Late Quaternary reconstruction of British-Irish Ice Sheet variability through the analysis of deep-water sediments from the Donegal Barra Fan and the Rockall Trough, North Atlantic.

Serena Tarlati

BSc, Geological and Earth Sciences, Alma Mater Studiorum, University of Bologna, Italy, 2010

MSc, Geology and Land Management (Curriculum b: Underground fluid resources), Alma Mater Studiorum, University of Bologna, School of Sciences, Italy, 2013

Thesis submitted for the degree of Doctor of Philosophy

School of Geography and Environmental Science,

Faculty of Life and Health Science,

Ulster University

September 2018

(I confirm that the word count is less than 100,000 words.)

Declaration on access to contents and condition of use

I hereby declare that with effect from the date on which the thesis is deposited in Ulster University Doctoral College, I permit:

1. The Librarian of the University to allow the thesis to be copied in whole or in part without reference to me on the understanding that such authority applies to the provision of single copies made for study purposes or for inclusion within the stock of another library.

2. The thesis to be made available through the Ulster Institutional Repository and/or EThOS under the terms of the Ulster eTheses Deposit Agreement which I have signed.

Summary

This research focusses on the evolution of the British-Irish Ice Sheet (BIIS) through the last glacial period and highlights its dynamic behaviour in terms of ice sheet advance and retreat, across the Irish and UK continental shelves. A multidisciplinary approach was applied to sediment cores retrieved from two different locations in the Rockall Trough, North East Atlantic Ocean, between 1000 and 3000 m water depth: from the glaciogenic Donegal-Barra Fan and the basin floor in the south-eastern portion of the trough. The methodologies used in this study include the interpretation of physical properties (in particular magnetic susceptibility and lightness), x-radiographs, grain size and stable isotopes analyses, radiocarbon dating, the determination of biofacies in planktonic foraminifera and the calculation of *Neogloboquadrina pachyderma (*sinistral*)* abundances, ice-rafted debris (IRD) concentrations and IRD fluxes. This research provides an overall interpretation on the sedimentary processes active along the North East Atlantic margin during the last 130 ka, in particular in relation to glacial and glaciomarine sedimentation linked to the BIIS. The presence of IRD of local origin in the deep water demonstrates how, during the last glacial period, the BIIS first extended offshore during MIS5b and later during MIS4 with marine-based calving margins. The BIIS maximum extent was reached before 20 ka BP, with a marine-terminating ice sheet that reached the shelf edge in most places. At this time, the maximum calculated value in sedimentation rates (13.8 cm/ka) suggests a significant input of sediment through meltwater plume deposition into the trough. Between 20 and 18 ka BP, the BIIS along the western Irish margin, north of the Porcupine Bank, was retreating through calving, shown by peaks in IRD concentrations and fluxes. The final stages of BIIS deglaciation are revealed by the cores from the Donegal-Barra Fan. Here glaciomarine sediments were delivered to the deep waters until around 16 ka BP. This is inferred to be the time when

the ice sheet had retreated entirely to an inshore or terrestrial position and therefore glacial sediment was no longer delivered to the shelf edge and outer shelf. Two distinct IRD-rich layers are related to two major BIIS calving events at 17.8 ka BP and 16.9 ka BP, which suggest that here the BIIS finally deglaciated by massive calving rather than a slow retreat across the shelf. An additional third IRD-rich layer is observed higher in the cores and dated at the Younger Dryas (ca. 12.7 ka BP). Icebergs responsible for the delivery of this last IRD pulse to the region are inferred to be sourced from a re-advancement and marine extension of the Scandinavian Ice Sheet at that time. Overall, the sediment record analysed in this study reveals how deep water sediments can provide a long and continuous record of glacial processes for large, marine-terminating ice sheets and can be used effectively for palaeoglaciological reconstructions. The results of this research can inform the current modelling of past ice sheet dynamics, which in turn will provide data for the prediction of possible future scenarios for present day marine-based ice sheets.

Table of contents

List of figures

List of tables

List of acronyms and abbreviations

ADS	Anton Dohrn Seamount
AMOC	Atlantic Meridional Overturning Circulation
AMS	Accelerator mass spectrometry
B1, 2, 3, 4, 5	Biofacies derived from two-way cluster analysis
B-C	BRITICE-CHRONO
BGS	British Geological Survey
BIIS	British-Irish Ice Sheet
BM	Extensively bioturbated mud
^{14}C BP	Conventional radiocarbon age
cal. a BP	Calibrated years before present
cal. ka BP	Calibrated thousand years before present
CHR	Clogher Head Readvance
CM	Chaotic mud
CO	Calcareous ooze
D	Donegal Lobe
$\delta\ ^{18}$O	Oxygen isotopic ratio
D-O	Dansgaard-Oeschger
D(4;3)	Mean volume weight value
DBF	Donegal Barra Fan
DNBC	Deep Northern Boundary Current
EIS	European Ice Sheet
ENAW	Eastern North Atlantic Water
FD	Feni Drift
FIS	Fennoscandia Ice Sheet
FM	Foraminifera-bearing mud
G	Galway Lobe
GC	Gravity corer

GGZW	Galway grounding zone wedge
HIS	Hebrides Ice Stream
HS	Hebrides Terrace Seamount
HS1	Heinrich stadial 1
ILM	Laminated mud rich in IRD
IRD	Ice rafted debris
[IRD]	IRD concentration, n° grains > 150µm /g of dry sediment > 63µm
ka BP	Thousand years before present
KPR	Killard Point Readvance
LIS	Laurentide Ice Sheet
LGM	Last glacial maximum
LSM	Laminated sand to mud couplet
LSW	Labrador Sea Water
mbsf	meter below sea floor
MIR	Mud rich in IRD
MIS	Marine isotopic stage
MiS	Malin Ice Stream
MS	Magnetic susceptibility
MSCL	Multi Sensor Core Logger
MSs	Malin Sea shelf
NAC	North Atlantic current
NADC	North Atlantic Deep Current
NADW	North Atlantic Deep Water
NCIS	North Channel Ice Stream
NEADW	North East Atlantic Deep Water
NERC	Natural Environment Research Council
NPS%	*Neogloboquadrina pachyderma* sinistral abundance
NRCF-East Kilbride	NERC radiocarbon facilities
NS	North Sea
OH	Outer Hebrides

PAST	Paleontological Statistics Software
PB	Porcupine Bank
PC	Piston corer
RB	Rockall Bank
RBSC	Rockall Bank Slide Complex
RmB	Rosemary Bank
RRS	Research Vessel
RT	Rockall Trough
RV	Research Vessel
SBP	Sub-bottom profiler system
SIS	Scandinavian Ice Sheet
SEC	Shelf Edge Current
SST	Sea surface temperature
UCD	University College Dublin
UUC	Ulster University Coleraine
WTROW	Wyville-Thompson Ridge Overflow Water
YD	Younger Dryas

Acknowledgements

I would like to thank my supervisors, the internals Sara Benetti and Paul Dunlop for their guidance and help during these past three and a half years, my external supervisors Aggeliki Georgiopoulou and Robin Edwards for advice during this time. In particular, I need to thank Sara for the immense support in these last few days of non-stop and crazy work. Also, thanks to the PhD examiners Ruth Plets and Bill Austin for their constructive comments on the manuscript and discussion during the Viva.

Next, I need to thank Ulster University and the Vice Chancellor Research Scholarship (VCRS) that funded this research and all the external institutions that supported the development of this work, such as the UK Natural Environment Research Council (NERC) grant NE/J007196/1 'Britice-Chrono', with AMS radiocarbon dating and the Marine Institute and the Quaternary Research Association (QRA) that allowed me to join international conferences and workshops.

I would like to thank the Captain and Crew, of *RV Celtic Explorer*, PI Aggie Georgiopoulou (UCD), Mr Áodhan Fitzgerald of the Marine Institute, for the cores acquisition during cruise CE10008. Then, I thank the Officers and Crew of the *RRS James Cook,* the PI Colm Ó Cofaigh (Durham University) for their help with data acquisition on the JC106 Cruise.

Thanks to Aggie for letting me work in UCD Dublin for grain size analysis and to Stephen McCarron at the National University of Ireland, Maynooth for the use of his GEOTEK multi-sensor core logger.

In these past years I had the chance to join two great experiences offshore, on board of the *RRS James Cook* during JC123 Cruise in the North Sea and on board of the *RV Celtic Explorer* during the Cruise CE16010 along the Newfoundland coastlines, Canada. Thanks to my supervisors for giving me these 'beautiful' opportunities.

I want to thank everybody that helped to keep myself more or less together in these Irish years. I start from the people I shared the most in this office, that I am not leaving now from days… Thanks to Jared, Kevin and Denise for everyday support, discussion and friendship. Then out of the office, thanks to Alex, Sabine, Magda, Tony, Gary, Eleonora and Davide, Federica, Klervi, Eduardo and many more that shared with me good time and with their presence make the time spent here rich of good memories. I have to thank Alex for supporting me with my moodiness and crying and craziness and lots of bad things in these last few months, thank you because you are probably one of the main reason I am now still sitting here. As last I want to thank the person I probably shared the most from the first day until the last, thank you Denise, for the laughs and all the extra travelling.

In the end, I want to say to myself that today, even with lots of problems and difficulties, something important is concluded, so don't only be critical but consider this moment as the achievement it represents.

A Nonno

Chapter 1: Introduction

1.1. Introduction and rationale

Reconstructing what happened in the past is an important tool for the understanding of current changing environments and the prediction of possible future scenarios (Leopold & Jones, 1947). Geological and environmental changes can occur over long periods of time and their direct observation is limited to the short timescale available to the human observers. For this reason, the use of paleo-archives is key for studying modern and changing environments (Seddon et al., 2014). This is particularly evident when investigating present ice sheets and glacial environments, where the extreme locations in addition to the 'time issue', make them inaccessible for many. Therefore, past archives of glacial processes, particularly in the form of sedimentary records from both terrestrial and marine locations, represent an important tool for investigating ice sheet dynamics and their evolution over long time-frames (Overpeck et al., 1997; Hambrey & McKelvey, 2000).

During the Pleistocene, the British-Irish Ice Sheet (BIIS) extended over Britain and Ireland; at times it extended onto the continental shelf and was therefore terminating in a marine environment. On several occasions it reached the shelf break along the North-east Atlantic continental margin (Stoker et al., 1994; Sejrup et al., 2005; Stoker et al., 2005). Onshore and offshore records have been analysed in the last 10-15 years to reconstruct and time constrain the behaviour of the BIIS during the last glacial period (Bowen et al., 2002; Ballantyne et al., 2008; Scourse et al., 2009; Chiverrell & Thomas, 2010; Clark et al., 2012a; J. Clark et al., 2012b; Hughes et al., 2014; Dove et al., 2015; Ballantyne et al., 2017; Ballantyne & Ó Cofaigh, 2017). The BIIS was inferred to extend along the North-

Atlantic margin at 70 ka BP and the analysis of deep water sediments has revealed a record of sub-millennial scale oscillations in the ice margin between 45 ka and 18 ka (Knutz et al., 2001; Wilson et al., 2002; Peck et al., 2007; Hibbert et al., 2010; Hall et al., 2011).

In most recent years, technological improvements in the acquisition of geophysical data, such as high resolution multi-beam echo-sounder bathymetry and seismic data, have supplied new material for research on the marine sectors of many former ice sheets, which moved the object of study away from the deep water to the glacial landforms observed in shallower locations on continental shelves (Ottesen et al., 2005; Shaw et al., 2009; Thorsnes et al., 2009; Anderson et al., 2014; Rignot et al., 2016). These new data have allowed large portions of the seafloor offshore of Ireland and UK to be mapped in the last 15 years and the interpretation of these new datasets has revealed a variety of glacial landforms, linked to the extension of the former BIIS on the UK and Irish continental shelves (Bradwell et al., 2006; Benetti et al., 2010; Howe et al., 2015; Peters et al., 2015). These glacial features are indeed recording the last BIIS glacial advance and retreat across the shelf. In addition, the mechanisms of ice sheet advance and retreat and the timing of the latter were inferred on the basis of the sediment records retrieved from certain landforms, such as mapped terminal moraines and grounding zone wedges (Bradwell et al., 2008; Dunlop et al., 2010; Ó Cofaigh et al., in press, Peters et al., 2015, 2016). These studies supplied a large amount of information, including the maximum extent of the former BIIS and the timing of its retreat at specific locations, such as the shelf offshore county Galway in Ireland (Peters et al., 2015, 2016). However, they do not provide a clear understanding about ice sheet dynamics before the last glacial maximum (LGM).

With this study, the focus switches back to the deep water environments, investigating sediment cores from the Donegal-Barra Fan and the south-eastern Rockall Trough: firstly,

for the possibility of retrieving longer sediment records, less disturbed, or influenced by erosion than in shallower water, and secondly, for the multi-proxy based information they can provide, including the analysis of ice rafted debris (IRD), oxygen isotopes, and microfossil assemblages. These proxies, when studied from suitable locations, have the potential to show the signal of alternation between glacial/interglacial, stadial/interstadial periods, as well as recording ice-sheet advances and retreats into the marine realm (cf. McManus et al., 1994; Bond et al., 1999; Scourse et al., 2009). This evidence can then be used to investigate ice sheets dynamics, over long and short periods of time and their general relationship to global climate. Therefore, palaeoenvironmental reconstructions obtained from deep water sediments can in turn provide key information for modelling the dynamic behaviour of modern marine-terminating ice-sheets, such as the West Antarctica Ice Sheet or the Greenland Ice Sheet, which is important for understanding their future trajectory in a warming world (DeConto & Pollard, 2003; Pritchard et al., 2012; Nick et al., 2013).

1.2. Hypothesis, research aim and objectives

This project wants to test the following hypothesis: **Deep water sediments can provide key information for the reconstruction of the behaviour of marine terminating ice sheets**; while attaining the final project aim of improving current knowledge about the variability of the BIIS.

This work focuses on the analysis of sediment cores collected from two specific areas in the Rockall Trough: the continental slope of the Donegal-Barra Fan and a deep-water location in the south-eastern portion of the trough. These areas represent two different depositional settings along the North Atlantic continental margin: a glaciogenic fan and

an open deep-water environment, which were both potentially influenced by the BIIS activity during the Late Quaternary as suggested by their proximity to mapped landforms that indicate ice-sheet extension to the shelf edge.

Specific objectives will help in testing the proposed hypothesis and at the same time reaching the project aim.

- The identification and interpretation of the lithofacies through the sediment record to better understand the modes of sediment delivery to the deep water environment and their potential links with glacial and glaciomarine processes.
- The construction of relevant age models using radiocarbon dating and correlation between the $\delta^{18}O$ record from foraminifera shells in the cores with local and global oxygen isotope records to allow the time-constraining of the sediment record.
- The investigation of ice-rafted debris concentration and fluxes over time as proxies for the extension of the BIIS into the marine environment and episodes of catastrophic ice retreat.
- The investigation of the planktonic foraminifera assemblages in the Rockall Trough as a tool for the analysis of changing climatic and oceanographic conditions and their relation with a marine extended ice sheet in the region.
- The overall reconstruction of the BIIS dynamics along the continental margin between 56 N and 53 N.

1.3. Previous research gaps

The BIIS is an intensively studied marine terminating paleo-ice sheet (see next chapter 2.3., 2.3.1.), where gaps in the understanding of its dynamics during the last glacial period are recognised and current research is working to fill them. These knowledge gaps are

recognised as driven by both geographical and chronological limitations (Clark et al., 2012a; Ó Cofaigh et al., 2012).

Firstly, gaps are recognised in the deep water sediment record where the majority of the previous works were based offshore the Malin Sea or the Porcupine Bight (Scourse et al., 2009) (see 2.3. and 2.3.1.) and very little work has been done on sediments along the north-west Irish margin, in particular in the south-eastern sector of the Rockall Trough. The area is still not well explored in relation to ice sheet dynamics and the BIIS extension on the continental shelf, considering how likely this zone could have been affected by an advanced BIIS offshore of western Ireland and Scotland (Peters et al., 2016; Callard et al., in review).

Secondly, high-resolution reconstructions of the BIIS advance and retreat events before the Marine Isotopic Stage (MIS) 2 and the last glacial maximum (LGM) are still scarce (see 2.3. and 2.3.1.) due to lack of long sediment records from suitable locations in shallow water and limited work in deep water (Hibbert et al., 2010). The sediment analysed in this project could likely provide long and continuous information able to extend current knowledge behind the MIS2.

And in the end, the reconstruction of the BIIS deglacial processes and their timing is still very limited, this is mostly due to the low resolution of the available datasets (Ó Cofaigh et al., 2012). In our case of study, deep sea sediments can provide long record allowing analysis at high resolution, for example the very long record from the Donegal Barra Fan. Therefore, it is highlighted how this research aims to help filling these gaps in knowledge, improving the current understanding of the BIIS dynamics through the use of deep sea sediments collected from two different locations.

1.4. Thesis structure

This PhD thesis revolves around two chapters written as scientific papers, both addressing the main research objectives and to be submitted to the journal Marine Geology. The respective datasets are extensively discussed in Chapters 4 and 5, each of these two chapters also include an introduction, regional setting and methodology section. These chapters are preceded by two introductory chapters where the 'Study area and background' and the 'Material and methods' are briefly presented. In Chapter 6 'General discussion and conclusions', the results from the two chapters are brought together and additionally discussed in order to highlight the implications of the results for the reconstruction of the BIIS dynamics across the entire region, thus addressing the last research objective. Because the chapters dealing with the datasets are structured as papers, some degree of repetition among each section is unavoidable and Chapter 2 and 3 have to be considered as a summary of the contents later included in the two papers. The structure of each chapter is outlined in the next paragraphs.

Chapter 2: Study Area and Background

In this chapter, the study area, the Rockall Trough, is introduced with reference to its geology, sedimentary history, bathymetry and oceanography. A short review on the previous work done on the BIIS is included with a general reconstruction of the BIIS history with particular attention to its western margin. A short summary of previous work on the reconstruction of BIIS dynamics based on deep water IRD records is included.

Chapter 3: Materials and methods

This chapter presents an overview of the material and the methodologies used during this research. The different techniques include sedimentological analysis, sampling

preparation, foraminiferal counts, assessment of biofacies, IRD counts, stable isotopes analysis and radiocarbon dating. The methods are successively presented in the specific sections of the full-length articles within Chapters 4 and 5.

Chapter 4: Late Quaternary deglacial history and meltwater events recorded on the southernmost glaciogenic fan of the North-east Atlantic, the Donegal-Barra Fan

In this paper, three sediment cores over 6 meters long collected from the cruise JC106 as part of the NERC-funded BRITICE-CHRONO project are analysed. The sedimentary evolution of Donegal-Barra Fan over the last 18,000 years BP is reconstructed. Sediment accumulation on the fan includes glaciogenic sediments delivered by a retreating BIIS and the renewal of contouritic deposition after 15,000 years BP. During the retreat, two BIIS inferred calving events are highlighted by IRD peaks at 17.8 and 16.9 ka BP. A Younger Dryas-dated glaciomarine deposit rich in IRD is recognised within the post-glacial sediments. It is interpreted as related to an ice-sheet re-advance of northern European origin rather than a Laurentide Ice Sheet origin due to the petrology of the IRD grains.

Chapter 5: Unravelling the history of the western sector of the British-Irish Ice Sheet over the entire last glacial period using NE Atlantic marine sediment cores: a multi-proxy approach

In this paper, the continuous sediment record from two piston cores up to 4 m long and recovered from approximately 3,000 m water depth is used to investigate the sedimentary evolution of the Rockall Trough basin. Six lithofacies are identified and the relatively sedimentary processes interpreted as related mostly to hemipelagic and glaciomarine

sedimentation. The use of stable oxygen isotopes guides in the time constraining of this sediment record, together with the abundance of the cold-water species *Neogloboquadrina pachyderma* sinistral and IRD concentrations. The pattern of sedimentation since the previous interglacial and through the entire last glacial period is then presented, with reference to the influence of the BIIS on the processes of sediment delivery. Biofacies, based on the planktonic foraminiferal content, supply a qualitative indication of sea-surface water temperature and IRD fluxes help in the investigation of the BIIS calving events recorded in the Rockall Trough.

Chapter 6: General discussion and conclusions

In this chapter, the findings obtained during this research are presented in conjunction with the results from previously published works with the aim of reconstructing the evolution of the BIIS and investigate its behaviour along the North Atlantic margin in the Late Quaternary. The deep water sediment is presented as an interesting tool for addressing known gaps in the BIIS knowledge and supporting the previous works done in shallower waters along the North-east Atlantic margin. Lastly, this chapter shortly summarizes the main results obtained during the development of this research and suggestions for future work are also presented.

The two main articles within this thesis are going to be soon submitted for peer-review and publication with co-authors. Co-authorship is typically an acknowledgement of a

combination of financial support, analytical collaborations, research cruise collaborations and advice on project development and results. Valuable support comes from co-authors with regard to editorial and organizational feedback. All writing and analysis for the accomplishment of this thesis were completed by the author.

Chapter 2: Study area and background

2.1. Climate forcing and glaciations

During the Quaternary, the global climate has undergone alternations of warm and cold climatic intervals, evident as interglacial and glacial periods (Bereiter et al., 2015). Glacial and interglacial periods followed a long-term periodicity, where ice masses extended to low latitudes and retreated towards the ice caps during the cold and warm intervals, respectively. These cycles are considered the result of orbital or astronomic forcing responsible for changes in the total solar insolation received by the Earth, due to the variability in the planet's orbital eccentricity, axis obliquity and precession (Milankovitch, 1941; Berger & Loutre 1991). These climatic cycles (i.e. Milankovitch cycles) are known to be repeating with different periodicities, varying between 100,000 and 23,000 years and are recorded in both marine and terrestrial records (Petit et al., 1999). Evidence of these climatic cycles have been provided from carbon dioxide (CO2) in ice cores and from the benthic $\delta^{18}O$ stack record in ocean sediments (Petit et al., 1999; Lisieki & Raymo, 2005).

Occurring during the last glacial period (~100,000 years) and at shorter time periodicities, the Dansgaard-Oeschger (D-O) cycles have been observed in ice core records from Greenland (Dansgaard et al., 1993). Deep marine sediment records indicate a similar trend, identified in changes within the foraminiferal contents, oxygen stable isotopes and through the presence of ice rafted debris (IRD) (McManus et al., 1994). Proposed drivers for the D-O climatic variability include orbital forcing and the presence of extended ice sheets in the northern hemisphere; however, the triggers of D-O cycles are still not well understood (Bond et al., 1999). In this second case, the ice sheets contribution of

freshwater to the oceans (i.e. evident in the planktonic fauna and stable isotopes) leads to a reduction of the Atlantic Meridional Overturning Circulation (AMOC) and is considered to be likely responsible for the transition to glacial conditions (Bond et al., 1999). The D-O cycles occur with an approximate duration of 2,000-3,000 years and are represented by an abrupt warming, reaching similar conditions to an interglacial period, followed by a gradual cooling (Dansgaard et al., 1993). Heinrich events (H-event) are acknowledged within the D-O cycles as the coldest events, occurring with an approximate 10,000 years periodicity. H-events are associated with the collapse of the Laurentide Ice Sheet (LIS), the marine terminating ice sheet covering the northern American continent, and with a large dispersal of icebergs in the North Atlantic (Heinrich, 1988). While the relative periodicity of these H-events has been identified, their driving causes are still under study (Hemming, 2004).

The British Irish Ice Sheet (BIIS), located along the eastern North Atlantic continental margin, was one of the ice masses sensitive to climatic changes experiencing periods of growth and retreat during Quaternary glaciations (Clark et al., 2012a). Evidence of the BIIS responding to these climatic cycles (i.e. ice-sheet extensions and retreats through time) are recognised in the glacial geomorphologies mapped in marine and terrestrial environments, including moraines, drumlins, grounding zone wedges and iceberg scours (Bradwell et al., 2008; Ó Cofaigh et al., 2012; Dunlop et al., 2010; Peters et al.,2016). BIIS dynamics also left evidence in the deep marine sediment records, representing the primary focus of this study. Our current understanding of the BIIS past extension, and subsequent response to climatic forcing, is presented in the next sections (i.e. sections 2.3. and 2.3.1.).

2.2. Study area

In this study the behaviour of the BIIS was investigated using deep-sea sediments from the North East Atlantic and in particular from the Rockall Trough (RT) (Fig. 2.1).

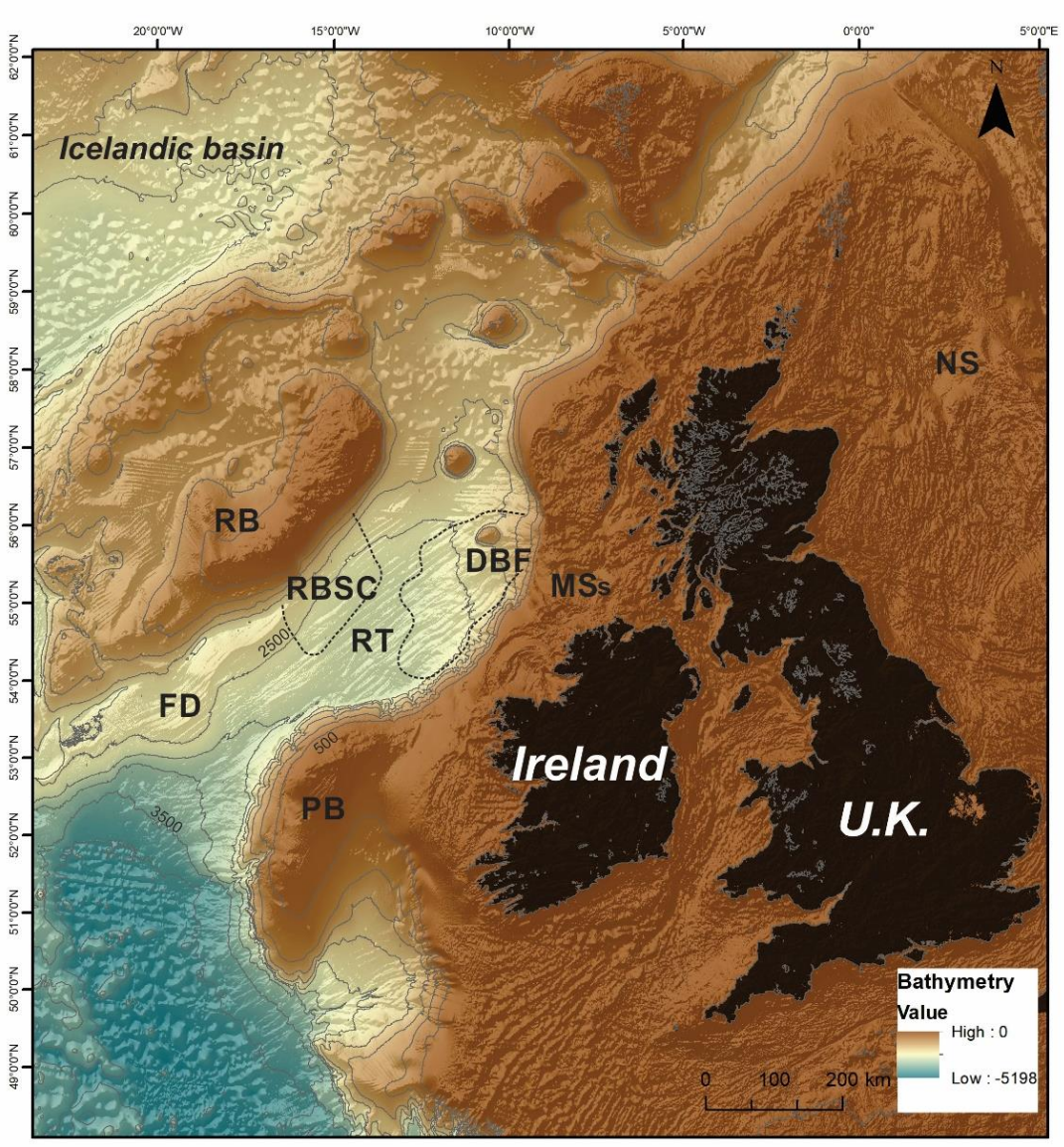

Figure 2.1: Overview of the north-eastern Atlantic margin from the General Bathymetric Chart of the Oceans (GEBCO). The Rockall Trough and the other main features in the region are labelled RT= Rockall Trough; RB= Rockall Bank; FD= Feni Drift; RBSC=Rockall Bank Slide Complex; DBF= Donegal Barra Fan; MSs= Malin Sea shelf; PB= Porcupine Bank; NS= North Sea).

The following sections provide a brief overview of the geography and glacial history of the study area, together with a review of the oceanographic setting of this sector of the North Atlantic. Both the regional setting and the rationale behind the work at the two specific locations, which were the focus of this research, are then dealt with more extensively in the relevant chapters.

2.2.1. Physiography and Geomorphology

The Rockall Trough (RT) is a deep elongate basin on the passive continental margin west of Ireland and UK, located between 60°N and 50°N of latitude and it has water depths ranging from 1,200 m in the northern sector up to 4,500 m in the southern (Shannon et al., 2001; Unnithan et al., 2001) (Fig. 2.1).

It is a narrow depression, ~1000 km long and approximately 200-250 km wide, bounded by steep flanks ranging between 3°and 7° (Stoker, 1995; Unnithan et al., 2001). The RT evolved from the late Palaeozoic to the early Cenozoic during the continental rifting and opening of the North Atlantic Ocean, through continental break up and subsidence (Stoker, 1997; Unnithan et al., 2001). It is separated from the Icelandic basin by the Rockall Bank, which is a high plateau or continental fragment that was formed during the Palaeozoic ocean opening (Naylor et al., 2009). During the Pleistocene, the RT has been largely influenced by the dynamic behaviour of the BIIS and by oceanic currents, delivering and winnowing sediments along the basin margins (Sejrup et al., 2005; Elliot et al., 2006; O'Reilly et al., 2007).

The main geomorphological features along this sector of the North Atlantic margin are, on the UK and western Irish continental slope, the Donegal Barra Fan (DBF) and an

intricate system of canyons with related depositional lobes in the trough (Cronin et al., 2005; Sacchetti et al., 2011; Sacchetti et al., 2012a) (Fig. 2.2).

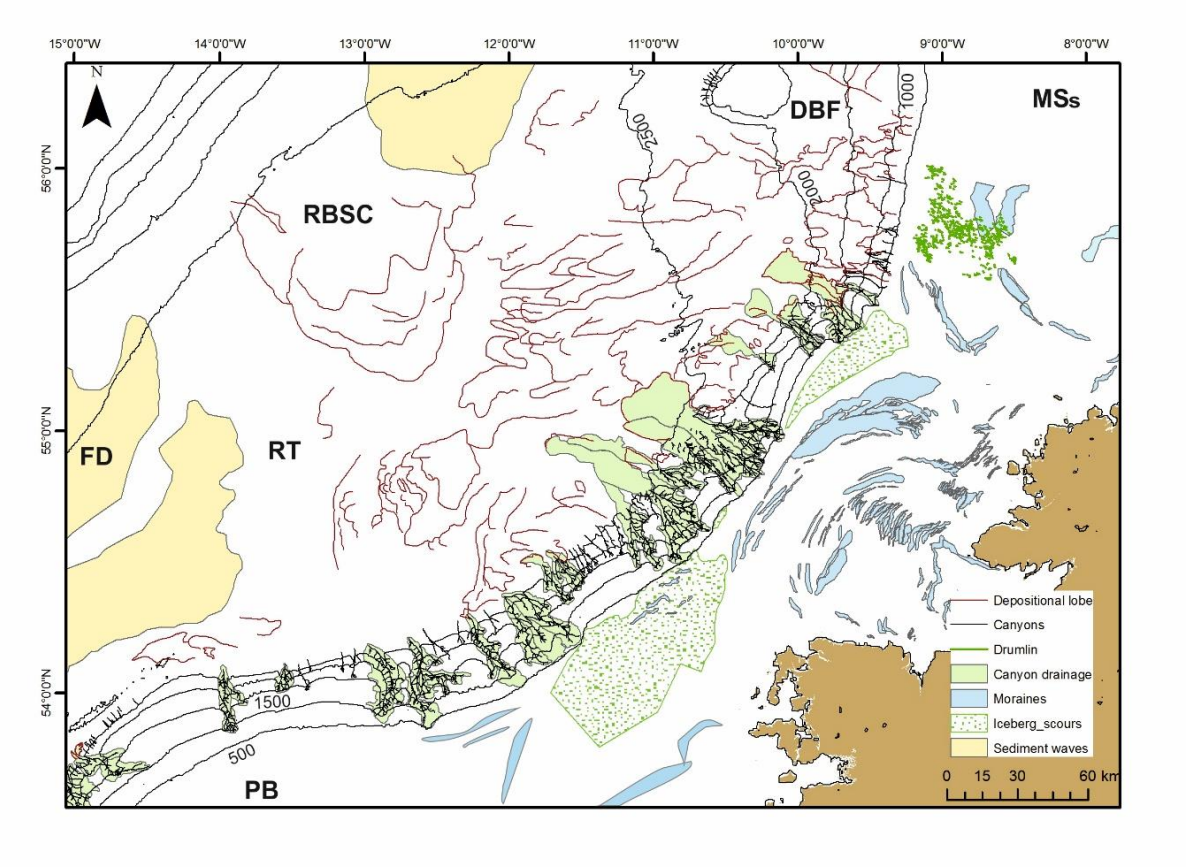

Figure 2.2: Sector of Irish shelf and slope with the main features mapped by Benetti et al., 2010, Sacchetti et al., 2011, Peters et al., 2015.

The DBF is a composite glaciogenic fan that was generated by the accumulation of numerous sediment lobes. These were delivered to the RT through down-slope movements by an extended BIIS on the Malin Sea shelf, during Pleistocene glaciations (Stoker, 1995; Armishaw et al., 1998; Holmes et al., 1998; Knutz et al., 2001). The overlapping sediment lobes of the DBF were deposited in an E-W direction, in the central RT, and in a NE-SW direction along the eastern flank, up to a distance of 250 km (Sacchetti et al., 2012a).

The canyons were formed along the Irish margin of the trough during the Mid-Cenozoic for slope rotation due to ocean opening with related subsidence (Unnithan et al., 2001; Elliot et al., 2006; O'Reilly et al., 2007) and then shaped by the BIIS glaciations during the Quaternary (O'Reilly et al., 2007; Ó Cofaigh et al., 2012; Sacchetti et al. 2012a).

The western flank of the RT is characterised by the presence of a large slope failure (Shannon et al., 2001), the Rockall Bank Slide Complex (RBSC) that seems to have occurred from 16 ka BP and during the current interglacial period (Figs. 2.1 and 2.2) (Flood et al., 1979; Faugeres et al., 1981; Shannon et al., 2001; Unnithan et al., 2001; Georgiopoulou et al., 2013). It is interpreted representing a three steps slope collapse generating a large slide complex with a suggested sediment volume between 265 and 765 km^3(Georgiopoulou et al., 2013).

The Feni Drift (FD) (Figs. 2.1 and 2.2) is a contourite drift along the western flank of the trough that was formed from bottom current activities beginning from the Eocene (Kidd & Hill, 1986; Stoker, 1997; Unnithan et al., 2001; Stoker et al., 2005). It is formed by large sediment waves, up to 60 m high, with wave length between 1 and 4 km and with crests between 2 and 20 km long, with a recognised parallel body on its eastward side (Sacchetti et al., 2012a) (Fig. 2.2).

On the Irish and UK continental shelves, other kinds of features are mapped, including moraines, drumlins, mega scale glacial lineations and iceberg scours (Bradwell et al., 2007; Benetti et al., 2010). Several complexes of arcuate and nested moraines are present across the shelf, together with drumlins on the Malin Sea shelf and icebergs scours along the shelf break, suggesting the activity of a dynamic marine-based ice-sheet west of Ireland and Scotland during the Late Quaternary (Sejrup et al., 2005; Benetti et al., 2010; Dunlop et al., 2010; Clark et al., 2012a; Ó Cofaigh et al., 2012; Peters et al., 2015; 2016). What is known about the history of the BIIS in the region is summarised in Sect. 2.3.

2.2.2. Oceanography and contourites deposition

The north-east Atlantic oceanography is characterised by the presence of the North Atlantic Current (NAC). The surface waters are largely influenced by this warm and saline current that moves northward, where it convectively overturns in the Nordic Seas. The deep waters are regulated by the Upper North Atlantic Deep Water (UNADW). UNADW forms from the Nordic Sea overflow waters (Iceland-Scotland Overflow Water-ISOW, Wyville-Thomson Overflow Water-WTOW) that enter in the NE Atlantic over the Wyville-Thomson and Iceland-Scotland Ridges, combining with the deep waters formed by convection in the Labrador Sea (i.e. Denmark Strait Overflow Water-DSOW) (Dickson et al., 2008) (Fig., 2.3).

The Rockall Trough (RT) is influenced by a large number of currents and water masses at different water depths promoting sediment transport and deposition on the margins of the trough and in the deep basin, predominantly during interglacial times (Knutz et al., 2002; Masson et al., 2010; Øvrebø et al., 2005; Toms, 2010; Sacchetti, 2012; Georgiopoulou et al., 2013). (Fig. 2.3).

These water masses can be broadly divided in superficial and deep. The Eastern North Atlantic Water (ENAW) flows from the Bay of Biscay towards northern latitudes, along the eastern side of the RT, moved by the Shelf Edge Current (SEC). The ENAW general velocity is 15-30 cm/s and has a thickness of approximately 400-600 m, between 0 and 600 m of water depth. It turns anticlockwise around the Hebrides Terrace Seamount (HS) and moves southward along the western RT margin (New & Smythe-Wright, 2001). The deeper North-Eastern Atlantic Deep Water (NEADW) moves slowly northward along the deepest part of the RT at water depths between 2,000 and 3,000 m. The current responsible for the flowing of this water mass is recognised in the North Atlantic Deep

Current (NADC), originating from the North Atlantic Current system (NAC) and flowing northward into the European basin (New & Smythe-Wright, 2001; Toms, 2010). Sediment is transported from the eastern to the western flank of the RT as a result of the currents activities (Shannon et al., 2001).

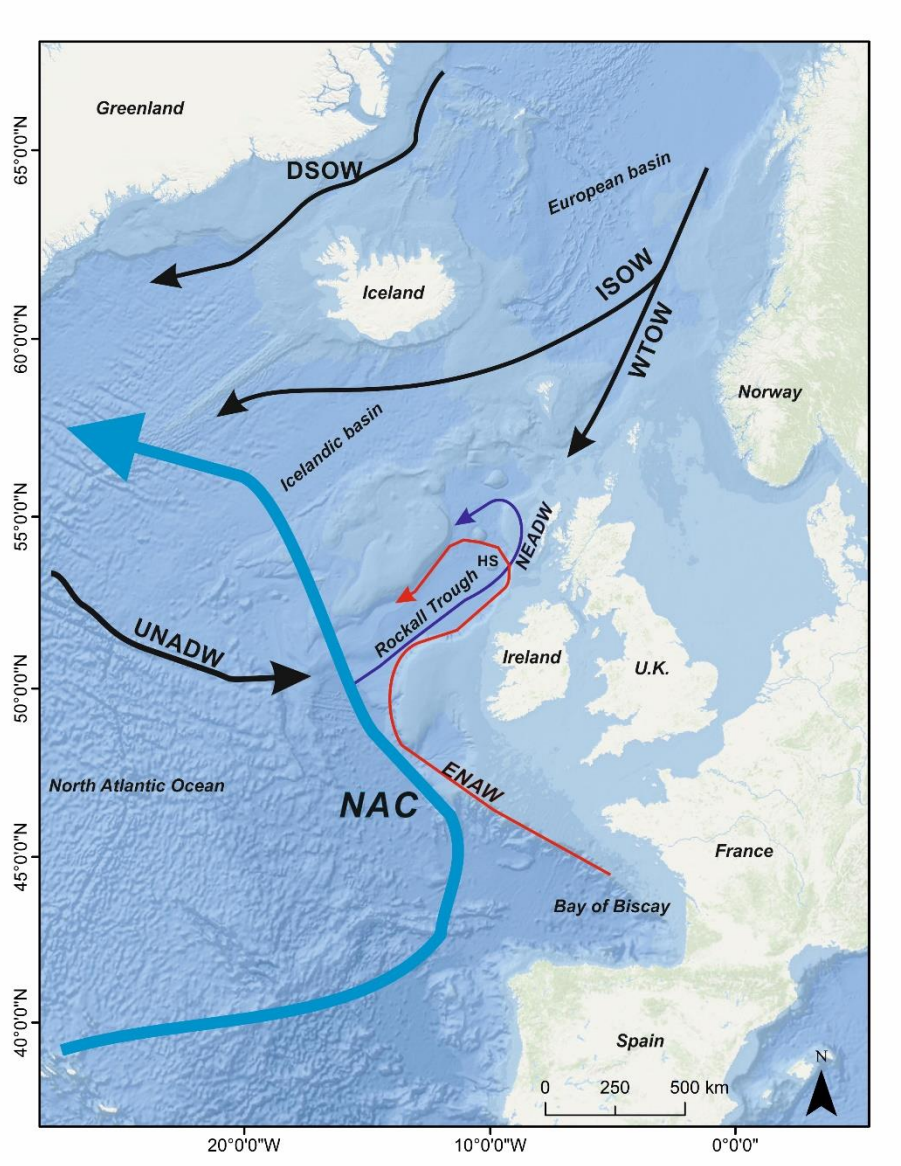

Figure 2.3: North-East Atlantic oceanographic settings. Direction of the North Atlantic Current (NAC) indicated by the light blue line. The red arrow indicates the main direction of Eastern North Atlantic Water (ENAW) in the Rockall Trough. The dark blue line is indicating the direction of the deeper North East Atlantic Deep Water (NEADW) in the Rockall Trough.

During Quaternary glacial intervals, large amounts of freshwater from melting marine terminating ice sheets were released into the oceans, having a central role on the deceleration or interruption of the Atlantic currents (Stanford et al., 2011; Bigg et al., 2012; Toucanne et al., 2015). The North-East Atlantic oceanographic setting was recognised to change during this time (Bigg et al., 2012). The Atlantic Meridional Overturning Circulation (AMOC), or ocean conveyor belt, experienced a reduction and migration to shallow water position during cold climatic intervals (Austin & Kroon, 2001). This was shown by studies on carbon and oxygen isotopic ratios, in accordance with investigation on the foraminiferal fauna, ocean sea-surface temperature (SST) and salinity reconstructions (Bond et al., 1999).

Studies based along the RT showed the interruption and slowing of currents along the UK and Irish margin, within the last glacial period and deglaciation (Austin & Kroon, 2001). During these cold intervals, the NEADW was suggested as largely reducing its formation as the result of the changing AMOC circulation (Austin & Kroon, 2001). Evidence for the interruption of the heat and salinity transport, along the trough flanks towards the Nordic seas, were provided by changes in the local SST, salinity and foraminiferal records (Austin & Kroon, 2001). In the RT, the SST and salinity experienced large oscillations between glacial and interglacial periods. These recorded accelerated alternations during deglaciation, also following a short D-O periodicity (Kroon et al., 1997).

Variations in RT waters display a similar timing with the Atlantic Ocean sediment and the Greenland ice records, making it possible to time constrain the local signals with the changing deep sea conditions of ventilation in the North Atlantic Ocean (Kroon et al., 1997; Austin & Kroon, 2001).

Sediment records from the North Atlantic show these oceanographic changes, as well as the restoration of typical interglacial oceanographic conditions following deglaciations (Rahmstorf, 2002; McManus et al., 2004).

This fluctuation in oceanography results in the observed alternating deposition of contourites and glacial or glaciomarine deposits along the Irish and UK margins (Austin & Kroon, 2001; Knutz et al., 2002). Contourites have been recognised along the RT flanks and the Donegal Barra Fan by previous research. These have been defined as the sediments deposited or significantly affected by the action of bottom currents on the sea-floor, recognized from muddy to gravel-lag in grain size, showing different compositions depending on the sediment supply to the system (Stow et al., 2002). Along the RT flanks, the contourites have been described as sandy and muddy sedimentary bodies, generally well-sorted, bioturbated, with a reduced thickness and a mottled character, deposited during warm or interglacial climatic intervals (Knutz et al., 2002; Masson et al., 2010; Øvrebø et al., 2005). The presence of glacial and glaciomarine deposits were also recognised by previous works (Kroon et al., 2000; Knutz et al., 2001). The BIIS marine-extension during glacial and deglacial intervals, with its ice margin reaching the shelf edge and retreating along the continental shelf, was responsible for the sediment delivery to these deep water locations (Knutz et al.,2002). In this case, the sedimentary deposits were largely represented by mass wasting deposits and turbidites (Kroon et al., 2000).

2.3. An overview of the BIIS over time

The BIIS has left behind a variety of landforms, both in terrestrial and marine settings (as mentioned above in Sect. 2.1.1.). The BIIS extent, dynamic changes and their timing in extension and retreat have been investigated using many different approaches, in the almost 150 years it has been under study (Agassiz, 1842; Wright, 1914; Bowen et al., 2002; Sejrup et al., 2005; Scourse et al., 2009; Clark et al., 2012a; Clark et al., 2012b; Ó Cofaigh et al., 2012).

Ice sheet activity was recorded starting from the Pleistocene with a series of extended glaciations along the majority of the UK-Irish margin (Stoker et al., 1994; Stoker, 1995; Sejrup et al., 2005). A glaciated shelf-edge along the North Atlantic was observed several times during different glacial periods, starting from Marine Isotopic Stage (MIS) 12 until the BIIS last glacial maximum (LGM) during MIS2 (Stoker et al., 1994; Sejrup et al., 2005). The past BIIS investigations largely focused on the last glaciation, and in particular on the BIIS behaviour during LGM and the subsequent deglaciation (Bowen et al., 2002; Bradwell et al., 2008; Chiverrell & Thomas, 2010; Clark et al., 2012a; Ó Cofaigh et al., 2012; Peters et al., 2016). During the Late Pleistocene, the BIIS is now known to have covered the majority of Ireland and Britain, with a maximum extent recorded between ~27-23 ka (Scourse et al., 2009; Clark et al., 2012a; Peters et al., 2015; Ballantyne & Ó Cofaigh, 2017). At that time, the BIIS also occupied part of the North Sea, connecting with the Fennoscandian Ice Sheet (FIS) and it extended along the western margin of the Irish and Scottish continental shelf (Wilson et al., 2002; Ó Cofaigh et al.,2010; Scourse et al., 2009; Clark et al., 2012a) (Fig. 2.4).

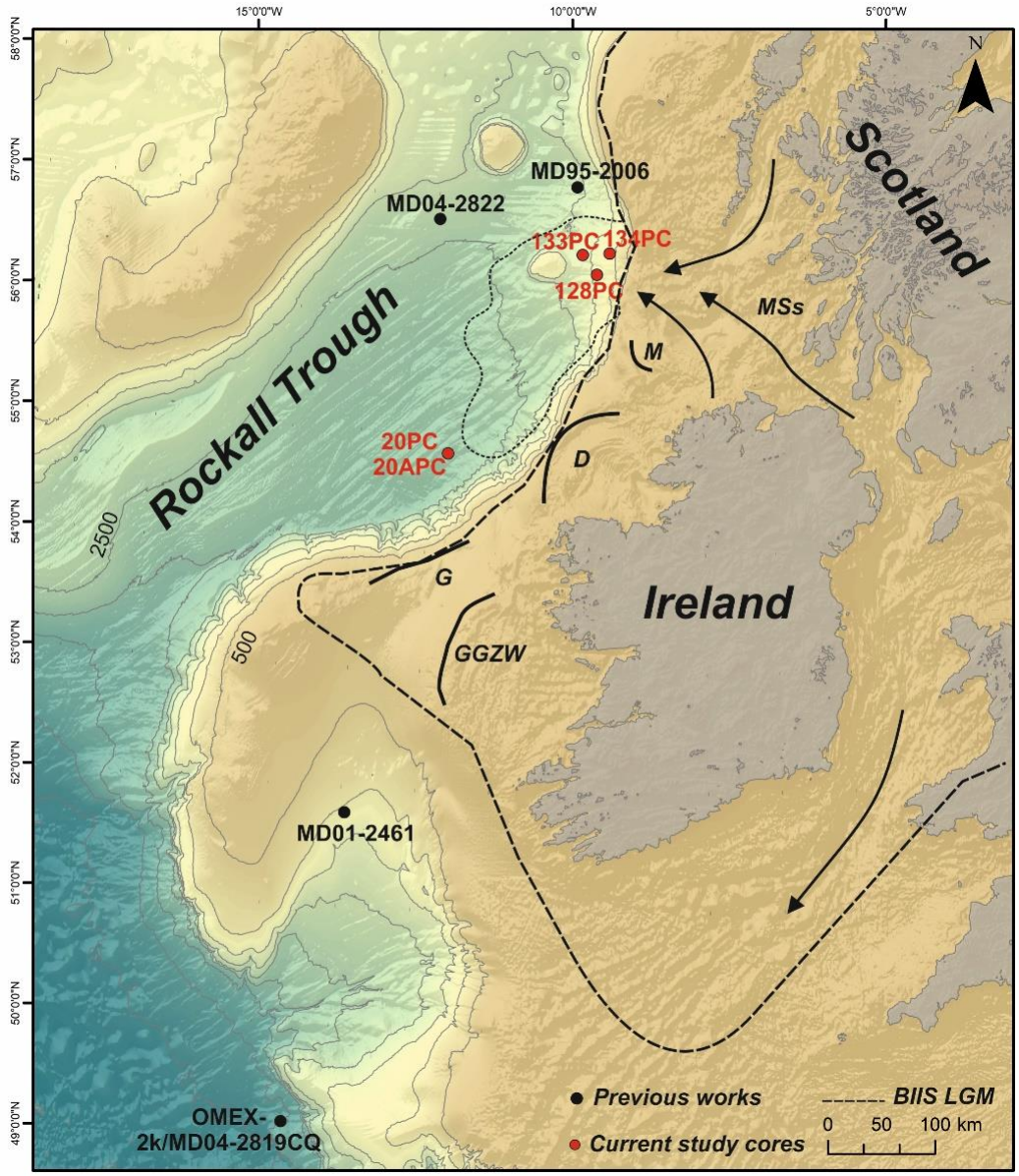

Figure 2.4: North west Irish and Scottish margin, from GEBCO bathymetry. The isobaths are represented every 500-m interval. The Malin Sea shelf (MSs) is indicated and the black arrows show ice-streamings active during the last glacial period. The Irish shelf displays several systems of moraines, results of the deglaciation and lobate aspect of the ice-sheet. M, D, G and GGZW indicate the largest ridges observed west of Ireland, along the Donegal Lobe (D) and the Galway Lobe (G) sectors of the BIIS. M=Malin Shelf moraines; GGZW=Galway grounding zone wedge. BIIS LGM after Clark et al., 2012a. Red dots represent location of the cores analysed within this study, abbreviations:133PC, 134PC, 128PC are from cruise JC106, 20PC=CE10008-20PC; 20APC=CE10008-20APC. Black dots represent previously investigated deep-water sediments from the area referred to into this chapter. From north to south: MD95-2006 used by Knutz et al., 2001; Scourse et al., 2009, Wilson & Austin, 2002. 57/-11/59 and 56/-10/36 used by Wilson et al., 2002. MD04-2822 used by Hibbert et al., 2010. MD01-2461 used by Peck et al., 2007, Scourse et al., 2009, Haapaniemi et al., 2010. OMEX-2k/MD04-2819CQ (Goban Spur) in Scourse et al., 2009, Haapanimei et al., 2010).

Along the Scottish margin, on the Malin Sea continental shelf (MSs), the BIIS was recorded reaching its maximum extension at 27 ka (Bradwell et al., 2008; Scourse et al., 2009). The Malin Ice Stream (MiS)/Hebrides Ice Stream (HIS) and the North Channel Ice Stream (NCIS) joined on the MSs delivering up to the 10% of the drainage water of the western BIIS to the DBF (Dove et al., 2015). Along the western Irish shelf, the BIIS reached its local maximum extent between 29 and 23 ka BP (Ó Cofaigh et al., 2012; Peters et al. 2015). BIIS retreat is inferred to have started at approximately 23 ka BP and, based on the observed landforms, then separated in distinct lobes along its marine termination until its total deglaciation after 15 ka (Clark et al., 2012a). After the LGM, along western Scotland the ice-streams retreated towards land and the HIS was recorded at the actual coast-line between 17 and 16 ka (Small et al., 2017). On the western Irish shelf, the BIIS sector offshore county Galway, the Galway Lobe (G) (Fig. 2.4) was recognised retreating from the shelf edge at 22 ka BP and was recorded in still-stand on the 200 m bath-isoline at approximately 21 ka with the formation of a grounding zone wedge (GGZW) (Peters et al., 2016). The following retreat for the lobe was observed after 21 ka (Peters et al., 2016). A different behaviour for the northerly located BIIS sector, the Donegal Lobe (D) has been observed. Here the maximum extent was dated between 29 and 23.7 ka (Ó Cofaigh et al., 2012; Purcell, 2014), and after it, the mapped nested arcuate moraines on the shelf suggested an episodic pattern of retreat, with minor re-advances during deglaciation (Ó Cofaigh et al., 2012). Until the BIIS final deglaciation, events of re-advance were observed. In particular, along the NE Irish coastlines, the Clogher Head Readvance (CHR) and the Killard Point Readvance (KPR) were dated at 18.4 ka BP and 17.3-16.6 ka BP (McCabe &Clark, 1998; Ballantyne & Ó Cofaigh, 2017). A dated re-advance at 18 ka BP was also recorded on the Western Irish shelf by Peters et al., 2016.

2.3.1. Previous BIIS reconstructions using the deep-water IRD record

The term IRD defines lithic grains coarser than 150 μm transported by iceberg drifting and embedded into muds, therefore representing a proxy of iceberg presence (Hemming et al., 2004; Peck et al., 2007). Deep water sediments have been used to reconstruct the BIIS growth and retreat over time through the record of IRD found offshore (Knutz et al., 2001; Peck et al., 2006; Scourse et al., 2009) (Fig. 2.4). In the majority of the IRD analysed in previous studies from the Rockall Trough and along the Irish margin, grains were recognised to be mainly delivered by the BIIS based on their composition, with the exclusion of Heinrich layers, which can be identified on this margin and whose IRD composition indicates a source in the Laurentide Ice Sheet (Peck et al., 2006; Scourse et al., 2009; Haapaniemi et al., 2010). The lithics recognised along the North Atlantic margin are mainly represented by quartzite, basalt, limestone and highly crystalline metamorphic grains; whilst those found in the Heinrich layers are generally represented by yellowish detrital dolomitic carbonate (Knutz et al., 2001; Peck et al., 2007). Studies on the presence and southward orientation of iceberg scours on the Rockall Bank supplied additional evidence of a main BIIS origin for the IRD observed. The Bank was indeed recognised as a large obstacle where icebergs flowing southward from Greenland and Iceland grounded during glacial intervals (Sacchetti et al., 2012b).

The analysis of IRD records from deep water locations allowed the observation of a marine-extended BIIS previous to the LGM and the MIS2 (Hibbert et al., 2010). BIIS extension offshore along western Britain was identified starting from the MIS4 and its evolution through time following a large scale response to the North Atlantic climate (Scourse et al., 2009; Hibbert et al., 2010). The IRD records display a millennial cyclicity starting from 45 ka BP and during MIS2, suggesting that iceberg discharge from the BIIS,

in the form of events of advance and retreat was also occurring on such timescales (Knutz et al., 2001; Peck et al., 2007; Scourse et al., 2009). These cycles followed a sub-Milankovich sequence identified in a Dansgaard-Oeschger (D-O) periodicity of 2-3 ka (Knutz et al., 2001; Wilson et al., 2002; Wilson & Austin, 2002; Peck et al., 2006; Scourse et al., 2009; Haapaniemi et al., 2010).

These previous investigations show how the deep water sediments and the IRD record can supply a large range of information about the BIIS dynamics and its relation to the North Atlantic climate and oceanography. However, the cores used in these previous studies were located in proximity of ice stream terminations, on the Donegal-Barra Fan, the Porcupine Seabight and the Goban Spur, and therefore not directly offshore of the main western margin of the BIIS identified from the glacial landforms on the shelf (Fig. 2.4).

Chapter 3: Materials and methods

In this chapter, a summary of all the material and the techniques used within this research are presented. The methodologies are summarized, together with their rationales, supplying an explanation of why they have been selected for the achievement of the research aim and objectives. All methods employed are moreover presented in Chapter 4 and 5.

3.1. Materials

A total of 5 sediment cores, up to 7 meters long, have been used in this study with the aim of reconstructing the BIIS dynamics during the Late Quaternary (Fig. 3.1).

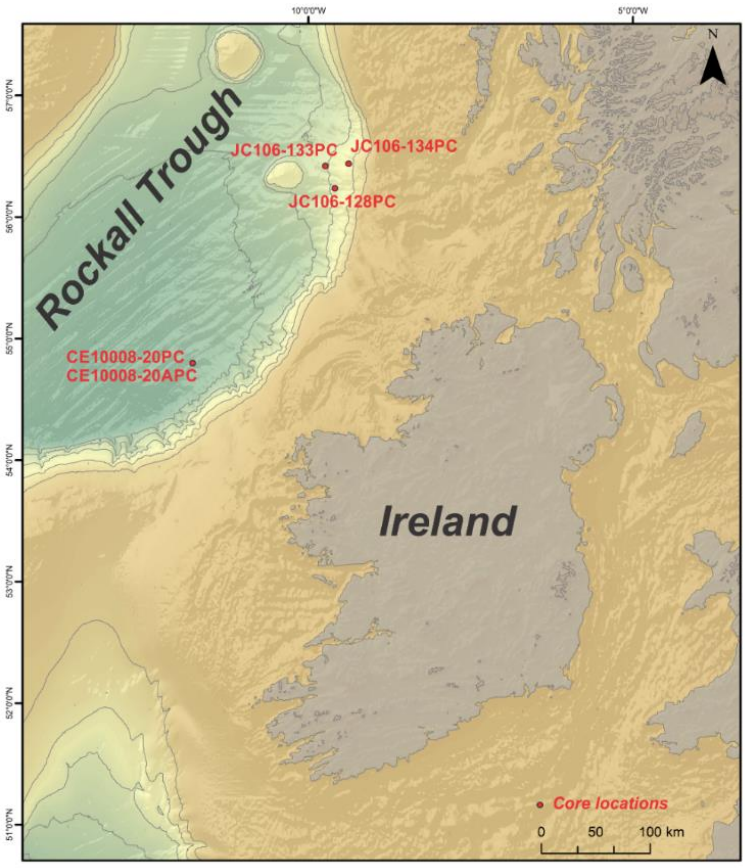

Figure 3.1: Core locations along the east margin of the Rockall Trough. Isobaths are shown with a 500-m interval.

The cores were collected by piston corer in the deep Rockall Trough during the CE10008 cruise on RV *Celtic Explorer* in 2010, and on the DBF during BRITICE-CHRONO cruise JC106 on the RV *James Cook* in 2014 (Fig.3.1) (Table 3.1; Appendix 1, 2).

Table 3.1: Sediment cores information.

Cruise	Core number	Latitude (N)	Longitude (W)	Water depth (m)	Length (cm)
CE10008	20PC	54.8063	-11.9343	2856	393
CE10008	20APC	54.8063	-11.9343	2856	400
JC106	128PC	56.1714	-9.6167	1475	668
JC106	133PC	56.4444	-9.6722	1537	661
JC106	134PC	56.4447	-9.3212	1036	672

Piston corers are typically used for the collection of muds and are deployed from the side of the ship. The piston corer (PC) has a trigger corer or gravity corer (GC) (Fig. 3.2). The GC touches the seafloor first and successively the PC is released. The PC penetrates the sea floor and passes through the soft sediment. The piston action creates a pressure differential at the top of the barrel that guides the movement of the soft material inside the core liner. Generally, piston cores have been observed as likely to record a certain grade of disturbance, this in the form of oversampling of the core top or compaction of the sediment due to the coring technique (Skinner & McCave, 2003).

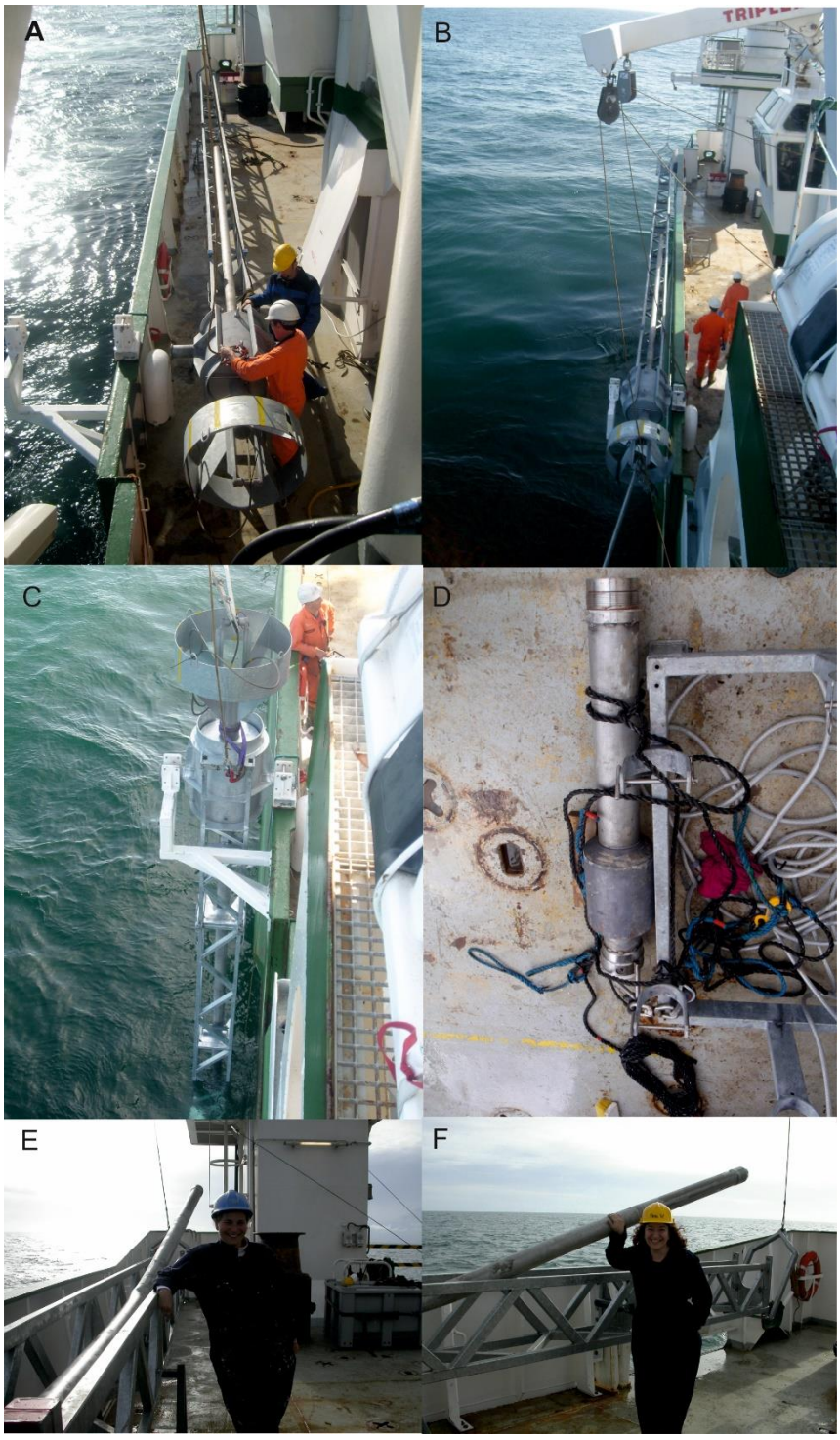

Figure 3.2: Piston coring on the RV Celtic Explorer. A-C: piston corer being prepared and deployed on the launching and recovery system (LARS). D: the trigger weight corer. E-F: coring in the Rockall Trough gone wrong when the corer hit a very thick sand interval during cruise CE10008 resulting in the bending of the core barrel (i.e. a "banana").

Cores were split in 1 m sections and initially described on board, wrapped in cling film and plastic tubing and successively stored at Ulster University Coleraine (UUC) and University College Dublin (UCD) in refrigerated cold rooms at 4-5°C, where the temperature is kept stable, ensuring the best preservation of the sediment record. The two sets of sediment cores (CE10008 and JC106) have been the object of different analytical procedures and, in the next sections, the individual work flow is described (Sect. 3.2). Specific results are presented in Chapter 4 and 5.

In addition to the cores, geophysical data, mostly sub-bottom, were acquired during the cruises and their preliminary interpretations guided the identification of the coring locations whilst on board. Only one seismic line from JC106 is presented in this study together with the sediment record (Chapter 4, Fig. 4.1), with the aim of providing a framework for the investigation of the sedimentary processes on the Donegal-Barra Fan. The data were acquired on board of the RV *James Cook*, with a hull-mounted Kongsberg SBP 120 sub-bottom profiler system, operates with a swept frequency of 2.5 kHz to 6.5 kHz. During data acquisition down the steep slopes, adjustments were made to the acquisition settings to ensure a good trade-off between penetration and resolution. Only one seismic line, providing information about the acoustic stratigraphy of approximately the first 50 meters below sea-floor, was recovered after the cruise and it is presented here in order to add context to the slope sedimentary settings. The data were imported into IHS Kingdom as 2D survey lines for visualisation and processed by the co-authors of the paper, presented in Chapter 4 (Dr Katrien Van Landeghem (Bangor University) and Dr Louise Callard (Durham University)). As part of this study, seismic units were identified and interpreted following the previous studies along the North Atlantic margin.

3.2. Methods

3.2.1. Physical properties and Sedimentology

The physical properties of all the cores were measured with a GEOTEK Ltd., Multi Sensor Core Logger (MSCL). The observation of physical properties was used for the identification of significant changes through the sediment record, such as the identification of boundaries or intervals with distinct values (Weaver & Schultheiss 1990). The analysis was run at the National University of Ireland in Maynooth for the cores collected during cruise CE10008, whilst the JC106 cores were analysed on board by the British Geological Survey (BGS) MSCL. Data include gamma density (g/cm^3), P-wave velocity (m/s), magnetic susceptibility ($SI \cdot 10^{-5}$), electrical resistivity (Ohm·m) and lightness (L) (St Onge et al., 2007). Gamma density represents the attenuation of gamma-rays traveling through the sediment; it is generally used for calculation of porosity and density of the sediments. P-wave velocity, the speed of the pressure waves crossing the sediment core, supplies measurements of sediment density and it is often used together with density measurements in calculation of acoustic impedance (density*acoustic velocity), in order to build seismic profiles and estimate depth on seismic reflectors. Magnetic susceptibility (MS) provides a measure of the extent a sediment can be magnetised by an external magnetic field; it can provide information on the chemistry and density of the sediment and peaks in MS normally represent high sediment density intervals. Electrical resistivity is used for measurements of the strength of sediment to be crossed by electric currents that, in combination with density, provide grain size and sediment permeability. Lightness quantifies sediment colour variability between 0 and 100, used for the identification of high in carbonate or organic matter layers (Balsam et al., 1998; St Onge et al., 2007). The data were acquired at either 1 cm or 2 cm intervals

and the spurious data were removed at top and bottom of each core section, in correspondence of possible empty spaces and the plastic caps, in order to avoid artefacts where the density of the sediment is uneven.

Within this study, magnetic susceptibility, p-wave velocity and lightness have been used preferentially over other physical properties because they seemed to be best representative of the variability in the sediment records. Magnetic susceptibility and lightness in particular guided the identification of lithofacies boundaries within the sediment record, even when not clearly visible to the naked eye. P-wave velocity was specifically used for the conversion from two-way times to mbsf in the JC106 seismic data for the Donegal-Barra fan.

X-radiographs were obtained for all the cores using a CARESTREAM DRX Evolution system at School of Radiology at Ulster University in Jordanstown. The X-radiographs provide a great, non-destructive, method for the investigation of deep sea sediments (cf. Howe, 1995; Principato, 2000; Lucchi et al., 2013). They allowed the identification of sedimentary structures not visible to the naked eye such as laminations, shear surfaces, bioturbation and burrowing, and additional presence of sand- and gravel-size lithic grains.

Grain size was measured through laser granulometry using a MALVERN Mastersizer 3000 (Sperazza et al., 2004), available at UUC and UCD. A total of 163 samples were analysed from the 5 cores. The cores were sampled at varying intervals between 10-20 cm, in order to cover the large majority of the record and sample all observed lithofacies. All the samples required pre-treatment, consisting of overnight soaking in 50 Ml 5% Calgon concentrated solution, to avoid flocculation of the fine particles and shaking on a rotating table.

The parameters selected for the measurements in the Malvern were:

Diffraction Index = 1.52

Absorption = 1.00

Blue light = tick to take the same parameters as above

Dispersion = water

Measurement = 30"

Obscuration = 12 - 20 and click on filter

Pump/Stirrer = 2750 - 3000 rpm

These values have been implemented after being tested in previous grain size analysis at UCD and UUC.

The results of the grain size were represented using two different outputs. In Chapter 4, the data were plotted considering the mean volume weight and presenting grain size variability along the core. In Chapter 5, the results were represented using their grain size spectrum at each sample location. In this second case, results have been calculated and plotted through the Excel worksheet GRADISTAT (Blott, 2001). These two grain size representations were selected to best present the data, in the first case the aim was to represent a trend along the core, while in the second present the single data point and characterise specific lithofacies.

Physical and sedimentological data were used in conjunction with visual core description for the identification of lithofacies, and the interpretation of sedimentary processes active along the North-east Atlantic margin. These were interpreted based on previous studies on sediment deposition along the North Atlantic and other glaciated and glacially-influenced margins (Middleton & Hampton, 1976; Stow, 1979; Lowe, 1979; Stow & Lovell, 1979; Lowe, 1982; Stow & Piper, 1984; Howe, 1995; Wang & Hesse, 1996; Hesse et al., 1997; Holmes et al., 1998; Hesse et al., 1999; Knutz et al., 2001; Ó Cofaigh &

Dowdeswell, 2001; Lucchi et al., 2002; Stow et al., 2002; Stow & Mayall, 2000; Wilson et al., 2002; Tripsanas & Piper, 2008; Rebesco et al., 2014).

3.2.2. Wet-sieving and samples preparation

A total of 227 samples were collected from the cores for planktonic foraminiferal studies and investigation on the Ice Rafted Debris (IRD) content, as well as radiocarbon dating and the analysis of oxygen stable isotopes (Table 3.2)

Table 3.2: Cruise, core number, length and analysis done for each core. In bracket the number of samples used for each analysis.

Cruise	Core	Length (cm)	MSCL	X-ray	Grain size	NPS%	IRD	Planktonic foraminifera assemblage	$\delta^{18}O$	^{14}C
CE10008	20PC	393		X	X (20)	X (20)	X (34)	X (20)		
CE10008	20APC	400	X	X	X (39)	X (31)	X (31)	X (31)	X (87)	X (2)
JC106	128PC	668	X	X	X (30)		X (34)			X (1)
JC106	133PC	661	X	X	X (33)	X (36)	X (36)			X (4)
JC106	134PC	672	X	X	X (34)		X (36)			X (2)

Samples were collected with the help of a spatula from the working half of the sediment cores. Generally, the sample was a one-cm thick slab, covering the full or half width of the core, with the exclusion of the sediment close to the liner (1 cm approximately on each side) to avoid possible contamination or coring disturbance. Samples were collected on a 20-cm interval for the JC106 cores; while, in CE10008 cores the sampling interval was approximately 5-10 cm. For both sets of cores, sampling avoided large signs of bioturbation and turbidites or other mass transport deposits as much as possible. Each sample was wet sieved through a 63 μm sieve, under running water. Once the sample was

clean, it was dried under infra-red lights and stored in appropriately labelled glass containers. The weight of the fraction > 63 μm was measured. Successively, only the fraction coarser than 150 μm was used for ensuing analytical work as discussed in the following sections. Previous works that investigated IRD and foraminifera in the region followed an analogue procedure (Austin & Kroon, 1996; Knutz et al., 2001; Peck et al., 2006; Scourse et al., 2009; Hibbert et al., 2010) and adopting the same work flow should allow an easier comparison of results.

3.2.3. *Neogloboquadrina pachyderma* sinistral abundance

Neogloboquadrina pachyderma sinistral (NPS) was recognized as a marker species for polar front migration and directly correlated with Greenland ice core record from previous studies (Bond et al., 1993; Peck et al., 2006; Scourse et al., 2009) and therefore it was decided to calculate its abundance through the sediment record in both sets of cores. This was done for 87 samples: 36 from JC106 and 51 from CE10008. The species was counted through the >150 μm fraction of the samples that were split into fraction containing a minimum number of planktonic foraminifera tests >300 beforehand. NPS relative abundance is then calculated as percentage of the species through each sample analysed (NPS %).

3.2.4. Ice Rafted Debris (IRD) concentration and fluxes

In the fraction coarser than 150 μm, a minimum of 300 lithic grains (or IRD) per sample were counted, when possible. A total of 171 samples, 65 from CE10008 and 106 from

JC106, were counted using a light microscope. The IRD record was represented as IRD concentration:

[IRD] = (n° lithic grains > 150μm) / (g of dry sediment > 63 μm)

(cf. Peck et al., 2007; Scourse et al., 2009; Haapaniemi et al., 2010).

Additionally, in Chapter 5, the [IRD] was converted to IRD fluxes for the CE10008 cores. The IRD fluxes represent a direct calculation of the IRD input over the linear sedimentation rates.

IRD flux= [IRD] X (LSR X ρDB)

Where: LSR=linear sedimentation rate and ρDB=dry bulk density;

(cf. Peck et al., 2007; Scourse et al., 2009; Haapaniemi et al., 2010; Hibbert et al., 2010).

Linear sedimentation rates (cm/ka) were calculated after the sediment record was time constrained; while the dry bulk density was derived by measured MSCL properties following the IODP protocol number 302.201.2008 (http://publications.iodp.org/proceedings/302/201/201_2.htm).

For the JC106 cores, in Chapter 4 only the [IRD] were presented. The conversion to flux was not calculated following the suggestion from previous works to remove in this way potential bias from the glaciogenic fan sediment record after the identification of several turbiditic intervals (Scourse et al., 2009). In fact, the down-slope deposits could have shown abrupt changes in the calculated sedimentation rates, obliterating the plumitic and hemipelagic setting investigated in the study.

3.2.5. Planktonic foraminifera assemblages and multivariate statistical analysis

The cores collected by the CE10008 Cruise were used for investigating changes in the planktonic foraminifera assemblages through time as the cores were found to cover the longest temporal record. The 51 samples collected from the CE10008 cores were analyzed in the fraction > 150 μm, with the aim of identifying the dominant planktonic foraminiferal species (Kennett & Srinivasan, 1983; Owen, 2010; http://www.foraminifera.eu). The specimens were identified to the species level and counted, at least 300 per sample, and a matrix with the relative abundances was built. The matrix was used for multivariate two-way cluster analysis. The output of two-way cluster analysis was represented by a dendrogram, where the different clusters were grouped to provide a measure of similarity through the samples and the specimens (Jones et al., 1999; Ceregato et al., 2007). Statistical analysis was run using the open source Paleontological Statistics Software PAST (Hammer & Harper, 2005). The index selected for the statistic used similarities correlation on un-weighted arithmetic averages (Correlation Distance Index) (Hammer et al., 2001). The two-way cluster analysis is often used on large datasets for observing similarities in the fossil content (Hendy & Kamp, 2004; Holland & Patzkowsi, 2004). In this study, the two-cluster analysis was applied to a relatively small matrix. This technique was chosen to observe changes within the planktonic foraminiferal assemblages and represent them in relation to their distribution along the cores. Each cluster was interpreted considering the main species representing the assemblages, with the aim of observing different climatic signals along core. An inferred sea surface paleotemperature (SST) was presented for each cluster based on the overall content of the planktonic foraminifera *Neogloboquadrina pachyderma* sinistral. The species has been recently observed shifting coiling from right to left between SST ranging from 11° to 6°

C (Eynaud, 2011), this property is here suggested also as a possible indicator of SST change through the biofacies identified.

3.2.6. Oxygen stable isotopes analysis

Eighty-seven samples from one of the two cores from cruise CE10008 (20APC) were submitted for oxygen stable isotopes analysis. The core was selected after it was recognized to cover the longest time interval (likely up to MIS6) of all cores included in this study and for recording a continuous sediment record with the absence of sedimentary hiatuses and only the occasional presence of thin redeposited layers. The sampling interval was approximately 5 cm and bioturbation and turbiditic beds were avoided as much as possible during samples collection. *Globigerina bulloides* (GB) was observed as the most common species along the North Atlantic during the Late Quaternary (Garvey, 2011; Allin, 2011) and was therefore selected for this analysis. Monospecific picks of GB, represented by 0.3-1 mg of weight per sample, were picked from the > 150 µm fraction when possible. The samples submitted were all represented by similar sized specimens, to avoid different isotopic record due to different development in the individual tests (Lab. Communication). The samples were submitted to Iso-Analytical (http://www.iso-analytical.co.uk/). Samples were weighed into clean Exetainer™ tubes and then flushed with 99.995 % helium. After flushing, phosphoric acid was added to the samples and they were allowed to react overnight to permit complete conversion of carbonate to CO_2. Reference and control materials were prepared the same way. The CO_2 gas liberated from samples was analysed by Continuous Flow-Isotope Ratio Mass Spectrometry (CF-IRMS). Carbon dioxide was sampled from the Exetainer™ tubes into a continuously flowing He stream using a double holed needle. The CO_2 was resolved on

a packed column gas chromatograph and the resultant chromatographic peak carried forward into the ion source of a Europa Scientific 20-20 IRMS where it was ionized and accelerated. Gas species of different mass were separated in a magnetic field then simultaneously measured using a Faraday cup collector array to measure the isotopomers of CO_2 at m/z 44, 45, and 46. The phosphoric acid used for digestion had been prepared for isotopic analysis in accordance with Coplen *et al.* (1983) and was injected through the septum into the vials. The reference material used during analysis of the samples was IA-R022 (Iso-Analytical working standard calcium carbonate, $\delta^{13}C_{V\text{-}PDB}$ = -28.63 ‰ and $\delta^{18}O_{V\text{-}PDB}$ = -22.69 ‰). IA-R022, NBS-18 (carbonatite, $\delta^{13}C_{V\text{-}PDB}$ = -5.01 ‰ and $\delta^{18}O_{V\text{-}PDB}$ = -23.20 ‰) and IA-R066 (chalk, $\delta^{13}C_{V\text{-}PDB}$ = +2.33 ‰ and $\delta^{18}O_{V\text{-}PDB}$ = -1.52 ‰) were run as quality control check samples. Acid preparations of samples and controls were measured directly against acid preparations of laboratory working calcium carbonate standard. This procedure removed the need to apply separate corrections for temperature dependent isotope fractionation. The results obtained for the NBS18 and IA-R066 controls were used to check and correct the data. Results for these were included in the tabulated results. IA-R022 has been calibrated against and is traceable to NBS-18 and NBS-19 (limestone, $\delta^{13}C_{V\text{-}PDB}$ = +1.95 ‰ and $\delta^{18}O_{V\text{-}PDB}$ = -2.2 ‰). IA-R066 has been calibrated against and is traceable to NBS-18 and IAEA-CO-1 (Carrara marble, $\delta^{13}C_{V\text{-}PDB}$ = +2.5 ‰ and $\delta^{18}O_{V\text{-}PDB}$ = -2.4 ‰). NBS-18, NBS-19 and IAEA-CO-1 are inter-laboratory comparison standard materials distributed by the International Atomic Energy Agency (IAEA). The analysis results were represented by a plotted curve, where heavy values of $\delta^{18}O$ were considered typical of cold surface water temperature and light values were characteristic of more temperate surface water temperatures (Emiliani, 1995; Wilson et al., 2002; McManus et al., 2004).

The $\delta^{18}O$ ratio was additionally used for the development of an initial age model, through the previously observed correlation between oxygen isotopic ratio and Greenland ice record from GRIP (Greenland Ice Core Project) (cf. Peck et al., 2006; Johnsen et al., 1997; Hibbert et al., 2010; Rasmussen et al., 2014).

3.2.7. Radiocarbon dating

Radiocarbon dating was used to provide an initial chronological framework for the cores included in this study. The samples submitted for dating were all represented by foraminiferal picks (Table 3.3). All the locations were selected after lithofacies identification and preliminary interpretation of the sedimentary processes. Samplings locations represented contacts between lithofacies, or specific intervals of interest, generally within glaciomarine sediments. Bioturbated and chaotic intervals were carefully avoided. Nine samples were radiocarbon dated through accelerator mass spectrometry (AMS). Five dates were included in the BRITICE-CHRONO (B-C) project. These have been dated at the NERC facilities, at the laboratory at the Scottish Universities Environment Research Centre (SUERC), and analysed using a 5MV tandem spectrometer. Four additional samples were dated at the private laboratory Beta-analytic, with the financial support of Ulster University.

Samples were calibrated using OxCal 4.2 (https://c14.arch.ox.ac.uk/oxcal.html) or Calib 7.1 (http://calib.qub.ac.uk/calib/calib.html), and the MARINE13 curve database (Ramsey, 2009; Talma & Vogel, 1993; Reimer et al., 2013). Three variable ΔR corrections were applied as for the proposed BRITICE-CHRONO protocol (0, 300, 700 (a)) on the samples collected from the JC106 cores. The calibrated ages were then quoted with the three ΔR corrections as the median value of the two σ range, with $\pm$ uncertainty.

These ΔR values have been selected (as 0, 300, 700) after that the main controls for the reservoir ages in deep and shallow waters were identified as related to the air-sea exchange mediated by the sinking of the Atlantic Meridional Overturning Circulation (AMOC) (Austin & Kroon, 2001). It was previously recognised that the AMOC is slowing down, interrupting or being present in shallow waters during glacial periods and the reservoir age can largely vary from the much reduced values (ΔR=0) characteristic of modern vigorous circulation (Austin, 2017). In addition, different water masses are recognised carrying a characteristic reservoir age based on their source and shelf hydrodynamics shows a strong control on shallow water reservoir (Wanamaker et al. 2012). It was measured how during the Younger Dryas (YD), the ΔR indicated a value of + 300 years (Austin et al., 1995). The value suggested how a reduction of the AMOC was the likely forcing cause for the cold YD event. Furthermore, during Heinrich (H) events and full glacial conditions ΔR values were measured reaching > 700 years in the deep North Atlantic (Waelbroeck et al. 2001; Peck et al. 2006), providing very strong evidence of AMOC interruption during H events.

The data in the text for the forthcoming Chapters were presented as calibrated with a ΔR correction=0, in accordance with the Britice-Chrono protocol for the JC106 cores (Austin, 2017); while the delta R correction for CE10008 cores, not included in the consortium, was calculated selecting the Rockall Trough /west Ireland/Scotland region. The values were then rounded to either the nearest decade or multiple of 5.

Table 3.3: Radiocarbon dates information. Cruise and core number, cm down-core, sample material and weight are indicated for all the samples. The conventional radiocarbon ages are expressed, together with the laboratory codes. In addition, the sampled lithofacies are presented (LSM: laminated sand to mud couplet; FM: foraminiferal-bearing mud; ILM: laminated mud rich in IRD; BM: extensively bioturbated mud; SMC: sand to mud couplet. G.B.= Globigerina bulloides; NPS= Neogloboquadrina pachyderma sinistral.

Cruise	Core	Depth (cm)	Sample material	Sample weight (mg)	^{14}C Age (yrs. BP)	Laboratory code	Surrounding lithofacies
CE10008	20APC	8.5	Monospecific NPS	8	19410±90	BETA 440618	LSM
CE10008	20APC	10	Monospecific G.B.	6	5930 ± 30	BETA 450230	FM
JC106	128PC	125-128	Monospecific NPS	10	13705 ± 40	SUERC-67943	ILM
JC106	134PC	60-61	Monospecific G.B.	7.9	13175 ± 40	SUERC-63572	BM
JC106	134PC	588-593	Mixed benthic forams	14	15020 ± 45	SUERC-63573	ILM
JC106	133PC	175-176	Monospecific NPS	6.7	11200 ± 30	BETA 441865	ILM
JC106	133PC	375-376	Mixed benthic forams	8	15270 ± 45	SUERC-67947	LSM
JC106	133PC	433-438	Monospecific NPS	10.8	14355 ± 40	SUERC-67948	ILM
JC106	133PC	583-588	Monospecific NPS	4.8	15050 ± 50	BETA 450231	ILM

Chapter 4: Late Quaternary deglacial history and meltwater events recorded on the southernmost glaciogenic fan of the North-east Atlantic, the Donegal Barra Fan.

Serena Tarlati*[1], S. Benetti[1], S.L. Callard[2], C. Ó Cofaigh[2], P. Dunlop[1], A. Georgiopoulou[3], R. Edwards[4], K. Van Landeghem[5], M. Saher[5], R. Chiverrell[6], D. Fabel[7], S. Moreton[8], C.D. Clark[9]

[1] School of Geography and Environmental Sciences, Ulster University, Coleraine, UK

[2] Department of Geography, Durham University, UK

[3]School of Earth Sciences, University College Dublin, Ireland

[4]School of Natural Sciences, Trinity College Dublin, Ireland

[5]School of Ocean Science, Bangor University, UK

[6]School of Environmental Sciences, University of Liverpool, UK

[7]Scottish Universities Environmental Research Centre, UK

[8]Natural Environment Research Council, Radiocarbon Facility, East Kilbride, UK

[9]Department of Geography, University of Sheffield, UK

*Tarlati-S@ulster.ac.uk

Abstract

During the last glaciation the British Irish Ice Sheet (BIIS) extended across the Malin Sea Shelf, between Ireland and Scotland. At its maximum extent, it was grounded at the shelf break delivering sediment to the Donegal Barra Fan (DBF), the southernmost glaciogenic fan of the Northeast Atlantic continental margin. In this study we analyse the high-resolution sedimentary record from three cores (greater than 6m long) and sub-bottom profiles from the DBF. The sediment record covers the time of final deglaciation of the last BIIS and the ensuing post-glacial period. Sedimentological analyses, X-radiographs and sediment physical properties of the cores allowed the discrimination of five

lithofacies. Bioturbated and foraminifera-rich muds are interpreted as hemipelagic and contourite deposits of the current interglacial period. Chaotic and laminated muds, ice-rafted debris (IRD)-rich layers, laminated sand and mud couplets are characteristic of sedimentation under glacial conditions. These are interpreted as mass transport deposits, plumites and turbidites, and appear to record ice sheet retreat across the shelf. IRD concentrations and *Neogloboquadrina pachyderma* sinistral abundances (NPS%) were calculated and their peaks are interpreted to represent the coldest intervals within the sediment record. At least two such intervals are recorded. Radiocarbon dates constrain these events to the latter part of the last deglaciation, specifically after 18 ka cal. BP. The dated glaciomarine sediments also constrain the timing of the last glacially-derived sedimentation on the slope between 17.8 and 16.8 ka cal. BP. This is interpreted as the last interval of active ice streaming on the Malin Sea shelf with a significant input of meltwater to this area. Following the deglaciation, a specific contourite interval rich in *Zoophycos* is indicative of the transition between stadial and interstadial conditions. The occurrence of this contourite facies also suggests a restoration of the flow of bottom currents, which previous works suggest were weakened during the glacial period. A peak in IRD concentration and NPS abundance, dating to the Younger Dryas (YD), suggests the presence of floating icebergs in the DBF region. Although the provenance of this ice is still unclear, we suggest a mostly European source based on the fact that these IRD grains appear in general composition very similar to those in the previous peaks.

4.1. Introduction

The North Atlantic continental margin can be subdivided into three sedimentary settings (i.e. glaciated, glacially-influenced and non-glaciated margin; cf. Weaver et al., 2000).

The contribution of different processes has produced distinct geomorphologies, including glaciogenic fans, complex canyon systems, areas of mass transport along the continental slope and large contourite drifts (Stoker, 1995; Holmes et al., 1998; Weaver et al., 2000; Piper, 2005; Sejrup et al., 2005; Stoker et al., 2005; Sacchetti et al., 2012a). North of 56°N, along the glaciated margin, glaciogenic fans are the main sedimentary features (Weaver et al., 2000; Sejrup et al., 2005; Stoker et al., 2005); they represent large sediment depocentres built during glacial periods through downslope mass wasting (Howe, 1995; Armishaw et al., 1998; Howe et al., 1998). South of 56°N and north of 26°N, the continental slope was shaped during the same time by downslope sediment transport, mostly in the form of turbidity currents and mass wasting, resulting in an intricate and dendritic system of canyons (Sejrup et al., 2005; Cronin et al., 2005; Ó Cofaigh et al., 2012; Sacchetti et al., 2012a).

Along the western Irish and UK margin, the extension of the British-Irish Ice Sheet (BIIS) on the continental shelf contributed to the development of these features both north and south of 56°N. The Donegal-Barra Fan (DBF), located north-west the island of Ireland (Fig. 4.1), was formed during Pleistocene glaciations and it represents the southernmost of the North Atlantic glaciogenic fans, as well as the largest fan associated with the western BIIS (Stoker, 1995; Clark et al., 2012a).

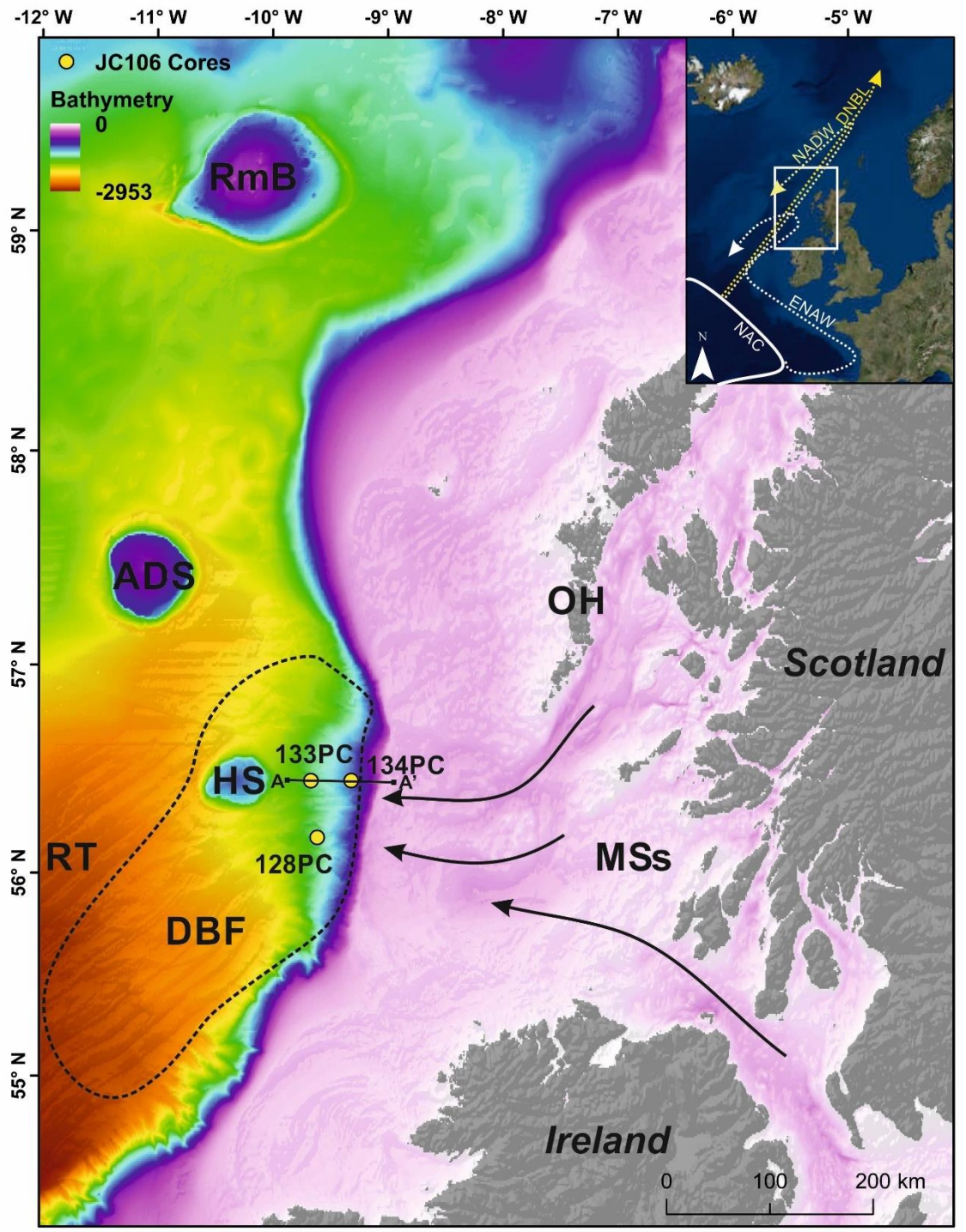

Figure 4.1: North Atlantic glaciated margin with the highlighted approximate extent of the Donegal-Barra fan and JC106 core locations. The direction of the ice-streams active during the last glacial period is indicated by the black arrows. On the top right, the map is positioned along the Atlantic margin and the main oceanic currents and water masses are indicated. The bathymetry data is supplied by the GEBCO, General Bathymetric Chart of the Ocean. A-A': seismic line location. Abbreviations: DBF=Donegal-Barra Fan, MSs= Malin Sea shelf, OH= Outer Hebrides, RT=Rockall Trough, HS=Hebrides Terrace Seamount, ADS=Anton Dohrn Seamount, RmB=Rosemary Bank, NAC=North Atlantic Current, NADW=North Atlantic Deep Water, DNBL= Deep Northern Boundary Current, ENAW=Eastern North Atlantic Water.

Sediments on the DBF were previously studied to better understand the margin's sedimentary evolution and the glacial history of the BIIS (Knutz et al., 2001; Wilson et al., 2002; Scourse et al., 2009). Although the concomitant sedimentation of down-slope and along-slope deposits (Howe, 1995; Stoker, 1995; Armishaw et al., 1998; Holmes et al., 1998; Owens, 2017) makes it a challenging deep-water location for investigation of sedimentary processes, these deep water sediments preserve a likely continuous and well-preserved glacially-derived sedimentary record. This record avoids the erosion and the hiatuses in sedimentation typically recognised in glacial and glaciomarine sediments from shallower waters. Within this study, we investigate a suite of three sediment cores from the DBF, each over 6 m long, to reconstruct the deglaciation of the BIIS through the interpretation of sedimentary processes and relevant proxy records, such as Ice Rafted Debris (IRD) concentration and foraminifera (*Neogloboquadrina pachyderma)* abundances. The aim of this paper is two-fold: 1) to describe and chronologically constrain the deglaciation of the BIIS using deep-water sediments and 2) to reconstruct the oceanographic and climatic conditions in this region from the last glacial to the present interglacial period.

4.2. Regional setting

4.2.1. Study area

The opening of the North Atlantic Ocean started shaping the east continental margin from 80-60 Ma (Stoker et al., 2005). The North West European margin was modified by Paleogene and Neogene tectonic activity, such as large subsidence, with relative deepening and uplifting, and compressive movements resulting in the margin complex aspect. Through the analysis of seismic lines all along the North East Atlantic, two main

unconformity bounded units were identified and classified as Miocene-Early Pliocene and Early Pliocene-Holocene sedimentary successions (Stoker, 1997; Stoker et al., 2005). In the Lower Neogene, deep water sedimentation was mostly influenced by bottom current activity along the margin. In the Upper Neogene unit, large erosion and subsequent progradation of the margin were recorded before the onset of the northern hemisphere glaciations (Stoker et al., 1994; Stoker et al., 2005). From the Plio-Pleistocene, the sedimentation along the margin is observed as driven by northern hemisphere extended glaciations (Howe, 1995; Stoker, 1995; Davidson & Stoker, 2002; Stoker et al., 2005; Sejrup et al., 2005; O' Reilly et al., 2007).

The DBF lies between 57° and 55° N along the North East Atlantic margin and started to form during the Pleistocene (Stoker, 1995; Armishaw et al.,1998). The fan has often been described as the largest sedimentary body resulting from the drainage of the western BIIS, occupying an area of 6300 km^2, with a maximum thickness between 400 and 700 m (Armishaw et al., 1998). It extends from the shelf edge, 200 m water depth, to about 2000 m, to the north and south of the Hebrides Seamount and along the eastern flank of the Rockall Trough, a deep elongate basin orientated NE-SW parallel to the continental margin (Fig. 4.1; Ó Cofaigh et al., 2012; Sacchetti et al., 2012b). Many sediment lobes, extending up to 250 km in length, have been identified in recent studies and interpreted as the result of episodes of large-scale downslope mass wasting related to ice streaming across the Malin Sea shelf during glacial intervals (Stoker, 1995; Knutz et al., 2002; Dunlop et al., 2010; Sacchetti et al., 2012a).

4.2.2. The British-Irish Ice Sheet and the sedimentary processes on the continental margin

The BIIS was a largely marine-influenced and highly dynamic ice sheet that covered most of Ireland and Britain during its maximum extent (Scourse et al., 2009; Chiverrell & Thomas, 2010; Clark et al., 2012a; Peters et al., 2015). Several phases of advances and retreats on the continental shelf during the last glacial period have been inferred on the basis of geomorphological and sedimentological evidence (Chiverrell & Thomas, 2010; Clark et al., 2012a; Ó Cofaigh et al., 2012; Peters et al., 2015). On the Malin Sea shelf, numerous glacial landforms (i.e. moraines, drumlins, iceberg scours and streamlines) have been mapped and interpreted as related to the dynamism of the last BIIS (Dunlop et al., 2010; Howe et al., 2012; Ó Cofaigh et al., 2012; Dove et al., 2015). These features suggest the presence of ice-streams flowing offshore from multiples directions, from north-west Ireland and western Scotland before converging on the continental shelf. These processes fed glaciogenic sediment to the shelf edge and by downslope transport to the DBF, during periods of the ice sheet maximum extent across the shelf (Knutz et al., 2001; Wilson et al., 2002; Bradwell et al., 2008; Dunlop at el., 2010; Dove et al. 2015; Ballantyne & Ó Cofaigh, 2017; Small et al., 2017).

During the last glacial period, the BIIS is inferred to have reached its maximum extent on the outer Malin Sea shelf at 27 ka (Ballantyne & Ó Cofaigh, 2017), followed by several phases of retreat and re-advance on the continental shelf at millennial scale that were identified in deep-water sediment records (Knutz et al., 2002; Wilson et al., 2002; Sejrup et al., 2005; Scourse et al., 2009). BIIS re-advances after the last glacial maximum were dated at 18.4 ka (Clogher Head re-advance; CHR), and at 17.3-16.6 ka (Killard Point re-advance; KPR) (McCabe &Clark, 1998; Ballantyne & Ó Cofaigh, 2017). These minor advances seem to correspond with the Dansgaard–Oeschger (D-O) multimillenial

climatic cycles recorded in the Greenland ice cores and in the North Atlantic deep-water sediments (Bond et al., 1993; Bond & Lotti, 1995; Bond et al., 1999; Wilson et al., 2002; Peck et al., 2007; Scourse et al., 2009).

4.2.3. Oceanography

During Quaternary glaciations, large amounts of freshwater released from melting ice sheets was recognised as having a fundamental role on the deceleration or interruption of the Atlantic currents (Stanford et al., 2011; Bigg et al., 2012; Toucanne et al., 2015). The North Atlantic sediments recorded these oceanographic changes, as well as the restoration of typical interglacial oceanographic conditions, following deglaciations (Rahmstorf, 2002; McManus et al., 2004). The eastern north Atlantic registers the presence of several complex water masses with different salinities and temperatures. These water masses tend to stratify within the water column and be moved by currents with different speeds (Pollard et al., 1996; Holliday et al., 2000; New & Smythe-Wright, 2001). The main surface current in the North Atlantic is the North Atlantic Current (NAC). NAC flows eastwards from the Gulf of Mexico across the Atlantic Ocean, then in an anticlockwise direction northward along the European coastline, before turning south as part of the sub-polar gyre. The Eastern North Atlantic Water (ENAW) originates from the NAC in the Bay of Biscay and is observed towards the north at ca. 1000-1500 m water depth on the eastern side of the Rockall Trough (Fig. 4.1 inset). It turns anticlockwise along the Hebrides Terrace Seamount and then moves south along the western margin of the trough (Holliday et al., 2000; Read, 2000). It is advected northward by the Shelf Edge Current (SEC) with an average speed of 15-30 cm/s (New & Smythe-Wright, 2001). The North Atlantic Deep Water (NADW) originates from the mixing of the NAC with the saline

flows from the southern Rockall Trough when they meet in the eastern North Atlantic (New & Smythe-Wright, 2001). It is observed deep along the Irish and UK slope, directing northward into the Norwegian Sea and the Norwegian basin (Fig. 4.1 inset). Driven by the NADW, the Deep Northern Boundary Current (DNBC) flows deep along the lower continental slope between 2-3 km (McCartney, 1992; Dickson & Kidd, 1987). All of these currents are thought to be responsible for both the winnowing of sediments and the deposition of contourites on the continental margin in this region (Faugeres et al., 1981; Howe, 1996; Howe et al., 1998; Stoker, 1997; Knutz et al., 2002; Masson et al., 2010; Georgiopoulou et al., 2012).

4.3. Material and methods

The sediment cores analysed in this study were collected as part of the BRITICE-CHRONO project in 2014 by piston coring during cruise JC106 on the *RRS James Cook* (Table 4.1; Fig. 4.1) (http://www.britice-chrono.group.shef.ac.uk/). The cores were retrieved from the slope between 1036 m and 1537 m water depth, with a recovery between 661 cm to 672 cm (Fig. 4.1; Table 4.1; Appendix 1). Core sites targeted the DBF (Fig. 4.1) and individual sites were picked using acoustic data collected with a hull-mounted Kongsberg SBP120 sub-bottom profiler. This chirp system operates with a swept frequency of 2.5 kHz to 6.5 kHz. During data acquisition down the steep slopes of the shelf edge, adjustments were needed to be made to the acquisition settings to ensure a good trade-off between penetration and resolution. The data were imported into IHS Kingdom as 2D survey lines for visualisation and processing. Only one seismic line, acquired running over the two piston core positions, is presented here and it was used for the identification of seismic units along the slope.

Table 4.1: Sediment core information.

Core	Latitude (°N)	Longitude (°W)	Water depth (m)	Core Length (cm)
JC106-128 PC	56.17147306	-9.616743611	1475	668
JC106-133PC	56.44449822	-9.672212722	1537	661
JC106-134PC	56.44471	-9.321229	1036	672

Cores were analysed with a Geotek Multi Sensor Core Logger (MSCL) at 2 cm intervals for physical properties, then split, photographed and described (Appendix 1). In this study, we focus on the magnetic susceptibility (MS) which best represents the variability of the lithofacies and their boundaries. MS data were cleaned by removing the spurious values at top and bottom of each core section; the 10 cm at the beginning and end of section were removed to avoid artefacts due to empty spaces and the plastic end caps. Core X-radiographs were collected at the School of Radiology at Ulster University, using a CARESTREAM DRX-Evolution System. X-radiographs were used to identify sedimentary structures not visible to the naked eye, including layers rich in ice-rafted debris (IRD), fine-scale laminations and shear surfaces (cf. Howe, 1995). Radiographs and MS data were used to aid facies interpretation and identification of boundaries between the different lithofacies. Grain size analyses were carried out using a 3000 MALVERN Mastersizer (Sperazza et al., 2004). Samples were collected ca. every 20 cm along the core, soaked in a 50 ml 5% Calgon concentrated solution, then placed on a shaking table overnight to guarantee the absence of flocculated particles. The results are reported in mean volume weight values (D(4;3)) (cf. Mingard et al., 2009; Rawle, 2011). The integration of these different techniques allowed the identification of lithofacies and the interpretation of the respective sedimentary processes.

Additionally, 1 cm thick slabs from one half of the core were collected, wet-sieved at 63 µm and dried under infrared lamps. These coarse fractions of each sample were then used for foraminifera identification and ice-rafted debris (IRD) counts. These took place on the > 150 µm fraction under a binocular microscope. The counting included at least 300 specimens for the foraminifera and 300 lithic grains, when recognised, for the IRD. IRD counts were carried on a total of 106 samples across the 3 cores. IRD concentration [IRD] was calculated as the number of lithic grains recognised in the fraction coarser than 150 µm on the total dry sediment weight (Haapaniemi et al., 2010; Peck et al., 2007; Scourse et al., 2009). Micropalaeontological analysis on planktonic foraminifera, in particular the calculation of the abundance for the polar species *Neogloboquadrina pachyderma* sinistral (NPS), was conducted with the aim of identifying colder stadials. Increases in the relative abundance of this cold species indicate southward migration of the polar front and associated sea ice (Bond et al., 1993; Peck et al., 2007; Haapaniemi et al., 2010). Foraminifera counts were conducted on 36 samples already collected for IRD counts and only in core JC106-133PC. The core was selected for the NPS analysis as it shows the most diverse sediment record of the three and is the furthest away from the former ice margin. Therefore, it potentially represents a more open-water environment, thus this location would likely be affected by regional climatic and oceanographic changes in addition to local and BIIS related proglacial processes.

Samples of hand-picked monospecific planktonic foraminifera, or mixed benthic foraminifera, were collected for radiocarbon dating from sediment slabs between 1 and 5 cm thick from one half of the core. A total of seven AMS (Accelerator Mass Spectrometer) radiocarbon dates were acquired for this study (Table 4.2; Appendix 1). Samples typically targeted lithofacies boundaries or distinct peaks in the IRD content and were dated at the UK Natural Environment Research Council (NERC) Radiocarbon

Facility (NRCF-East Kilbride) and the private analytical laboratory Beta Analytic. They were then calibrated using OxCal 4.2 (Ramsey, 2009) with the Marine13.14c calibration curve (Reimer et al., 2013) which has an inbuilt 400-year marine reservoir correction. The radiocarbon and calibrated dates used three separate age simulations, with ΔR values of 0, 300 and 700 years (BRITICE-CHRONO protocol). These were used to account for uncertainty over the spatial and temporal variation in the marine reservoir effect ages in the North Atlantic and adjoining continental shelves, since the LGM (e.g. Wanamaker et al., 2012; Table 4.2). For clarity, all calibrated ages are presented; however, only the calibrated ages with a ΔR of 0 years are used to describe the timing of events in the text. This BRITICE-CHRONO protocol for reporting radiocarbon ages allows results to be easily comparable. All the samples, except for 133PC 375-376 cm, were used during the study. The aforementioned sample was eliminated from the age reconstruction because, after further core analysis and unexpected dating result, it was found to be collected in a disturbed interval. The radiocarbon dates were successively used for measurements of sedimentation rates (interpreted mass transport deposits and turbidites were excluded from the calculations).

4.4. Results

4.4.1. Acoustic data

4.4.1.1. Description

The sub-bottom profiler data provides a context for core analysis. The survey lines ran perpendicularly to the margin, from the shelf edge to the base of the continental slope. Several seismic units are delineated and described along three sections showing a different internal organisation depending on the location on the slope, hereby described

as lower, middle and upper slope. These are beyond 1200 m water depth; between 900 and 1200 m water depth and above 900 m water depth, respectively (Fig. 4.2).

In the lower section of the slope (1400-1600 m water depth in Fig. 4.2a), there are no reflectors visible in the deepest seismic unit in the profile (Unit 1a). Its upper boundary (green in Fig. 4.2a) is a low amplitude, wavy reflector, identified continuously along the lower slope. The overlying seismic unit 2a is between 25 and 20 m thick, characterised by sub-parallel, undisturbed reflectors and is recognised along the entire lower slope (Fig. 4.2). Its upper boundary is a high amplitude reflector, also wavy (as the lower boundary) and continuous on the lower slope (bright purple in Fig. 4.2a). Above seismic unit 2a, the uppermost seismic unit 3a shows a thickness of approximately 3 m and is acoustically represented by low amplitude sub-parallel reflectors. Its upper boundary is the seabed, which is characterised by a high amplitude, undulated and continuous reflector (dark blue in Fig. 4.2a). JC106-133PC was recovered from the lower slope and sampled seismic unit 3a and the top part of seismic unit 2a.

Along the middle slope, between 900 - 1200 m water depth (Fig. 4.2), reflectors are not visible in the lowest seismic unit 1b. Above it, seismic unit 2b displays a thickness between 45 and 30 m with undulating, wavy reflectors of variable amplitude with asymmetrical aspect and up-slope progradation (Fig. 4.2b). The bounding surfaces are both wavy continuous reflectors; the lower boundary is represented by a low amplitude reflector (light green in Fig. 4.2b) and the upper boundary by a high amplitude reflector (pink reflector in Fig. 4.2b). The overlying seismic unit 3b ranges between 5 and 10 m of thickness and is internally characterised by low amplitude sub-parallel reflectors. Its upper boundary is a discontinuous, high amplitude reflector (yellow in Fig. 4.2b). The uppermost seismic unit 4b is bounded by the yellow reflector and the seabed (dark blue reflector in Fig. 4.2b). It has a thickness generally less than 3 m and is represented by

acoustically low amplitude reflectors. On the seabed, a ~6 m high escarpment is recognised at 1095 m water depth. Core JC106-134PC was collected from this part of the slope (Fig. 4.2b) and it sampled seismic unit 4b and 3b.

The upper slope, above 900 m deep (Fig. 4.2), shows a lowermost seismic unit 1c that is deeper than 30 meters below sea floor (mbsf), with low amplitude, wavy, sub-parallel reflectors. The upper boundary of this unit is represented by a continuous low amplitude reflector (dark purple in Fig. 4.2c), but no basal boundary is visible and is likely due to lack of return for the seismic signal. The overlaying seismic unit 2c, with a varying thickness between 10 and 30 m, is bounded by low amplitude reflectors (dark purple and light blue in Fig. 4.2c) and it shows an acoustically semi-transparent and chaotic character. Seismic unit 3c, ranging between 5 and 10 m, displays low amplitude sub-parallel reflectors. Its lower boundary is the light blue low amplitude continuous reflector, while the upper boundary is represented by a low amplitude, undulated and discontinuous reflector (light yellow in Fig. 4.2c). Above the light yellow reflector, seismic unit 4c is represented by a thin, acoustically transparent and discontinuous unit, less than 3 m thick. Its upper boundary is the high amplitude reflector of the seabed (Fig. 4.2c). Two escarpments (between 5 and 15 m high) are visible in the uppermost seismic unit and at the seafloor, accounting for some of the discontinuity in the unit. No sediment cores were retrieved from this part of the slope.

A direct correlation along slope between the seismic units, described into the singular slope sections, is not possible due to slope length and steep angle. Although, similar trends can be recognised. Below ~35 mbsf no acoustic signal is recognised, between 30 and 10 mbsf the seismic units 2 (a, b, c), 3b and 3c show their maximum thickness with largely high reflectance, wavy and/or subparallel internal reflectors. Above these, seismic units

3a, 4b, and 4c are thinner (3 m or less) and display general low amplitude or transparency. Escarpments are predominantly found within these units.

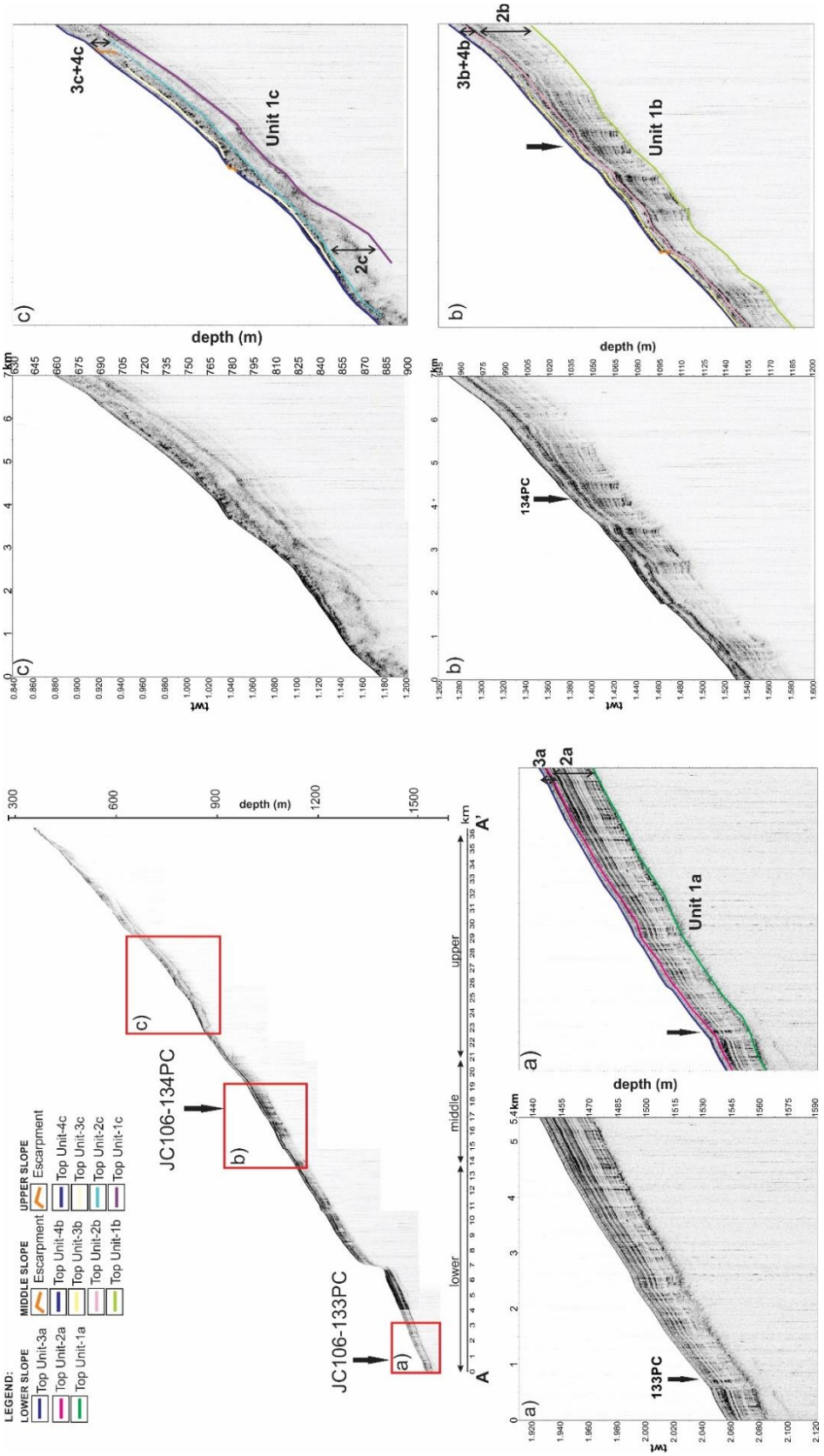

Figure 4.2: Seismic profile of the slope with the coring location for 134PC and 133PC indicated. The boundaries between seismic units are identified and indicated by coloured lines.

4.4.1.2. Interpretation

The seismic line across the DBF shows a 2° steep (on average) slope interrupted by several escarpments (Fig. 4.2). The lowermost seismic units (units 1a, 1b and 1c) are interpreted as Plio-Pleistocene glaciogenic mass transport deposits. This corresponds withprevious research analysing seismic and sedimentological/borehole records from the North Atlantic margin, which identified the Upper MacLeod sequence, a stack (up to 60 m thick) of reworked glaciomarine sediments (Stoker et al., 1994; Stoker, 1995). The character of the seismic units here corresponds with the acoustically transparent character of the lower acoustic unit of the Upper MacLeod Sequence, which is interpreted as debris flow deposits (Stoker et al., 1993).

Units 2a, 2b, and 2c, together with 3b and 3c, are interpreted as consisting of Late Pleistocene glaciomarine sediments and are also part of the Upper MacLeod sequence. In the lower and middle slope, (Fig. 4.2a and 4.2b), these units show continuous and subparallel reflectors. Additionally, in the middle slope, unit 2b displays upslope-climbing sediment waves (Fig. 4.2b). This conformation is typical of wave migration during intervals of large sedimentary input and high sedimentation rates, which could be related to both downslope and alongslope sediment transport (Wynn & Stow, 2002).

The upper acoustic unit of the Upper MacLeod sequence is also characterised by continuous, wavy and subparallel reflectors and it was interpreted as distal glaciomarine sediments redistributed by different mass flow processes, as mass wasting and turbidites along the Hebrides slope and the Barra Fan (Stoker et al., 1994; Stoker, 1995; Armishaw et al. 1998; Knutz et al., 2002). The character of the upper slope (unit 2c; Fig. 4.2c) is slightly different (i.e. chaotic and semi-transparent). A similar acoustic unit, interpreted as debrites, is found on the Donegal Barra Fan in correspondence of the Peach Slide

(Owen et al., 2018). The occurrence of the buried escarpments specifically within this unit seems also to suggest that the upper slope was likely affected by down-slope mass movements and slumps.

The uppermost seismic units along the entire slope (3a, 4b and 4c) are interpreted as recording Holocene hemipelagic and contouritic deposition as elsewhere on the fan, where similar acoustic facies and sediments are again identified and dated (Armishaw et al., 1998; Knutz et al., 2002; Owen et al., 2018). Their reduced thickness compared to the underlying units (3-10m vs. 30-40m) suggests a reduced sediment input compared to the previous conditions during the Late Pleistocene.

4.4.2. Chrono- and lithostratigraphy

4.4.2.1. Lithofacies description

Lithofacies are defined based on lithology, sediment colour, internal sedimentary structures observed in the X-radiographs, mean grain size (volume weight mean D (4;3)) and magnetic susceptibility. Five lithofacies are recognised and presented (Fig. 4.3).

Foraminifera-bearing mud (FM)

A light brown, sandy foraminiferal mud was recognised only at the top of core JC106-128PC. This facies shows bioturbation, clearly visible in the X-radiographs (Fig. 4.3). The mean volume grain size is 30-40 µm, with the foraminifera representing the coarser fraction. It has a thickness of approximately 5 cm and there is a gradual contact with the darker underlying lithofacies. The acquisition of physical properties was not possible in this facies because of its limited thickness and position at the core top.

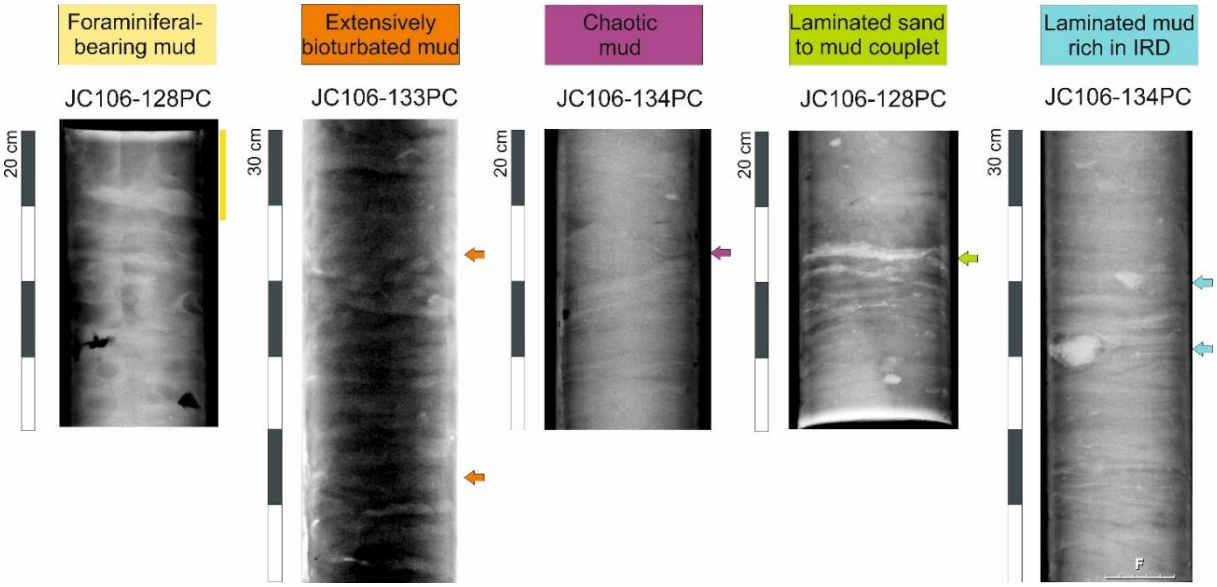

Figure 4.3: Five lithofacies identified, illustrated with x-radiographs. Foraminiferal-bearing mud: Lithofacies is identified by the yellow lateral bar; Extensively bioturbated mud: Zoophycos borrows are highlighted in orange. The x-radiograph image is presented with inverted colour to better display the ichnofacies; Chaotic mud: Inclined shear surface in purple; Laminated sand to mud couplet: Ripple highlighted in green; Laminated mud rich in IRD: Lamination and IRD, larger lithics indicated by blue arrows.

Extensively bioturbated mud (BM)

This lithofacies is a brown sandy mud, well sorted, rich in foraminifera and extensively bioturbated (Fig. 4.3), showing an abundant presence of *Zoophycos* burrows. *Zoophycos* is an ichnofacies, characterised by long tubular structures parallel and sub-horizontal within the sediment, with a thickness not less than 1 cm (cf. Löwemark et al., 2006). It is characteristic of a low energy environment and it is used as a palaeoceanographic tool in studies on climatic cyclicity for deep-water environments (Howe et al., 1998; Dorador et al., 2016). The ichnofacies appears to be dominant and showing a well-developed burrowing in deep-water ecosystems within the transition between cold and warm climatic stages, during glacial terminations (Dorador et al., 2016). Generally, in the JC106 cores, the ichnofacies distribution changed through the record, from high frequency at the facies base then reducing moving upwards. The BM facies is found in

all of the three piston-cores collected from the DBF, at the core top of JC106-133PC and JC106-134PC, following the foraminifera-bearing mud lithofacies in core JC106-128PC (Figs., 4.4, 4.5 and 4.6).

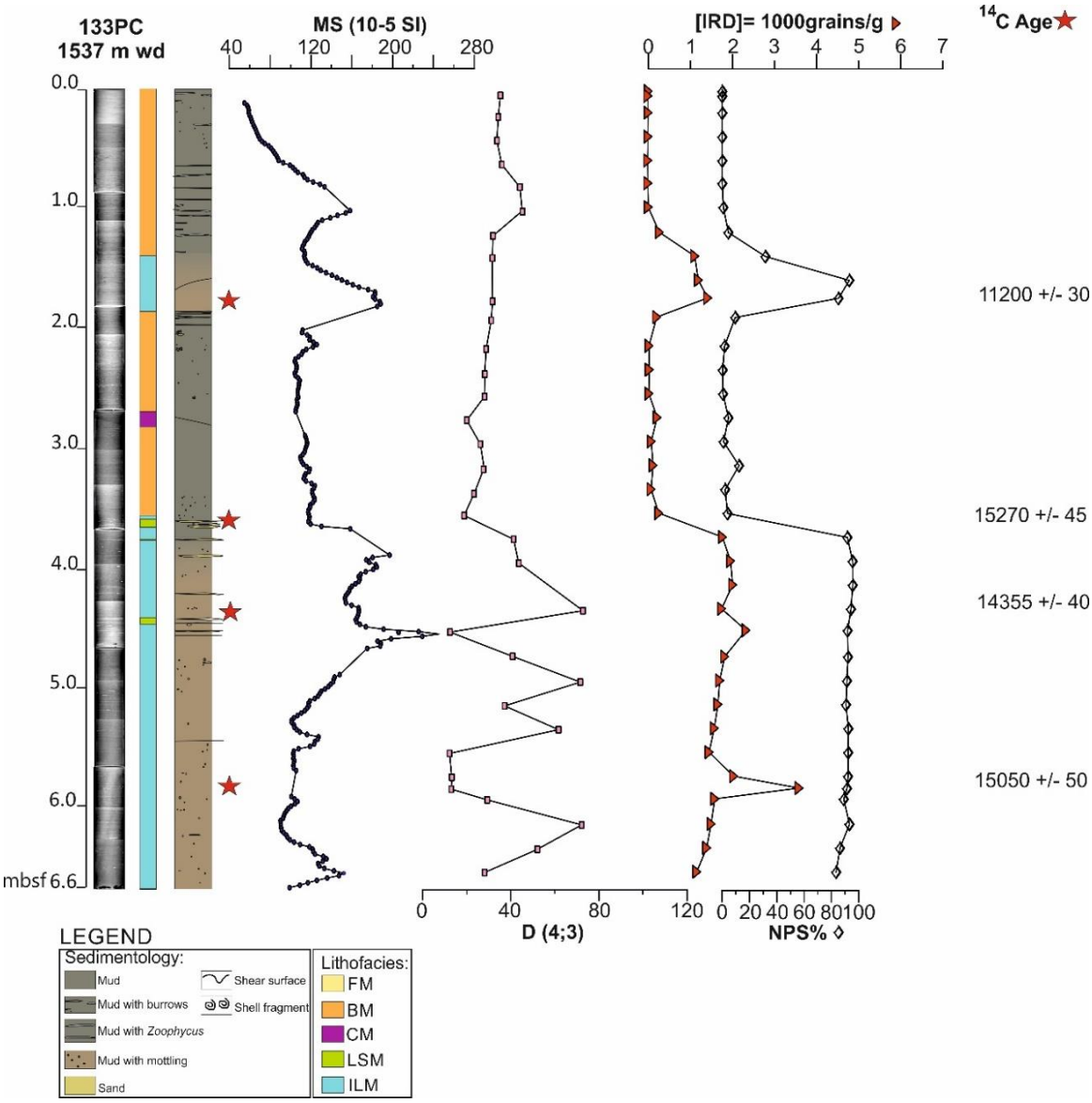

Figure.4.4: Core JC106-133PC: X-radiographs, lithofacies identification and corelog. Magnetic susceptibility (MS), mean volume grain size (µm), IRD concentration [IRD] and abundance of Neogloboquadrina pachyderma sinistral (%NPS) and conventional radiocarbon ages are reported. MS data from Figs. 4 to 6, present a wider spacing, approximately every meter, in correspondence of the end of the core sections. Lithofacies: FM=Foraminiferal-bearing mud, BM=Extensively bioturbated mud, CM=Chaotic mud, LSM=Laminated sand to mud couplet, ILM=Laminated mud rich in IRD.

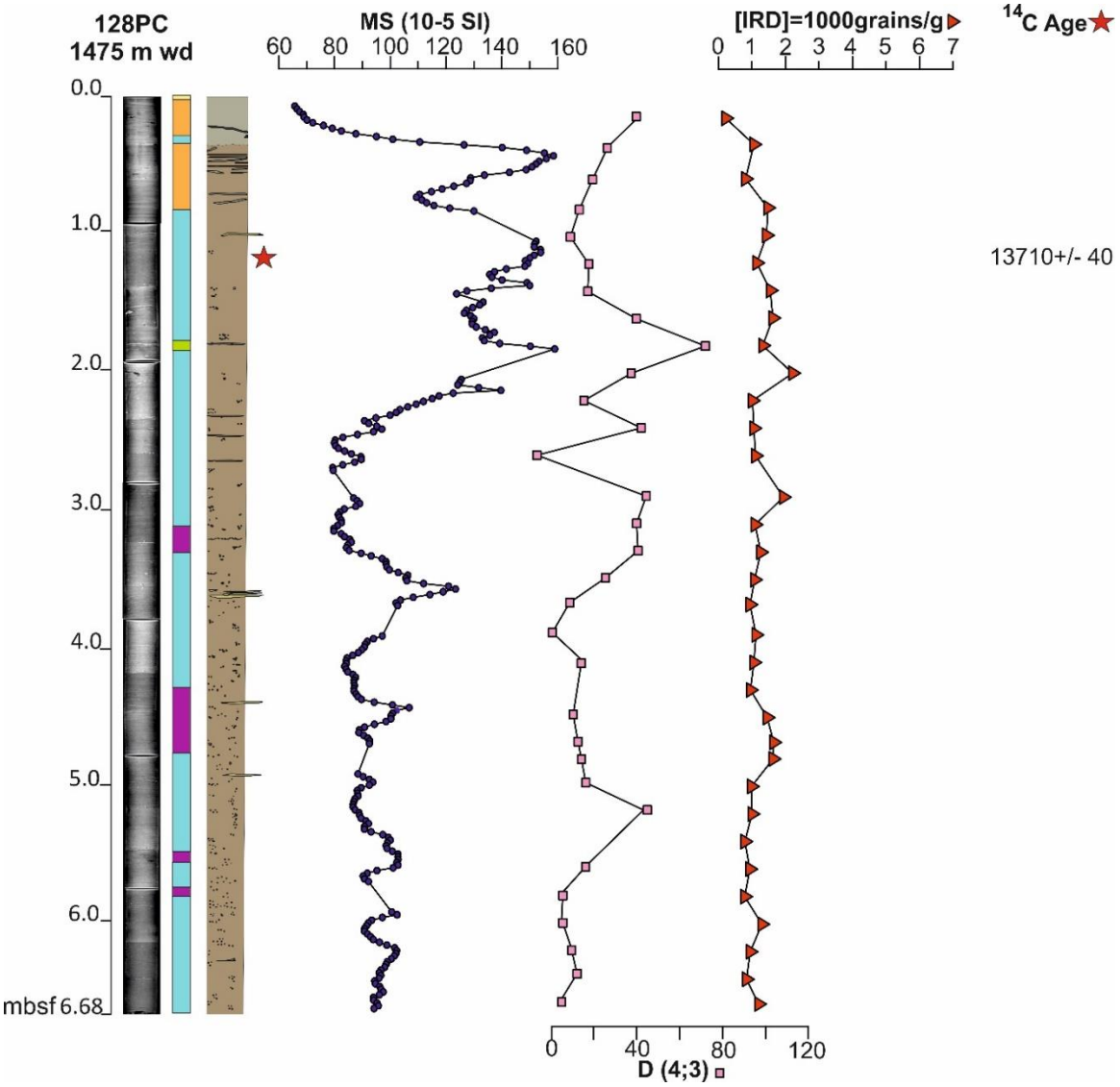

Figure 4.5: Core JC106-128PC: X-radiographs, lithofacies identification and corelog. Magnetic susceptibility (MS), mean volume grain size (D), IRD concentration [IRD] and conventional radiocarbon age are reported.

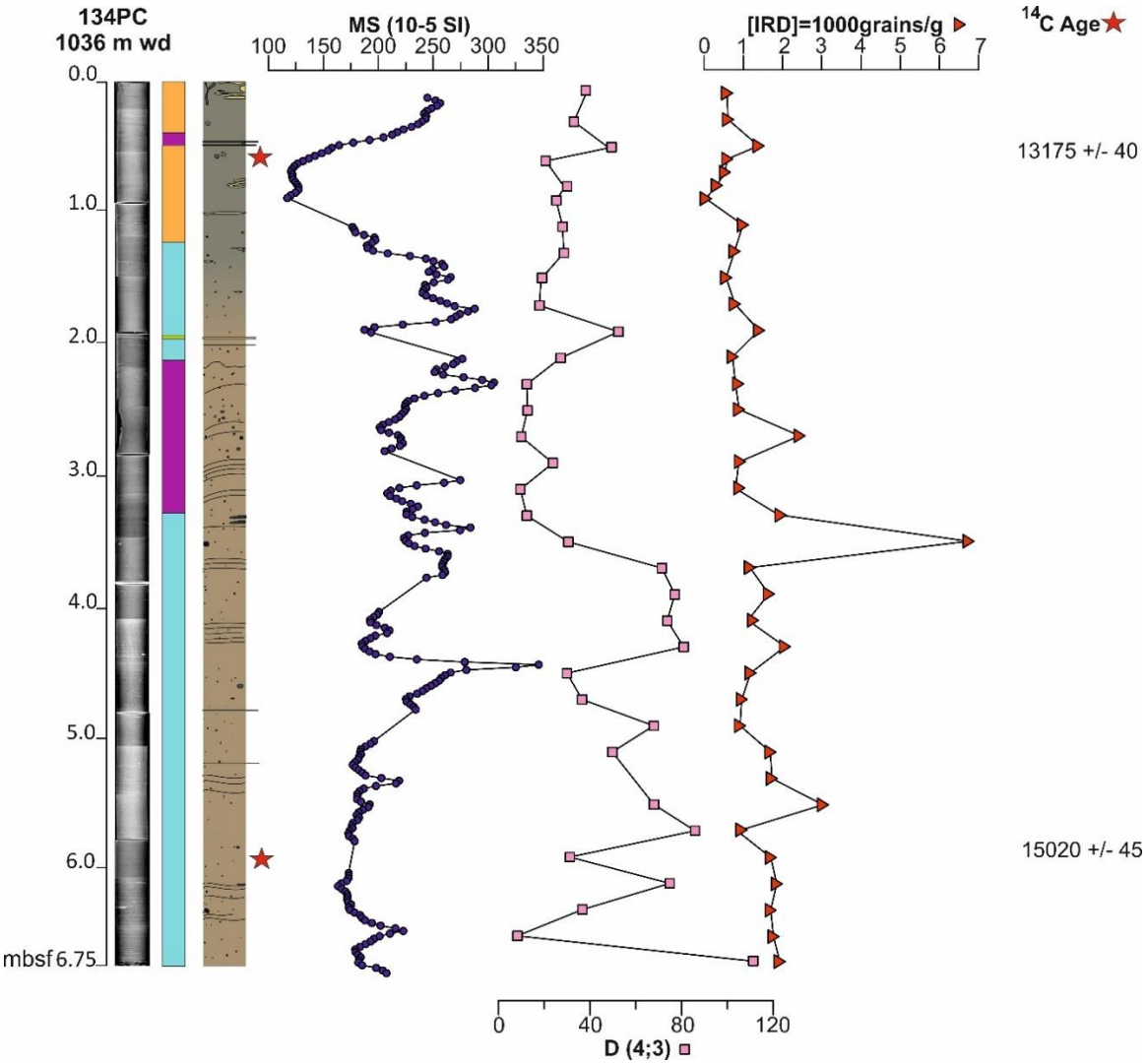

Figure 4.6: Core JC106-134PC: X-radiographs, lithofacies identification and corelog. Magnetic susceptibility (MS), mean grain size values (D), IRD concentration [IRD] and conventional radiocarbon ages are indicated.

BM is up to 2 m thick and generally darker than the sedimentary unit above (FM). Within this lithofacies both fining and coarsening upward trends in grain size are observed, with both sharp and gradual basal and upper contacts. The grain size characteristic of this facies is calculated between 20 and 30 µm in volume weight D(4;3) and have a high content of foraminifera. The MS varies between 40-120 (10^{-5} SI) (Figs. 4.4, 4.5 and 4.6). No primary sedimentary structures are visible.

Chaotic mud (CM)

This lithofacies is an olive-brown, chaotic mud, poorly sorted, devoid of foraminifera, with well-defined shear surfaces and occasional mud clasts. No primary sedimentary structures are present, but seldom wispy and dipping lamination due to possible faulting (Fig.4.3). It is present in all the cores and shows a thickness varying from 20 cm to ca. 50 cm (Figs. 4.4, 4.5 and 4.6). The grain size is measured as < 20 µm in volume weight D(4;3).

Laminated sand to mud couplet (LSM)

Olive-brown laminated sand to mud couplets, with well-sorted laminated basal sand and sharp basal contacts are observed in all cores. This lithofacies has a fining upward trend; the coarser sand base is generally well-sorted, then the sorting decreases moving upwards within the unit. Ripples are recognised within the sandy interval, bioturbation is absent and foraminifera are scarce (Fig. 4.3). Generally, the couplets are thin, between 5 cm to 10 cm. The mean grain size in volume weight is calculated between 40 µm and 100 µm and the facies is marked by high peaks in magnetic susceptibility, with values between 160 and 270 (10^{-5} SI) (Figs. 4.4, 4.5 and 4.6).

Laminated mud rich in IRD (ILM)

The lithofacies is described as an olive-brown laminated mud rich in ice-rafted debris (IRD). The diameter of the lithic grains, observed on the split sediment core and by the x-radiographs, ranges from a few mm to 5-6 cm and is not equally distributed within the facies. Laminations are not always visible to the naked eye but clearly evident on the X-radiographs (Fig. 4.3). Bioturbation is lacking and foraminiferal content is low. The mean volume grain size is extremely variable due to the IRD content, fluctuating from 10 to

100 µm. The MS ranges between 80 and 150 (10^{-5} SI). This laminated IRD-rich mud is found in all three piston cores, constitutes the majority of the sediment record and has a thickness of up to 3.5 m (Figs. 4.4, 4.5 and 4.6).

4.4.2.2. Lithostratigraphy

Core JC106-133PC, the deepest and most westerly located core (Figs. 4.1 and 4.4) contains extensively bioturbated mud (BM) from the core top down to 135 cm core depth. BM changes gradually over 5 cm into the laminated, IRD-rich mud facies (ILM), which is ca. 50 cm thick. Below ILM, BM is recognized again between 185 cm and 370 cm down core. Within BM, a chaotic mud (CM) interval was recognised at 275 cm, with a 7 cm thickness. Below 370 cm, there is a gradual contact over 10 cm from the bioturbated mud into laminated and IRD-rich mud, which extends to the bottom of the core. Three intervals of laminated sand to mud couplets (LSM), with thicknesses varying between a few cm to 7-8 cm, were identified around 380 cm, 390 cm and 444 cm down-core.

Foraminifera-bearing mud (FM) is found exclusively at the core top of JC106-128PC (Figs. 4.1 and 4.5). FM gradually transitions into BM over a few cm. BM then extends down to 95 cm core depth, but is interrupted by a 5 cm thick laminated mud at 30-35 cm with sharp basal and gradual top contact with the BM. Below 95 cm down-core, IRD-rich laminated muds (ILM) are the dominant lithofacies. Four chaotic mud (CM) deposits, bounded by inclined and sharp planes, are identified through the ILM interval at 310 cm, 449 cm, 547 cm and 590 cm down-core, with thickness ranging between 5 and 25 cm. A LSM interval at 182 cm down-core displays a sharp basal contact and a thickness of 8 cm, it is well visible in the MS record with a peak reaching 160 (10^{-5} SI).

In the more proximal to the shelf edge location, in core JC106-134PC (Figs. 4.1 and 4.6), the BM facies extends from the core top to 120 cm down-core. A CM deposit, <10 cm

interval, was recognised at 50 cm. This unit is wedge shaped and marked by two inclined (up to 45°) sharp surfaces, bounded with fine silt (Fig. 4.3). From 120 cm down-core, with a gradual top contact, the ILM represents the main lithofacies recorded in 134PC. A 1m-thick chaotic mud deposit was recognised between 210 cm and 310 cm, with an inclined sharp surface at the top and faint and inclined lamination following it within the muddy layers. A laminated sand to mud couplet (LSM) is observed at 195 cm, it is indicated by an increase in the mean volume grain size and a peak in MS of 200 (10^{-5} SI). At 444 cm down-core a sharp increase is seen in the magnetic susceptibility signal (Fig. 4.6), with a high value of 346 (10^{-5} SI) which correspond to large lithic grains, easily recognised at the x-rays.

Overall, the three cores show a similar alternation of lithofacies from top to bottom, and result in a similar internal organisation (Figs 4.4, 4.5 and 4.6), although core JC106-128PC differs in that it contains a large number of chaotic mud deposits compared with the other two. Generally, the IRD-rich laminated mud constitutes the majority of the sediments and the facies is recognised covering the lower half of the record. At the top of ILM, in transition to BM, the laminated sand to mud couplets (LSM) are identified in all the three cores. The LSM are always recognised in the upper part of the ILM. The same trend is not recognised for the chaotic mud lithofacies, these intervals are present through the record without an apparent trend. The BM facies is characteristic of the upper part of JC106-133PC and JC106-134PC, but not of JC106-128PC. A thin (5 cm) interval of foraminiferal-bearing mud (FM) is recognised at the top of 128PC (Fig. 4.5). This facies does not seem to be present in the other two sediment cores. An IRD-rich mud interval is identified through the BM facies in JC106-133PC and JC106-128PC, with a thickness reducing from 45 to 5 cm moving towards the shelf edge; it is not recognised in JC106-

134PC. The interval is characterised by high values of MS, ranging between 160 and 200 (10^{-5} SI) (Figs. 4.4 and 4.5).

4.4.2.3. Radiocarbon dating and sedimentation rates

Radiocarbon ages constrain most of the sediment record to the end of the last glacial interval (Marine Isotopic Stage 2 - MIS2). In the cores the youngest age of 12,690 ± 90 cal. BP is found at 175 cm down-core in JC106-133PC, within the ILM lithofacies (Fig. 4.4). The oldest age is observed in the same ILM lithofacies, between 583 and 588 cm in the same core, corresponding to 17,825 ± 175 cal. BP. The available ages constrain the boundary between the laminated mud rich in IRD and the extensively bioturbated mud ranging from 16 to 15.2 ka cal. BP (Figs. 4.4, 4.5, 4.6 and 4.7).

*Table 4.2: Radiocarbon results. Sample indicated by * was not taken into account for age reconstruction as it was at a later stage recognized to be in a re-deposited/disturbed interval. All the values are rounded to the nearest decade or multiple of 5. NPS=Neogloboquadrina pachyderma sinistral, G.B.= Globigerina bulloides.*

Core	Depth (cm)	Sample material	^{14}C Age (yrs. BP)	Calibrated age (yrs. BP) ΔR=0	Calibrated age (yrs. BP) ΔR=300	Calibrated age (yrs. BP) ΔR=700	Surrounding lithofacies	Laboratory code
128PC	125-128	Mono. NPS	13710 ± 40	15995 ± 180	15550 ± 220	14960 ± 230	ILM	SUERC-67943
134PC	60-61	Mono. G.B.	13175 ± 40	15240 ± 140	14635 ± 360	13955 ± 135	BM	SUERC-63572
134PC	588-593	Mixed benthic forams	15020 ± 45	17800 ± 170	17445 ± 180	16865 ± 225	ILM	SUERC-63573
133PC	175-176	Mono. NPS	11200 ± 30	12690 ± 90	12440 ± 150	11655 ± 250	ILM	441865
133PC	375-376*	Mixed benthic forams	15270 ± 45	18070 ± 170	17750 ± 175	17250 ± 195	LSM	SUERC-67947
133PC	433-438	Mono. NPS	14355 ± 40	16915 ± 220	16455 ± 210	15930 ± 175	ILM	SUERC-67948
133PC	583-588	Mono. NPS	15050 ± 50	17825 ± 175	17465 ± 195	16885 ± 240	ILM	450231

The sedimentation rates are calculated for the laminated mud rich in IRD lithofacies. In the ILM facies these values are calculated as 166 cm/ka for JC106-134PC (closest to the

continental shelf break), and as 131.8 cm/ka for JC106-133PC (furthest from the shelf break).

4.4.2.4. Ice-rafted debris (IRD) concentration and Neogloboquadrina pachyderma abundance

IRD is mainly represented by crystalline quartzite, granite and basalt. These petrologies were recognised as typical of the Irish and Scottish geology (Knutz et al., 2001), and therefore, the most likely to be delivered by the BIIS during its advances and retreats in the Late Quaternary. IRD is found within the laminated mud lithofacies at an average concentration of 960 grains/g of dry sediment in JC106-133PC, 1150 grains/g in JC106-128PC and 1350 grains/g in JC106-134PC (Figs 4.4, 4.5 and 4.6). The lowest [IRD] values are generally measured at the core tops and within the BM lithofacies. The highest concentrations are observed in lithofacies ILM, 6730 grains/g of dry sediment, at 350 cm down-core in JC106-134PC, the most proximal core to the shelf edge (Fig. 4.6).

In core JC106-133PC, [IRD] is very low within the BM lithofacies, with values close to 0 (Fig. 4.4). In the ILM, the [IRD] increases to at least 1000 grains/g. Three main IRD peaks are observed at 175 cm, 453 cm and 585 cm with respective values of 1420, 2340 and 3600 grains/g. These peaks are relatively sharp and represent a two- to three-fold increase in IRD concentration compared to the values above and below them. Core JC106-133PC shows consistently high [IRD] in the bottom half (Fig. 4.4), on average 1656 grains/g per sample. Within the upper part of the core, a high in IRD interval is recognised between 140 and 175 cm, the [IRD] reaches 1428 grains/g. In core JC106-128PC, the [IRD] shows an irregular pattern, displaying many small peaks with maximum values of 2180 and 1910 grains/g (Fig. 4.5). The lowest values are measured in the BM

lithofacies; while in the ILM, minor peaks are observed between values of 1030 and 1620 grains/g. These peaks are found within chaotic muds. In core JC106-134PC, the lowest [IRD] are measured through the BM lithofacies with values between 0 and 1000 grains/g (Fig. 4.6). A general increase is observed in the ILM lithofacies, with an average of 1547 grains/g per sample. As previously observed in JC106-128PC, the increase in [IRD] can sometimes be correlated to the presence of chaotic mud deposits along core. Two [IRD] peaks within the ILM are recognised at 350 and 550 cm with measured values of 6730 and 3026 grains /g.

In addition, the abundance of the planktonic foraminifera *Neogloboquadrina pachyderma* sinistral (NPS%) calculated in core JC106-133PC shows an alternation between high and low values (Fig. 4.4). The NPS% abundance mirrors the IRD curve, with high NPS% corresponding with IRD peaks and characterising the ILM lithofacies. NPS% is low at the core top, with values <10% of the planktonic foraminifera assemblage between the core top and 120 cm of core depth. Further down the core, a sudden increase between 140 and 195 cm is recorded with NPS% >=80%. Between 195 cm and 355 cm down-core, the NPS% is reduced again to values <10 %. At 375 cm of core depth, the NPS abundance increases suddenly and significantly, exceeding values of 80%, and stays high for the rest of the core to the bottom.

4.4.2.5. Facies interpretation and chrono-stratigraphy

The five lithofacies are identified corresponding to five different sedimentary processes, all characteristic of sedimentation along a glaciated margin (Hesse et al., 1997; Weaver et al., 2000; Ó Cofaigh & Dowdeswell, 2001). Based on the available radiocarbon dates and the correlation between the pattern on distribution of IRD, the entire sediment record

appears to be younger than 18 ka cal. BP and therefore time constrained to the Marine Isotopic Stage (MIS) 1 and the latter part of MIS2 (Figs. 4.7 and 4.8).

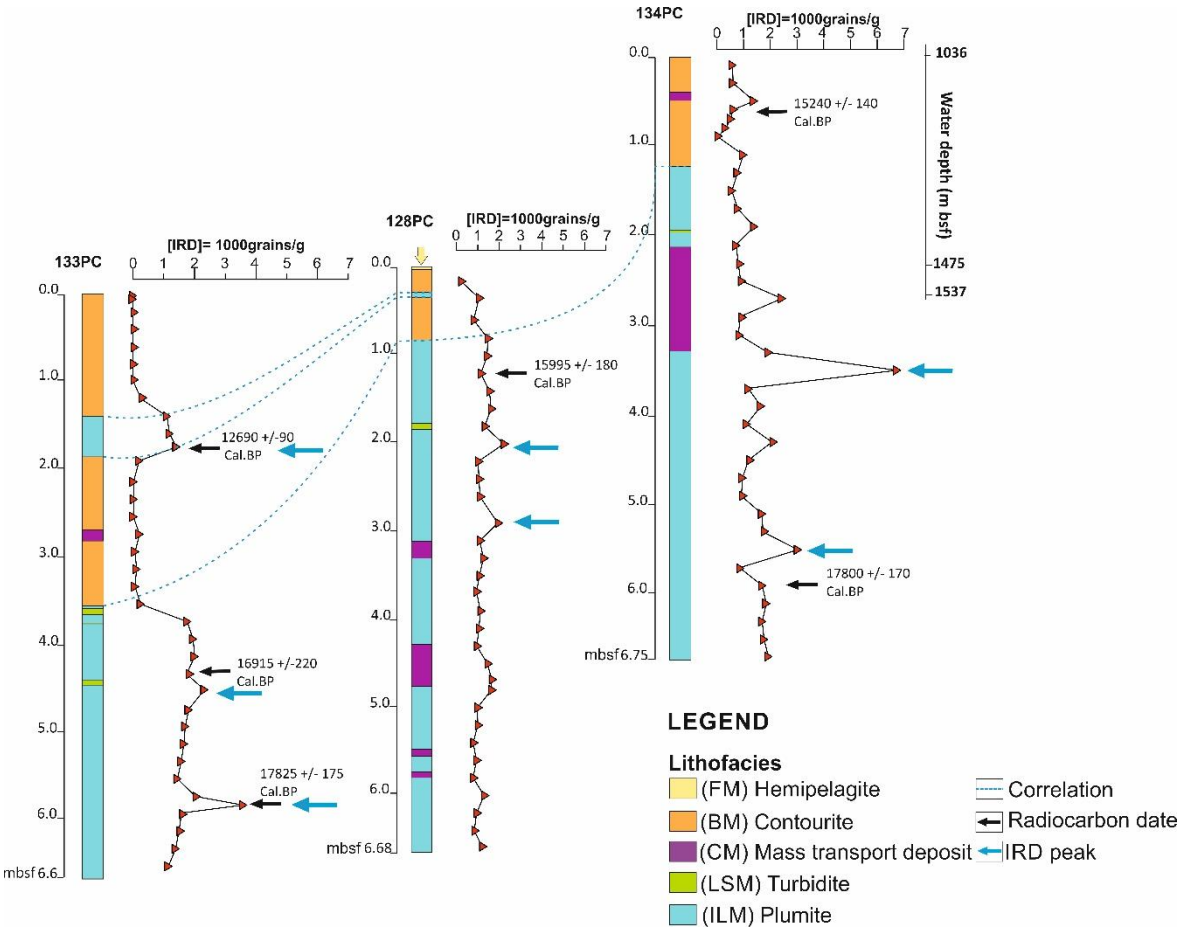

Figure 4.7: Correlation between the three DBF sediment cores (JC106-133PC, JC106-128PC, JC106-134PC) based on lithofacies identified, [IRD] concentration and cal. radiocarbon dating. The lithofacies were indicated with different colour shown in the legend, the yellow arrow at the 128PC core top highlight the thin FM facies.

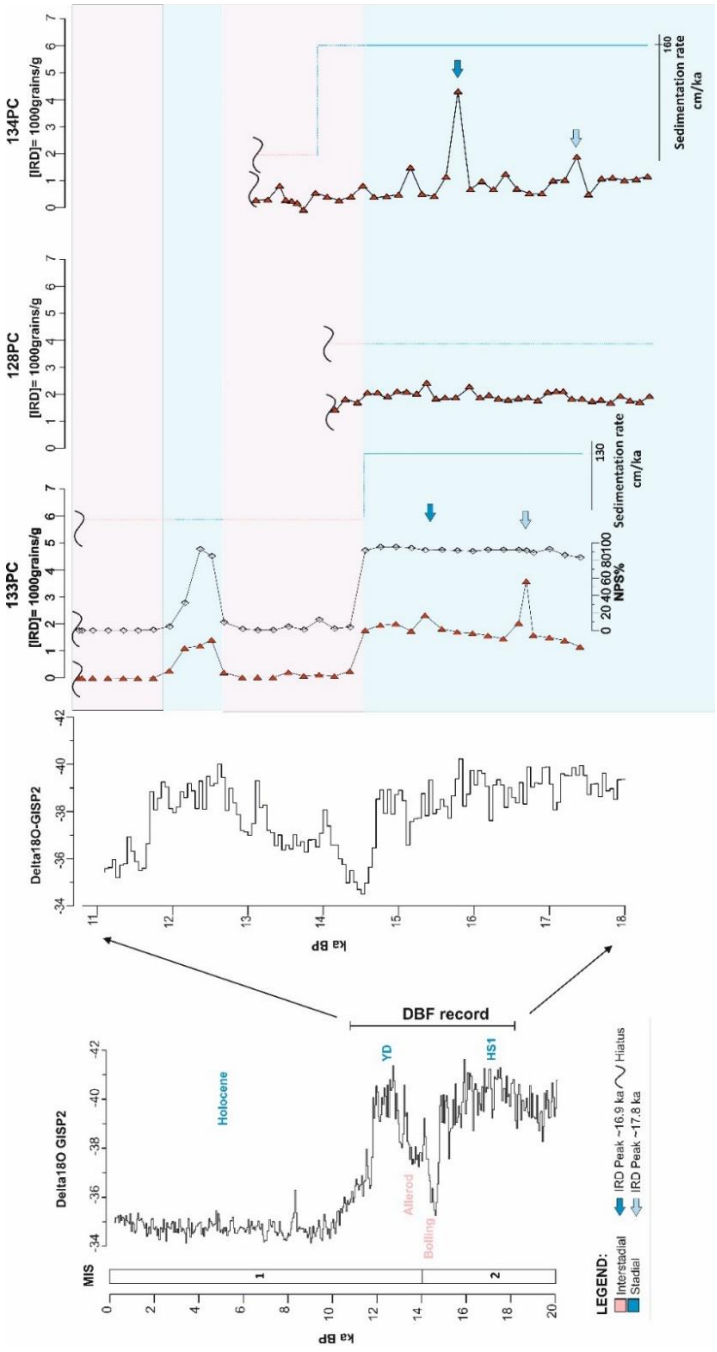

Figure 4.8: Reading from left to right- Marine Isotopic Stages (MIS) indicated for the last 20ka, with stadials and interstadials. In light blue the cold intervals, in light pick the warm. The δ18O record is registered from the GISP2 ice core record from Greenland (Rasmussen et al., 2014; Seierstad et al., 2014). The DBF sediment record represents a specific interval of the GISP2 curve, it is indicated by the two black arrows. The DBF record timing is included between 11 and 18 ka. A sedimentary hiatus or high compact record is identified after 11 ka. The stadials and interstadials are indicated (HS1- Heinrich Stadial 1, Bolling-Allerod warm stadial, YD- Younger Drays, Holocene). The [IRD] is used to identify and time constrain the record within the three cores in the DBF. The dark blue arrow indicated the high peak in IRD concentration dated ~16.9 ka cal. BP, the light blue arrow the older rich in IRD event dated ~17.8 ka cal. BP. Sedimentation rate has been calculated for the JC106-134PC and JC106-133PC, the rates for the glaciogenic sediment are indicated by the blue line.

The laminated mud rich in IRD lithofacies (ILM) is interpreted as plumite deposits, resulting from meltwater events with presence of icebergs (Wang & Hesse, 1996; Hesse et al., 1997; Hesse et al., 1999; Ó Cofaigh & Dowdeswell, 2001; Evans et al., 2002; Lucchi et al., 2002). Plumite deposition in the DBF was observed occurring until ~16 ka cal. BP (Fig. 7), with calculated sedimentation rates ranging from 160 to 130 cm/ka. These values are lower in core JC106-133PC, the most distal one from the shelf edge. Within the facies, the lithic content does not show any particular variations and high [IRD] were interpreted as large release of IRD due to calving events and presence of icebergs. Sedimentation rates are considered relatively high for the margin setting and water depths (Dowdeswell et al., 2008; Carvalho et al., 2011), without considering a meltwater input. Meltwater plumes along the Canadian margin and Antarctica were recognised able to deliver plumites as far as 250 km from basal ice sheet melt-out locations (Hesse et al., 1997; Prothro et al., 2018). The proximal source of meltwater to the DBF is suggested as localised on the Malin Sea Shelf, along Western Scotland and the Hebrides, at a maximum of 150 km from the fan. Within the plumites, the laminated sand to mud couplets (LSM) are interpreted as turbidites. The sedimentary structures, the thickness and grain sizes suggest that these are deposits of dilute, low-density turbidity currents (Middleton & Hampton, 1976; Lowe, 1979; Lowe, 1982; Wang & Hesse, 1996; Hesse et al., 1997; Hesse et al., 1999). Their age is approximately 17 ka cal. BP and their occurrence is inferred as related to the meltwater release (Fig. 4.7 and Table 4.2). Overlying the plumites, the extensively bioturbated mud facies (BM) is interpreted on the basis of grain size, thickness and internal organisation representing a contourite, sediment reworked and winnowed by bottom-currents (Stow, 1979; Stow & Lovell, 1979; Stow & Piper, 1984; Stow et al., 2002; Rebesco et al., 2014). With reference to the mean grain size (<30 μm), the contouritic deposits were classified as muddy-contourite using the

Stow et al., 2002 classification (Stow et al., 2002; Rebesco et al., 2014). The transition from the plumites to the contourites occurs between ~16 and ~15.2 ka cal. BP (Fig. 4.7 and Table 4.2). We do not have a date for the top of the contourites, but the facies is recognised up to JC106-133PC and JC106-134PC core tops (Fig. 4.7). In cores JC106-134PC and JC106-128PC, the BM unit is only between 120 and 95 cm thick, which seems to suggest a very condensed Holocene sediment record or the presence of a sedimentary hiatus. The decrease in *Zoophycos* burrows toward the core top in BM is interpreted as due to an increasing bottom current velocity and temperature through time, representing a transition to modern climatic conditions. The inferred increased current speed, with the related increased winnowing of the sediment record, could be responsible for the limited thickness of this lithofacies. In core JC106-133PC, the contouritic unit is 360 cm thick but it is interrupted by a 50-cm thick plumite interval that corresponds to an increase in [IRD] and NPS% (Fig. 4.4). Within the plumites, three high [IRD] are identified and interpreted as large releases of IRD due to possible calving events and presence of icebergs. A tentative correlation of the IRD content identify two main events before 16 ka cal. BP, where one is directly dated at ~17.8 ka cal. BP, whilst the youngest is inferred on the sedimentation rate at ~16.9 ka cal. BP (blue arrows in Fig. 4.7). The third IRD peak is dated at ~ 12.7 ka cal. BP, which is during the Younger Dryas (YD) (Alley, 2000). A similar, but much thinner, plumite interval is also recognised within contourites of JC106-128PC (Fig.4.7).

The chaotic muds (CM) occur throughout the plumites and the contourites (Fig. 4.7). The facies is interpreted as mass transport deposits due to slope instability (Holmes et al., 1998; Tripsanas & Piper, 2008). The interpretation is supported by the identification of inclined, up to 45°, sharp contacts inferred as shear surfaces, and presence of mud clasts within the muds. Similar deposits have been identified within glaciogenic sediment record

along all the glaciated margins (Aksu & Hiscott, 1989; Tripsanas & Piper, 2008; Garcia et al., 2011). As the mass transport deposits are found within the plumites, we consider a likely triggering mechanism the oversteepening and overpressurisation of the slope due to the high sedimentation rates and rapid sediment accumulation that fed the plumites.

The thin (5 cm) interval of foraminiferal-bearing mud (FM) at the top of JC106-128PC (highlighted in Fig. 4.7 by the yellow arrow) is interpreted as a hemipelagite. It is the result of slow settling of fine mud and foraminiferal tests, where bioturbation is common and the depositional environment is characterised by low energy (Stow et al., 1996; Stow & Mayall, 2000; Howe, 1995; Knutz et al., 2001). The hemipelagite is not directly dated, but interpreted as Holocene because of similarities with other deposits reported in the vicinity, such as characteristic colour, presence of foraminifera and the core top position (along the Irish margin: Howe,1995; Knutz, et al., 2002; the DBF: Howe, 1996; Knutz et al., 2001; Wilson et al., 2002; and the Rockall Trough: Howe, 1995; Georgiopoulou et al., 2012). The hemipelagite does not seem to be present in JC106-133PC and JC106-134PC. Its absence is attributed to potentially different processes occurring on the slope.

The variation of the depositional processes over time is reconstructed using the radiocarbon dates together with *Neogloboquadrina pachyderma* sinistral abundance (NPS%) and the IRD record. NPS % is commonly used to indicate changes in sea-surface temperature as it is known to represent the most abundant polar species during cold intervals (Peck et al., 2006; Haapaniemi et al. 2010). NPS% has been observed having a direct correlation with BIIS-delivered IRD and air temperature changes recorded in ice masses, making it possible to correlate with the GISP2 ice-record from Greenland (Seierstad et al., 2014; Rasmussen et al., 2014; Peck et al., 2006; Peck et al., 2007; Scourse et al., 2009; Haapaniemi et al., 2010). In core JC106-133PC, the NPS% shows a direct correlation with the IRD concentration [IRD] (Fig. 4.4). The [IRD] is used to time

constrain the sediment record and correlate it with the GISP2 ice-record from Greenland with the final aim to identify stadial and interstadial periods (Fig. 4.8). The observed alternation of cold and warm characteristic lithofacies allow this identification within the DBF sediments (Fig. 4.8). The Heinrich stadial 1 (HS1) (18.2-16.7 ka BP) is identified within the deglacial sediment as a cold interval with low temperature; after this, the passage to the warm Bolling-Allerod interstadial (14.7-12.8 ka BP) is recorded at 14.7 ka. The YD stadial is extended between 12.9 to 11.5 ka BP. After it, the Holocene is identified. The passage between MIS2 and 1 is dated following Lisiecki & Raymo, 2005 at 14 ka BP (Fig. 4.8).

4.5. Discussion

4.5.1. Late Quaternary sedimentary processes on the Donegal-Barra Fan

The lithofacies described in the results are characteristic of different sedimentary styles and their timing from the radiocarbon dates is used to interpret how the sedimentation in the DBF developed during the Late Quaternary. Based on their thicknesses, seismic units 3a, 2a, 3b and 4b (Fig. 4.2) contain all the lithofacies observed in the cores and these are therefore interpreted as representing sedimentation post last glacial maximum (LGM). Previous studies on deep-sea environments, along the North Atlantic margin, showed that the sediment cores collected from similar water depths, within the region of interest, present an incomplete record in time, making their interpretation difficult (Howe, 1995; Scourse et al., 2009). Our results, even with the presence of an extremely compact in thickness deposit with potential hiatuses in the post glacial sediments, demonstrate that combining sedimentology, with proxies such as [IRD], NPS% and radiocarbon dates, it

is possible to reconstruct the deglacial history of the DBF post ~18 ka and its transition to modern climatic conditions (Fig. 4.9).

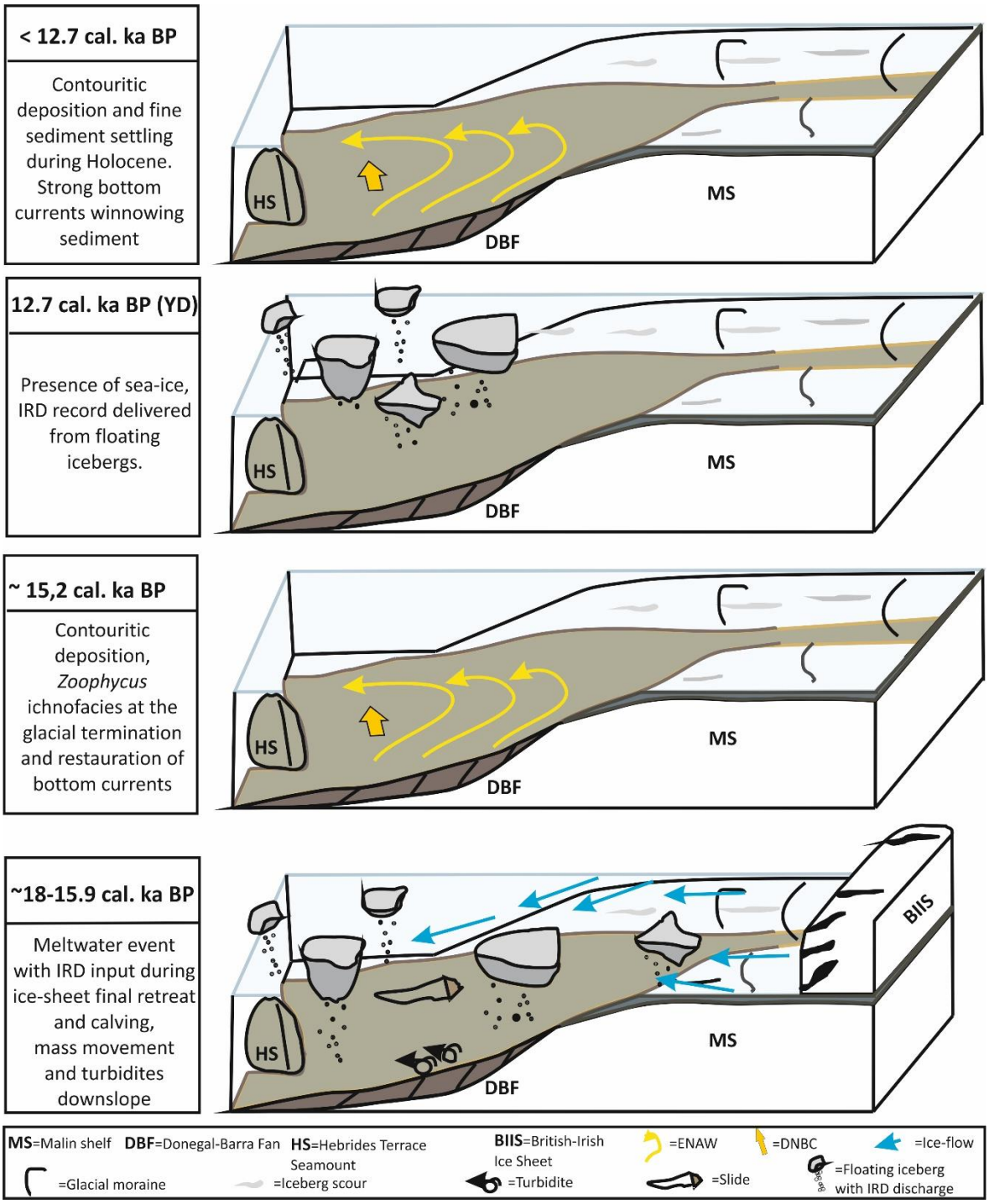

Figure 4.9: Schematic depositional model for the DBF. The sedimentation is represented by meltwater events with large discharge of icebergs and mass movements, laminar and turbulent, downslope. The meltwater and iceberg presence are recorded for sediments older than 15.9 ka cal. BP and for Younger Dryas age. Contouritic deposition is recognised for sediment dated after 15.2 cal. ka BP. Currents abbreviations: ENAW= Eastern North Atlantic Water; DNBC= Deep Northern Boundary Current.

The DBF, during the BIIS LGM, was fed by the Hebrides Ice Stream (HIS) and the North Channel Ice Stream (NCIS) (Dunlop et al., 2010; Dove et al., 2015). The ice streams converged on the Malin Sea shelf (MSs) delivering large amounts of meltwater and sediment to the DBF; the HIS alone was calculated as draining between 5-10 % of the former BIIS (Dove et al., 2015). After the LGM, the previously investigated IRD record from the Northeast Atlantic deep-water sediments described the BIIS as an extremely dynamic ice sheet. Several phases of advances and retreats with relative discharge of icebergs were observed through the IRD record, following a millennial variability (Knutz et al., 2001; Wilson et al., 2002; Peck et al., 2006; Scourse et al., 2009; Haapaniemi et al., 2010).

The core correlation (Fig. 4.7) shows inferred meltwater deposits in the DBF dated between ~ 18 ka cal. BP and 16 ka cal. BP. These are interpreted as glaciomarine sediments delivered by meltwater plumes during the last moments of BIIS marine extension. Given the proximity of the DBF to the Outer Hebrides (~100km), we suggest that the plumitic facies we see in our cores is a record of the BIIS last extension on the Malin Sea shelf (MSs), likely from the Hebrides sector.

Total deglaciation for the marine extended portion of the BIIS on the MSs, with retreat of the ice-limit to the actual coast line and consequent interruption of the HIS, was dated between 17-16 ka (Bradwell et al., 2008; Small et al., 2017; Ballantyne & Ó Cofaigh, 2017). Evidence along western Scotland and the Hebrides suggested the BIIS was marine-extended up to ~16 ka (Dove et al., 2015; Small et al., 2017). Post LGM, BIIS re-advances were additionally recognised along the north east of Ireland during the CHR at 18.4 and KPR between 17.3 and 16.6 ka (McCabe & Clark, 1998; McCabe et al., 2007; Ballantyne & Ó Cofaigh, 2017). Also in Northern Ireland with the Ballycrampsey Readvance (BR) a post glacial re-advance was identified (McCabe & Clark, 2003). The simultaneous dates

for these Irish events were interpreted as a potential regionally-significant event of ice margin extension during that time (McCabe et al., 2007).

Within the studied DBF deglacial record, the high sedimentation rates in the plumites suggest these have been delivered through concentrated meltwater plumes, supporting the presence of a melting BIIS along western Scotland, along the Hebrides and with a potential Irish contribution. In addition, the identification of turbulent flows along the margin (Fig. 4.9) supports a greater downslope input of sediment due to the final BIIS melting with consequent slope instability during deglaciation. Similar behaviour along polar and north Atlantic margins has been observed in a rhythmic turbidic activity along the glaciated margins, used as a proxy for meltwater delivery during the last deglaciation (Dowdeswell et al., 1998; Roger et al., 2013).

Following the deglaciation, contouritic deposits are dated around 15.2 ka cal. BP and recognised until the core tops, presenting approximately ~1 m of thickness (Fig. 4.8). The contourites are interpreted as representing a condensed unit with the likely possibility of sedimentary hiatuses in the upper part. In addition, the *Zoophycos*-enriched interval allows for the identification of an initial restoration of the bottom currents after their weakening during glacial times, still experiencing intermediate climatic conditions. *Zoophycos* is visible after the BIIS deglaciation and recognised after YD deposits, suggesting during these intervals an increase in temperature and in ocean currents speed. This environmental reconstruction was previously observed along the Atlantic margin, between glacial and interglacial conditions, during periods with high and seasonal productivity and sedimentation rates ranging between 5 and 20 cm/ka (Dorador et al., 2016). The contouritic unit is interpreted as being initially deposited during the transition between stadial and interstadial conditions, with *Zoophycos* and relative higher sedimentation rates. It moves then to a muddy contourite with likely a condensed aspect

and sedimentary hiatuses due to an increased current speed. Hiatuses in the DBF record were previously observed and attributed to the NADW current, winnowing or not allowing hemipelagic deposition during Late Pleistocene and Holocene along the North East Atlantic continental slope (Knutz et al., 2002).

Within MIS 1, the cold YD stadial is characterised by a high [IRD] and NPS%. There is no record of BIIS marine re-advance during this time interval, and the origin of the plumites coinciding with YD needs to be investigated. Previous investigation of sediment cores, collected from the North East Atlantic margin, showed an enrichment in IRD during the YD (Scourse et al., 2009); however, a different origin, not directly connected with the Laurentide Ice Sheet (LIS) for this sediment was never hypothesised. The main oceanic currents were recorded either interrupting or slowing down during the previous glacial periods (Knutz et al., 2002; Peck et al., 2006; Toucanne et al., 2015). A similar behaviour was observed during the cold YD stadial as for the previous LIS meltwater events (Bond et al., 1999; Adams et al., 1999; Alley, 2000; Broecker et al., 2010; Lynch-Stieglitz et al., 2011). Recent evidence indicated that the Scandinavian Ice Sheet (SIS) extended as marine-based off the south-west of Norway during the cold YD stadial (Broecker et al., 2010; Mangerud et al., 2016). One possible interpretation for the YD deposit of the DBF could be a re-advance of the Scandinavian Ice Sheet (SIS) at that time. Based on published works investigating the ice-sheets extension along the North East Atlantic margin, in particular during the YD (Hughes et al., 2015; Mangerud et al., 2016), we postulate that in this time the DBF received a high IRD discharge likely related to a secondary re-advance of the SIS and an associated arrival of icebergs flowing south along the Atlantic margin. A SIS origin is suggested considering that the IRD petrographies in the YD-dated interval are represented largely by quarzite, basalt and highly metamorphic grains, corresponding with a European origin/geology. These petrologies are typically

found along the Scandinavian margin as well as the southern located UK and Irish margin, and they represent the majority of the lithics identified by this study along the DBF sediment record. The IRD petrologies, together with a non-previous recognized BIIS marine extension able to deliver meltwater plume and iceberg to the fan during the YD, is interpreted as potentially related to icebergs from the documented extended SIS. A detailed investigation of the IRD record, with calculations of relative abundance of the IRD petrologies was not part of the project and is strongly suggested for future studies as it may provide clear evidence for icebergs provenance.

After the YD, at the transition to the Holocene, post-glacial sedimentation is restored with contourites deposition becoming dominant (Fig. 4.9). The contourite reduced thickness during the Holocene suggests the presence of strong bottom currents flowing northward between 1000 and 1500 m water depth. The presence of a strong current would potentially represent one possible explanation for the missing YD plumite in the most proximal core to the shelf edge, together with a no-deposition of the plume in that location (Fig. 4.7). The occurrence of bottom currents along the North Atlantic margin and in particular the eastern Rockall Trough flank was observed between 1000 and 1500 m water depth, with large erosive power manifested in short core recoveries and reduced thickness for post-glacial deposits (Howe, 1996; Knutz et al., 2002).

Hemipelagite deposition is not particularly prominent here. A thin hemipelagic layer is present at the core top of only one core, JC106-128PC. We can only speculate that the reduced hemipelagic thickness represents recent sedimentation, and could relate to changes in the oceanic current regime for the study area. However, our data is too limited to discuss this any further.

4.5.2. British-Irish Ice Sheet contribution to continental margin sedimentation

Most of the JC106 sediment record from the DBF is interpreted as representing the sedimentation occurring during the final stages of the BIIS deglaciation, at the end of the Late Midlandian glaciation (MIS2). Between ~18 and ~16 ka cal. BP, the DBF is observed receiving meltwater plumes deposits from the BIIS before its total ice-depletion. This interpretation is based on the sedimentation rates calculated through the DBF plumitic facies (130-160 cm/ka). This suggests that meltwater and iceberg discharge during the latter part of the deglaciation continued to contribute to the build-up of the DBF, in addition to the observations occurring during the broader last glacial interval (Howe, 1995; Stoker, 1995; Armishaw et al., 1998; Holmes et al., 1998; Sejrup et al., 2005). In the current study, the high input of glaciomarine sediment and the IRD record observed within the plumites are inferred as representing BIIS meltwater event deposits, with additional higher IRD signal delivered from a larger number of floating icebergs during possible calving events. The meltwater is supposed to be BIIS delivered as it was discovered that until 16 ka BP, there was melting ice coming from fjords along the Hebrides and Western Scotland (Small et al., 2017; Arosio et al., in press). This does not exclude the presence of icebergs coming from different locations but implies that the main signal recorded within the plumite was delivered by the drained BIIS. Sediment provenance studies may be able to resolve the relative contributions. The sediment record correlates well with the larger BIIS reconstruction (Clark et al., 2012a; Ó Cofaigh et al., 2012; Ballantyne & Ó Cofaigh, 2017). On the Malin Sea shelf, the deglaciation of the marine sector and HIS interruption was inferred between 17-16 ka (Small et al., 2017). In addition, along the north east of Ireland, the BIIS re-advanced at 18.4 ka (CHR) and 17.3-16.6 ka (KPR) (Ballantyne & Ó Cofaigh, 2017).

The post-17 ka turbidites may indicate a meltwater release with delivery of a large amount of sediment at the end of deglaciation. Intense turbulent flows have been noted at the transition between glacial and post-glacial deposits along the North Atlantic and Canadian margins (Holmes et al., 1998; Knutz et al., 2002; Roger et al., 2013). In a similar setting within deglaciation, along the Canadian margin, turbiditic events displayed a 1-2 ka cyclicity, following a Dansgaard-Oeschger periodicity (Roger et al., 2013). Although the DBF record is not old enough for a full correlation with the Canadian records, the turbidites are recorded at the end of the cold Heinrich Stadial 1, showing a correlation in the sedimentation style between the two Atlantic margins (Figs. 4.7 and 4.8).

The two observed distinct peaks in IRD concentration during deglaciation and the one during YD suggest episodes of increased iceberg release along the margin. That means that there was a large presence of icebergs at ~17.9 ka cal. BP, ~16.8 ka cal. BP and during the YD at 12.7 ka cal. BP. The likely cause of these high IRD concentrations are interpreted as calving events of the European Ice Sheet (EIS) (i.e. BIIS and SIS) during that time. The calving locations are potentially related to a retreating Hebrides Ice Stream, a BIIS southern cap on the southern Outer Hebrides and Western Scotland or to a marine-extended southern ice-margin of the SIS, south of Norway.

4.5.3. Implication for the reconstruction of the North Atlantic Ocean currents

BIIS calving events and iceberg releases were interpreted as independently regulated by the internal ice sheet dynamics on a millennial (D-O) scale (Knutz et al., 2001; Peck et al., 2006; Haapaniemi et al., 2010). From a broad perspective, a synchronicity between the final deglaciation of European Ice Sheets (EIS) (i.e the BIIS, the Scandinavian Ice Sheet, the Svalbard-Barents-Kara Seas, the Channel River Hydrographic Network) along

the North East Atlantic was recorded (Hughes et al., 2015). The DBF sediments in this study identify the last portion of the BIIS deglaciation, where the observed meltwater releases correlate with the other EIS melting events.

The EIS with its large amount of freshwater delivered to the North Atlantic Ocean has been interpreted as responsible for global climatic changes (Bigg et al., 2012; Hughes et al., 2015; Toucanne et al., 2015). The high dynamic behaviour of the BIIS, in part reconstructed using the DBF sediment record, fits perfectly within the European scenario. The BIIS together with the other European Ice Sheets can therefore be considered having an active and contributing role on the North Atlantic climate. Sediment retrieved from the Bay of Biscay displayed two large discharges of meltwater from the EIS occurring at 18.2 ± 0.2 and 16.7 ± 0.2 ka (Toucanne et al., 2015). The IRD peaks recorded in the DBF and inferred as large releases of freshwater with potential calving during BIIS deglaciation potentially correspond with the ones from the Bay of Biscay.

The lithofacies identified from the DBF sediments showed how the Atlantic Meridional Overturning Circulation (AMOC) was acting differently during the deglaciation, allowing the undisturbed deposition from meltwater plumes. Following this, contourites dating from 15.2 ka cal. BP, offer evidence for the AMOC restoration. Subsequently, another plumitic deposit is observed during the Younger Dryas at 12,690 ± 90 cal. a BP, with the AMOC brief interruption, eventually restored again and present today. AMOC weakness was hypothesised corresponding with the European meltwater events (Hall et al., 2006; McManus et al., 2004; Toucanne et al., 2015). In the DBF, it is observed that the BIIS was unstable between 18 and 16 ka cal. BP, registering a meltwater input on the Malin Sea shelf with two large intervals rich in floating icebergs dated in this study.

The synchronicity in the deglacial meltwater release between the BIIS and the EIS shows a potential climatic relationship, present between the Eastern North Atlantic ice sheets, at

least in their final deglaciation. The stadial H1, dated between 18.2 and 16.7 ka, represents the time frame where the Laurentide Ice Sheet (LIS) instability reached its maximum, including the Heinrich 1 event (Heinrich, 1988). It is additionally supported by this study that the EIS, in particular the deglaciating BIIS, acted during the same time span with a similar unstable behaviour. Furthermore, the presence of icebergs recognised during MIS1 and the YD stadial not attributed to LIS calving, supports the recent works on the European Ice Sheets advance during this last cold period of time (Mangerud et al., 2016) and opens a new question about the role of the EIS during MIS1.

4.6. Conclusions

The investigation of the deep water sediments retrieved from the DBF allowed the reconstruction of the final stages of the BIIS deglaciation and the transition to modern climatic conditions.

- The DBF sedimentary history from the last ~ 18,000 years was reconstructed. This record was interpreted as large meltwater plumes with high sedimentation rates during the final BIIS deglaciation, with a post-glacial restoration of oceanic currents and deposition of contourites during the Holocene.
- The different proxies used, in particular the IRD concentration (n° IRD > 150 grains/g of dry sediment), allowed for the identification of two intervals during deglaciation, at ~17.8 and ~16.9 ka cal. BP, implying the presence of floating icebergs in the area of the DBF. The provenance of the IRD record, based on the lithic grains petrologies, suggest European Ice Sheet calving events, potentially BIIS calving events from the Hebrides and Western Scotland.

- During the Younger Dryas, an IRD-rich interval was related to a European Ice Sheet marine advance and following calving, potentially the Scandinavian Ice Sheet, on the basis of similar composition in the lithic grains petrologies and the recorded marine extension at that time.
- A potential key sedimentary facies was identified in the contourites. The interval rich in *Zoophycos* ichnofacies could represent evidence for the transition between stadial and interstadial climatic conditions. This lithofacies can potentially be identified along any continental margin and represents a useful climatic tool.
- The British-Irish Ice Sheet deglaciation recorded from the DBF sediment and IRD record fits within the observed behaviour of the European Ice Sheet during the Late Quaternary and in particular at the transition between Marine Isotopic Stages 2 and 1. By releasing a large amount of freshwater, the BIIS likely could have had an active role on the Atlantic Meridional Oceanic Current reduction registered and the North Atlantic climate.

Chapter 5: Unravelling the history of the western sector of the British-Irish Ice Sheet over the entire last glacial period using NE Atlantic marine sediment cores: a multi-proxy approach

Abstract

Sediment cores collected from 3000 m water depth in the south-eastern Rockall Trough, North-East Atlantic Ocean, are used to reconstruct the sedimentary evolution of the basin starting from the last interglacial period. Particular interest is focussed on the British-Irish Ice Sheet (BIIS) contribution to the sedimentation in the deep water location. The methodologies used in this study include sedimentological analysis, interpretation of physical properties, planktonic foraminifera abundances, ice rafted debris (IRD) and oxygen stable isotope analysis. Six lithofacies, 5 biofacies, *Neogloboquadrina pachyderma* sinistral abundance, IRD concentration and $\delta^{18}O$ ratios have been used to describe the sedimentary evolution in the trough as mostly represented by hemipelagic settling and related to meltwater plume deposition. In addition, the biofacies identified provide a relative indication of sea-surface temperature at the time of deposition. Oxygen isotope ratios are used for the creation of an age model that constrains the Rockall Trough sedimentary record to the last 130 ka and allows the identification of Marine Isotopic Stages. IRD fluxes are calculated to investigate the evolution of the BIIS through time. A previously unrecognised BIIS marine extension is inferred during MIS5b, with plumitic deposition and IRD fluxes between 85 and 80 ka BP suggesting a retreating ice-margin. After this, the BIIS is observed as re-advancing during MIS4, with recorded high sedimentation rates within plumites and an inferred retreat due to calving at ~60 ka BP.

The BIIS maximum extent then follows, with recorded sedimentation rates up to 13.8 cm/ka in the plumitic facies. BIIS maximum extent is inferred occurring before 20 ka BP during MIS2, when high IRD fluxes suggest a calving ice-margin. A calving location is suggested along the Irish shelf break, north of the Porcupine Bank, supported by mapped iceberg scours following the maximum extent.

5.1. Introduction

Deep sea sediments can supply a continuous archive of past environments and climatic conditions presenting a potential long record that avoids hiatuses and erosional events typical of shallower marine locations. In this study, the sedimentary record from two cores collected from approximately 3000 meters of water depth in the Rockall Trough, east North Atlantic, is investigated (Fig. 5.1).

The Rockall Trough flanks are characterised by strong down-slope and along-slope activity (Shannon et al. 2001; Øvrebø et al., 2005). Along its western margin, the Feni Drift and the Rockall Bank Slide Complex (RBSC) represent the results of bottom current activity and slope failure (Stoker, 1997; Shannon et al., 2001; Georgiopoulou et al., 2013). The eastern flank is mostly shaped by the BIIS, responsible for excavation and sediment delivery along the slope to the basin from the Plio-Pleistocene onwards (Stoker, 1995; Sejrup et al., 2005; Ó Cofaigh et al., 2012; Sacchetti et al., 2012a). The cored location is selected in the south-east part of the trough, approximately 50 km distant from these large features and canyon systems (Fig. 5.1). The area was selected for this study due to its apparent quiet depositional character, suggested by the distance to the main depositional lobes and canyons, revealed by previous regional mapping (Sacchetti et al., 2012). The cored location was selected as likely representing an area with mainly hemipelagic

deposition and lack of down-slope deposits. These conditions allowed for the recovery of a largely continuous sedimentological record without significant reworking or bioturbation, in the form of two twin sediment cores up to 4 m long. Sedimentology, physical properties, planktonic foraminiferal content, IRD record and oxygen stable isotope allowed for the reconstruction of the sedimentary evolution of this area.

The main aim of this study is to investigate the sedimentary processes that occur in this deep part of the Rockall Trough and to reconstruct the sedimentary evolution of this part of the basin, through time. There are two specific objectives. The first is to use oxygen isotope ratios to time constrain the sediment record. The second objective is to investigate BIIS dynamics and assess if the sediment record and the IRD can be used to analyse the progressive growth of the BIIS during the last glaciation and subsequent deglaciation.

5.2. Regional Setting

5.2.1. Physiography and Geomorphology

The Rockall Trough (RT) is an elongate deep-water basin, oriented NNE-SSW, along the eastern North Atlantic continental margin. Its water depth varies between 1200 m in the northern sector and 4500 m in the southern respectively (Fig. 5.1). Its flanks are narrow and steep, with angles ranging from 3° to 7° (Shannon et al., 2001; Unnithan et al., 2001; Sejrup et al., 2005; Øvrebø et al., 2005; Elliot et al., 2006). The RT flanks show the presence of both depositional and erosional features. These are identified in numerous canyons on the eastern side, while a large slope failure, the Rockall Bank Slide Complex (RBSC), is evident on the western flank (Flood et al., 1979; Faugeres et al., 1981; Shannon et al., 2001; Øvrebø et al., 2005; Sacchetti et al., 2011; Sacchetti et al., 2012; Georgiopoulou et al., 2013). The eastern flank of the Rockall Trough is characterised by

a present-day undersupply of sediment on the continental slope (Shannon et al., 2001). The slope is marked by large canyon and gully systems formed during Mid-Cenozoic subsidence, linked to widespread slope rotation (Elliot et al., 2006; O'Reilly et al., 2007). The canyons have been successively deepened by the advances of the BIIS onto the continental shelf during glacial intervals as they constituted the main delivery systems for glaciogenic sediment along the Irish continental margin (Cronin et al., 2005; O'Reilly et al., 2007; Ó Cofaigh et al., 2012; Sacchetti et al., 2011; Sacchetti et al. 2012). These have been recognised to actively deliver sediment during the Late Pleistocene to the trough during glacial intervals, in relation to an extended BIIS on the continental shelf (Sacchetti et al., 2012). On the Irish continental shelf, the BIIS extension left additional evidence of advance and retreat in the form of moraines and iceberg scours (Benetti et al., 2010; Ó Cofaigh et al., 2012; Peters et al., 2015). Arcuate moraines are mapped along the shelf-break and mid-Irish shelf, north of the Porcupine Bank, while iceberg scours are evident all along the shelf edge (Benetti et al., 2010; Peters et al., 2015) (Fig. 5.1). Also the northern sector of the Rockall Trough has been greatly influenced by the BIIS. Through the delivery of vast quantities of sediment to the shelf edge through the Malin Sea paleo-ice stream, a trough-mouth fan (the Donegal-Barra Fan – DBF) was formed on the slope between UK and Irish waters (Armishaw et al., 1998; Holmes et al., 1998; Howe, 1995). On the western flank of the Rockall Trough, the main sedimentary features are represented by the Rockall Bank Slide Complex (RBSC) and the Feni Drift (Stoker, 1997; Unnithan et al., 2001; Shannon et al., 2001; Georgiopoulou et al., 2013). The contouritic Feni Drift testifies an active regime of bottom currents along the western trough margin, with the drift ranging in age from the Eocene to the Early Pliocene (Kidd & Hill, 1986; Stoker, 1997; Stoker et al., 2005). The RBSC represents a multiphase slope collapse generating elongated slides through the Rockall Trough (Unnithan et al.,2001; Elliot et

al., 2009; Georgiopoulou et al., 2013). It has been active at least since the Mid-Pleistocene and was recorded active up until the current interglacial (Flood et al., 1979; Faugeres et al., 1981; Øvrebø et al., 2005; Georgiopoulou et al., 2013).

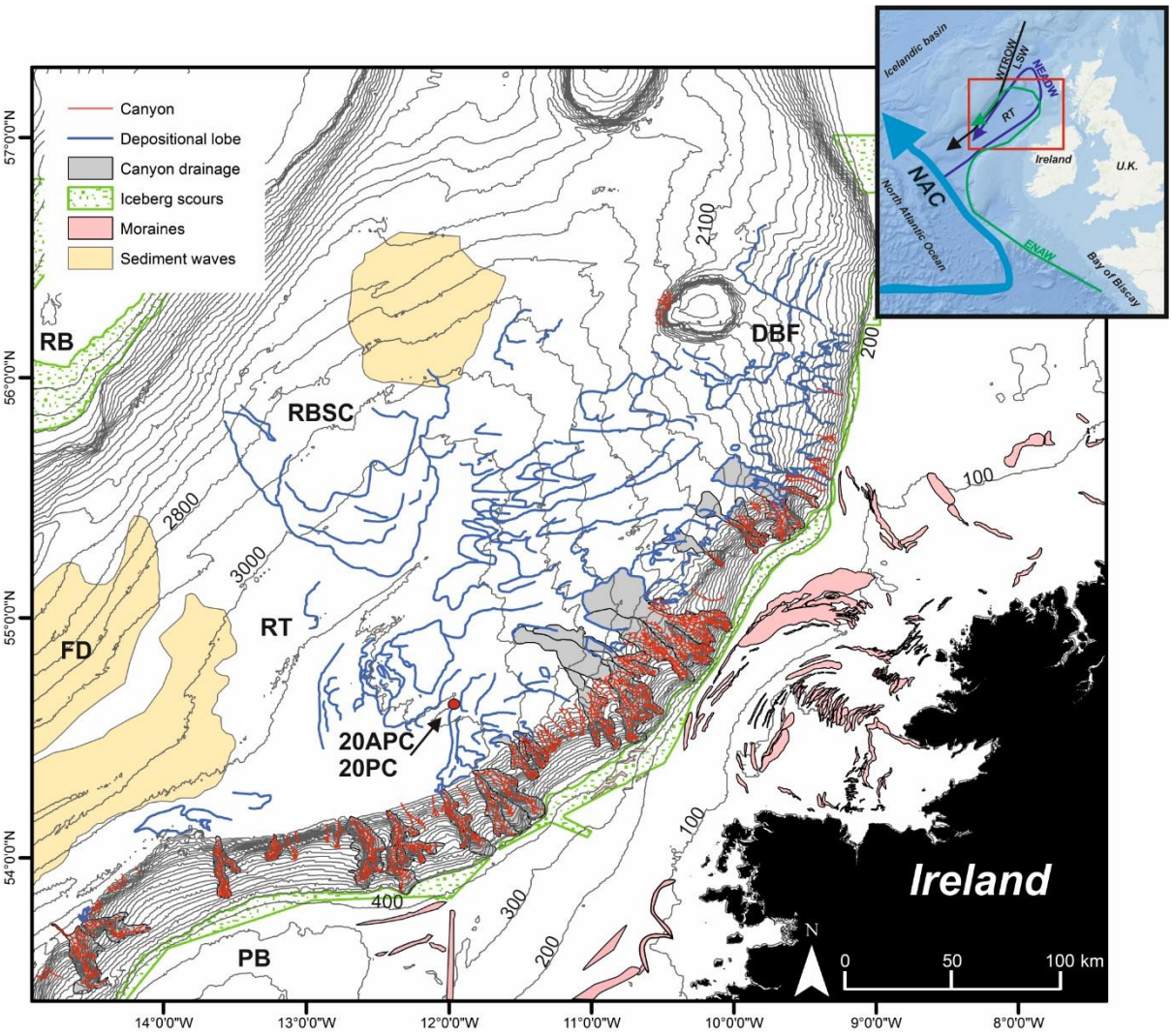

Figure 5.1: Location map, the twin cores location is indicated by the red dot. The sedimentary features mapped along the margin are indicates as DBF (Donegal-Barra Fan), FD (Feni Drift), RBSC (Rockall Bank Slide Complex). RT= Rockall Trough, RB= Rockall Bank, PB=Porcupine Bank; in the inset map: ENAW (Eastern North Atlantic Water), WTROW (Wyville-Thompson Ridge Overflow Water), LSW (Labrador Sea Water), NEADW (North-Eastern Atlantic Deep Water). Mapped features after Benetti et al., 2010, Sacchetti et al.,2012; Peters et al., 2015.

5.2.2. Oceanography

The Rockall Trough's oceanographic setting is complex with variable water masses at different water depths. In the trough the currents flow towards the north on the eastern flank, turn anticlockwise around the Hebrides Terrace Seamount and move southwards along the trough western margin (Fig. 5.1). The Eastern North Atlantic Water (ENAW) is recognised as the main surface water mass. It originates in the Bay of Biscay, as part of the North Atlantic current (NAC) and it flows with the Shelf Edge Current (SEC) at an average velocity of 15-30 cm/s (Pingree, 1993; New & Smythe-Wright, 2001). The ENAW moves northward along the eastern flank of the trough, turns around the Hebrides Terrace Seamount and then flows southward along the trough western flank (New & Smythe-Wright, 2001). The lower part of the water column is dominated by the Wyville-Thompson Ridge Overflow Water (WTROW) and the Labrador Sea Water (LSW) originating north, in the Norwegian and Labrador Seas, flowing towards the south along the western flank of the trough between 1,000 and 2,000 m of water depth (Lee & Ellet, 1965; van Aken, 2000). The north-eastern Atlantic Deep Water (NEADW) is recognised as flowing northward along the eastern side of the trough (i.e. between 2,000 and 3,000 m), driven by the North Atlantic Deep Current (NADC), generated by the North Atlantic Current (NAC) (New & Smythe-Wright, 2001; Toms, 2010), before turning southward along the western Rockall Trough (McCartney & Mauritzen, 2001). The current regime has changed through time and these changes are observed within the sediment record, where characteristic lithofacies along the trough flanks mark an alternation from interglacial and glacial periods, implying a weakened current regime during cold climatic intervals (Kidd & Hill, 1986; Toms, 2001; Øvrebo et al., 2005).

5.3. Material and methods

In 2010, the RV *Celtic Explorer* collected many sediment cores by piston coring in deep-sea locations along the Irish continental margin during cruise CE10008. Two cores from this cruise were retrieved from a deep sector of the Rockall Trough, at ~50 km from the complex canyons systems on the Irish continental slope and the lobes of the DBF (Fig. 5.1). These cores, the longest recovered cores from the cruise (i.e. up to 4m long), were collected from the same site and were referred to as twin cores, 20PC and 20APC (Table 5.1; Appendix 2). The twin cores were split after collection and an initial description presented an apparent undisturbed and continuous sedimentation (Allin, 2011).

For this reason, the twin cores have been selected for this study as likely not recording thick down-slope mass transport deposits and allowing investigation of the sedimentary evolution of the basin without large event of rework or erosion (Fig. 5.1; Table 5.1).

Table 5.1: Sediment core general information

Cruise	Core Number	Latitude	Longitude	Water-depth (m)	Recovery (cm)
CE10008	20PC	54.8063 N	11.9343 W	2856	393
CE10008	20A PC	54.8063 N	11.9343 W	2856	400

Within this work, the twin cores were thoroughly described and analysed using multiple different techniques presented in the next sections. Core 20APC was most intensively investigated because of its longer record in terms of time in comparison with 20PC, which is instead used to reinforce description and interpretation of the sedimentary processes through time.

5.3.1. Sedimentology

Prior to a new and accurate sedimentological logging, x-radiographs were acquired on the twin cores using a CARESTREAM DRX Evolution system at the Faculty of Radiology, Ulster University in Jordanstown (Appendix 2). The use of x-radiographs allowed for the identification of sedimentary structures not visible to the naked eye and intervals of increased IRD content (cf. Howe, 1995; Lucchi et al., 2013).

Core 20APC was scanned with a Geotek Multi Sensor Core Logger (MSCL) at 1 cm intervals at the National University of Ireland, Maynooth, to measure physical properties, such as P-wave velocity (m/s), bulk density (gm/cm^3), magnetic susceptibility ($SI*10^{-5}$) and lightness (L) (Appendix 2).

These data have supported the identification of boundaries within the sediment record and guided the recognition of specific lithofacies, such as high magnetic susceptibility for turbiditic events not recognised to the naked eye and high lightness values for facies high in carbonate content (Weaver & Schultheiss, 1990; Balsam et al., 1999; Knutz et al., 2001).

After a detailed core description, 59 samples were collected for grain size analysis from both cores, at approximately 10 cm interval. The samples were pre-treated, soaked in a 5% Calgon solution overnight and shaken on a rotating table in order to avoid flocculation of the fine particles. Grain size was calculated using a Malvern 3000 (cf. Sperazza et al., 2004) at University College Dublin (UCD) and at Ulster University, Coleraine. The results were represented as a full spectrum through the use of the Excel spread-sheet GRADISTAT (Blott, 2001) and used in the lithofacies identification.

5.3.2. Foraminiferal analyses

Fifty-one half-slab samples, 1 cm thick samples, were collected approximately every 10 or 20 cm for microfossil analysis on both cores following lithofacies identification. The samples were wet washed and sieved with a 63 μm sieve, then dried under an infrared lamp. The fraction >150 μm was used for the investigation of the planktonic foraminiferal content. The planktonic foraminifera assemblages, with relative abundance of the dominant planktonic species, were calculated counting at least 300 foraminiferal specimens for each sample, when applicable (Peck et al., 2006; Hibbert et al., 2010). Particular attention was paid to the relative abundance of *Neogloboquadrina pachyderma* sinistral (NPS%), as it has been found by previous studies to be strongly associated with changes in polar front migration and has been used in correlation with ice-core records from Greenland (Bond et al., 1993; Peck et al., 2006; Haapaniemi et al., 2010).

In addition, relative abundances of the dominant species were used to conduct two-way cluster analysis (Pang-Ning Tan et al., 2006; Ceregato et al., 2007). The statistics were calculated using the open source Paleontological Statistics Software, PAST (Hammer & Harper, 2005). A Correlation Distance index was used to observe similarity within the matrix, utilising an un-weighted pair-group method with arithmetic averaging (i.e. UPGMA) (Hammer et al., 2001). This multivariate technique produces dendrograms used for the identification of biofacies. These in turn are indicative of different climatic or environmental conditions, recorded in the sediment record (cf. Hendy & Kamp, 2004; Holland & Patzkowsi, 2004).

5.3.3. Stable isotopes analyses

Eighty-seven samples represented by monospecific picks of the planktonic foraminifera *Globigerina bulloides* were selected for stable isotope analysis from core 20APC. The location of the samples included all the lithofacies, avoiding clear evidence of bioturbation and turbiditic beds and aiming for a full coverage of the sediment record, with an average of 5 cm interval between the samples. The *Globigerina bulloides* species was chosen for the analysis due to its large geographic distribution in the North Atlantic and its high abundance during different climatic periods (Garvey, 2011; Allin, 2011). The specimens were picked from the fraction >150 μm when possible (Lab. communication) and a minimum of 0.3 mg per sample was analysed at Iso-Analytical (http://www.iso-analytical.co.uk/). Measurements were made on a Continuous Flow Isotope Ratio Mass Spectrometry (CF-IRMS) and the calculated oxygen isotope values are expressed as ‰ Vienna Pee Dee Belemnite standard (VPDB) (Appendix 2). The $\delta^{18}O$ record was used for the identification of Marine Isotopic Stages (MIS) through correlation with SPECMAP and Lisieki & Raymo stack lines and the acquisition of climatic information. These include qualitative changes in sea-surface temperature, ice sheet extent or presence of sea-ice (Imbrie et al., 1984; Emiliani, 1955; Lisieki & Raymo, 2005; Peck et al., 2006). The $\delta^{18}O$ record was then compared with the Greenland Ice Core Project (GRIP) $\delta^{18}O$ for the creation of an age model for core 20APC. The GRIP curve was selected for the comparison with the 20APC record, after the lithofacies interpretation and the identification of an inferred last interglacial interval at the core bottom. GRIP is well known as presenting a very long and extended record for the MIS5, even if some uncertainty is presented for the interstadial 5.e or Eemian (Johnsen, et al., 1997). Following the age model creation, sedimentation rates through time for 20APC were

calculated after removing turbidites or debrites from the core length, in order to avoid abrupt changes in the rates produced by down-slope deposits (Dowdeswell et al., 2002; Scourse et al., 2009).

5.3.4. Radiocarbon dating

Two radiocarbon dates were obtained from monospecific picks of *Neogloboquadrina pachyderma* sinistral and *Globigerina bulloides* from a sample at 8.5 and at 10 cm down-core in 20APC. They were dated by Beta Analytics and the results were calibrated using Calib14 and Marine13 database, with ΔR=-16±55 (Talma & Vogel, 1993; Reimer et al., 2013).

The sample at 8.5 cm was successively observed being collected from a disturbed interval. Only the sample from 10 cm was then included in the age model as a control point. Both dates are presented in Table 5.2 with conventional radiocarbon age and calibrated results.

Table 5.2: Radiocarbon dates information

Core depth(cm)	**Sample material**	**^{14}C Age (ka BP)**	**Calibrated age (ka BP)**	**Surrounding lithofacies**	**Laboratory code**
8.5	Mono NPS	19410 ± 90	22872 ± 250	LSM	440618
10	Mono G.B.	6340 ± 30	6820 ± 155	FM	450230

5.3.5. IRD analysis

Sixty-five samples from both cores wet washed and sieved, as previously described for foraminiferal analyses, were used for the additional investigation of the IRD present within the sediment record. The sampling interval follows a 10-15 cm resolution, in order to provide good coverage of the two cores. IRD concentration [IRD] was calculated for

the fraction > 150 μm as number of IRD grains/g of dry sediment (cf. Peck et al., 2006; Scourse et al., 2009; Haapaniemi et al., 2010). [IRD] from 20APC was converted to IRD fluxes using the following formula from Peck et al., 2007:

IRD flux= [IRD] X (LSR X ρDB)

Where: LSR=linear sedimentation rate obtained from 20APC (cm/ka) and ρDB= dry bulk density obtained from 20APC measured physical properties (g/cm^3).

After the lithofacies interpretation, IRD fluxes were calculated excluding the high IRD concentrations within the inferred turbiditic layers and Heinrich event intervals, focusing on the BIIS-discharged IRD content within the 20APC sediment record.

5.4 Results

5.4.1. Description

5.4.1.1 Lithofacies

Six lithofacies are recognised within the Rockall Trough sediments (Fig. 5.2) and classified based on their lithology, grain size sorting and average foraminiferal content, x-rays and physical properties.

Foraminifera bearing-mud (FM)

Light brown-grey sandy mud, rich in foraminifera, is identified at the core top and towards or at the bottom of both twin cores. The thickness of this facies varies between 10 cm and 70 cm (Fig. 5.3). Contacts appear as a gradual passage from, or to, grey muds. Bioturbation is present and burrows are identified on the core surface and on x-radiographs. The grain size spectrum shows a moderately sorted sandy mud (Fig. 5.2). L

values are measured around 50-60 and magnetic susceptibility shows values of 10-20*10^{-5} SI (Fig. 5.3).

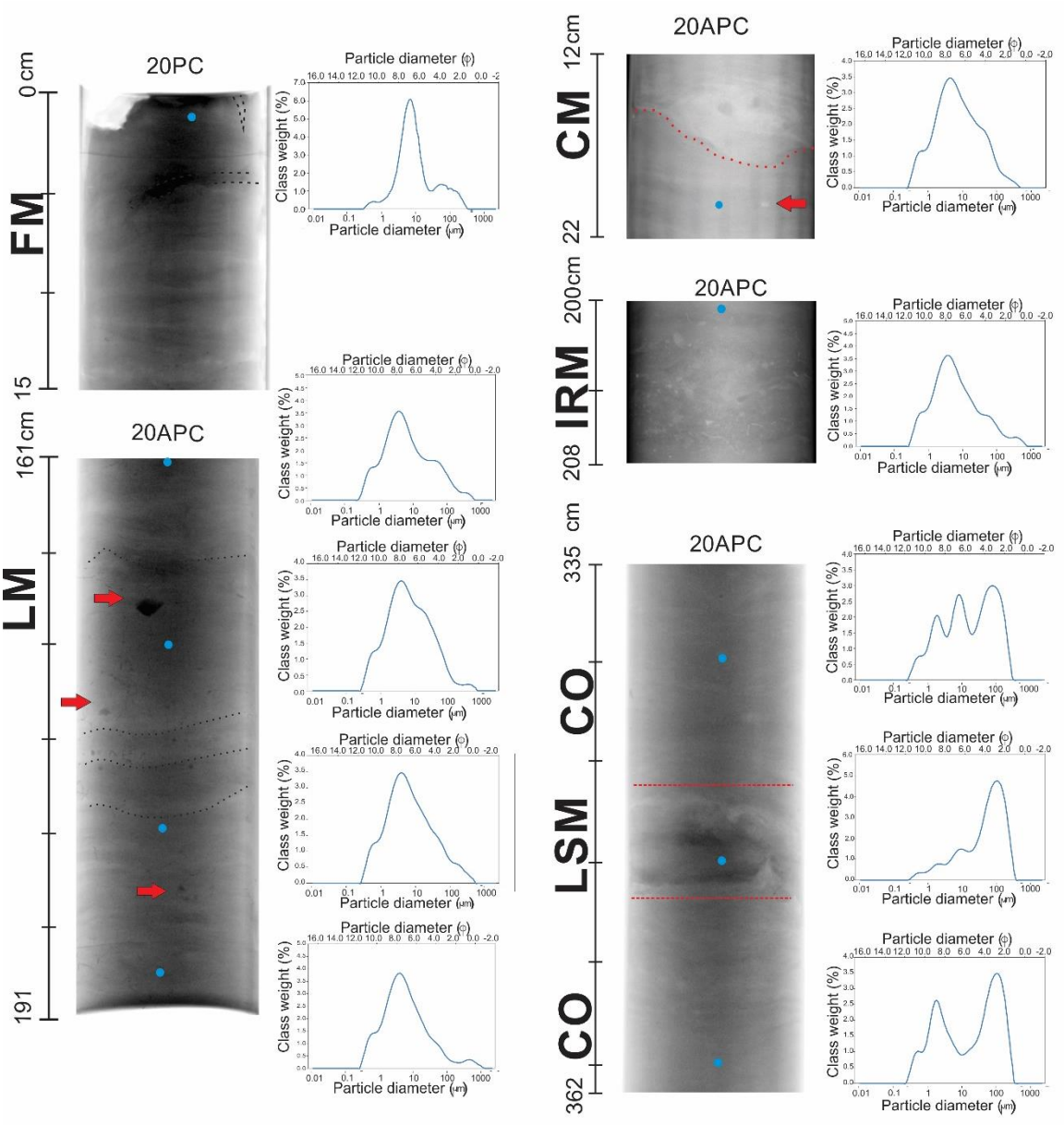

Figure 5.2: Examples of the six lithofacies on the x-radiographs. The grain size distribution of selected samples is shown (blue dots show the sampled location). Burrows, wavy laminations and a sharp contact with ripples are indicated by the dotted lines. The red arrows point to granule- and gravel-sized IRD grains. (FM=Foraminiferal-bearing mud; LM=laminated IRD-rich mud; CM=Chaotic mud; IRM=IRD-rich mud; CO=Calcareous ooze; LSM=Laminated sand to mud couplet).

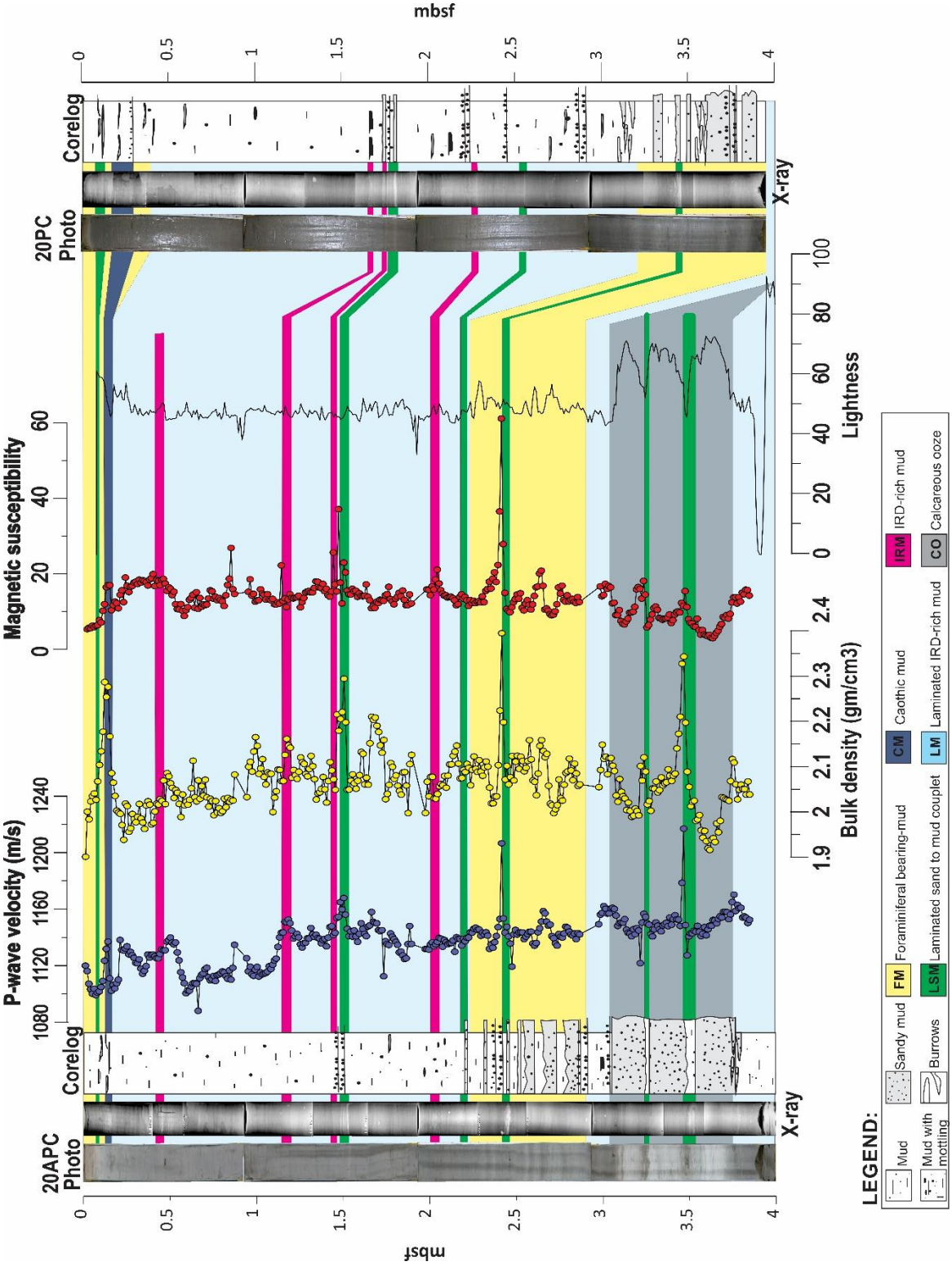

Figure 5.3: 20APC and 20PC lithostratigraphy. The lithofacies are identified by the different colours shading. The CO is identified only at the core bottom of 20APC. Above it, the two cores display the same stratigraphy.

Calcareous ooze (CO)

This facies contains white sandy mud, where the sand fraction is mostly composed of mm-scale foraminifera (over 50%). The facies is recognised only at the bottom of core 20APC in three intervals, with a thickness between 20-30 cm (Fig. 5.3). X-radiographs show light bioturbation and burrowing. Grain size analysis of several samples in this facies show a trimodal or polimodal distribution and very poor sorting (Fig. 5.2). The ooze presents low MS values, never higher than $10*10^{-5}$SI, and the maximum lightness values of all of the analysed sediment record, with peaks of 80 L (Fig. 5.3).

Laminated IRD-rich mud (LM)

The facies is a wavy-laminated, olive-brown mud, with sparse lithic clasts (Fig. 5.2). The laminations are not always visible to the naked eye but are evident in the x-radiographs throughout this facies. The facies shows a variable thickness, ranging from 5 cm to over 1 m along core (Fig. 5.3). Contacts with the bordering lithofacies are generally gradual. Grain size spectrum for the facies shows a unimodal (centred around 50 μm), poorly sorted sediment, with high clay content (i.e. 22.4%, 18.3%), coarse silt (i.e. 13.8%, 9.7%), and sand (i.e. up to 14%, 14.6 %) (Fig. 5.2). The LM lithofacies has low values of lightness, measured at approximately 50 L. Bulk density varies between 2 to 2.4 g/cm^3 and MS shows values around $20*10^{-5}$ SI (Fig. 5.3). The IRD content is represented mainly by limestone, basalt, quartzite, shale including mica and schist with variable sizes, ranging from a few mm to 2-3 cm.

IRD-rich mud (IRM)

The lithofacies is a greyish, light coloured, mud with thickness varying between 2 and 5 cm and largely lacking laminations of any kind (Fig. 5.3). IRD is abundant, grains have

a millimetric to centimetric diameter clearly visible on the x-radiographs, these are largely represented by calcareous whitish-yellowish grains (Fig. 5.2). Bioturbation is absent. Grain size analysis displays a unimodal, very poorly sorted sediment. A small increase in L values is recorded in correlation with this facies. Physical properties increased within the layers, with MS showing values between 20-40*10^{-5} SI (Fig. 5.3).

Laminated sand to mud couplets (LSM)

This facies is olive brown in colour with a thickness between a few cm and a maximum of 13 cm. LSM is represented by a laminated sand to mud couplets, with basal, well-sorted sand fining upward into mud. Six LSM are observed within 20APC, while only 4 are visible through 20PC. These intervals are largely observed within the foraminifera-bearing mud and the calcareous ooze lithofacies. The basal contact is generally sharp or erosive, and ripples are visible (Fig. 5.2). Bioturbation is absent and foraminifera content is scarce. All physical properties, and in particular the magnetic susceptibility (MS), reach high values in correspondence to these intervals, where MS is measured between 30-60*10^{-5} SI (Fig. 5.3).

Chaotic mud (CM)

The facies is a dark grey mud, massive and poorly sorted, with presence of sparse grains and sharp base contact (Fig. 5.2). No sedimentary structures are visible. It is only recognised at the core top of 20APC and 20PC, with a thickness varying between 5 cm to 15 between the two cores respectively. It passes gradually at the top to foraminiferal-bearing mud. High values of MS, p-wave velocity and bulk density are recorded through the physical properties (Fig. 5.3).

5.4.1.2. Biofacies and cluster analysis

Two-way cluster analysis built on the planktonic foraminifera relative abundances provides the dendrograms observed in Figure 5.4. Along the Q-MODE clusters, the clusters are grouped for similarities between the samples (numbers 1 to 7), whilst along the R-MODE, the clusters identify the similarities between the species (letters A to F). Five biofacies are identified and labelled on the crossed matrices as B1, B2, B3, B4 and B5, and are reported on the left hand side of the figure.

Biofacies 1 (B1) is represented by *Globigerina bulloides* (d'Orbigny, 1826), *Turborotalita quinqueloba* (Natland, 1938) and *Neogloboquadrina pachyderma* dextral (NPD) or *Neogloboquadrina incomputa* (Cifelli, 1961), dominating the assemblage. *Biofacies 2* (B2) is mainly represented by *Globigerina bulloides,* in association with *Turborotalita quinqueloba*. Few specimens of *Globorotalia menardii* (d'Orbigny, 1826) and *Globorotalia truncatulinoides* (d'Orbigny, 1839) are recognised within the B1 and B2 (Appendix 3). *Biofacies 3* (B3) shows a mix of temperate and sub-polar species, such as *Globigerina bulloides*, *Globigerina inflata* (d'Obrigny, 1838) and NPD, at the same time with a relative high abundance of *Neogloboquadrina pachyderma* sinistral (NPS) (Ehrenberg, 1861). *Biofacies 4* (B4) is represented exclusively by NPS and *Globigerina bulloides*. In *Biofacies 5* (B5) the polar species NPS, and the *Globigerina bulloides* still dominate but there is an increase in the abundance of *Turborotalita quinqueloba* and *Globorotalia scitula* (Brady, 1882).

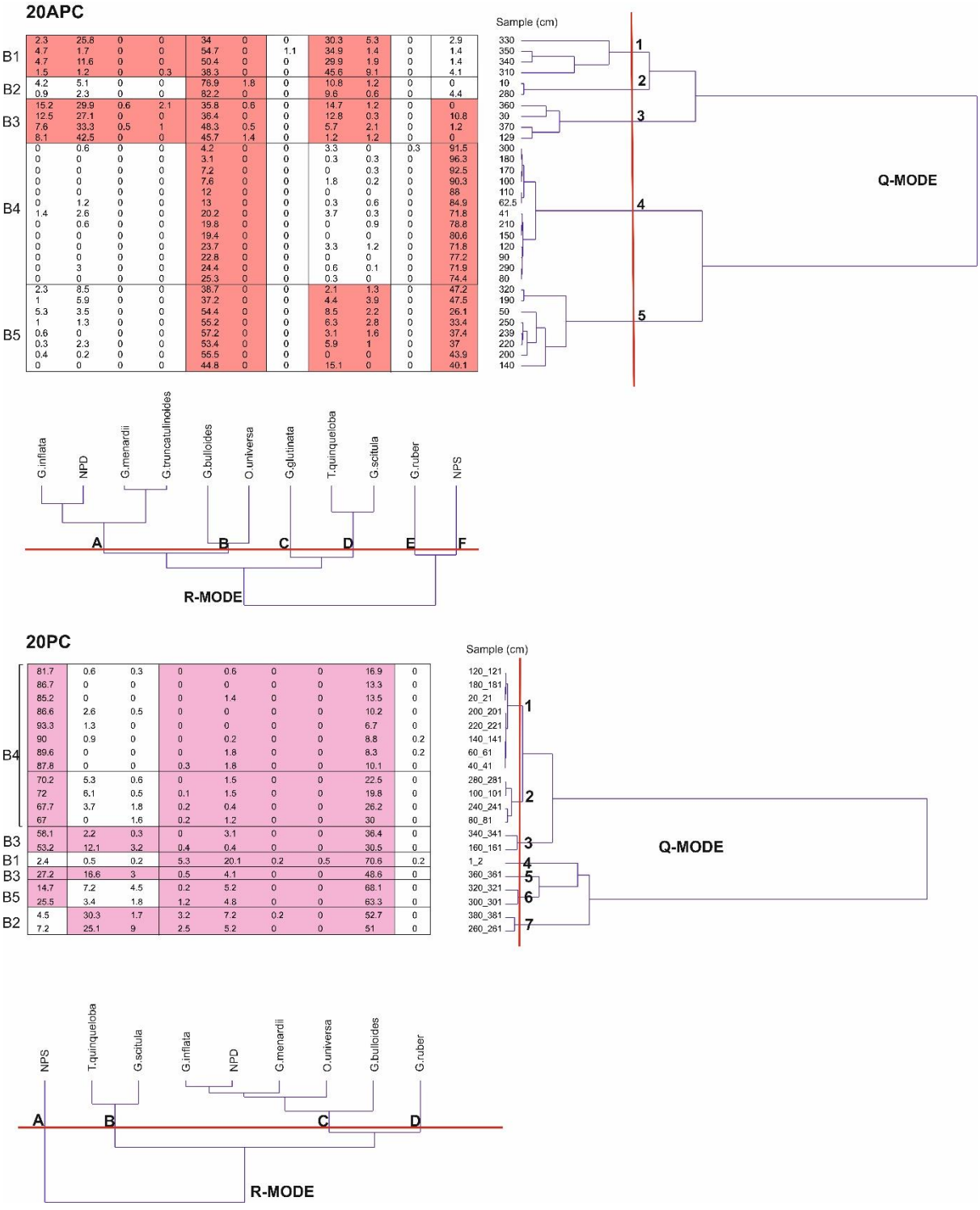

Figure 5.4: Two-way cluster analysis for 20APC and 20PC. The shading on the matrix represents the crossing between Q-mode and R-mode clusters used for the biofacies identification and description. The 5 biofacies identified are reported on the left-hand side and are discussed in the text. NPS=Neogloboquadrina pachyderma sinistral; NPD=Neogloboquadrina pachyderma dextral.

In 20A PC (Fig. 5.5), B1 is recognised at the core-bottom, across four samples between 310 cm and 350 cm down-core and corresponds with the calcareous ooze. B2 is recognised towards the top of the core at 10 cm and in the bottom half at 280 cm down-core, within the foraminifera-bearing mud. B4 is found in 13 of 22 samples between 30 cm and 300 cm down-core, within the laminated IRD-rich mud. Interspersed among laminated IRD-rich mud biofacies B3 (2 of 22 samples) and B5 (7 of 22) are observed. Two B3 facies are between 360 and 370 cm down-core, within the calcareous ooze, together with a B5 at 320 cm down-core.

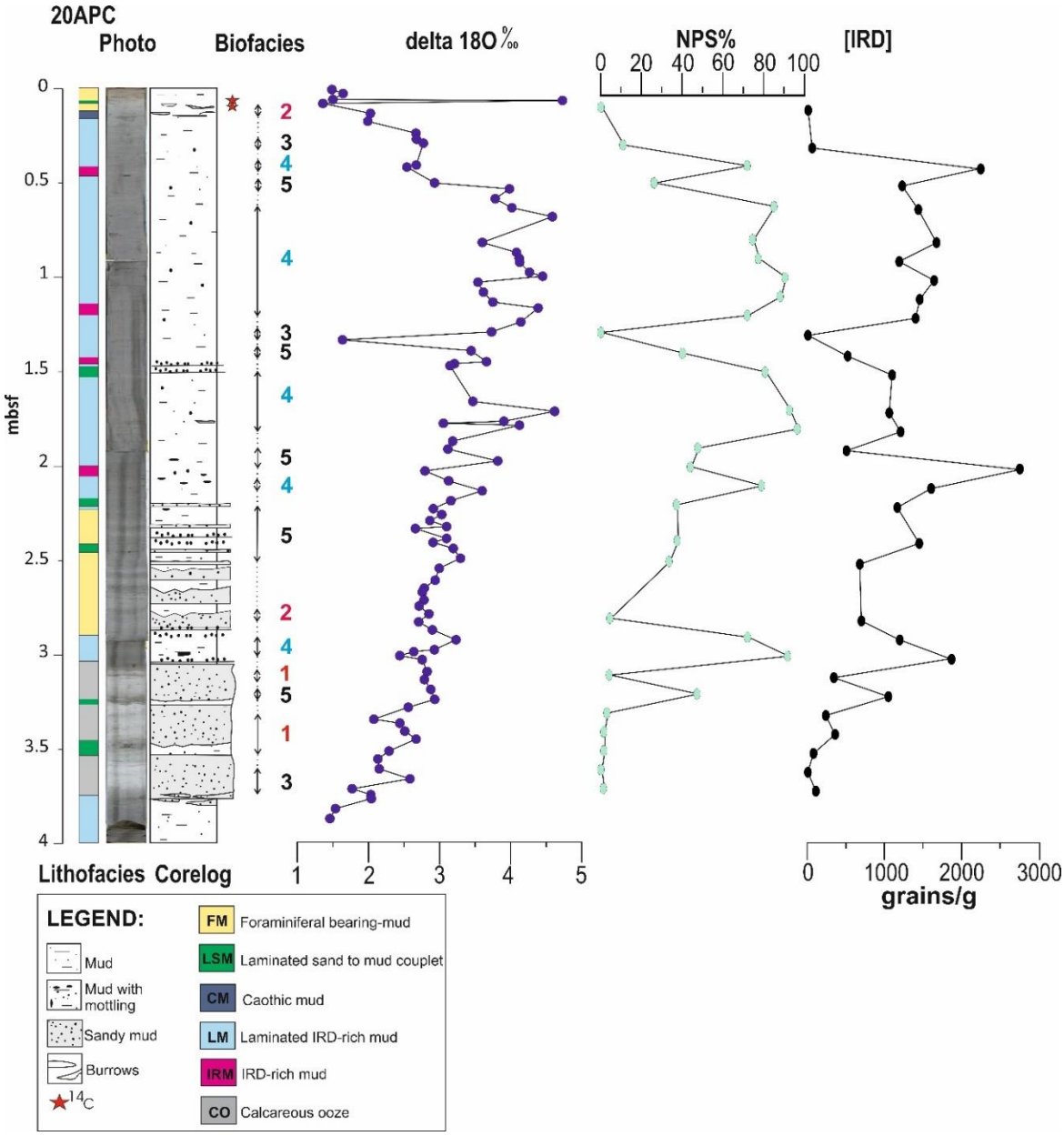

Figure 5.5: 20APC results with oxygen isotopic ratio, NPS% and [IRD] concentrations. High values in $\delta^{18}O$ correspond to high NPS% and [IRD], suggesting cold glacial intervals. Conversely, low values in all three parameters are indicative of warmer conditions such as interglacial and interstadial periods. The biofacies are marked in red for warm/temperate species assemblages, blue for cold assembles and black for assemblages representing intermediate conditions.

In core 20PC (Fig. 5.6), B1 is identified at the core-top where the sample was collected within the foraminifera-bearing mud, at 1 cm down-core. Between 20 cm and 280 cm, B4 was found within the laminated IRD-rich mud in 12 out of 14 samples. The core bottom

shows B5, B3 and B2 between 300 and 380 cm, with two samples each for B3 and B5 and one representing B2 at 380 cm down-core. The samples are collected from foraminiferal-bearing mud and upper contact with laminated mud IRD-rich lithofacies. B3 is also observed at 160 cm, within LM.

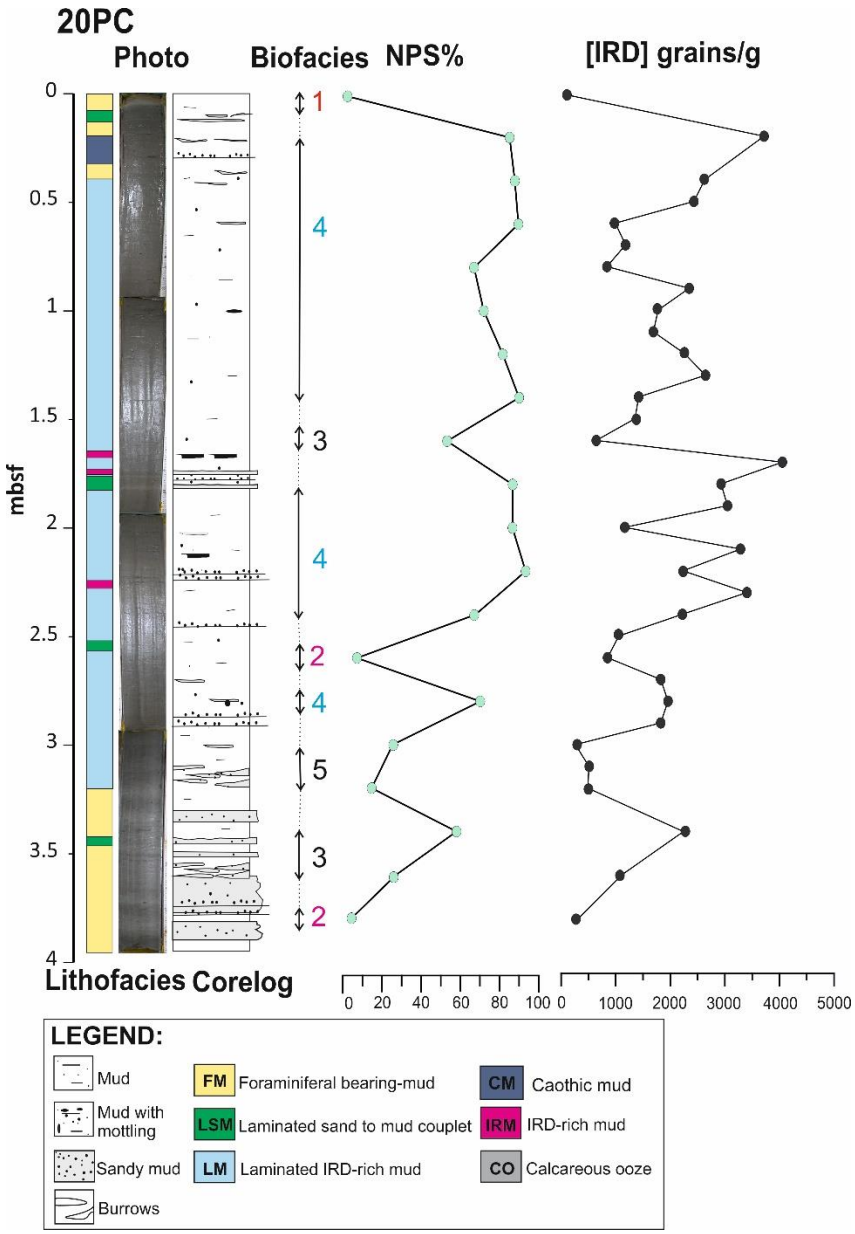

Figure 5.6: 20PC results with NPS%, [IRD] and biofacies. High values in NPS% and [IRD] suggest cold glacial intervals. Low values are indicative of warmer conditions. Biofacies as before are indicated in red for temperate foraminifera assemblages, blue for cold assemblages and black for intermediate conditions.

5.4.1.3. Oxygen isotope ratios

The oxygen isotopic ratios measured on the 87 samples, from core 20APC, range between light values of 1.5‰ and a heaviest of 4.7‰. The core top (down to 19 cm) and bottom (between 320 and 370cm) display similar values around 1.5‰. Corresponding with a laminated sand and mud couplet interval, the heaviest value in $\delta^{18}O$ (4.73‰) is observed 8.5 cm down-core. This value is considered as an outlier and therefore not used for this study because is collected from a reworked interval. Moreover, a sample for radiocarbon dating was collected from the same core location (see Table 5.2). This provided a conventional radiocarbon age of 19410 ± 90, comparable with the past glacial period and resulting in the heavy $\delta^{18}O$ (4.73‰), reinforcing the interpretation that the interval has been reworked.

From 10 cm down to 67 cm, a constant increase is observed, with $\delta^{18}O$ reaching 4.6‰. A more constant and heavy $\delta^{18}O$ is then observed with relative heavy values down to 129 cm, where an isolated light peak (1.63‰) is recorded (Fig. 5.5). Below 129 cm, the isotopic ratio rises again up to 4.6‰ at 165 cm down-core. After this point, a gradual decreasing pattern, with alternation of heavy and light ratio, is observed until the bottom of the core.

A correlation with the previously identified lithofacies and biofacies is also observed (Fig. 5.5). The $\delta^{18}O$ record displays light ratios in correspondence with the foraminiferal mud and calcareous ooze, while generally the heaviest values and intervals are recognised within the laminated IRD-rich mud. No particular correlation is observed within the LSM, CM and IRM. In relation to the biofacies, heavy isotope ratios are recorded along the same intervals where biofacies 4 is recognised; while biofacies 1 and 2 are generally observed corresponding to the light ratios (Fig. 5.5). Biofacies 3 and 5 are generally

observed in correlation to intermediate values, with the exception of the samples at 129 cm down-core, where the $\delta^{18}O$ as 1.63‰, is light (Fig. 5.5).

5.4.1.4. Neogloboquadrina pachyderma (sinistral)

The NPS abundance calculated through the 20APC sediment record shows an alternation of high and low values between 0% and 96% (Fig. 5.5). NPS is low at the core top, with values below 20%. Further down the core, a high percentage of NPS (>70%) is observed around 40 cm down core and again between 62 cm and 120 cm, reaching up to 85% at 62.5 cm. Below this interval, the abundance suddenly drops to 0%, but then it increases dramatically to values above 80% and reaches 96% between 150 and 180 cm. After this interval another decrease in abundance is observed to around 45% at 2 m down-core, with an overall gradual decrease in abundance to the bottom core. It is punctuated by several positive peaks at 210 cm (NPS >75%), at 300 cm (NPS >90%) and a smaller one at 320 cm (NPS > 45%). Below this bottom peak, the NPS% displays constant low values (< 3%) to the end of the core (Fig. 5.5). The NPS% mirrors the $\delta^{18}O$ curve, with high NPS% corresponding to heavy oxygen isotopic ratio. As observed for the $\delta^{18}O$ record, high NPS% is characteristic of the laminated IRD-rich muds and correlates well with biofacies 4, while low abundances correspond to foraminiferal mud and calcareous ooze lithofacies and biofacies 1, 2, 3 and 5.

In 20PC core (Fig. 5.6), NPS% is high between 20 cm and 60 cm down-core with NPS% > 80%, between 70% and 90% at 100 cm, 120 cm and 140 cm down-core. High abundance is also observed between 180 cm and 220 cm, with values > 85% (Fig. 5.6). After 220 cm, the abundance decreases towards lower values, until reaching < 5% at the core bottom. As seen for the twin core, in 20PC NPS% is high within the laminated IRD-rich mud lithofacies (LM) and Biofacies 4.

5.4.1.5. IRD concentration

IRD concentration along 20APC is on average 960 grains per gram of dry sediment per sample (Fig. 5.5). The highest value is recorded 200 cm down-core with 2750 grains/g of dry sediment, while the lowest values as low as 0 grains/g of dry sediment were measured at the core top, around 130 cm and at the core bottom. Generally, higher IRD concentrations [IRD] are recorded in correspondence to the peaks in NPS% and $\delta^{18}O$ ratios, in relation to the laminated IRD-rich muds (Fig. 5.5).

In 20PC, [IRD] is measured with an average value of 1520 grains/gr of dry sediment per sample. The highest peaks are at 20 cm, 170 cm and 190 cm down-core, in correspondence to IRD-rich mud lithofacies (IRM) and laminated sand and mud couplet lithofacies (LSM), with values of 3730, 4060 and 3060 grains/g respectively. Four peaks were recognised within the laminated mud lithofacies rich in IRD (LM): at 100 cm, 130 cm, 180 cm and 210 cm, their values range between 1700 and 3300 grains/g. The lowest [IRD] were calculated for the real top and bottom samples (1 cm and 380 cm down-core with values as low as 0), with 2-4% of NPS abundance and B1 and B2 in correlation (Fig. 5.6).

5.4.2. Interpretation

5.4.2.1. Lithofacies interpretation

The six described lithofacies were interpreted with reference to the specific depositional processes that can occur in a deep water environment, including deposition from turbidity currents and hemipelagic deposition with a contribution from meltwater plumes and iceberg rafting during glacial times (cf. Stow & Piper, 1984; Hesse et al., 1997; Stow & Mayall, 2000; Ó Cofaigh & Dowdeswell, 2001).

Hemipelagites

The foraminiferal-bearing mud FM is interpreted as a hemipelagite, a result of fine sediment settling through the water column (Howe, 1995; Stow et al., 1996). The facies is rich in foraminifera and bioturbation recognised through the presence of burrows. These features support the hypothesis of deposition in a quiet environment, allowing for the proliferation of infaunal organisms (Stow et al., 1996; Stow & Mayall, 2000; Howe, 1995; Knutz et al., 2002). The lithofacies was recognised at the top of the twin cores, at the bottom of 20PC and between 225-300 cm down-core in 20APC. The lithofacies is also characterised by biofacies 1 and 2, where the relevant foraminifera species are indicative of relatively warm climatic conditions, together with low NPS abundance, suggesting deposition during the Holocene and the previous interglacial period.

Also the calcareous ooze lithofacies is interpreted as a hemipelagite, characteristic of an intense warm interval and quiet environment (Howe, 1995; Stow et al., 1996). Calcareous ooze was not recognised in core 20PC; however, it was observed between 306 cm to 360 cm down-core in 20A PC. The coarser grain size and the higher values in lightness differentiates this facies from the FM. A similar sediment has been recognised in the North Atlantic and has been ascribed to deposition under a climate warmer than today and in particular as characteristic of the past interglacial period (McManus et al., 1994; Ovrebo et al., 2005; Zhuravleva et al., 2017). Biofacies 1 is present through the facies supporting a warm climatic condition during deposition, where *Globorotalia meanardii* and *Globorotalia truncatulinoides* allow comparison of this facies to the past interglacial (Ericson & Wollin, 1968, Broecker & van Donk, 1970).

Plumites

The LM lithofacies is interpreted as a meltwater plume deposit with a contribution of IRD deposition from floating icebergs (Wang & Hesse, 1996; Hesse et al., 1999; Ó Cofaigh & Dowdeswell, 2001; Evans et al., 2002; Lucchi et al., 2002). The facies is inferred as delivered by a turbid meltwater plume from the BIIS grounding on the Irish continental shelf, with the addition of melting icebergs. It is recognised in both the cores, between a depth of 35 cm to 315 cm for 20PC and between 50 cm and 225 cm down-core for 20APC. It is interpreted as characteristic of cold, glacial conditions during the BIIS extension. B4 is largely the most recognised biofacies within the lithofacies, where the high relative abundance of NPS% suggests cold climatic conditions and a southward extended polar front during deposition (Bond et al., 1993; Johannessen et al., 1994).

Heinrich layers

The IRM lithofacies, with its high content in whitish IRD grains, low thickness and visible light grey colour on the surface of the split core is interpreted as Heinrich (H) event layers (Heinrich, 1988; Hemming, 2004). Four inferred H-layers are recognised within the sediment record, they were interpreted as IRD delivered by floating icebergs from the Laurentide Ice Sheet (LIS).

Turbidites and mass transport deposits

The LSM is interpreted as a turbidite, a turbulent down-slope flow deposit (Middleton & Hampton, 1976; Lowe, 1979; Lowe, 1982). Sedimentary structures such as ripples, planar lamination, erosional basal contacts, high peaks in magnetic susceptibility and reduced thickness suggest that these are deposits of dilute, low-density turbidity currents (Wang

& Hesse, 1996; Hesse et al., 1997; Hesse et al., 1999; Knutz et al., 2002). The variable magnetic susceptibility values recorded are interpreted as variability in the chemical imprint of the sediments delivered. The Rockall Trough was influenced by down-slope flows, their origin was identified as terrigenous sediments delivered from the channel system on the eastern flank, or down-slope movements from the western flank, likely triggered by slope instability (Øvrebo et al., 2005; Georgiopoulou et al., 2012; Sacchetti et al., 2012). Although evidence suggests that the cores were retrieved in a quiet depositional environment, the Rockall Trough basin was known to receive down-slope deposits from different locations and some turbulent flows reached the studied location. The turbidites are inferred flowing through channels on the eastern margin of the RT, from the Donegal Barra Fan (DBF), generally active during the glacial intervals, with a marine extended BIIS, or triggered due to slope instability on the western RT side (Øvrebo et al., 2005; Georgiopoulou et al., 2012; Sacchetti et al., 2012).

A debrite or mass transport deposit is additionally inferred in the chaotic mud at the top of 20APC and 20PC. It is interpreted as result of a cohesive debris flow after identification of an erosive basal contact and the absence of internal structures (Holmes et al., 1998; Tripsanas & Piper, 2008). The interval is inferred as representing downslope deposit from one of the trough flanks as observed for the turbidites (Øvrebo et al., 2005; Georgiopoulou et al., 2012; Sacchetti et al., 2012).

5.4.2.2. Biofacies interpretation

The biofacies represent the result of correlation between the foraminifera assemblages and their distribution along the sediment record. The relative abundance of polar, sub-polar and temperate species within the clusters can be interpreted as representing relative

warm or cold climatic condition on the basis of previous reconstructed foraminiferal records in the North Atlantic Ocean (de Abreu et al., 2003; Hall et al., 2011). Moreover, an inferred sea-surface palaeotemperature (SST) is now presented for each biofacies, based on modern studies on coiling direction of *Neogloboquadrina pachyderma* in arctic environments. The species, already recognised as a qualitative proxy for polar front migration (Bond et al., 1993; Johannensen et al., 1994) is observed changing its coiling from right to left, between 11° and 6° C of SST (Eynaud, 2011). In this study, we infer low NPS abundance within the biofacies (between 5-10%) as representing SST > 11°, whilst high NPS% (>70%) as characteristic of SST < 6°C. Intermediate SST conditions, between 6° and 11°, are inferred considering the relative abundances of the species present in the specific biofacies. B1 is represented by sub-polar and temperate species, indicative of a relatively warm environment, where NPS% is lower than 4% and the SST is inferred as >11°C. B2 is still interpreted as representing relatively warm conditions for its abundance of temperate and sub-polar species, where NPS% is lower than 8% and the SST is inferred as approximately 11°. Modern SST measurements in the North Atlantic show values between 11° and 13°C, supporting the inferred SST in the biofacies as likely representing realistic values (http://www.ospo.noaa.gov/Products/ocean/sst/contour/). B4 is interpreted identifying colder climatic conditions than B2 and B1, with a non-diversified foraminiferal assemblage and NPS% >70%. The SST is inferred as <6 °. B3 and B5 are considered representing intermediate conditions between B1 and B4, where B3 is considered warmer than B5, because of the more diversified foraminiferal assemblage (i.e. *Globigerina inflata* and *Turborotalita quinqueloba*).

The five biofacies identified through cluster analysis present a particular distribution along core and consequently through time. In particular, B1 and B2 are recorded at the core tops and bottom, (Figs. 5.5 and 5.6), showing within the foraminiferal assemblage

specimens of *Globorotalia menardii* and *Globorotalia truncatulinoides*. The presence of these species are considered to be representative of modern Holocene climatic conditions or as likely related to the past interglacial (Ericson & Wollin, 1968, Broecker & van Donk, 1970). The sediment record analysed from the deep Rockall Trough is then interpreted to range from the last interglacial period (i.e. MIS5e), in correspondence of the calcareous ooze at the core bottom of 20APC, to the modern Holocene at the core top.

5.4.2.3. Age model framework

The NPS% and [IRD] results on the twin cores display a similar internal organisation, in accordance to the comparable stratigraphy shown in Fig. 5.3. 20APC is inferred as recording a longer and more compressed record in comparison to 20PC. This is interpreted as the result of the different piston coring procedures. The two cores were retrieved from the same location using two different barrel lengths, 12 m for 20APC and 6 m barrel for 20PC. The different barrel lengths and internal pressure responsible of the sediment recovery are likely responsible for the 20APC compaction (Skinner & McCave, 2003). 20APC is consequently the longer record acquired and therefore the one used for the age model.

An age model is presented for core 20APC by correlation of the $\delta^{18}O$ record with the oxygen isotope ratios from the Greenland Ice Core Project (GRIP) (Johnsen, et al., 1997). This was done following an initial correlation between *Neogloboquadrina pachyderma* sinistral abundance (NPS%), IRD concentration [IRD] and $\delta^{18}O$ record from 20APC (Fig. 5.5) with the $\delta^{18}O$ of SPECMAP (Imbrie et al., 1984) and Lisiecki & Raymo (2005) stack lines (Fig. 5.7). This allowed for the dentification of Marine Isotope Stages, up to MIS6,

and supported the tentative correlation of the 20APC $\delta^{18}O$ record with the Greenland Ice Core Project (GRIP) record (Johnsen, et al., 1997).

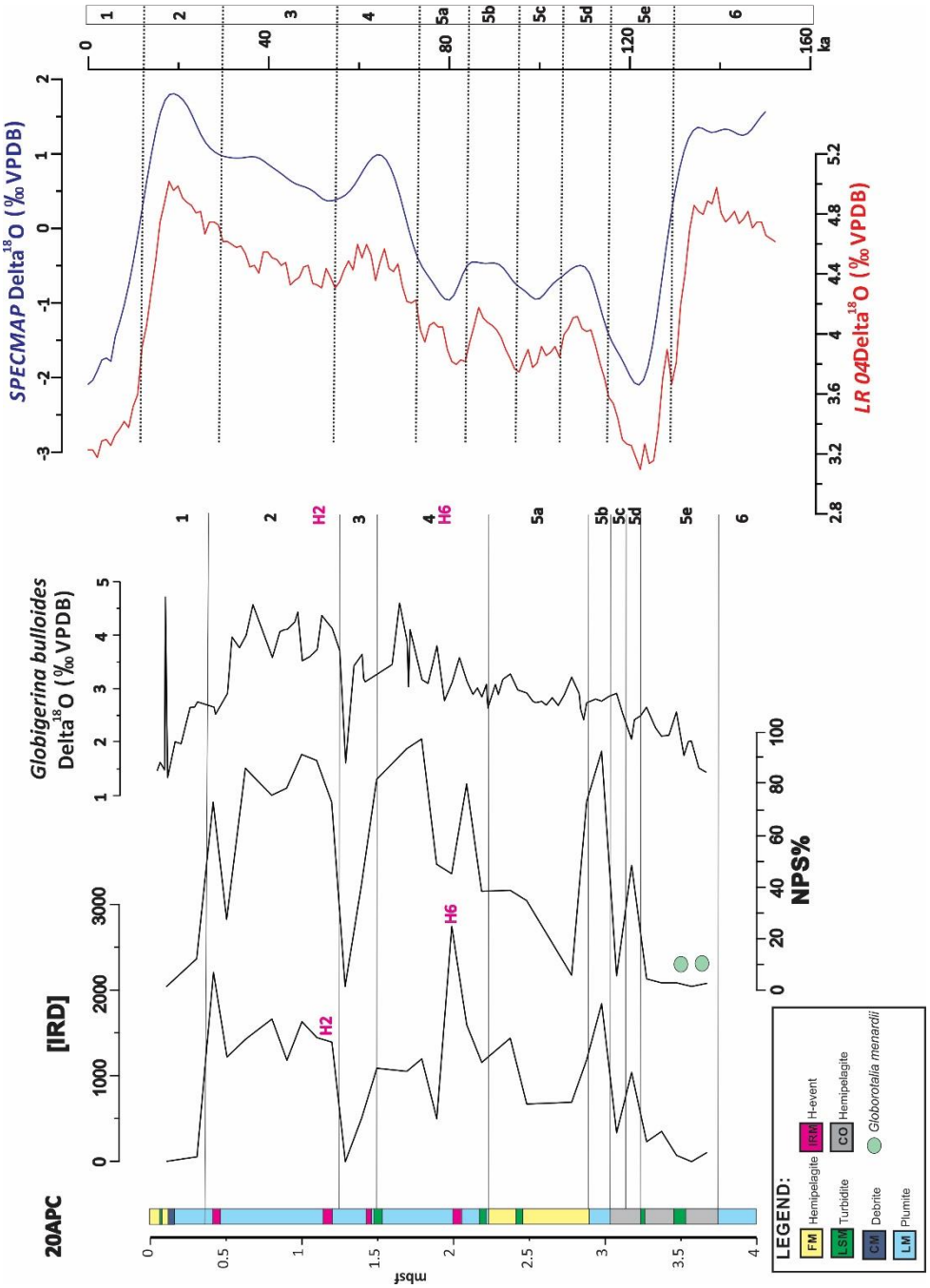

Figure 5.7: Lithofacies, [IRD] and NPS% show similar pattern with SPECMAP and LR04 stack lines. The MIS are shown on the 20APC record, with additional evidence from the Globorotalia menardii identification and the Heinrich events 6 and 2 highlighted through the IRD record.

Six marine isotopic stages are identified in the 20APC sediment record after the analysis of lithofacies, fossiliferous content, $\delta^{18}O$ record, NPS abundance and IRD content. The presence of the marker species *Globorotalia menardii* (light green dots in Fig. 5.7) suggests the deposition of calcareous ooze (CO in Fig. 5.7) during the last interglacial period (MIS5e). A similar facies, characterised by very high foraminiferal content was presented as characteristic of Eemian interstadial deposition, along the North Atlantic margin and the Rockall Trough flanks (Øvrebø et al., 2005). NPS% shows a correlation with polar front migration and display high and low values in accordance with transition between stadial and interstadial periods (Bond et al., 1993), such as low values during MIS 5e, 5a, MIS3 and the MIS1. A much higher abundance is observed occurring during MIS5b, MIS4 and MIS2 (Fig. 5.7). Within the IRD record, two intervals collected within the inferred H events at 200 and 110 cm downcore are observed under the microscope. The identification of whiteish calcareous IRD grains suggest that these intervals likely represent H events that, based on the stratigraphy, are recognised to occur during MIS2 and MIS4, respectively. These [IRD] rich events are suggested as representing H-2 and H-6, after considering their stratigraphic position along the core and the average sedimentation rates (average for similar water depth between 0.5 and 3 cm/ka) measured in the North-east Atlantic (Carvalho et al., 2011).

In addition, the $\delta^{18}O$ record shows a similar trend with the stack lines, highlighting increasing values within the plumites (MIS2, MIS4 and MIS5b), and generally low values within hemipelagites (MIS1, MIS3, MIS5e). Following the identified similarity with SPECMAP (Imbrie et al., 1984) and Lisiecki & Raymo (2005) stack lines, an initially 'event based' chronostratigraphy (Austin & Hibbert, 2012) can be proposed for 20APC.

5.4.2.3.1. 20APC and GRIP correlation

The proposed 20APC chronostratigraphy is based on an initial orbital tuning of the planktonic *Globigerina bulloides* $\delta^{18}O$ record and the single ^{14}C radiocarbon date from 20APC with the GRIP ice-core $\delta^{18}O$ record from Greenland (Fig. 5.8).

The features established for the chronostratigraphy included positive and negative peaks in $\delta^{18}O$ record for 20APC. Fourteen control points are identified and tuned within the records, labelled A to N, based on visual identification (Fig. 5.8). The two $\delta^{18}O$ curves (20APC and GRIP) show mirrored trends and in Fig. 5.8 the MIS are indicated for both the records. Tie points between the records are selected. A is recognised within MIS1 as the first high peak. B, C and D are selected sequentially within MIS2, after peak D was recognised in correspondence of an IRM layer, inferred as Heinrich event 2 (~ 25 ka). Following these, F and G are identified in MIS4, where F is observed as H6 event at ~61 ka and G follows as the next positive peak. Peak E, in MIS3, is inserted between the previously identified as the lowest values in between D and F. Peak H follows as the next largest decrease in $\delta^{18}O$ as transition to MIS5, then I is identified as the highest peak before a general decreasing trend. Inside this decreasing pattern, J, K, L, M and N are identified as the major fluctuations (highest-lowest peaks). The chronology of the upper part of the core is additionally constrained using the one radiocarbon date obtained at 10 cm down-core, with a calibrated age of 6,820 ± 155 a BP (Table 5.2). Marine Isotopic Stages (MIS) and their boundaries are inserted after Lisiecki & Raymo (2005) (Fig. 5.8). The qualitative interpretation for this correlation is considered as the main limitation of this work. The proposed age model presents a high level of uncertainty and requires the further testing of this correlation with future analysis.

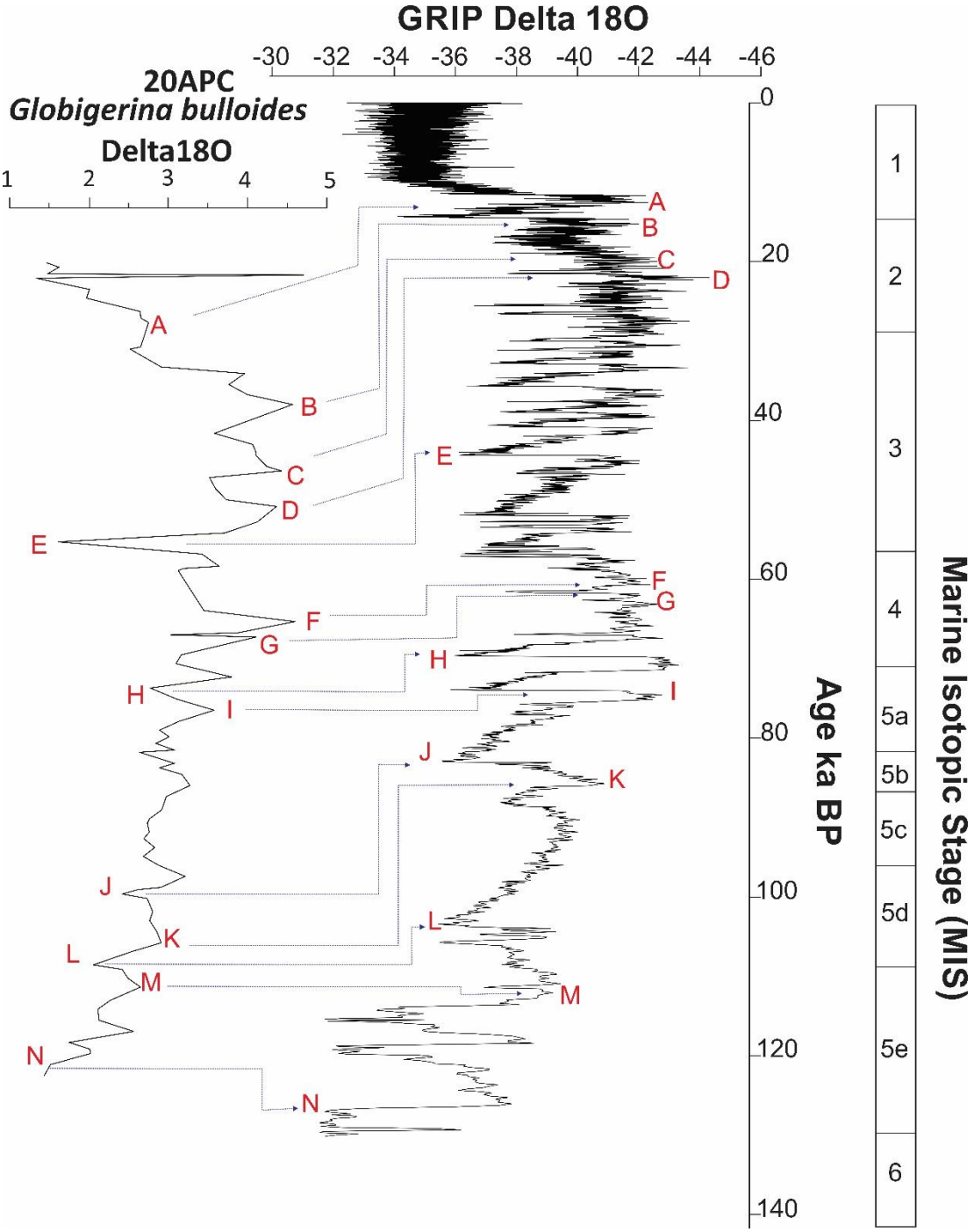

Figure 5.8: Initial tuning of CE20APC $\delta^{18}O$ record, with GRIP from Greenland ice core $\delta^{18}O$ record. 14 peaks were identified and correlated, the peaks are identified also through [IRD] and NPS%. The red letters identified the points used for the creation of the age model.

The calculated age model is reported in Figure 5.9 and shows that the sediment record is therefore constrained to the last 130 ka BP.

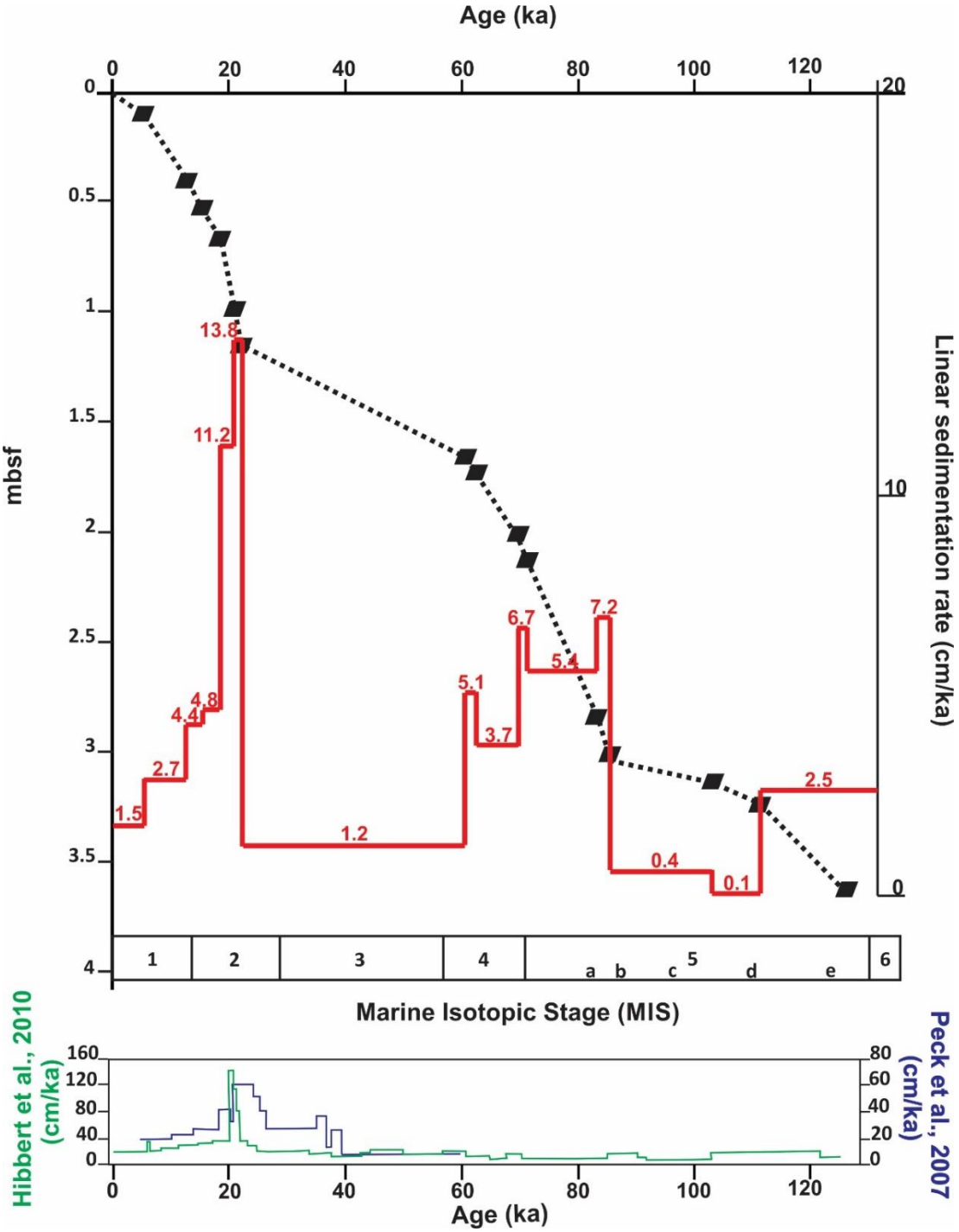

Figure 5.9: Composite age model for 20APC based on radiocarbon date and previous orbital tuning. Linear sedimentation rates are calculated on the basis of the age model and indicated by the red line. MIS boundaries are marked following Lisiecki & Raymo (2005). Linear sedimentation rates from vicinity cored locations show how the highest rates are recorded during MIS2.

5.4.2.4. Sedimentation rates and IRD fluxes

Based on the calculated age model for core 20APC (Fig. 5.9), linear sedimentation rates were calculated between each pair of adjoining samples and are shown in figure 5.9 by a red line against time. The variability in sedimentation rates through time is clearly apparent and indicated by the compact record of 20APC, also interpreted as representing minimum rates.

During MIS5, values range from a minimum of 0.1 cm/ka, to a maximum of 7.2 cm/ka. The highest rates are observed during MIS5a and MIS5b (Fig. 5.9), with values of 5.4 cm/ka and 7.2 cm/ka, respectively. Extremely low values (i.e. 0.1 and 0.4 cm/ka) are measured between MIS5d and MIS5c; while MIS5e records 2.5 cm/ka. During MIS4, rates are relatively high, with a maximum value of 6.7 cm/ka (Fig. 5.9). MIS3 shows a rather sharp decrease in sedimentation, with a rate of 1.2 cm/ka. A significant increase is observed at the passage to MIS2, where the calculated sedimentation rates are between 13.8 cm/ka and 11.2 cm/ka and are the highest within the 20APC sediment record. Previously calculated sedimentation rates along the BIIS western margin showed how the ice sheet was delivering sediment to the deep water with maximum values reached during the MIS2 (Peck et al., 2007; Hibbert et al., 2010). A decrease in sedimentation rates then follows into MIS1, from 4.8 cm/ka to 2.7 cm/ka and 1.5 cm/ka during the last 6,000 years. The values calculated for the 20APC are lower than the ones reported from previous studies, supporting the inferred compaction of the analysed sediment record. The difference in sedimentation rates is also justified by the different character of sedimentation, as the trough location is characterised by slow settling of meltwater plume sediments; while the other locations experienced deposition from ice streaming.

The calculation of the rates allowed for the conversion of IRD concentrations into IRD fluxes (Fig. 5.10), used to highlight the IRD deposition that can be attributed to the BIIS. Three main periods of BIIS-sources IRD deposition seem to be recorded within core 20APC, during MIS5b, MIS4 and MIS2. The values vary from a maximum 30000 (grains cm^{-2} ka^{-1}) between 20 and 18 ka BP, to 2500 (grains cm^{-2} ka-1) following 60, and 20000 (grains cm^{-2} ka^{-1}) between 85-80 ka (Fig. 5.10).

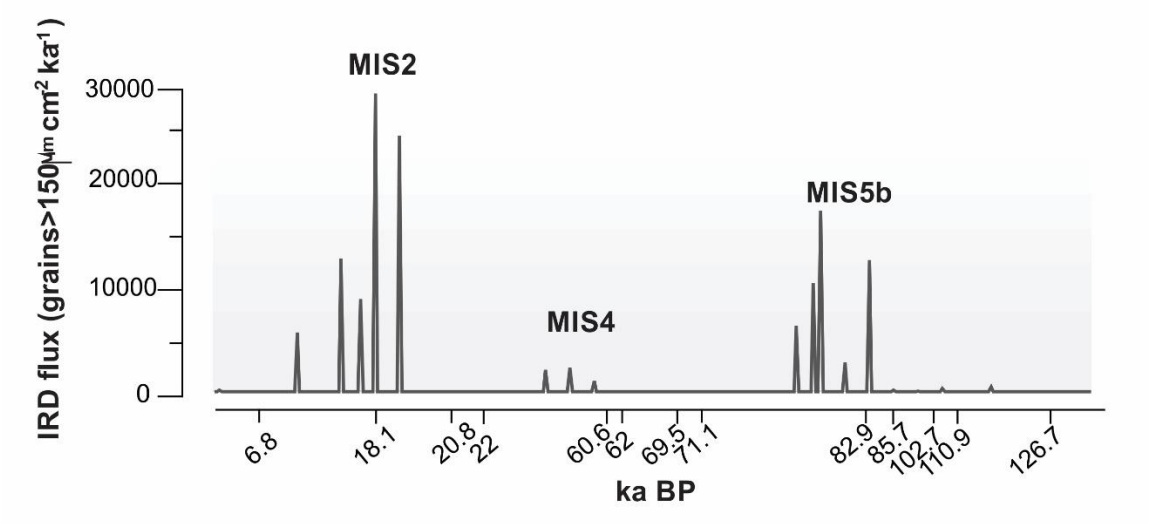

Figure 5.10: IRD fluxes calculated for 20APC. The MIS are inserted to indicate the relative Marine Isotopic Stages.

5.5. Discussion

5.5.1. Sedimentary processes and climate in the Rockall Trough since the previous interglacial

The sediments described in 20APC and 20PC are interpreted as a mostly continuous record, with no obvious hiatuses or large erosional surfaces, representing the last ~130 ka of depositional history of the Rockall Trough (Fig. 5.11).

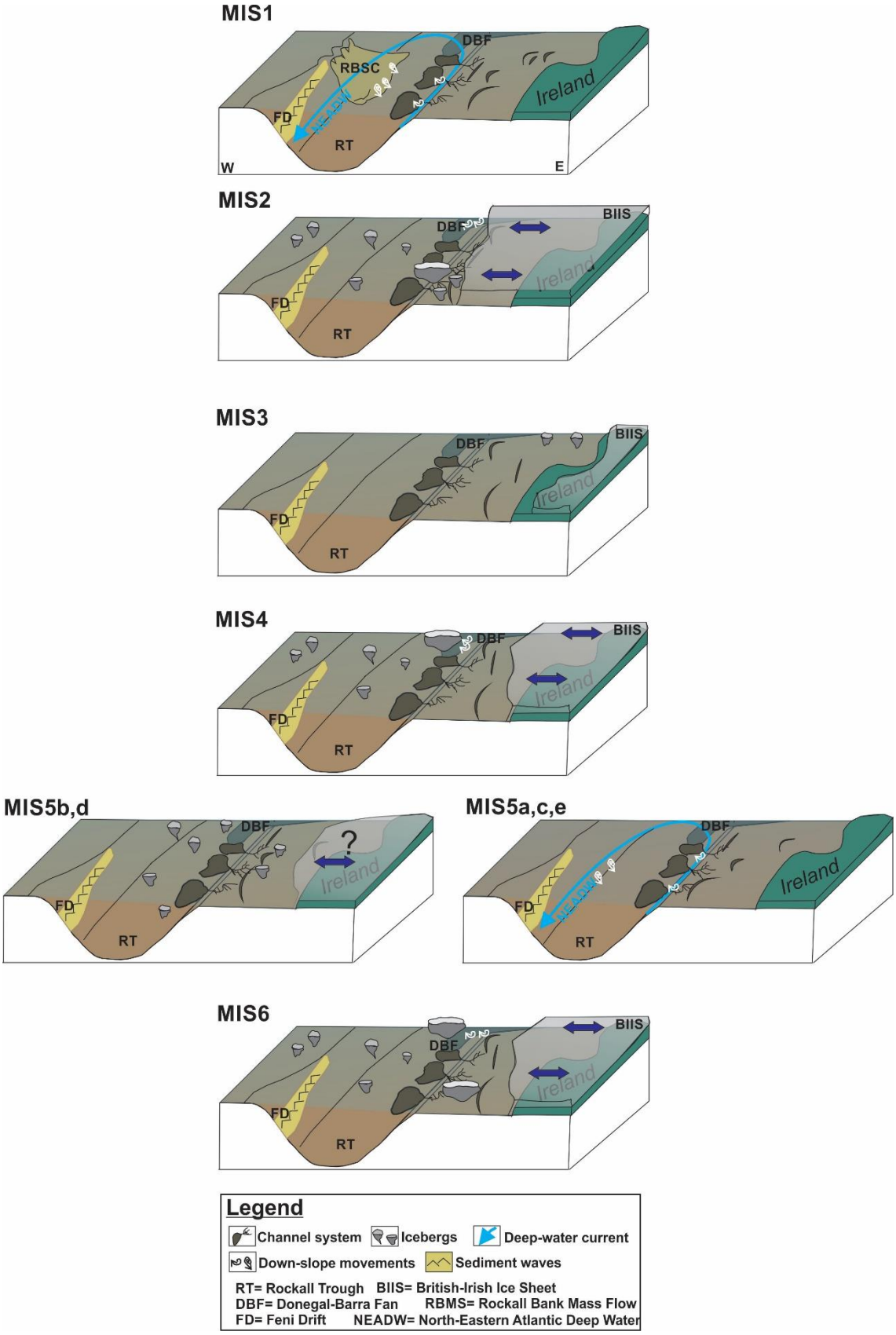

Figure 5.11: Reconstruction of the sedimentary evolution of the Irish margin since the end of MIS6 glaciation, with illustrated relative depositional processes.

These cores record changes in the sedimentary processes, in a relative quiet depositional area, not influenced by large down-slope movements (covering approximately 7.5% of the core length) but where the sedimentation was reconstructed as mainly as hemipelagic and plumitic (over 90%).

At the bottom of the sediment record, the glaciomarine sediment constituted by the laminated IRD-rich mud is inferred to be likely recording the termination of the glacial period occurring during MIS6 (Fig. 5.11).

The BIIS extension within MIS6 was previously recognised using seismic data along Western Britain and Ireland and from an IRD record investigation in deep water areas in the North Atlantic, on the western border of the Barra Fan (Sejrup et al., 2005; Hibbert et al., 2010). The presence of IRD showed a marine-extended BIIS at that time, and allowed the inference of a BIIS calving margin along the Hebrides continental shelf, west of Scotland (Hibbert et al., 2010). The following retreat and passage to interglacial conditions was interpreted as the result of rapid withdrawal of the polar front towards northern latitudes, and an increase in sea-level (Hibbert et al., 2010; Shackleton et al., 2000; Siddall et al., 2003). The IRD at the bottom of core 20APC shows the presence of icebergs as far south as 54°N and therefore suggests a possible ice sheet presence also occurring along the Irish sector of the BIIS at that time (Fig. 5.11).

The sediment record from the Rockall Trough thus allows a full reconstruction of the processes occurring during the various stages of MIS5 (Fig. 5.11). During MIS5, sedimentation appears to be mostly hemipelagic or plumitic, with the rare occurrence of turbiditic flows reaching this part of the basin.

MIS5 stadial and interstadial periods are shown within the sediment record by fluctuating sedimentation rates (from 7.2 cm/ka in MIS5b to 0.1 cm/ka in MIS5d; Fig. 5.9) and the

alternation between relatively low and high values in the three proxies: $\delta^{18}O$ ratio, NPS% and [IRD] (Fig. 5.12).

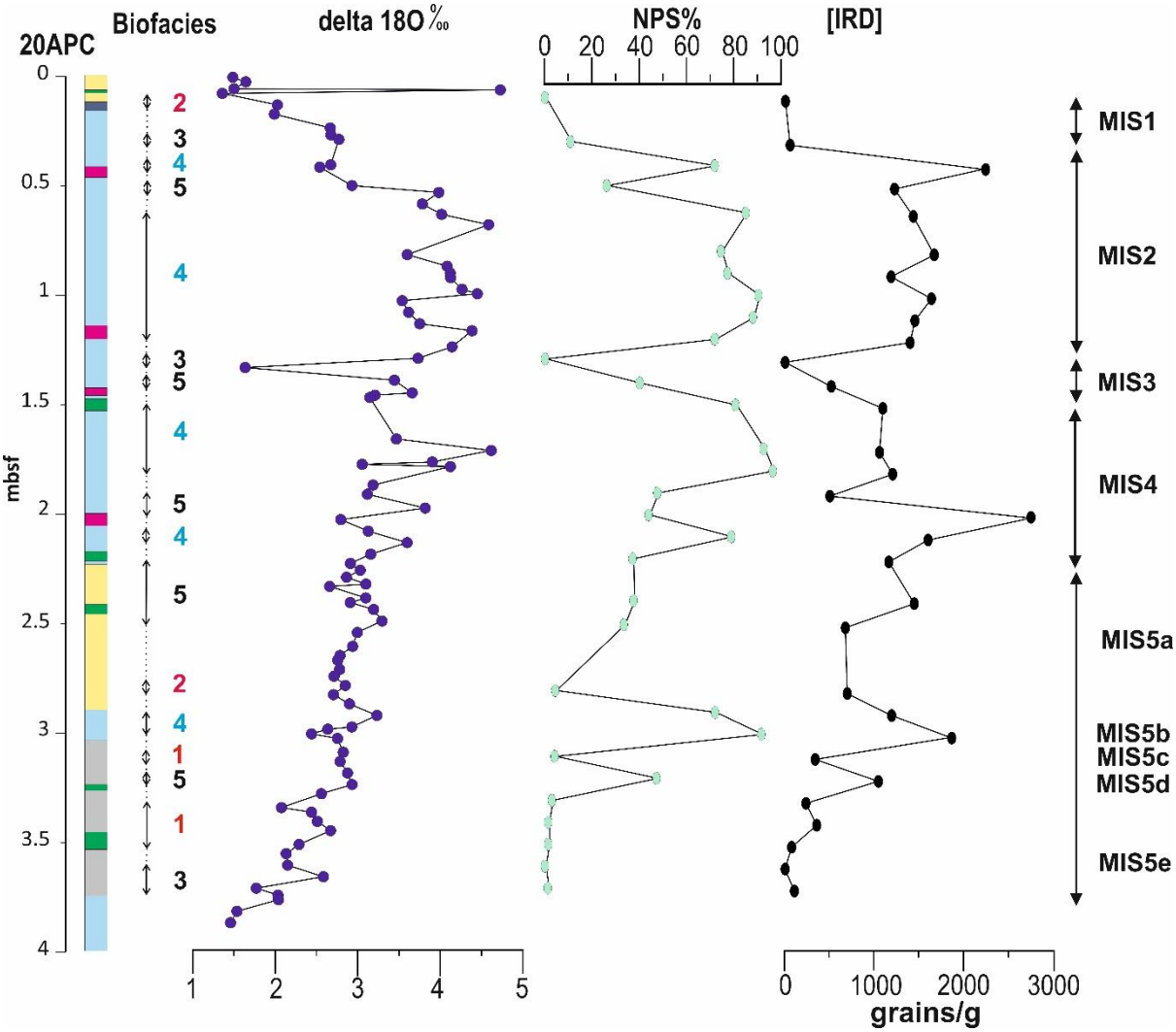

Figure 5.12: Summary of the results from 20APC, the MIS intervals are reported on the right.

During MIS5e hemipelagic sediment, with a calculated sedimentation rates of 2.5 cm/ka is recognised with $\delta^{18}O$ between 1.5 and 2 ‰, <3% NPS% and no recorded IRD grains. B1 and B3 suggest a progressively increase in SST, reaching values > 11 °C. The recognition of B1 with a large foraminiferal diversification within the assemblage, together with *Globorotalia menardii*, supports deposition of the sediments during the past

interglacial period (Ericson & Wollin, 1968; Broecker & van Donk, 1970). Within the interstadials MIS5a and MIS5c a relatively low NPS% (reaching a maximum of 30%), low IRD concentrations and increasing (2.5-3.5‰) $\delta^{18}O$ values are identified, together with inferred SST decreasing from 11°C towards lower values up to MIS5a (Fig. 5.12).

The stadial periods MIS5b and MIS5d are characterised by peaks in the IRD concentration, a heavy $\delta^{18}O$ and high NPS% in correlation with B4 and B5, representing SST <6°C. The proxies suggest a general transition to a colder climate, with gradual decrease in SST. An increase in the sedimentation rate is also observed within MIS5b, where [IRD] are measured within a plumite reaching 1840 grains/g.

On the basis of this evidence, the Rockall trough is recording relatively warm climatic conditions, where fine sediment settling represents the main depositional process during MIS5e (Fig. 5.11). Following this period, the BIIS marine-extension and meltwater plume deposition is evident. A BIIS marine termination is inferred advancing during MIS5b, delivering meltwater and icebergs to the Rockall Trough (Fig. 5.11). The relative age of the IRD record analysed in the study, suggests a BIIS retreating during MIS5b with large discharge of icebergs in the trough recorded between 85 and 80 ka BP (Fig. 5.11). Intermediate condition, between MIS5e and MIS5b are inferred for MIS5a, with a no-marine extended BIIS.

Starting from the MIS5d, IRD have been observed within the North Atlantic and are related to the initial development of ice masses, with increase in ice-volume and consequent marine ice sheet extension (Broecker et al., 1993; McManus et al., 1994; Chapman & Shackleton, 1999). This growth in ice-extent is guided by changes in oceanic circulation (i.e. AMOC) responsible for heat distribution to northern latitude, provoking the end of the interglacial period and forcing the beginning of the glacial period during MIS5d (Adkins et al., 1997; Hald et al., 2001; McManus et al., 2004). In the Rockall

Trough, this trend is observed in the IRD record, NPS% and $\delta^{18}O$ (Fig. 5.12). The trough sediment record is consequently interpreted as free from the influence of an extended BIIS during MIS5e and recording a growing BIIS, during the transition from MIS5d up to MIS5b (Fig. 5.11).

During MIS4 the sedimentation in the trough is observed as largely related to meltwater plume deposition, where two Heinrich event intervals are highlighted by layers enriched in IRD. Sedimentation rates are calculated with a maximum value of 6.7 cm/ka and a minimum of 3.7 cm/ka and are higher than during the previous MIS (Fig. 5.9). The $\delta^{18}O$ record displays several heavy points in the ‰ ratios, reaching 3.5-4 ‰. NPS% increases over 70% and the [IRD] extent to a maximum of 2740 grain/g (Fig. 5.12). In addition, B4 largely represented within the planktonic foraminifera biofacies suggests a SST < 6°C.

Plumites with high sedimentation rates support an extended BIIS along the Irish continental shelf, where larger amount of icebergs with related IRD deposition are recorded ~ 60 ka BP (Fig. 5.10).

During MIS4 global ice-volume has been recorded to have increased (Chapman & Shackleton, 1999), with evidence of the extension of northern European ice sheets at the same time (Sejrup et al., 2000; Gemmell et al., 2007). Also, the BIIS was recorded extending offshore during this period (Hibbert et al., 2010). Calving of the BIIS ice-margin and deposition of IRD along the western side of the Barra Fan were inferred as demonstrating ice-sheet retreat after oscillation of the sea-level that likely drove the BIIS ice-margin to collapse during MIS4 (Arz et al., 2007; Hibbert et al., 2010).

In the Rockall Trough, the transition to MIS3 is identified within the plumites through a recorded increase in sea-surface temperature with B3 and B5, together with a very light oxygen isotopic ratio (1.63‰). A similar decrease is reported in the NPS%=0 and there

is no record in the [IRD] (Fig. 5.12). The rise in SST is suggesting a transitional warming environment, between the two cold stadials MIS4 and MIS2.

MIS3 is interpreted as an interval with a small extended BIIS along its western margin, where sedimentation rates are low, ~1.2 cm/ka with a scarce deposition from melting icebergs (Fig. 5.11). The marine-based BIIS likely occurring around Scotland during that time observed by Hibbert et al., 2010, could support the light $\delta\,^{18}O$ ratio, correlated with SST values between 6° and 11°C.

The Rockall Trough sediment record during MIS 2 is represented by plumites. Sedimentation rates are between 13.8 cm/ka and 4.4 cm/ka, showing the highest values measured within the record analysed (Fig. 5.9). $\Delta^{18}O$ ratio reaches 4.58‰, NPS% is over 70% and [IRD] increases to an average value of 1520 grains/g, together with the identification of B4 and an inferred SST < 6°C (Fig. 5.12). During MIS2 the sedimentation in the trough is largely related to meltwater plume deposition, together with icebergs floating and consequently IRD discharge coming from the BIIS (Fig. 5.11). Abundant IRD are observed following 20 ka BP (Fig. 5.10), these are interpreted as representing BIIS western extent retreat through calving. Ice sheet maximum extent is suggested pre-dating these IRD fluxes as occurring before ~20 ka BP. BIIS retreating on the shelf is inferred through IRD from the Rockall Trough up to 18 ka BP. Previous studies along the Irish slope and continental shelf show that the BIIS maximum extent along the shelf break was reached during MIS2, and in particular likely before the global LGM around 21 ka BP (Sacchetti et al., 2012, Ó Cofaigh et al., 2012; Peters et al., 2016). Within this marine isotopic stage, the BIIS is interpreted to have reached its maximum south-west extension along the north Atlantic margin with its highest measured sedimentation rates (Fig. 5.11).

The increase in SST, shown by the following decrease in NPS%, suggests a backward migration of the polar front (Fig. 5.12). This can be interpreted as a potential cause of the BIIS final retreat, as it was hypothesized for the transition between MIS6 and MIS5 (Hibbert et al., 2010; Shackleton et al., 2000; Siddall et al., 2003).

Sedimentation during MIS1 is represented by hemipelagites and down-slope deposits (Fig. 5.11). The NPS%, [IRD] and $\delta^{18}O$ ratio all present minimum values. In the sediments from MIS1, biofacies B1 and B2 suggest similar climatic condition to the previous interglacial, MIS5e, and a SST >11°C. Sedimentation rates are measured between 2.7 cm/ka and 1.5 cm/ka (Fig. 5.9), similar as well to the values measured during the previous interglacial, MIS5e.

Overall, the sedimentation in the Rockall Trough occurred predominantly by settling of fine-grained sediment and large scale down-slope movements during interglacials, and with deposition from glacial meltwater plumes and ice rafting during glacial and stadial intervals. Turbidites are observed occurring during interglacial and interstadial periods. These may potentially be related to larger slope instability from the trough flanks during interglacial and interstadial, such as the Rockall Bank Slide Complex which is known to have been active following the last glacial period (Georgiopoulou et al., 2013).

5.5.2. IRD record in deep water and BIIS calving margins

The BIIS was a marine-terminating ice sheet that has been intensively studied in recent times and its past behaviour has been under investigation because its implication in providing a meaningful analogue for modern ice sheets (i.e. West Antarctica), as well as information about past climate change across the North Atlantic Ocean (Bradwell et al., 2008; Clark et al., 2012a; Ó Cofaigh et al., 2012; Ballantyne & Ó Cofaigh, 2017).

Analysis of seismic data showed that the BIIS extended several times across the North Atlantic continental shelf during glacial periods and, on occasions, as far as the shelf edge (Stoker et al., 1995). Transport of glaciogenic sediments across the continental margin seems to have started in the Early Pleistocene (Elliot et al., 2006), however limited evidence exists on the glacial advances before the last BIIS glacial maximum (LGM) and most of the recent studies actually focussed on its last maximum extent and subsequent deglaciation (Ó Cofaigh et al., 2012; Clark et al., 2012a; Ballantyne & Ó Cofaigh, 2017). The BIIS largely extended across the Irish and UK continental shelf during the last glaciation (Knutz et al., 2001; Bradwell et al., 2008; Scourse et al., 2009; Benetti et al.; 2010; Ó Cofaigh et al., 2012; Peters et al., 2015; 2016). It reached its maximum extent at the Irish shelf-edge at ~24 ka (Ó Cofaigh et al., 2012; Peters et al., 2016). Limited dating on the deglaciation from marine sediments suggests that the ice had started retreating from the shelf break around 22 ka, possibly due to a rise in sea level (Ó Cofaigh et al., 2012; Peters et al., 2015; 2016). The limitation of these previous works on the BIIS dynamics is related to the fact that the results were obtained working with shallow water (i.e. shelf) sediments, generally displaying a short recovery and major reworking compared to the deeper water records.

In this study, the cores are from a deep-water location, which was largely unaffected by mass transport and reworking; therefore, a longer sediment record, covering the entire last glacial period, can be analysed. The calculation of the IRD fluxes presented in this study, now opens the possibility of investigating the dynamic behaviour of the BIIS through the entirety of the last glaciation. The attempted chronology of 20APC, based on oxygen isotope ratios in correlation with ice core record from Greenland, represents an initial time constrain for the sedimentary history recorded in the SE RT. The timing of

the IRD discharge to the deep water environment appears to fit with the previous reconstructions of the western extent of the BIIS.

Peaks in IRD fluxes in the Rockall Trough are identified during MIS2, MIS4 and MIS5b (Fig. 5.10). The oldest interval is recognised between 85 ka and 80 ka, corresponding to MIS5b. The sediment record during this period is represented by meltwater plume deposits with relatively high IRD concentration. Studies based on deep sea oxygen isotopic ratios and global ice volume reconstruction showed a gradual building up of the continental ice sheets between MIS5e and MIS5d (McManus et al., 1994; Chapman & Shackleton, 1999). A similar behaviour can be suggested for the BIIS, with initial build up and a marine extension with meltwater plume deposition and consequent marine-termini collapse, through the stadial and interstadial periods of the MIS5. IRD fluxes have been observed with a similar timing in the northern Rockall Trough by earlier studies, and interpreted as delivered by floating icebergs moved by changes in oceanographic context and not related to an advanced BIIS (Hibbert et al., 2010). Within the current IRD record in the Rockall Trough, no particular petrological differences have been observed between the fluxes, and for this reason the BIIS can be suggested as the main delivering source of icebergs. These fluxes could represent the first recorded BIIS advance offshore within the last glacial period and additional chemical analysis and provenance studies are highly recommended to verify this interpretation.

During MIS4, IRD fluxes are identified within meltwater deposits at approximately 60 ka. The BIIS is inferred as marine-extended during this interval of time (Fig. 5.11) and the IRD record is used in support of the identification of a BIIS retreating margin through calving after 60 ka. An offshore extended BIIS was previously recorded through IRD investigations and it was constrained to 70 ka BP along the North-West Britain (Hibbert

al., 2010). The lower IRD input recorded during MIS4, compared to MIS5b (Fig. 5.10) can be justified by a farther located ice-margin.

During MIS2, significant IRD peaks are recognised between 20 and 18 ka (Fig. 5.10). The shelf record suggests that approximately at this time the BIIS had started retreating from its maximum extent along the shelf break, north of the Porcupine Bank, across the mid-western Irish shelf (Peters et al., 2016). Radiocarbon dates, from the western Irish margin, showed an ice margin retreat from its maximum extent after 22 ka BP, with the Porcupine sector of the Irish shelf being free of grounding ice by 19 ka cal. BP. The presence of a grounding zone wedge is recognised all along the mid-Irish shelf, as the result of an ice shelf north of the Porcupine Bank, during ice sheet steady state on the middle western shelf up to approximately 18 cal. Ka BP (Peters et al., 2016). The BIIS retreat was interpreted as a break-up of the ice-margin, with large iceberg calving events after the identification of a criss-crossing pattern of iceberg scours on the outer shelf, at approximately 200-500 m of water depth (Ó Cofaigh et al., 2012). Iceberg scours are observed to overwrite moraines and glacial deposits and for this reason are interpreted as representing the result of BIIS calving margins, following the maximum extent.

The two most abundant fluxes in the Rockall Trough record are identified in this study between 20 and 18 ka BP. This seems to be in accordance with the interpretation of a fast initial ice sheet collapse and retreat to a mid- to inner-shelf position that was then occupied for some time, until possibly 18.5 ka BP. Smaller peaks, with lower IRD fluxes are seen until around 18 ka BP and interpreted as smaller events of ice-margin calving during the overall ice sheet retreat.

Iceberg scouring on the outer shelf between 200 and 500 m of water depth (Ó Cofaigh et al., 2012; Peters et al., 2016) supports the identification of an extended ice-margin calving location along the mid-western Irish shelf following 20 ka BP. The orientation of these

erosional features on the sea-bed likely represents the direction of the paleo-currents active during the beginning of deglaciation (Ó Cofaigh et al., 2012). These currents are interpreted as responsible for the delivered IRD record to the studied location in the trough.

Overall, through the IRD fluxes presented, the deglacial pattern of the BIIS can be described as marked by large calving events of its marine-termini within the last glacial period.

Antarctica marine-based ice sheets, such as the Ross Sea Ice Sheet, are observed retreating through large calving events, episodically, or they are characterised by retreat through slow melting (Dowdeswell et al., 2008). The BIIS behaviour during deglaciation on the mid-western Irish shelf north of the Porcupine Bank, can be described as a mixing of these methods. The IRD record describes an ice sheet calving at 20 ka BP, with large ice margin collapse and icebergs dispersal. At this initial stage, a slower melting follows. A fast initial retreat through a massive ice-shelf break up with large calving and an associated grounding line retreat is also proposed by numerical modelling that have simulated the evolution for similar ice-margins (Andreassen et al., 2014).

5.6 Conclusions

The Rockall Trough sediment record analysed within this study represents a continuous sedimentation without large hiatus or erosional events during the last 130 ka. It records the full length of previous interglacial and glacial periods. It supplied the opportunity to observe the sedimentary evolution in the basin in relation of different advance of the BIIS during the stadial periods of the last glaciation. It supplies new evidence of ice sheet growth, predating the last glacial maximum, and shows how the deep water record can support data from shallower locations and strengthen glacial reconstructions.

The major conclusions achieved during this research can be summarised as follows:

- ^{14}C, NPS abundance, IRD concentrations and $\delta^{18}O$ record allowed to constrain the sampled sediments to the last 130 ka and the subdivision of the sediment record in marine isotopic stages;
- Rockall Trough sedimentary evolution was reconstructed during the last 130 ka, displaying an alternation between hemipelagic sedimentation during interglacials and a predominately glaciomarine sedimentation from meltwater plumes and ice rafting throughout the last glacial period;
- In relation to the BIIS, a first ice sheet build up and retreat is hypothesised during MIS5d and MIS5b, with recorded IRD fluxes in the Rockall Trough suggesting retreat through calving between 85 and 80 ka BP.
- A second marine extension is recognised during MIS4 and a glacial retreat is inferred as due to calving at 60 ka.
- During MIS2 the BIIS maximum extent is interpreted on the basis of the highest recorded sedimentation rates into the Rockall Trough occurring before 20 ka BP.
- Between 20 and 18 ka BP the ice sheet is retreating through calving events and the location of calving is suggested along the Western-Irish margin, north of the Porcupine Bank.
- The unrecorded presence of IRD fluxes after 18 ka BP allow to define the BIIS deglaciation along its western Irish extent as characterised by the large calving events and a subsequent phase of slow melting.

Chapter 6: Discussion and conclusions

The aim of this research was to investigate the dynamic behaviour of the paleo marine-terminating BIIS. This was achieved using different proxies, such as NPS%, IRD concentrations, oxygen stable isotopes and radiocarbon dating on deep water sediments, collected at the boundary between the North Atlantic glaciated and glacially-influenced margins (cf. Weaver et al., 2000; Fig. 6.1).

The specific results of this research provided new evidence of the BIIS growth and decay during the entire last glacial period and the key findings for the two specific locations are discussed in Chapters 4 and 5. In Chapter 4, the sediment record retrieved from the Donegal-Barra Fan by the *RRS James Cook*, during the BRITICE-CHRONO Cruise JC106, supplied a detailed reconstruction of the final deglaciation of the Malin Sea Shelf sector of the BIIS. In Chapter 5, twin cores collected from the deep Rockall Trough during cruise CE10008 on the *RV Celtic Explorer* allowed for the first time the reconstruction of the style of sediment delivery to the basin and a better understanding of the BIIS contribution to the sedimentation in deep water offshore western Ireland. The two records represent the result of sedimentary processes in two different depositional settings, a glaciogenic fan and a deep-water basin, and over different time scales. The oldest date for the Donegal-Barra Fan was observed at approximately 18 ka BP and for the Rockall Trough basin was inferred at around 130 ka BP. This makes the direct correlation between the two sedimentary records not straightforward and requires the integration with the previous scientific literature on this region. The aim of this chapter is, therefore, to present these very different deep-water records in a larger context, with the support of previously published works on the IRD record and deglaciation of the BIIS. This chapter, in particular, is going to explore what appears to be the main process for deep-water

sediment deposition (i.e. meltwater plumes) and its relation to BIIS calving margins. Additionally, the chapter will provide a summary of the phases of ice sheet advance and retreat during the entire last glacial period, including a discussion of what was happening in the region during the Younger Dryas.

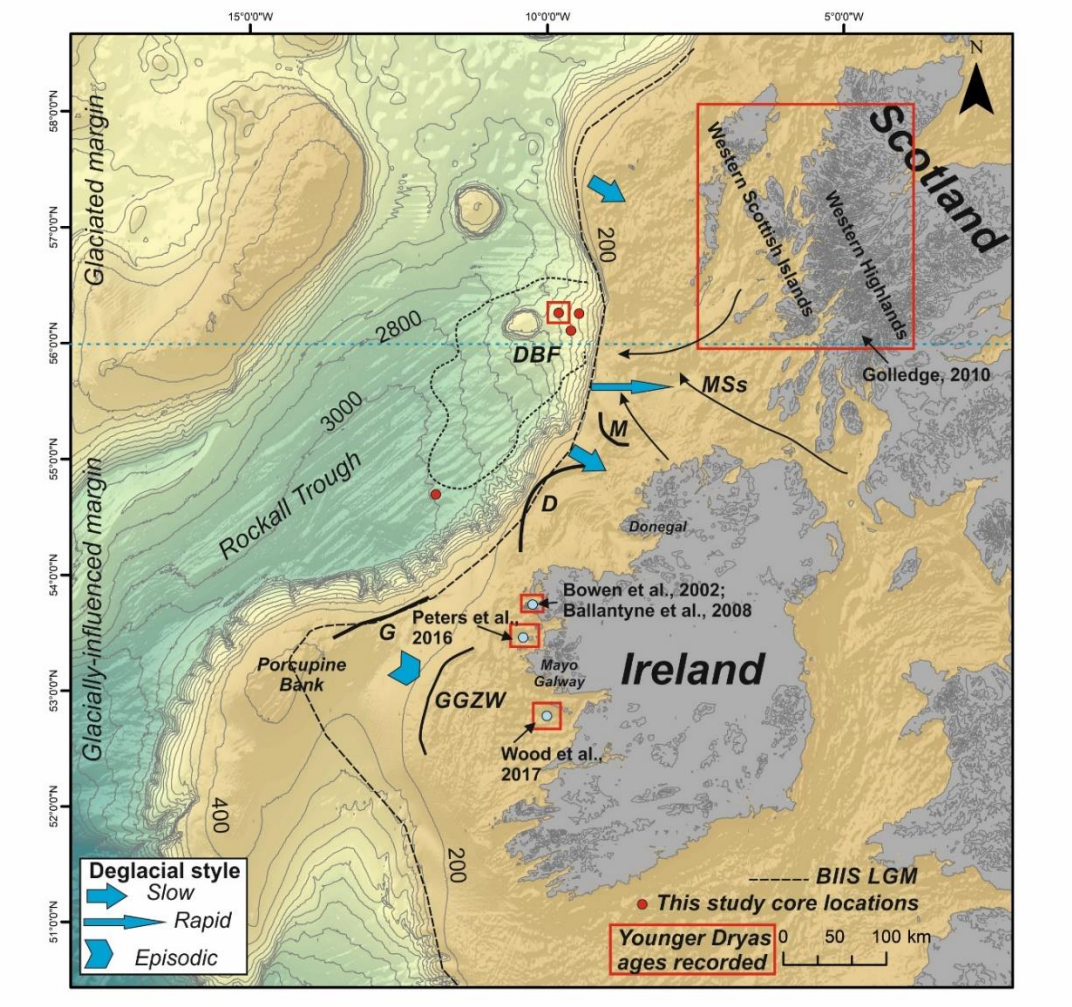

Figure 6.1.: Rockall Trough and North Atlantic continental margin. Limit between glaciated and glacially-influenced margin: light blue dotted line at 56°N (after Weaver et al, 2000). Bathymetry from GEBCO (https://www.gebco.net/); isobaths at a 200-m interval. Black arrows are inferred direction of the main ice flow to the DBF during the LGM (after Clark et al., 2012a). Dashed line indicates the BIIS possible maximum extent based on the position of the main mapped moraines shown by black lines. Malin Sea shelf=MSs; DBF=Donegal-Barra Fan (after Sacchetti et al., 2012); Moraines: D= Donegal (Benetti et al., 2010); G=Galway and GGZW=Galway grounding zone wedge (Peters et al., 2016); M= Malin moraines (Dunlop et al., 2010). The YD dated glacial and glaciomarine deposits in Scotland, Ireland and offshore are highlighted by the red boxes.

6.1. North-east Atlantic deep water records

Sediment cores from the deep North-east Atlantic have been analysed with the aim of investigating ice sheet dynamics and oceanography (de Abreu et al., 2003; Peck et al., 2006; Scourse et al., 2009; Hibbert et al., 2010). Particular attention here is focused on the chronostratigraphies built during these studies using oxygen isotope data (de Abreu et al., 2003; Hibbert et al., 2010). In the selected cases (de Abreu et al., 2003; Hibbert et al., 2010), $\delta^{18}O$ records were obtained from a single sediment core, analysed with high sampling resolution. This allowed for a time constrain of the observed sedimentary processes and the oceanographic changes within the identified Marine Isotope Stages (MIS). On the left section of Fig. 6.2, modified from Austin & Hibbert (2012), the correlation between $\delta^{18}O$ record from the MD04-2822 cored location, SPECMAP and LR05 benthic stack lines is presented. A similar technique has been used for the creation of the age model for core 20APC from the SE Rockall Trough (Chapter 5). Within this project, the sediment record has been time constrained to the last 130 ka BP, using the $\delta^{18}O$ data and their correlation with SPECMAP and LR05 stack lines (Fig. 5.7). Oxygen stable isotopes, together with NPS abundance, IRD concentration and presence of the planktonic foraminifera *Globoratalia menardii* helped in identifying Marine Isotope Stages, from MIS5e to MIS1, with an additional tentative correlation of SE Rockall Trough $\delta^{18}O$ with the GRIP Greenland ice core record (Fig. 5.8).

Within the following section, the study will show how a general agreement is recognised between the newly produced data and the previously observed and dated $\delta^{18}O$ record from the North-east Atlantic, moving from the Northern Rockall Trough to the Iberian margin to the south.

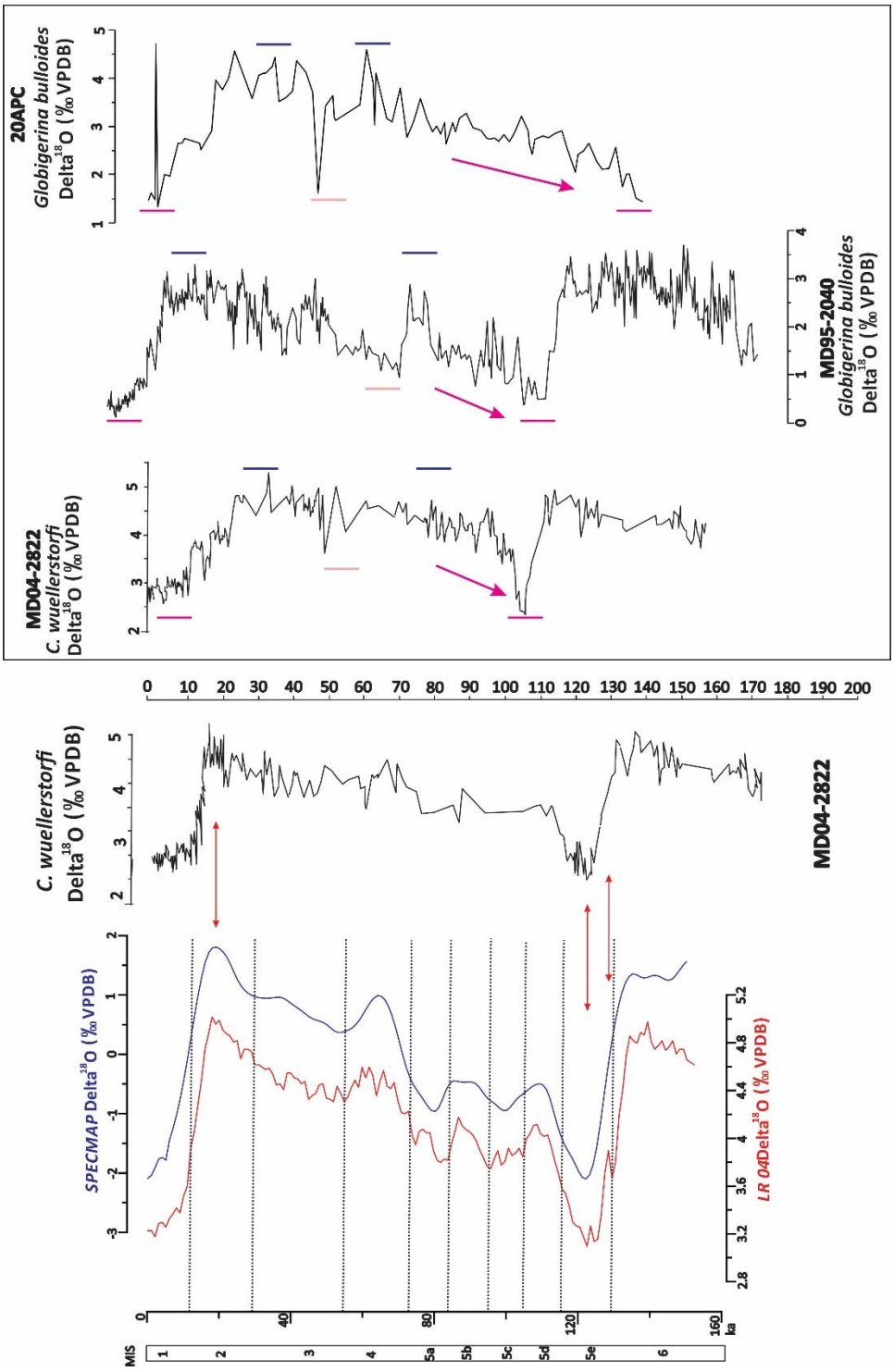

Figure 6.2: On the left, from Austin & Hibbert, 2012, correlation of $\delta^{18}O$ data with stack lines. On the right, oxygen isotope ratios for three sediment cores collected from the North East Atlantic Ocean. 20APC is the piston core analysed within the study and collected from the south-eastern Rockall Trough; MD95-2040 is collected along the Iberian margin and presented in the study of de Abreu et al., 2003; MD04-2822 is used by Hibbert et al., 2010 and the record is from the North sector of the Rockall Trough, on the western margin of the DBF.

The $\delta^{18}O$ record from 20APC is presented together with the MD95-2040 record from the Iberian margin and the MD04-2822 from the western extent of the Donegal Barra Fan, Northern Rockall Trough (Fig. 6.2). The $\delta^{18}O$ records present similar values, with similar trends observed between the plots (Fig. 6.2). It is recognised and highlighted by the purple horizontal lines, that the lightest $\delta^{18}O$ values are at the core top and bottom of 20APC (Fig. 6.2). These values are suggested to represent the current and previous interglacial conditions, during MIS1 and MIS5e. Following MIS1, an increased oxygen ratio is observed in all the three records presented, showing within MIS2, the heaviest $\delta^{18}O$ values along 20APC. This increasing trend is suggested to represent the transition and reach of glacial and stadial conditions, during MIS2 and MIS4. In agreement with what is observed in 20APC, the $\delta^{18}O$ records of MD95-2040 and MD04-2822 showed the heaviest values within these intervals. Highlighted by the purple arrow, decreasing trends in $\delta^{18}O$ are observed along the three cores between the stadial MIS4 and the previous interglacial period MIS5e. A clearly repetitive pattern is recognised between all the cores, where the blue and purple horizontal lines indicate the correlated intervals (Fig. 6.2) and the light pink suggests the MIS3 interstadial, supporting the initial chronological representation designed for 20APC in Chapter 5.

Within this study, an additional step forward towards a more detailed chronostratigraphy was proposed through the correlation of the 20APC oxygen ratios with the $\delta^{18}O$ of GRIP (Greenland Ice Core Project) (Johnsen, et al., 1997). This was done with the aim of helping in the identification of the stadial and interstadial periods pre-dating the MIS5e. The GRIP ice record has been selected for the correlation after it was observed to record the longest signal of the MIS5 in Greenland, even if some uncertainty was presented for the MIS5e (i.e. the last interglacial) likely due to the ice layers internal organization (Johnsen, et al., 1997). Considering the level of resolution within the current study, which

is much lower than the ice layers' annual resolution, the 5e uncertainty was easily bypassed and the record was chosen for the correlation because of the longest MIS5 signal. Limitations of the correlation with the GRIP record are clearly stated in Chapter 5, although an agreement is observed between the age model created in this study and the previously published $\delta^{18}O$ signals for the North-east Atlantic records. A further testing of the 20APC chronology is strongly recommended for future studies, as the deep sea record from the SE Rockall Trough displayed a high potential in recording past climatic and BIIS-related information (Chapter 5).

Furthermore, a general agreement is recognised between the results of the current study together with previously analysed North Atlantic sediment records. For instance, focusing on the sedimentation rates calculated in deep water environments, in relation to BIIS extension offshore during the last glacial period. A general increase in rates through time is recognised along the North-east Atlantic margin, suggesting a progressive ice sheet growth, with values reaching their maximum during MIS2 in particular predating 20 ka BP (i.e. 120-60 cm/ka in Hibbert et al., 2010, Peck et al., 2007). The sedimentation rates measured after the BIIS maximum extent, during deglaciation, showed rapid decrease with sediment delivered to the deep water up to 16 ka BP (Peck et al., 2007). The current study shows agreement with previous investigations. Furthermore, it adds new evidence to the current BIIS paleoenvironmental reconstruction. This includes the previously unrecognised ice sheet marine extension and meltwater plume deposition at ~90 ka BP (Chapter 5) and the deglaciation of the Malin Sea Shelf sector, characterised by calving events up to 16 ka BP (Chapter 4). The BIIS reconstruction for its western offshore extent is presented in section 6.4., where the new data produced by this study are presented and merged with the previous works in deep water.

6.2. Plumites and IRD concentration and their relationship with calving margins

Plumites, interpreted as the result of meltwater plume deposition (cf. Hesse et al., 1997; Dowdeswell et al., 1998), represent the majority of the sediment record analysed in the cores. This facies is a dark brown laminated mud, rich in silty intervals, with sparse sand-sized or gravel-sized lithic clasts. In the context of sedimentation on continental margins and in deep water, in a region affected by former ice sheets, the facies is interpreted as being deposited mostly by settling of fine-grained sediment from meltwater plumes, in conjunction with fine size sediments and ice-rafted debris >150 μm in diameter from icebergs (cf. Dowdeswell et al., 1998; Evans et al., 2002; Lucchi et al., 2002; Lloyd et al., 2005; Roger et al., 2013; Prothro et al., 2018). Meltwater plumes have been observed to deliver fine sediment up to 250 km from the basal ice sheet meltout location (Hesse et al., 1997; Prothro et al., 2018) and in this study the cores are retrieved at a maximum of 100 km from the inferred and closest ice-margin, when the ice extended onto the continental shelf (Fig. 6.1). The presence and absence at times of plumites in the cores has therefore been used in this study as a diagnostic tool to assess the distance of the ice margin from the core locations.

Additionally, within the meltwater deposits, peaks in IRD concentrations and fluxes have been related to ice-margin calving events (Figs. 4.7 and 5.10). Plumites have generally very fine grain size (average in this study approximately 50 μm or lower) (cf. Andrews, 2000). The peaks of a coarser grain size at these locations are related to icebergs being able to carry sand-sized particles to distal locations and a relative enrichment in icebergs is related to calving from the ice sheet margin (Andrews, 2000; Scourse et al., 2009).

On the DBF, glaciogenic sediments constitute the large majority of the sediment record and they have an age between 18 and 16 ka BP (Fig. 4.7). Due to the proximity of the

Malin Sea, these are interpreted as being deposited by meltwater plumes from an ice margin that was no longer at the shelf edge, but centred around western Scotland and the Outer Hebrides (~100 km from the cores location). Other studies on the Malin Sea shelf have provided evidence for an ice margin retreating from the shelf edge from 27 ka cal. BP, with a final retreat onshore following 16 ka cal. BP (Small et al., 2017; Callard et al., in review). This is additionally supported by studies on the DBF, showing higher sedimentation rates than those measured within our study, during periods corresponding to the BIIS maximum extent at the shelf edge (Knutz et al., 2001). The peaks in IRD concentration are interpreted as an episodic increase in icebergs reaching the fan. Calving events are suggested as the dominant source of icebergs and IRD found in the DBF at this time. These were possibly localised along Western Scotland, the Outer Hebrides and the southern extent of the Scandinavian Ice Sheet. These locations are suggested based on published reconstructions of the European ice sheets behaviour during the last glacial period and deglaciation (Hughes et al., 2015). Furthermore, the main IRD petrologies (which include basalts, quartzite and highly metamorphic rocks), are recognised as typical of the UK, Irish and Scandinavia margin. The Hebrides Ice Stream is thought to have retreated on the Malin Sea shelf during deglaciation (Small et al., 2016), likely representing the closest source of icebergs delivered to the fan up to 16 ka cal. BP. The dated re-advance of the Scandinavian Ice Sheet during the Younger Dryas (Mangerud et al., 2016) is suggested as the potential source location for icebergs, as it represents the only large marine terminating ice-sheet recorded in vicinity of the fan during this time.

Another potential source of IRD delivered to the fan could possibly originate in the northern sector of Ireland due to the similar geology; however, this is not supported by an extended and well time constrained ice sheet reconstruction for this section of the BIIS, up until this point. The dated re-advances of the Irish Ice Sheet, occurring during

deglaciation, and following 18 ka BP, are in fact largely localised along the eastern extent of Ireland. In addition, the behaviour of the North Channel Ice stream, following LGM, is also largely unknown adding to the uncertainty of BIIS dynamics during this time. The further study of the deglaciation for the Irish sector of the BIIS, along the northern part of Ireland and the North Channel, is needed in order to provide additional evidence on the provenance of the IRD record observed within this study. In addition, a Greenland-Icelandic provenance is excluded after studies recognising in the Rockall Bank an obstacle to iceberg migration from these locations towards the Rockall Trough (Sacchetti et al., 2012b).

The continuous deep-water record in the SE Rockall Trough also shows predominantly plumite deposition throughout the last glacial period. The core location is actually approximately 60 km from the BIIS ice margin at its maximum extent, therefore well within the reach of meltwater plumes (Fig. 6.1). The provenance of the plumes that delivered sediment to this location is inferred to be the central-western ice-margin of the BIIS, and in particular from the BIIS sector north of the Porcupine Bank. In this case, the origin of the IRD is inferred as the BIIS ice margin north of the Porcupine Bank. The IRD record from the SE RT does not show large variation within the lithic grains petrologies and the calving ice margins are suggested based on the previous studies about the Western BIIS extent, during the last glacial period (Hibbert et al., 2010; Ó Cofaigh et al., 2012; Peters et al., 2016). The observed IRD fluxes are interpreted as recording separate episodes of ice calving during deglacial events within MIS5b, MIS4 and MIS2. The icebergs provenance is inferred to be the Malin Sea shelf during MIS4, based on previously identified IRD fluxes in the northern Rockall Trough. This supports an interpretation of an instable ice margin delivering icebergs to the western extent of the Barra Fan (Hibbert et al., 2010). The western Irish margin, north of the Porcupine Bank,

corresponding to the Donegal-Galway sector of the BIIS is suggested to be the main source of icebergs and IRD in the RT between 20 and 18 ka BP (MIS2). The interpretation is based on the pattern of iceberg scours on the outer shelf, shelf break and other published data suggesting a fast initial BIIS collapse for the area (Ó Cofaigh et al., 2012; Peters et al., 2016).

This information on the distance of the ice margin from core locations and on the inferred provenance of icebergs was then used to reconstruct the variability of the BIIS over time since the previous interglacial and this is outlined in the following section.

6.3. Growth, evolution and deglaciation of the BIIS

In order to reconstruct the evolution of the BIIS over time, during the last glacial period, a series of inferences were made:

- The degree of the BIIS extension on the western Irish continental shelf is inferred based on the presence of the plumites in the Rockall Trough (Figs. 5.5 and 5.11). When plumites are absent, the ice margin is inferred to be over 250 km away (Prothro et al., 2018).
- High sedimentation rates calculated in the basin are used as a proxy for the amount of fine sediment delivered by meltwater plumes to deep water, as hemipelagic deposition for similar water depths in similar settings generally has much lower sedimentation rates, on average between 0.5 and 3 cm/ka (cf. Carvalho et al., 2011).
- Furthermore, the observed IRD fluxes (Fig. 5.10) are considered characteristic of ice-margin retreat through calving events and the exact position of such calving locations are based on published works on the BIIS on the continental shelf and

in deep water (specifically, Hibbert et al., 2010; Ó Cofaigh et al., 2012; Peters et al., 2016).

Based on the sediment record discussed in this thesis, it is possible to shed new light on the BIIS variability starting at approximately 130,000 years ago.

During MIS5e, predominantly interglacial conditions existed in the region of the Rockall Trough. These are shown in the deep-water sediment record as hemipelagic deposition, low NPS abundance and identification of warm climatic conditions through the foraminifera assemblages. Signals of an initial development of the BIIS are suggested during MIS5d around 100 ka BP (Fig. 6.3).

A gradual and steady increase in the oxygen isotopic ratio, together with an increase in NPS abundance and presence of IRD support an initial growth. The growth of the BIIS at this time coincides with a widespread record of expanding ice masses around the globe and of the cessation of interglacial conditions suggesting global climate as the driver for BIIS initial expansion (McManus et al., 1994; Chapman & Shackleton, 1999).

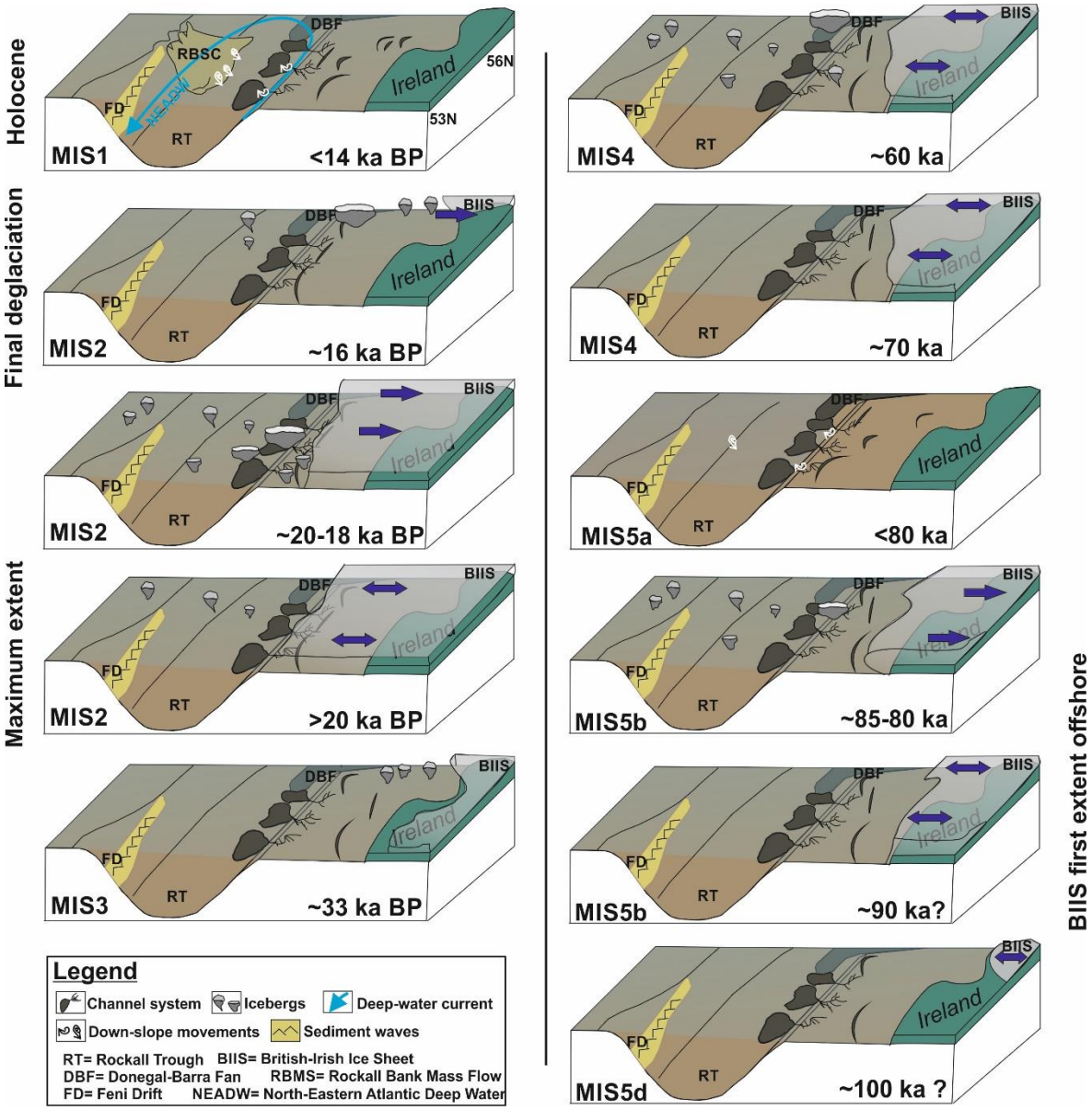

Figure 6.3: BIIS evolution along the North Atlantic continental margin during the last glacial period.

The first extension of the BIIS offshore western Ireland and recorded with plumites in deep water is hypothesised by this study during MIS5b, where the data suggest an ice sheet advanced on the continental shelf. This is based on oxygen isotope values, reaching 3.5‰ and an inferred SST of < 6°C (Fig. 5.5). Similar values in $\delta^{18}O$ from *Globigerina bulloides* were observed in other studies representing a low SST and glacial conditions, between 27 and 18 ka BP (cf. Peck et al., 2006, Hall et al., 2011 with observed values

during glacial $\delta^{18}O \geq 3.5‰$) Additionally, relatively high sedimentation rates (7.2 cm/ka) during this period suggest a sediment source close to the area and therefore a BIIS provenance for both fine-grained sediment and IRD found in the sediment cores. IRD fluxes recognized in association with plumites between 85 and 80 ka BP (Fig. 6.3) suggest episodes of retreat across the shelf through calving events.

After 80 ka BP, during MIS5a, the BIIS is not recognised extending offshore. The reduced sedimentation rates in the trough (down to 5.4 cm/ka) and the lack of IRD fluxes suggest different environmental conditions. The low NPS abundance (lower than 30%) and relatively warm biofacies, together with a lighter $\delta^{18}O$ record compared to MIS5b suggest conditions close to an interstadial period (Figs. 6.3 and 5.11).

Successively, a marine-extended BIIS is recognised again after 70 ka BP, during MIS4, through plumite sedimentation, a distinct increase in IRD content, high NPS abundances, the identification of characteristic cold biofacies (SST<6ºC; *Neogloboquadrina pachyderma* sinistral and *Globigerina bulloides*) and a progressively heavier $\delta^{18}O$ record. Sedimentation rates in the trough, with values between 6.7 and 3.7 cm/ka, higher than during the previous interstadial, additionally support a BIIS extension on the continental shelf with meltwater plume sedimentation in the deep-water. Other studies have previously suggested a BIIS extension during this period of time, together with ice sheet expansion in Norway and North Scotland (Hibbert et al., 2010; Sejrup et al., 2000; Gemmel et al., 2007; Mangerud et al., 2004). Based on a series of IRD fluxes, with discharge up to 5000 IRD grains*cm^{-1}*ka^{-1}, an unstable ice-margin, retreating through calving, is inferred at approximately 60 ka BP (Chapter 5, Fig. 5.10; Fig. 6.3). In the northern Rockall Trough, high IRD fluxes were also recorded at 70.2 ka and 61.7 ka by Hibbert et al., 2010, showing a similar timing with those further to the south observed here.

During MIS3 the BIIS was still marine-terminating, but not across the entire western Irish shelf. Offshore of the western Irish margin the sedimentation rates drastically decrease from 5.1 to 1.2 cm/ka and IRD fluxes are absent (Fig. 5.10). The $\delta^{18}O$ record decreases towards values typical of observed interglacial and modern conditions (Fig. 5.5) and planktonic foraminiferal biofacies (B5 and B3), characteristic of intermediate to relatively warm SST, are also identified. Other studies reported a continuous IRD record along the western extent of the Barra Fan and on the Porcupine Seabight, both located in proximity of ice-streaming locations (i.e. Hebrides Ice Stream and Irish Sea Ice Stream). In these studies, IRD fluxes strongly suggest a marine-extended BIIS, with a steady increase in IRD from 40 ka onward demonstrating ice sheet expansion (Peck et al., 2007; Hibbert et al., 2010). It appears that the BIIS marine extension at this time was occurring mainly in the Malin Sea shelf and in the Irish and Celtic Seas, with ice probably only present in mountain areas in counties Mayo and Galway. This is suggested by the low sedimentation rates in the SE trough during MIS3 (Fig. 5.9), which are lower than the values presented for the cored locations in proximity of ice-streams, showing a progressive ice sheet growth during this time (Peck et al., 2007; Hibbert et al., 2010). Terrestrial evidence actually suggests ice expansion over mainland Ireland starting at 32 ka BP (Ballantyne & Ó Cofaigh, 2017; McCabe et al., 2007). The BIIS is thought to have reached its maximum extent some time during MIS2 (Clark et al., 2012a). However, the timing of this is still under debate. Current reconstructions suggest that different portions of the ice sheet reached their maximum extent at different times along the North Atlantic margin (Wilson et al., 2002; Clark et al., 2012a; Ó Cofaigh et al., 2012; Peters et al., 2015). Along the Malin Sea shelf, the BIIS is inferred to have extended to the shelf edge between 29 and 27 ka BP, with a large ice stream feeding sediment to the Donegal-Barra Fan (Scourse et al., 2009). Along the western coast of Ireland, the BIIS is identified reaching its maximum

extension at the shelf edge before 26 ka cal BP offshore Donegal, and at approximately 24 ka cal BP offshore counties Mayo and Galway with an extension to the Porcupine Bank (Peters et al., 2015; Ó Cofaigh et al., in press). After reaching its maximum extent, smaller advances and retreats are observed through the IRD record, microfossils and stable isotopes following a millennial D-O periodicity (Wilson et al., 2002; Peck et al., 2007; Scourse et al., 2009). In the Rockall Trough, during MIS2 sedimentation rates reach a maximum of 13.8 cm/ka (a particularly high value for a deep water hemipelagic setting; cf. Carvalho et al., 2011: 0.5-3 cm/ka sed. rates in deep water), with deposition occurring mostly from meltwater plumes. The highest recorded sedimentation rates, heavy $\delta^{18}O$ and the identified biofacies (B4 with *Neogloboquadrina pachyderma* sinistral and *Globigerina bulloides*), suggesting a SST below 6°C, all strongly support the presence of the BIIS at the shelf edge and along the entire north-west Irish continental margin for an extended period of time during MIS2 with the delivery of abundant sediment-laden meltwater to the margin (Fig. 6.3). IRD fluxes, with maximum values of 30000 grains*cm^{-1}*ka^{-1}, are also observed during MIS2 between 20 and 18 ka BP (Fig. 5.10). These are interpreted as recording deglaciation, which is then time-constrained to approximately 20 ka BP (Fig. 5.11). This suggests that along this portion of the margin, the BIIS maximum extent actually pre-dates the LGM (Fig. 6.3). IRD fluxes are recorded until ~18 ka BP. After this time, plumite deposition is still identified in the sediment record with lower sedimentation rates and therefore it is likely that the ice margin had retreated to a mid-shelf or more landwards position.

The sediment record of the DBF actually allows a better record of the final stages of deglaciation. Here plumites, dated between 18 and 16 ka cal. BP, suggest a progressive retreat of the BIIS from the Malin Sea shelf at this time (Fig. 4.7). After 16 ka cal BP, the sediment record shows a transition from glaciomarine sedimentation to a contourite

sedimentation, characterised by abundant traces of *Zoophycos* burrows. This ichnofacies is recognised appearing in deep water environments generally during glacial terminations (Dorador et al., 2016), supporting the BIIS total deglaciation on the Malin Sea shelf after 16 ka BP.

Holocene contourite sedimentation in the DBF is interrupted by a distinct plumite layer, rich in IRD (Fig. 4.7) that was dated at the Younger Dryas. Although the exact provenance of the IRD would need to be confirmed by additional chemical analysis, the petrology of IRD grains seems characteristic of a European origin, being mainly represented by basalts and highly crystalline metamorphic grains. As during the Younger Dryas, ice extension over Ireland and UK seems to have been currently known only as confined to the terrestrial west coast of Ireland (Lough Accorymore), the western Scottish Islands and Western Highlands (Bowen et al., 2002; Ballantyne et al., 2008; Golledge, 2010; Small & Fabel., 2016), in this study the origin of IRD is suggested to be the Scandinavian Ice Sheet, with iceberg migration towards southern latitudes. This ice sheet was recently discovered with a marine extension along its southern margin, with a maximum advance dated at ~11.5 ka BP (Mangerud et al., 2016).

It is interesting to notice how recent works along western Ireland (Fig. 6.1) display an increase in dated YD glaciomarine deposits along Irish coastal areas. These records were not correlated to the Laurentide Ice sheet activity but directly connected to the BIIS. A YD age is obtained from a glacio-tectonised till 53 km offshore of the coast line of Connemara (Peters et al., 2016). Moving south towards Galway Bay, off the coast of the Aran Islands, west of Galway Bay, a glaciomarine mud, IRD rich interval, is dated at 12.8 (Wood et al., 2017). These modern discoveries along western Irish marine environments could likely soon supply evidence for a BIIS re-advance during this time, opening (maybe?) the way for a new investigation along the North-eastern Atlantic margin. A

possible Irish contribution to the IRD content, dated at the YD in the DBF, is considered because of the petrologies recognised; however, the lack of an extensive reconstruction of re-advance along the north and west sectors of Ireland during this time, makes it highly speculative and currently not supported by additional evidence. A supplementary process has to be taken in consideration as possibly responsible for the YD interval, observed in the DBF. This is suggested as the result of polar front migration and the presence of sea ice at that time. The sea-ice could have produced the plumitic interval but it would have required an external input of icebergs carrying sand size particles. The Scandinavian Ice Sheet, with its dated YD re-advance, is the most probable origin for icebergs, at least within the current state of knowledge.

6.4. Comparison between glacially-related sedimentary processes in the Rockall Trough with other glaciated margins.

Plumite deposits are observed along all the continental margins where ice sheets extend into the marine environment, from Antarctica, to the Canadian and Norwegian margins (Hesse et al., 1997; Lekens et al., 2005; Lucchi & Rebesco, 2007). The sediments analysed in this study are mostly represented by meltwater plume deposits, a striking difference from the Norwegian margin further to the north, where the glacial sedimentary record is generally presented by prograding trough-mouth fans and down slope mass transport deposits (Taylor et al., 2000). The Canadian margin, however, seems to provide an analogue for what is being observed along the Irish margin, where meltwater processes had a great influence on the sedimentation in deep water (Piper, 1988; Piper et al., 1990; Piper, 2005). Meltwater plumes and sandy erosive, high density, hyperpycnal flows contributed to the formation of the canyons system on the Canadian margin and deposition of thick plumitic intervals in deep waters (Piper, 1988; Piper & Gould, 2004).

These meltwater plumes seem to have an increasing contribution to sedimentation moving south along the margin, where ice loss from the southern portion of the LIS was observed occurring more likely by melting than by other processes due to the thermal gradient along the margin (Piper, 1988).

Similarities between the Canadian canyons, in particular along the Nova Scotian sector of the margin, with the canyons along the eastern flank of the Rockall Trough, have suggested how similar processes related to meltwater discharge were responsible for shaping the Irish slope and carving of Irish canyons (Sacchetti et al., 2012). This geomorphological evidence, together with the sedimentological data outlined in this study, strongly suggests the occurrence of similar processes along the Canadian and Irish margins during glacial times and in particular the presence of turbid meltwater plumes along the BIIS margin.

Within the Antarctic glaciated margin, different styles of deglaciation are observed for marine-based ice sheets and their classification is based on specific features on the continental shelves, such as grounding zone wedge, transverse ridges and mega scale glacial lineations, interpreted as representing three different speeds in ice-margin retreat: slow (i.e. recessional pattern), episodic (i.e. with calving and stationary phases normally forming GZWs) and rapid (Dowdeswell et al., 2008).

After the BIIS reached its maximum extent, a re-organization in lobes occurred following the initial iceberg wasting and retreat from the shelf edge position (Clark et al., 2012a). Over 26,000 mapped glacial features support our understanding of this retreat (Clark et al., 2012a; Clark et al., 2017). They can be used to characterize the style of deglaciation for the BIIS lobes (although ages for these landforms are often not available) together with the deep water record analysed within this study. The BIIS deglaciation is thought to have occurred relatively slowly in the intra ice-stream sections north and south of the

Malin Sea Shelf on the base of the presence of mapped moraines (Bradwell et al., 2008; Benetti et al., 2010; Dunlop et al., 2010) suggesting a step-by-step like ice sheet retreat. Conversely, a fast ice retreat within the ice-stream in the MSs is suggested by the presence of mega-scale glacial lineations mapped by Howe et al. (2012) and Dove et al. (2015). This study also suggests that the final stages of deglaciation were characterised by large calving events and meltwater pulses. South of 54°N, deglaciation for the BIIS ice margin is instead interpreted as episodic, on the basis of the presence of an extensive grounding zone wedge offshore counties Galway and Mayo (Peters et al., 2015) and a calving ice margin on the shelf break north of the Porcupine Bank as recognised in this study (Chapter 5).

Observing the bathymetry of the western UK and Irish shelf, it is easy to notice how the shelf width changes along the western Irish and UK continental margin. The shelf is relatively narrow offshore northern Scotland and Donegal in Ireland (around 80 to 100 km width), whilst it is significantly wider in the Malin Sea (between 150 and 200 km) and even more south of 54°N, where, including the Porcupine Bank, it reaches a width of over 200 km (Fig. 6.1). It is suggested that the style of deglaciation might have been partially influenced by this factor. An episodic or rapid retreat is mostly common on a wider shelf, whereas a slower retreat is more likely along narrower one. This is potentially explained due to a higher internal ice sheet stability on a less extended continental shelf. This interpretation correlates with what was observed in the Ross Sea (Antarctica) by Dowdeswell et al. (2008): a narrower shelf with slow retreat, in between the ice-streams, and an ice-margin experiencing still stand and grounding zone wedges formations in correspondence of a more extended continental shelf.

6.5. Conclusions

Overall, this research revealed BIIS dynamics through the entire last glacial period. The BIIS extension on the continental shelf of Ireland and UK is shown to have a significant impact on the sedimentation in deep water. Deep-water sediment cores, collected from designated locations, recorded a long and generally continuous record and the relation to glacial processes, avoiding reworking and erosion typical of continental shelves and coastlines. The deep water sediments not only supply new knowledge about the BIIS but, they are shown as potentially useful for testing hypotheses based on the less continuous and shallower sediment record. The new insight on the BIIS dynamic behaviour during the last glacial period (i.e. a previously unrecognised first marine extension and calving ice margins within deglaciation) can now be inserted on long term models used to predict future dynamics for marine-terminating ice sheets with similar aspect, such as the West Antarctica Ice Sheet.

The investigation of the sediment from the Donegal Barra fan highlighted the transition between the end of the last deglaciation and the modern interglacial period. The analysis of lithofacies, IRD counts, NPS abundance and radiocarbon dating in particular showed that:

- The final BIIS deglaciation along the Malin Sea shelf occurred between 18 and 16 ka BP.
- This period was still characterised by the accumulation of plumites onto the continental slope, thus providing evidence for a marine extension of the BIIS on the Malin Sea shelf until at least 16 ka BP.

- The deglaciation was also characterised by large and episodic events of iceberg calving, two of which distinctly occurred at 17.8 ka BP and 16.9 ka BP.
- Contouritic facies, rich in *Zoophycos* ichnofacies, characterise the transition between the end of the deglaciation and the renewal of interglacial conditions and this litho-ichnofacies could represent a diagnostic tool for the study of passive margin sedimentary evolution.
- During the Younger Dryas, there was the deposition of an IRD-rich plumite layer. It was interpreted as recording the presence of icebergs on the Donegal-Barra Fan at that time. The origin of such icebergs is inferred to be a European ice sheet, possibly the Scandinavian Ice Sheet, after it is recognised marine extended at this time.

Additionally, the analysis of the sediment record from the SE Rockall Trough allowed the reconstruction of the sedimentary evolution of the basin since 130 ka BP and highlighted the contribution of the BIIS to deep water sedimentation in the form of intermittent IRD and plumite deposition during the entire last glacial period. In particular:

- Oxygen stable isotopes, radiocarbon dating, *Neogloboquadrina pachyderma* sinistral abundance and IRD concentration were used to create a sound age model and time constrain the sediment record to the last 130 ka BP.
- Hemipelagic deposition and settling from meltwater plumes of glacially-derived fine sediments are recognised as the main sedimentary processes in the Rockall Trough during the last 130 ka BP.
- A BIIS marine extension during MIS5b was identified for the first time in this sediment record from meltwater plume deposits, heavy $\delta^{18}O$, NPS abundance and

high sedimentation rates. IRD fluxes suggested a BIIS retreating ice margin between 85-80 ka BP.

- IRD fluxes also identified BIIS calving events along western Irish ice margin at ~60 ka BP (MIS4) and between 20 and 18 ka BP (MIS2).
- High sedimentation rates within plumite deposits were used to infer a BIIS maximum extension before 20 ka BP.
- A series of calving events between 20 and 18 ka BP characterise the BIIS deglaciation. Based on the geomorphological features, such as iceberg scours mapped along the Western Irish margin, the calving location was suggested to be between the northern Porcupine Bank and the Malin Sea.
- The 5 biofacies identified through planktonic foraminifera assemblages and interpreted as characteristic of different sea surface temperature values provided a qualitative description of oceanic conditions during this time.

The initial research hypothesis '**Deep water sediments can provide key information for the reconstruction of the behaviour of marine terminating ice sheets**' is here clearly demonstrated. This is shown by the specific results obtained from the two locations that, merged with published reconstructions of the BIIS, provides a better understanding of the ice sheet dynamics. It fills some of the research gaps highlighted in the introductory chapter, such as observing records predating ice sheet maximum extent and introducing high resolution data in the deglacial records.

Key findings added to previous knowledge about the BIIS are summarised as:

- A glaciomarine fine mud rich in IRD in the region records episodes when the BIIS was marine-terminating. The episodic increase in IRD concentration and fluxes has been correlated with ice calving from the ice sheet margins.
- A BIIS marine extension during MIS5b is identified for the first time in this study, thus suggesting an earlier episode of ice sheet growth during the last glacial period.
- BIIS maximum extent along the entire western Irish margin, north of the Porcupine Bank, occurred before 20 ka BP and therefore before the global LGM, and by this time the BIIS had already started retreating. This could possibly be related to local changes in sea level due to glacioisostatic depression as suggested by studies on the shelf.
- The final BIIS deglaciation along the Malin Sea shelf occurred between 18 and 16 ka BP and was characterised by large and episodic events of iceberg calving, two of which distinctly occurred at 17.8 ka BP and 16.9 ka BP.
- During the Younger Dryas, the deposition of an IRD-rich glaciomarine plumitic layer on the DBF records the presence of icebergs in the region at that time. The origin of such icebergs is inferred to be a European ice sheet, possibly the Scandinavian Ice Sheet.

6.6. Suggestions for future work

The main limits of this project are represented by the sampling interval for foraminiferal and IRD investigation along the cores. These have been selected so to achieve optimal coverage of the events in the time available for the project. Given the significance and temporal resolution of the recovered sediment records, future studies should consider a smaller sample spacing for a finer resolution and a better understanding of the climatic and oceanographic processes between the previous interglacial and the Holocene.

A series of additional avenues of research to improve the work done on the BIIS through the current study and to advance the knowledge acquired about deep sea sedimentation in the region include:

- The investigation on the ice rafting processes and provenance of IRD.
- The identification of possible differences in the IRD record delivered by the British and the Irish sectors of the BIIS.
- The investigation on modern and palaeo-currents, together with investigation of paleo-current strengths along the margin, to be carried out on contourites using the sortable silt fraction.
- The study of the Younger Dryas-age marine deposits, IRD provenance, benthic foraminiferal assemblages, etc.
- An increased sampling resolution for Oxygen stable isotopes and a stronger testing for the CE10008 chronology.
- A refined biofacies identification and statistical analysis to assess its potential for the investigation of the polar front migration.

References

Adams, J., Maslin, M., Thomas, E. (1999) Sudden climate transitions during the Quaternary. *Progress in Physical Geography*, 23(1), 1-36.

Adkins, J.F., Boyle, E.A., Keigwin, L. and Cortijo, E. (1997) Variability of the North Atlantic thermohaline circulation during the last interglacial period. Nature, 390(6656), p.154.

Agassiz, L. (1838) On glaciers, and the evidence of their having once existed in Scotland, Ireland, and England. *In:* On glaciers, and the evidence of their having once existed in Scotland, Ireland, and England. *Proceedings of the Geological Society of London.* Nov. 1838 to June 1842, Part II (1840-1841), no.72, 327-332.

Aksu, A.E., Hiscott, R.N. (1989) Slides and debris flows on the high-latitude continental slope of Baffin Bay. *Geology*, 17(10), 885-888.

Alley, R.B. (2000) The Younger Dryas cold interval as viewed from central Greenland. *Quaternary Science Reviews*, 19(1–5), 213-226.

Allin, J. (2011) *Stable isotope, foraminiferal and lithological evidence of palaeoceanographic change in the Rockall Trough from core CE10008_20A.* MSc. in Environmental Science ed. Trinity College Dublin.

Anderson, J.B., Conway, H., Bart, P.J., Witus, A.E., Greenwood, S.L., McKay, R.M., Hall, B.L., Ackert, R.P., Licht, K., Jakobsson, M., Stone, J.O. (2014) Ross Sea paleo-ice sheet drainage and deglacial history during and since the LGM. *Quaternary Science Reviews*, 100, 31-54.

Andreassen, K., Winsborrow, M.C.M., Bjarnadóttir, L.R., Rüther, D.C. (2014) Ice stream retreat dynamics inferred from an assemblage of landforms in the northern Barents Sea. *Quaternary Science Reviews*, 92, 246-257.

Andrews, J.T. (2000) Icebergs and iceberg rafted detritus (IRD) in the North Atlantic: facts and assumptions. *Oceanography*, 13,3/2000, 100-108.

Armishaw, J.E., Holmes, R.W., Stow, D.A.V. (1998) Morphology and sedimentation on the Hebrides Slope and Barra Fan, NW UK continental margin. *Geological Processes on Continental Margins: Sedimentation, Mass-Wasting and Stability. Geological Society, London, Special Publications*, 129, 81-104.

Arosio, R., Crocket, K.C., Nowell, G.M., Callard,S.L., Howe, J.A., Benetti, S., Fabel, D., Moreton, S., Clark, C.D. (2017) Weathering fluxes and sediment provenance on the SW Scottish shelf during the last deglaciation. *Marine Geology*, in press

Arz, H.W., Lamy, F., Ganopolski, A., Nowaczyk, N., Pätzold, J. (2007) Dominant Northern Hemisphere climate control over millennial-scale glacial sea-level variability. *Quaternary Science Reviews,* 26(3–4), 312-321.

Austin, W.E.N. (2017) Marine radiocarbon dating in Britice-Chrono: A protocol. Version2: 29 May, 2007.

Austin, W.E., Bard, E., Hunt, J.B., Kroon, D. and Peacock, J.D. (1995) The 14 C age of the Icelandic Vedde Ash: implications for Younger Dryas marine reservoir age corrections. *Radiocarbon*, 37(1), 53-62.

Austin, W.E.N., Kroon, D. (1996) Late glacial sedimentology, foraminifera and stable isotope stratigraphy of the Hebridean Continental Shelf, northwest Scotland. *Geological Society, London, Special Publications,* 111(1), 187-213.

Austin, W.E.N., Kroon, D. (2001) Deep sea ventilation of the northeastern Atlantic during the last 15,000 years. *Global and Planetary Change*, 30(1-2),13-31.

Austin, W.E., Hibbert, F.D. (2012) Tracing time in the ocean: a brief review of chronological constraints (60–8 kyr) on North Atlantic marine event-based stratigraphies. *Quaternary Science Reviews*, 36, 28-37.

Ballantyne, C.K., Fabel, D., Gheorghiu, D., Rodés, Á., Shanks, R., Xu, S. (2017) Late Quaternary glaciation in the Hebrides sector of the continental shelf: cosmogenic nuclide dating of glacial events on the St Kilda archipelago. *Boreas*, 46 (4), 605-621.

Ballantyne, C.K., Ó Cofaigh, C. (2017) The last Irish Ice Sheet: extent and chronology. *Advances in Irish Quaternary Studies*, 1, 101-149.

Ballantyne, C.K., Stone, J.O., McCarroll, D. (2008) Dimensions and chronology of the last ice sheet in Western Ireland. *Quaternary Science Reviews,* 27(3), 185-200.

Balsam, W.L., Deaton, B.C., Damuth, J.E. (1999) Evaluating optical lightness as a proxy for carbonate content in marine sediment cores. *Marine Geology*, 161(2), 141-153.

Beaman, R.J., Harris, P.T. (2003) Seafloor morphology and acoustic facies of the George V Land shelf. *Deep Sea Research Part II: Topical Studies in Oceanography,* 50(8), 1343-1355.

Benetti, S., Dunlop, P., Ó Cofaigh, C. (2010) Glacial and glacially-related features on the continental margin of northwest Ireland mapped from marine geophysical data. *Journal of Maps,* 6:1, 14-29.

Bereiter, B., Eggleston, S., Schmitt, J., Nehrbass-Ahles, C., Stocker, T.F., Fischer, H., Kipfstuhl, S. and Chappellaz, J., (2015) Revision of the EPICA Dome C CO2 record from 800 to 600 kyr before present. *Geophysical Research Letters,* 42(2), 542-549.

Berger, A., Loutre, M.F., (1991) Insolation values for the climate of the last 10 million years. *Quaternary Science Reviews,* 10(4), 297-317.

Bigg, G.R., Clark, C.D., Greenwood, S.L., Haflidason, H., Hughes, A.L.C., Levine, R.C., Nygård, A., Sejrup, H.P. (2012) Sensitivity of the North Atlantic circulation to break-up of the marine sectors of the NW European ice sheets during the last Glacial: A synthesis of modelling and palaeoceanography. *Global and Planetary Change,* 98–99, 153-165.

Blott, S.J., Pye, K. (2001) GRADISTAT: a grain size distribution and statistics package for the analysis of unconsolidated sediments. *Earth Surface Processes and Landforms,* 26(11), 1237-1248.

Bond, G.C., Broecker, W., Johnsen, S., McManus, J., Labeyrie, L., Jouzel, J., Bonani, G. (1993) Correlations between climate records from North Atlantic sediments and Greenland ice. *Letters to Nature,* 365, 143-147.

Bond, G.C., Lotti, R. (1995) Iceberg discharge into the North Atlantic on millennial time scale during the last glaciation. *Science,* 267, 1005-1010.

Bond, G.C., Showers, W., Elliot, M., Evans, M., Lotti, R., Hajdas, I., Bonani, G., Johnson, S. (1999) The North Atlantic's 1-2 kyr climate rhythm: relation to Heinrich events, Dansgaard/Oeschger cycles and Little Ice Age. *Mechanism of Global Climate Change at Millennial Time Scale, Geophysical Monograph,* 112, 35-58.

Bowen, D.Q., Phillips, F.M., McCabe, A.M., Knutz, P.C., Sykes, G.A. (2002) New data for the Last Glacial Maximum in Great Britain and Ireland. *Quaternary Science Reviews,* 21(1), 89-101.

Bradwell, T., Stoker, M., Larter, R. (2007) Geomorphological signature and flow dynamics of The Minch palaeo-ice stream, northwest Scotland. *Journal of Quaternary Science,* 22(6), 609-617.

Bradwell, T., Stoker, M.S., Golledge, N.R., Wilson, C.K., Merritt, J.W., Long, D., Everest, J.D., Hestvik, O.B., Stevenson, A.G., Hubbard, A.L., Finlayson, A.G., Mathers, H.E. (2008) The northern sector of the last British Ice Sheet: Maximum extent and demise. *Earth-Science Reviews,* 88(3–4), 207-226.

Broecker, W.S., van Donk, J. (1970) Insolation changes, ice volumes, and the O18 record in deep-sea cores. *Reviews of Geophysics,* 8(1), 169-198.

Broecker, W., Bond, G. and McManus, J. (1993) Heinrich events: Triggers of ocean circulation change? In Ice in the climate system (pp. 161-166). Springer, Berlin, Heidelberg.

Broecker, W.S., Denton, G.H., Edwards, R.L. and Cheng, H., Alley, R.B., Putnam, A.E. (2010) Putting the Younger Dryas cold event into context. *Quaternary Science Reviews,* 29(9–10), 1078-1081.

Callard, S.L., Ó Cofaigh, C., Benetti, S., Chiverrell, R.C., Van Landeghem, K. J.J., Saher, M.H., Gales J.A., Small, D., Clark, C.D., Livingstone, S.J., Fabel, D., Moreton, S.G. (2018) Extent and retreat history of the Barra Fan Ice Stream offshore western Scotland and northern Ireland during the last glaciation. *Submitted to Quaternary Science Reviews*.

Carvalho, F.P., Oliveira, J.M., Soares, A.M.M. (2011) Sediment accumulation and bioturbation rates in the deep Northeast Atlantic determined by radiometric techniques. *ICES Journal of Marine Science,* 68(3), 427-435.

Ceregato, A., Raffi, S., Scarponi, D. (2007) The circalittoral/bathyal paleocommunities in the Middle Pliocene of Northern Italy: The case of the Korobkovia oblonga–Jupiteria concava paleocommunity type. *Geobios,* 40(5), 555-572.

Chapman, M.R., Shackleton, N.J. (1999) Global ice-volume fluctuations, North Atlantic ice-rafting events, and deep-ocean circulation changes between 130 and 70 ka. *Geology,* 27(9), 795-798.

Chiverrell, R.C., Thomas, G.S.P. (2010) Extent and timing of the Last Glacial Maximum (LGM) in Britain and Ireland: a review. *Journal of Quaternary Science,* 25(4), 535-549.

Clark, C.D., Ely, J.C., Greenwood, S.L., Hughes, A.L.C., Meehan, R., Barr, I.D., Bateman, M.D., Bradwell, T., Doole, J., Evans, D.J.A., Jordan, C.J., Monteys, X., Pellicer, X.M., Sheehy, M. (2017) BRITICE Glacial Map, version 2: a map and GIS database of glacial landforms of the last British–Irish Ice Sheet. *Boreas* 47(1), 11-e8.

Clark, C.D., Hughes, A.L.C., Greenwood, S.L., Jordan, C., Sejrup, HP. (2012a) Pattern and timing of retreat of the last British-Irish Ice Sheet. *Quaternary Science Reviews,* 44, 112-146.

Clark, J., McCabe, A.M., Bowen, D.Q., Clark, P.U. (2012b) Response of the Irish Ice Sheet to abrupt climate change during the last deglaciation. *Quaternary Science Reviews,* 35(Supplement C), 100-115.

Cronin, B.T., Akhmetzhanov, A.M., Mazzini, A., Akhmanov, G., Ivanov, M., Kenyon, N.H. (2005) Morphology, evolution and fill: Implications for sand and mud distribution in filling deep-water canyons and slope channel complexes. *Sedimentary Geology,* 179(1), 71-97.

Davison, S., Stoker, M.S. (2002) Late Pleistocene glacially-influenced deep-marine sedimentation off NW Britain: implications for the rock record. *Geological Society, London, Special Publications,* 203(1), 129-147.

Dansgaard, W., Johnsen, S.J., Clausen, H.B., Dahl-Jensen, D., Gundestrup, N.S., Hammer, C.U., Hvidberg, C.S., Steffensen, J.P., Sveinbjörnsdottir, A.E., Jouzel, J., Bond, G. (1993) Evidence for general instability of past climate from a 250-kyr ice-core record. *Nature,* 364(6434), 218.

de Abreu, L., Shackleton, N.J., Schönfeld, J., Hall, M., Chapman, M. (2003) Millennial-scale oceanic climate variability off the Western Iberian margin during the last two glacial periods. *Marine Geology,* 196(1–2), 1-20.

DeConto, R.M., Pollard, D. (2003) A coupled climate–ice sheet modeling approach to the Early Cenozoic history of the Antarctic ice sheet. *Palaeogeography, Palaeoclimatology, Palaeoecology,* 198(1), 39-52.

Dickson, R.R., Kidd, R.B. (1987) Deep circulation in the southern Rockall Trough-the oceanographic setting of site-610. *Initial Reports of the Deep Sea Drilling Project,* 94, 1061-1074.

Dorador, J., Wetzel, A., Rodríguez-Tovar, F.J. (2016) *Zoophycos* in deep-sea sediments indicates high and seasonal primary productivity: Ichnology as a proxy in palaeoceanography during glacial–interglacial variations. *Terra Nova,* 28(5), 323-328.

Dove, D., Arosio, R., Finlayson, A., Bradwell, T., Howe, J.A. (2015) Submarine glacial landforms record Late Pleistocene ice-sheet dynamics, Inner Hebrides, Scotland. *Quaternary Science Reviews,* 123, 76-90.

Dowdeswell, J.A., Elverhfi, A., Spielhagen, R. (1998) Glacimarine sedimentary processes and facies on the polar north Atlantic margins. *Quaternary Science Reviews,* 17(1), 243-272.

Dowdeswell, J.A., Ó Cofaigh, C., Noormets, R., Larter, R.D., Hillenbrand, C.-D., Benetti, S., Evans, J., Pudsey, C.J. (2008b) A major trough-mouth fan on the continental margin of the Bellingshausen Sea, West Antarctica: The Belgica Fan. *Marine Geology,* 252(3), 129-140.

Dowdeswell, J.A., Ó Cofaigh, C., Taylor, J., Kenyon, N.H., Mienert, J., Wilken, M. (2002) On the architecture of high-latitude continental margins: the influence of ice-sheet and sea-ice processes in the Polar North Atlantic. *Geological Society, London, Special Publications,* 203(1), 33-54.

Dowdeswell, J.A., Ottesen, D., Evans, J., Ó Cofaigh, C., Anderson, J.B. (2008a) Submarine glacial landforms and rates of ice-stream collapse. *Geology,* 36(10), 819-822.

Dunlop, P., Shannon, R., McCabe, M., Quinn, R., Doyle, E. (2010) Marine geophysical evidence for ice sheet extension and recession on the Malin Shelf: New evidence for the western limits of the British Irish Ice Sheet. *Marine Geology,* 276, 86-99.

Elliott, G.M., Shannon, P.M., Haughton, P.D.W., Praeg, D., O'Reilly, B. (2006) Mid- to Late Cenozoic canyon development on the eastern margin of the Rockall Trough, offshore Ireland. *Marine Geology,* 229(3), 113-132.

Emiliani, C. (1955) Pleistocene Temperatures. *The Journal of Geology,* 63(6), 538-578.

Evans, J., Dowdeswell, J.A., Grobe, H., Niessen, F., Stein, R., Hubberten, H-W., Whittington, R.J. (2002) Late Quaternary sedimentation in Kejser Franz Joseph Fjord and the continental margin of east Greenland. *Geological Society, London, Special Publications,* 203(1), 149-179.

Ericson, D.B. and Wollin, G. (1968) Pleistocene climates and chronology in deep-sea sediments. Science, 162(3859), 1227-1234.

Eynaud, F. (2011) Planktonic foraminifera in the Arctic: potentials and issues regarding modern and quaternary populations. *In:* Planktonic foraminifera in the Arctic: potentials and issues regarding modern and quaternary populations. *IOP Conference Series: Earth and Environmental Science.* IOP Publishing, 012005.

Faugeres, J.C, Gonthier, E., Grousset, F., Poutiers, J. (1981) The Feni Drift: The importance and meaning of slump deposits on the eastern slope of the Rockall Bank. *Marine Geology,* 40(3), M49-M57.

Flood, R.D., Hollister, C.D., Lonsdale, P. (1979) Disruption of the Feni sediment drift by debris flows from Rockall Bank. *Marine Geology,* 32(3), 311-334.

García, M., Ercilla, G., Alonso, B., Casas, D., Dowdeswell, J.A. (2011) Sediment lithofacies, processes and sedimentary models in the Central Bransfield Basin, Antarctic Peninsula, since the Last Glacial Maximum. *Marine Geology*, 290(1), 1-16.

Garvey, D. (2011) *Evaluation of the potential use of Planktonic foraminifera as palaeoceanographic indicators in the Rockall Trough and Hatton Bank regions of the North East Atlantic.* Unpublished M.Sc. Thesis ed. Trinity College, Dublin:

Gemmell, A.M.D., Murray, A.S., Connell, E.R. (2007) Devensian glacial events in Buchan (NE Scotland): A progress report on new OSL dates and their implications. *Quaternary Geochronology,* 2(1), 237-242.

Georgiopoulou, A., Benetti, S., Shannon, P., Haughton, P.D.W., McCarron, S. (2012) Gravity flow deposits in the deep Rockall Trough, northeast Atlantic. *In:* Yamada, Y.e.a. ed. *Submarine mass movements and their consequences, Advances in natual and technological hazards research.* 31st ed. Netherlands: Springer, 695-707.

Georgiopoulou, A., Shannon, P.M., Sacchetti, F., Haughton, P.D.W., Benetti, S. (2013) Basement-controlled multiple slope collapses, Rockall Bank Slide Complex, NE Atlantic. *Marine Geology,* 336, 198-214.

Golledge, N.R. (2010) Glaciation of Scotland during the Younger Dryas stadial: a review. *Journal of Quaternary Science,* 25(4), 550-566.

Haapaniemi, A.I., Scourse, J.D., Peck, V.L., Kennedy, H., Kennedy, P., Hemming, S.R., Furze, M.F.A., Pienkowski, A.J., Austin, W.E.N., Walden, J., Wadsworth, E., Hall, I.R. (2010) Source, timing, frequency and flux of ice-rafted detritus to the Northeast Atlantic margin, 30-12 ka: testing the Heinrich precursor hypothesis. *Boreas an International Journal of Quaternary Research,* 39, 576-591.

Hald, M., Dokken, T. and Mikalsen, G. (2001) Abrupt climatic change during the last interglacial–glacial cycle in the polar North Atlantic. Marine Geology, 176(1-4), pp.121-137.

Hall, I.R., Moran, S.B., Zahn, R., Knutz, P.C., Shen, C.-C., Edwards, R.L. (2006) Accelerated drawdown of meridional overturning in the late-glacial Atlantic triggered by transient pre-H event freshwater perturbation. *Geophysical Research Letters,* 33(16).

Hall, I.R., Colmero-Hidalgo, E., Zahn, R., Peck, V.L., Hemming, S.R. (2011) Centennial-to millennial-scale ice-ocean interactions in the subpolar northeast Atlantic 18-41 kyr ago. *Paleoceanography,* 26, PA2224.

Hambrey, M.J, McKelvey, B. (2000) Major Neogene fluctuations of the East Antarctic ice sheet: Stratigraphic evidence from the Lambert Glacier region. *Geology,* 28(10), 887-890.

Hammer, O., Harper, D. ed. (2005) *Paleontological data analysis.* Oxford: Wiley-Blackwell.

Hammer, Ø., Harper, D.A.T., Ryan, P.D. (2001) Paleontological statistics software: Package for education and data analysis. *Palaeontologia Electronica,* (4)

Heinrich, H. (1988) Origin and consequences of cyclic ice rafting in the northeast Atlantic Ocean during the past 130,000 years. *Quaternary Research,* 29(2), 142-152.

Hemming, S.R. (2004) Heinrich events: Massive late Pleistocene detritus layers of the North Atlantic and their global climate imprint. *Reviews of Geophysics,* 42(1), 2003RG00128.

Hendy, A.J.W., Kamp, P.J.J. (2004) Late Miocene to early Pliocene biofacies of Wanganui and Taranaki Basins, New Zealand: Applications to paleoenvironmental and sequence stratigraphic analysis. *New Zealand Journal of Geology and Geophysics,* 47(4), 769-785.

Hesse, R., Khodabakhsh, S., Klaucke, I., Ryan, W.B.F. (1997) Asymmetrical turbid surface-plume deposit near ice-outlets of the Pleistocene Laurentide ice sheet in the Labrador Sea. *Geo-Marine Letters,* 17(3), 179-187.

Hesse, R., Klauck, I., Khodabakhsh, S., Piper, D. (1999) Continental slope sedimentation adjacent to an ice margin. III. The upper Labrador Slope. *Marine Geology,* 155(3–4), 249-276.

Hibbert, F.D., Austin, W.E.N., Leng, M.J., Gatliff, R.W. (2010) British Ice Sheet dynamics inferred from North Atlantic ice-rafted debris records spanning the last 175 000 years. *Journal of Quaternary Science,* 25(4), 461-482.

Holland, S.M., Patzkowsky, M.E. (2004) Ecosystem structure and stability: Middle Upper Ordovician of central Kentucky, USA. *Palaios,* 19(4), 316-331.

Holliday, P.N., Pollard, R.T., Read, J.F., Leach, H. (2000) Water mass properties and fluxes in the Rockall Trough, 1975–1998. *Deep Sea Research Part I: Oceanographic Research Papers,* 47(7), 1303-1332.

Holmes, R., Long, D., Dodd, L.R. (1998) Large-scale debrites and submarine landslide on the Barra Fan, west of Britain. *Geological Processes on Continental Margins: Sedimentation, Mass-Wasting and Stability. Geological Society, London, Special Publications,* 129, 67-79.

Howe, J.A. (1995) Sedimentary processes and variations in slope-current activity during the last Glacial-Interglacial episode on the Hebrides Slope, northern Rockall Trough, North Atlantic Ocean. *Sedimentary Geology,* 96(3), 201-230.

Howe, J.A. (1996) Turbidite and contourite sediment waves in the northern Rockall Trough, North Atlantic Ocean. *Sedimentology,* 43, 219-234.

Howe, J.A., Dove, D., Bradwell, T., Gafeira, J. (2012) Submarine geomorphology and glacial history of the Sea of the Hebrides, UK. *Marine Geology,* 315-318(Supplement C), 64-76.

Howe, J.A., Harland, R., Hine, N.M., Austin, W.E.N. (1998) Late Quaternary stratigraphy and palaeoceanographic change in the northern Rockall Trough, North Atlantic Ocean. *Geological Processes on Continental Margins: Sedimentation, Mass-Wasting and Stability. Geological Society, London, Special Publications,* 129, 269-286.

Hughes, A.L.C., Clark, C.D., Jordan, C.J. (2014) Flow-pattern evolution of the last British Ice Sheet. *Quaternary Science Reviews,* 89(Supplement C), 148-168.

Hughes, A.L.C., Gyllencreutz, R., Lohne O.S., Mangerud, J., Svendesen J.I. (2015) The last Eurasian Ice Sheet - a chronological database and time-slice reconstruction, DATED-1. *Boreas an International Journal of Quaternary Research,* 45, 1-45.

Imbrie, J., Hays, J.D., Martinson, D.G., McIntyre, A., Mix, A.C., Morley, J.J., Pisias, N.G., Prell, W.L., Shackleton, N.J. (1984) The orbital theory of Pleistocene climate: support from a revised chronology of the marine d18O record.

Johannessen, T., Jansen, E., Flatøy, A., Ravelo, A.C. (1994) The relationship between surface water masses, oceanographic fronts and paleoclimatic proxies in surface sediments of the Greenland, Iceland, Norwegian Seas. *In:* Anon. *Carbon cycling in the glacial ocean: constraints on the ocean's role in global change.* Springer, 61-85.

Johnsen, S.J., Clausen, H.B., Dansgaard, W., Gundestrup, N.S., Hammer, C.U., Andersen, U., Andersen, K.K., Hvidberg, C.S., Dahl-Jensen, D., Steffensen, J.P., Shoji, H., Sveinbjörnsdóttir, Á.E., White, J., Jouzel, J., Fisher,D. (1997) The δ18O record along the Greenland Ice Core Project deep ice core and the problem of possible Eemian climatic instability. *Journal of Geophysical Research: Oceans,* 102(C12), 26397-26410.

Jones, R.L.l., Whatley, R.C., Cronin, T.M., Dowsett, H.J. (1999) Reconstructing late Quaternary deep-water masses in the eastern Arctic Ocean using benthonic Ostracoda. *Marine Micropaleontology,* 37(3), 251-272.

Kennett, J.P., Srinivasan, M.S. (1983) *Neogene planktonic foraminifera: a phylogenetic atlas.* Hutchinson Ross.

Kidd, R.B., Hill, P.R. (1986) Sedimentation on mid-ocean sediment drifts. North Atlantic Palaeoceanography. *Geological Society, London,* 21, 87-102.

Knutz, P.C., Austin, W.E.N., Jones, E.J.W. (2001) Millennial-scale depositional cycles related to British Ice Sheet variability and North Atlantic paleocirculation since 45 kyrs B.P., Barra fan, U.K. margin. *Paleoceanography,* 16, 53-64.

Knutz, P.C., Jones, E.J.W., Austin, W.E.N., van Weering, T.C.E. (2002) Glacimarine slope sedimentation, contourite drifts and bottom current pathways on the Barra Fan, UK North Atlantic margin. *Marine Geology,* 188(1–2), 129-146.

Kroon, D., Austin, W.E.N., Chapman, M.R. and Ganssen, G.M. (1997) Deglacial surface circulation changes in the northeastern Atlantic: Temperature and salinity records off NW Scotland on a century scale. *Paleoceanography and Paleoclimatology*, 12(6), 755-763.

Kroon, D., Shimmield, G., Austin, W.E.N., Derrick, S., Knutz, P., Shimmield, T. (2000) Century-to millennial-scale sedimentological–geochemical records of glacial–Holocene sediment variations from the Barra Fan (NE Atlantic). *Journal of the Geological Society,* 157(3), 643-653.

Lee, A., Ellett, D. (1965) On the contribution of overflow water from the Norwegian Sea to the hydrographic structure of the North Atlantic Ocean. *Deep Sea Research and Oceanographic Abstracts,* 12(2), 129-142.

Lekens, W.A.H., Sejrup, H.P., Haflidason, H., Petersen, G.Ø., Hjelstuen, B., Knorr, G. (2005) Laminated sediments preceding Heinrich event 1 in the Northern North Sea and Southern Norwegian Sea: Origin, processes and regional linkage. *Marine Geology,* 216(1), 27-50.

Leopold, A., Jones, S.E. (1947) A Phenological Record for Sauk and Dane Counties, Wisconsin, 1935-1945. *Ecological Monographs,* 17(1), 81-122.

Lisiecki, L. E., Raymo, M.E. (2005) A Pliocene-Pleistocene stack of 57 globally distributed benthic δ18O records. *Paleoceanography,* 20(1), PA1003.

Lloyd, J.M., Park, L.A., Kuijpers, A., Moros, M. (2005) Early Holocene palaeoceanography and deglacial chronology of Disko Bugt, west Greenland. *Quaternary Science Reviews,* 24(14), 1741-1755.

Lowe, D.R. (1979) Sediment gravity flows: their classification and some problems of application to natural flows and deposits. In: Doyle, L.J., Pilkey, O.H. ed. Geology of continental slopes. Special Publication, 27 ed. Tulsa, Oklaoma: Society of economic paleontologists and mineralogists, 75-84.

Lowe, D.R. (1982) Sediment gravity flows: II. Depositional models with special reference to the deposits of high density turbidity currents. Journal of Sedimentary Petrology, 52, 279-297.

Löwemark, L., Lin, H.L., Sarnthein, M. (2006) Temporal variations of the trace fossil Zoophycos in a 425 ka long sediment record from the South China Sea: implications for the ethology of the Zoophycos producer. Geological Magazine, 143(1), 105-114.

Lucchi, R.G., Camerlenghi, A., Rebesco, M., Colmenero-Hidalgo, E., Sierro, F.J., Sagnotti, L., Urgeles, R., Melis, R., Morigi, C., Bárcena, M.-A., Giorgetti, G., Villa, G., Persico, D., Flores, J.-A., Rigual-Hernández, A.S., Pedrosa, M.T., Macri, P., Caburlotto, A. (2013) Postglacial sedimentary processes on the Storfjorden and Kveithola trough mouth fans: Significance of extreme glacimarine sedimentation. *Global and Planetary Change*, 111(Supplement C), 309-326.

Lucchi, R.G., Rebesco, M. (2007) Glacial contourites on the Antarctic Peninsula margin: insight for palaeoenvironmental and palaeoclimatic conditions. *Geological Society, London, Special Publications*, 276(1), 111-127.

Lucchi, R.G., Rebesco, M., Camerlenghi, A., Busetti, M., Tomadin, L., Villa, G., Persico, D., Morigi, C., Bonci, M.C., Giorgetti, G. (2002) Mid-late Pleistocene glacimarine sedimentary processes of a high-latitude, deep-sea sediment drift (Antarctic Peninsula Pacific margin). *Marine Geology*, 189(3–4), 343-370.

Lynch-Stieglitz, J., Schmidt, M.W., Curry, W.B. (2011) Evidence from the Florida Straits for Younger Dryas ocean circulation changes. *Paleoceanography*, 26(1), PA1205.

Mangerud, J. (2004) Ice sheet limits on Norway and the Norwegian continental shelf. *Quaternary Glaciations—Extent and Chronology*, 1, pp.271-294.

Mangerud, J., Aarseth, I., Hughes, A.L.C., Lohne, Ø.S., Skår, K., Sønstegaard, E., Svendsen, J.I. (2016) A major re-growth of the Scandinavian Ice Sheet in western Norway during Allerød-Younger Dryas. *Quaternary Science Reviews*, 132, 175-205.

Masson, D.G., Plets, R.M.K., Huvenne, V.A.I., Wynn, R.B., Bett, B.J. (2010) Sedimentology and depositional history of Holocene sandy contourites on the lower slope of the Faroe–Shetland Channel, northwest of the UK. *Marine Geology*, 268(1), 85-96.

McCabe, A.M., Clark, P.U. (1998) Ice-sheet variability around the North Atlantic Ocean during the last deglaciation. *Nature*, 392(6674), 373-377.

McCabe, A.M., Clark, P.U. (2003) Deglacial chronology from County Donegal, Ireland: implications for deglaciation of the British–Irish ice sheet. *Journal of the Geological Society*, 160(6), 847-855.

McCabe, A.M., Clark, P.U., Clark, J., Dunlop, P. (2007) Radiocarbon constraints on readvances of the British–Irish Ice Sheet in the northern Irish Sea Basin during the last deglaciation. *Quaternary Science Reviews*, 26(9), 1204-1211.

McCartney, M.S. (1992) Recirculating components to the deep boundary current of the northern North Atlantic. *Progress in Oceanography,* 29(4), 283-383.

McCartney, M.S., Mauritzen, C. (2001) On the origin of the warm inflow to the Nordic Seas. *Progress in Oceanography,* 51(1), 125-214.

McCullagh, D. (2018) *Palaeoenvironmental evolution of Galway Bay, western Ireland, from the post-glacial to present.* PhD thesis ed. Coleraine: Ulster University.

McManus, J.F., Bond, G.C., Broecker, W.S., Johnsen, S., Labeyrie, L., Higgins, S. (1994) High-resolution climate records from the North Atlantic during the last interglacial. *Nature,* 371(6495), 326-329.

McManus, J.F., Francois, R., Gherardi, J.M., Keigwin, L.D., Brown-Leger, S. (2004) Collapse and rapid resumption of Atlantic meridional circulation linked to deglacial climate change. *Letter to Nature,* 428, 834-837.

Middleton, G.V., Hampton, M.A. (1976) Subaqueous sediment transport and deposition by sediment gravity flows. *Marine Sediment Transport (Eds.D.J.Stanley and D.J.P.Swift), 197-218. Wiley, New York.*

Milankovitch, M., (1941) History of radiation on the Earth and its use for the problem of the ice ages. *K. Serb. Akad. Beogr*.

Mingard, K., Morrell, R., Jackson, P., Lawson, S., Patel, S., Buxton, R. (2009) Good practice guide for improving the consistency of particle size measurements.

Mitchum, R.M., Vail, P.R., Sangree, J.B. (1977) Seismic stratigraphy and global changes of sea level: Part 6. Stratigraphic interpretation of seismic reflection patterns in depositional sequences: Section 2. Application of seismic reflection configuration to stratigraphic interpretation. *In:* Anon. *Seismic stratigraphy- applications to hydrocarbon exploration.* AAPG Special Volumes, 117-133.

Naylor, D., Shannon, P.M., Holland, C.H., Sanders, I.S. (2009) Geology of offshore Ireland. *The Geology of Ireland,* , 405-460.

New, A.L., Smythe-Wright, D. (2001) Aspects of the circulation in the Rockall Trough. *Continental Shelf Research,* 21(8–10), 777-810.

Nick, F.M., Vieli, A., Andersen, M.L., Joughin, I., Payne, A., Edwards, T.L., Pattyn, F., van de Wal, R.S.W. (2013) Future sea-level rise from Greenland/'s main outlet glaciers in a warming climate. *Nature,* 497(7448), 235-238.

Ó Cofaigh, C., Dowdeswell, J.A. (2001) Laminated sediments in glacimarine environments: diagnostic criteria for their interpretation. *Quaternary Science Reviews,* 20(13), 1411-1436.

Ó Cofaigh, C., Dunlop, P., Benetti,S. (2012) Marine geophysical evidence for Late Pleistocene ice sheet extent and recession off northwest Ireland. *Quaternary Science Reviews,* 44, 147-159.

Ó Cofaigh, C., Weilbach, K., Lloyd, J.M., Benetti, S., Callard, S.L., Purcell, C., Chiverrell, R.C., Dunlop, P., Saher, M., Livingstone, S.J., Van Landeghem, K.J.J., Moreton, S.G., Clark, C.D., Fabel, D. (in press) Early deglaciation of the Atlantic shelf northwest of Ireland driven by glacioisostatic depression and high relative sea level. Quaternary Science Reviews

O'Reilly, B.M., Shannon, P.M., Readman, P.W. (2007) Shelf to slope sedimentation processes and the impact of Plio–Pleistocene glaciations in the northeast Atlantic, west of Ireland. *Marine Geology,* 238(1), 21-44.

Ottesen, D., Dowdeswell, J.A., Rise, L. (2005) Submarine landforms and the reconstruction of fast-flowing ice streams within a large Quaternary ice sheet: The 2500-km-long Norwegian-Svalbard margin (57–80 N). *Geological Society of America Bulletin,* 117(7-8), 1033-1050.

Overpeck, J., Hughen, K., Hardy, D., Bradley, R., Case, R., Douglas, M., Finney, B., Gajewski, K., Jacoby, G., Jennings, A. (1997) Arctic environmental change of the last four centuries. *Science,* 278(5341), 1251-1256.

Øvrebø, L.K., Haughton, P.D.W., Shannon, P.M. (2005) Temporal and spatial variations in Late Quaternary slope sedimentation along the undersupplied margins of the Rockall Trough, offshore west Ireland. *Norwegian Journal of Geology/Norsk Geologisk Forening,* 85(4)

Owens, M. (2017) *The role of alongslope and downslope sedimentary processes in the construction of Cenozoic large-scale mounded features: A 3D seismic study from the NE Rockall Trough.* Research Master's thesis ed. Dublin: University College Dublin.

Owen, N.L. (2010) A multi-proxy palaeoceanographic investigation of slope deposits on the Porcupine bank, NE Atlantic Ocean. Unpublished PhD thesis, Geology, Trinity College Dublin.

Peck, V.L., Hall, I.R., Zahn, R., Elderfield, H., Grousset, F., Hemming, S.R., Scourse, J.D. (2006) High resolution evidence for linkages between NW European ice sheet instability and Atlantic Meridional Overturning Circulation. *Earth and Planetary Science Letters,* 243(3–4), 476-488.

Peck, V.L., Hall, I.R., Zahn, R., Scourse, J.D. (2006b). Progressive reduction in NE Atlantic intermediate water ventilation prior to Heinrich events: Response to NW European ice sheet instabilities? Geochemistry, Geophysics, Geosystems, 8(1).

Peck, V.L., Hall, I.R., Zahn, R., Grousset, F., Hemming, S.R., Scourse, J.D. (2007) The relationship of Heinrich events and their European precursors over the past 60 ka BP: a multi-proxy ice-rafted debris provenance study in the North East Atlantic. *Quaternary Science Reviews*, 26(7–8), 862-875.

Peters, J.L, Benetti, S., Dunlop, P., Ó Cofaigh, C. (2015) Maximum extent and dynamic behaviour of the last British–Irish Ice Sheet west of Ireland. *Quaternary Science Reviews*, 128, 48-68.

Peters, J.L., Benetti, S., Dunlop, P., Ó Cofaigh, C., Moreton, S.G., Wheeler, A.J., Clark, C.D. (2016) Sedimentology and chronology of the advance and retreat of the last British-Irish Ice Sheet on the continental shelf west of Ireland. *Quaternary Science Reviews*, 140(Supplement C), 101-124.

Petit, J.R., Jouzel, J., Raynaud, D., Barkov, N.I., Barnola, J.M., Basile, I., Bender, M., Chappellaz, J., Davis, M., Delaygue, G. and Delmotte, M., (1999) Climate and atmospheric history of the past 420,000 years from the Vostok ice core, Antarctica. *Nature*, 399(6735), 429.

Pingree, R.D. (1993) Flow of surface waters to the west of the British Isles and in the Bay of Biscay. *Deep Sea Research Part II: Topical Studies in Oceanography*, 40(1), 369-388.

Piper, D.J. (1988) DNAG# 3. Glaciomarine sedimentation on the continental slope off eastern Canada. *Geoscience Canada*, 15(1).

Piper, D.J.W., Mudie, P.J., Fader, G.B., Josenhans, H.W., MacLean, B. and Vilks, G. (1990) Quaternary geology. *Geology of the continental margin of Eastern Canada*. Geological survey of Canada, Geology of Canada, (2), pp.475-607.

Piper, D.J. and Gould, K. (2004) Late Quaternary geological history of the continental slope, South Whale Subbasin, and implications for hydrocarbon development, southwestern Grand Banks of Newfoundland. *Natural Resources Canada*, Geological Survey of Canada.

Piper, D.J.W. (2005) Late Cenozoic evolution of the continental margin of eastern Canada. *Norwegian Journal of Geology,* 85, 305-318.

Pollard, R.T., Griffiths, M.J., Cunningham, S.A., Read, J.F., Pérez, F.F., Ríos, A.F. (1996) Vivaldi 1991 - A study of the formation, circulation and ventilation of Eastern North Atlantic Central Water. *Progress in Oceanography*, 37(2), 167-192.

Principato, S. (2005) X-ray radiographs of sediment cores: a guide to analyzing diamicton. *Image Analysis, Sediments and Paleoenvironments,* 165-185.

Pritchard, H.D., Ligtenberg, S.R.M., Fricker, H.A., Vaughan, D.G., Van den Broeke, M.R., Padman, L. (2012) Antarctic ice-sheet loss driven by basal melting of ice shelves. *Nature,* 484(7395), 502-505.

Prothro, L.O., Simkins, L.M., Majewski, W., Anderson, J.B. (2018) Glacial retreat patterns and processes determined from integrated sedimentology and geomorphology records. *Marine Geology,* 395, 104-119.

Purcell, C.S. (2014) *Late Quaternary glaciation of the continental shelf offshore of NW Ireland.* Durham theses. Durham University.

Rahmstorf, S. (2002) Ocean circulation and climate during the past 120,000 years. *Nature,* 419(6903), 207-214.

Ramsey, C.B. (2009) Bayesian analysis of radiocarbon dates. *Radiocarbon,* 51(1), 337-360.

Rasmussen, S.O., Bigler, M., Blockley, S.P., Blunier, T., Buchardt, S.L., Clausen, H.B., Cvijanovic, I., Dahl-Jensen, D., Johnsen, S.J., Fischer, H., Gkinis, V., Guillevic, M., Hoek, W.Z., Lowe, J.J., Pedro, J.B., Popp, T., Seierstad, I.K., Steffensen, J.P., Svensson, A.M., Vallelonga, P., Vinther, B.M., Walker, M.J.C., Wheatley, J.J., Winstrup, M. (2014) A stratigraphic framework for abrupt climatic changes during the Last Glacial period based on three synchronized Greenland ice-core records: refining and extending the INTIMATE event stratigraphy. *Quaternary Science Reviews,* 106(Supplement C), 14-28.

Rawle, A.F. (2011) *Basic principles of particle size analysis.*

Read, J.F. (2000) CONVEX-91: water masses and circulation of the Northeast Atlantic subpolar gyre. *Progress in Oceanography,* 48(4), 461-510.

Rebesco, M., Hernández-Molina, F.J., Van Rooij, D., Wåhlin, A. (2014) Contourites and associated sediments controlled by deep-water circulation processes: State-of-the-art and future considerations. *Marine Geology,* 352, 111-154.

Reimer, P.J., Bard, E., Bayliss, A., Beck, J.W., Blackwell, P.G., Ramsey, C.B.,Buck, C.E., Cheng, H., Edwards, R.L., Friedrich, M., Grootes, P.M., Guilderson, T.P., Haflidason, H., Hajdas, I., Hatté, C., Heaton, T.J., Hoffmann, D.L., Hogg, A.G., Hughen, K.A., Kaiser, K.F., Kromer, B., Manning, S.W., Niu, M., Reimer, R.W., Richards, D.A., Scott, E.M., Southon, J.R., Staff, R.A., Turney, C.S.M., van der Plicht, J. (2013) IntCal13 and Marine13 Radiocarbon Age Calibration Curves 0–50,000 Years cal BP. *Radiocarbon,* 55(4), 1869-1887.

Rignot, E., Fenty, I., Xu, Y., Cai, C., Velicogna, I., Ó Cofaigh, C., Dowdeswell, J.A., Weinrebe, W., Catania, G., Duncan, D. (2016) Bathymetry data reveal glaciers vulnerable to ice-ocean interaction in Uummannaq and Vaigat glacial fjords, west Greenland. *Geophysical Research Letters,* 43(6), 2667-2674.

Roger, J., Saint-Ange, F., Lajeunesse, P., Duchesne, M.J., St-Onge, G. (2013) Late Quaternary glacial history and meltwater discharge along the northeastern Newfoundland shelf. *Canadian Journal of Earth Sciences,* 50, 1178-1194.

Sacchetti, F., (2012) Late Quaternary sedimentation associated with the British-Irish Ice Sheet on the NW Irish continental slope: a marine geological and geophysical investigation. PhD thesis, School of Environmental Science, Ulster University.

Sacchetti, F., Benetti, S., Georgiopoulou, A., Dunlop, P., Quinn, R. (2011) Geomorphology of the Irish Rockall Trough, North Atlantic Ocean, mapped from multibeam bathymetric and backscatter data. *Journal of Maps,*7(1), 60-81.

Sacchetti, F., Benetti, S., Georgiopoulou, A., Shannon, P.M., O'Reilly, B.M., Dunlop, P., Quinn, R., Ó Cofaigh, C. (2012a) Deep-water geomorphology of the glaciated Irish margin from high-resolution marine geophysical data. *Marine Geology,* 291–294, 113-131.

Sacchetti, F., Benetti, S., Ó Cofaigh, C., Georgiopoulou, A. (2012b) Geophysical evidence of deep-keeled icebergs on the Rockall Bank, Northeast Atlantic Ocean. *Geomorphology,* 159–160, 63-72.

Scourse, J.D., Haapaniemi, A.I., Colmenero-Hidalgo, E., Peck, V.L., Hall, I.R., Austin, W.E.N., Knutz, P.C., Zahn, R. (2009) Growth, dynamics and deglaciation of the last British–Irish ice sheet: the deep-sea ice-rafted detritus record. *Quaternary Science Reviews,* 28(27–28), 3066-3084.

Seddon, A.W.R., Mackay, A.W., Baker, A.G., Birks, H.J.B., Breman, E., Buck, C.E., Ellis, E.C., Froyd, C.A., Gill, J.L., Gillson, L. (2014) Looking forward through the past: identification of 50 priority research questions in palaeoecology. *Journal of Ecology,* 102(1), 256-267.

Seierstad, I.K., Abbott, P.M., Bigler, M., Blunier, T., Bourne, A.J., Brook, E., Buchardt, S.L., Buizert,C., Clausen, H.B., Cook, E., Dahl-Jensen, D., Davies, S.M., Guillevic, M., Johnsen, S.J., Pedersen, D.S., Popp, T.J., Rasmussen, S.O., Severinghaus, J.P., Svensson, A., Vinther, B.M. (2014) Consistently dated records from the Greenland GRIP, GISP2 and NGRIP ice cores for the past 104 ka reveal regional millennial-scale δ18O gradients with possible Heinrich event imprint. *Quaternary Science Reviews,* 106(Supplement C), 29-46.

Sejrup, H.P., Larsen, E., Landvik, J., King, E.L., Haflidason, H., Nesje, A. (2000) Quaternary glaciations in southern Fennoscandia: evidence from southwestern Norway and the northern North Sea region. Quaternary Science Reviews, 19(7), 667-685.

Sejrup, H-P., Hjelstuen, B.O., Torbjørn, D.K.I., Haflidason, H., Kuijpers, A., Nygård, A., Praeg, S., Stoker, M.S., Vorren, T.O. (2005) Pleistocene glacial history of the NW European continental margin. *Marine and Petroleum Geology,* 22(9–10), 1111-1129.

Shackleton, N.J., Hall, M.A., Vincent, E. (2000) Phase relationships between millennial-scale events 64,000–24,000 years ago. *Paleoceanography,* 15(6), 565-569.

Shannon, P.M., O'Reilly, B.M., Readman, P.W., Jacob, A.W.B., Kenyon, N. (2001) Slope failure features on the margins of the Rockall Trough. *The Petroleum Exploration of Ireland's Offshore Basins,* Geological Society of London, Special publication (188), 455-464.

Shaw, J., Todd, B.J., Brushett, D., Parrott, D.R., Bell, T. (2009) Late Wisconsinan glacial landsystems on Atlantic Canadian shelves: New evidence from multibeam and single-beam sonar data. *Boreas,* 38(1), 146-159.

Siddall, M., Rohling, E. J., Almogi-Labin, A., Hemleben, C., Meischner, D., Schmelzer, I., Smeed, D.A. (2003) Sea-level fluctuations during the last glacial cycle.*423*(6942), 853-8.

Skinner, L.C., McCave, I.N. (2003) Analysis and modelling of gravity-and piston coring based on soil mechanics. *Marine Geology,* 199(1-2), 181-204.

Small, D., Benetti, S., Dove, D., Ballantyne, C.K., Fabel, D., Clark, C.D., Gheorghiu, D.M., Newall, J., Xu, S. (2017) Cosmogenic exposure age constraints on deglaciation and flow behaviour of a marine-based ice stream in western Scotland, 21–16 ka. *Quaternary Science Reviews,* 167, 30-46.

Small, D., Fabel, D. (2016) Was Scotland deglaciated during the younger Dryas? *Quaternary Science Reviews,* 145, 259-263.

Sperazza, M., Moore, J.N., Hendrix, M.S. (2004) High-resolution particle size analysis of naturally occurring very fine-grained sediment through laser diffractometry: research methods papers. *Journal of Sedimentary Research,* 74(5), 736-743.

Stanford, J.D., Rohling, E.J., Bacon, S., Roberts, A.P., Grousset, F.E., Bolshaw, M. (2011) A new concept for the paleoceanographic evolution of Heinrich event 1 in the North Atlantic. *Quaternary Science Reviews,* 30(9–10), 1047-1066.

Stoker, M.S. (1995) The influence of glacigenic sedimentation on slope-apron development on the continental margin off Northwest Britain. *The Tectonics, Sedimentation and Palaeoceanography of the North Atlantic Region, Geological Society Special Pubblication,* 90, 159-177.

Stoker, M.S. (1997) Mid- to la Cenozoic sedimentation on the continental margin off NW Britain. *Journal of the Geological Society, London,* 154, 509-515.

Stoker, M.S., Leslie, A.B., Scott, W.D., Briden, J.C., Hine, N.M., Harland, R., Wilkinson, I.P., Evans, D., Ardus, D.A. (1994) A record of late Cenozoic stratigraphy, sedimentation and climate change from the Hebrides Slope, NE Atlantic Ocean. *Journal of the Geological Society,* 151(2), 235-249.

Stoker, M.S., Praeg, D., Hjelstuen, B.O., Laberg, J.S., Nielsen, T., Shannon, P.M. (2005) Neogene stratigraphy and the sedimentary and oceanographic development of the NW European Atlantic margin. *Marine and Petroleum Geology*, 22(9–10), 977-1005.

St-Onge, G., Mulder, T., Francus, P., Long, B. (2007) Chapter two continuous physical properties of cored marine sediments. *Developments in Marine Geology,* 1, 63-98.

Stow, D.A.V. (1979) Distinguishing between fine-grained turbidites and contourites on the Nova Scotia deep water margin. *Sedimentology,* 26, 371-387.

Stow, D.A.V., Lovell, J.P.B. (1979) Contourites: Their recognition in modern and ancient sediments. Earth-Science Reviews, 14(3), 251-291.

Stow, D.A.V., Piper, D.J.W. (1984) Deep-water fine-grained sediments: facies models. Fine-Grained Sediments: Deep Water Processes and Facies. Blackwell Scientific Publication for the Geological Society, 661-644.

Stow, D.A.V., Reading, H.G., Collinson, J.D. (1996) Deep seas. Sedimentary Environments: Processes, Facies and Stratigraphy, 3, 395-453.

Stow, D.A.V., Mayall, M. (2000) Deep-water sedimentary systems: New models for the 21st century. Marine and Petroleum Geology, 17(2), 125-135.

Stow, D.A.V., Faugeres, J-C., Howe, J.A., Pudsey, C.J., Viana, A.R. (2002) Bottom currents, contourites and deep-sea sediment drift: current state-of-the-art. Deep-Water Contourite Systems: Modern Drifts and Ancient Series, Seismic and Sedimentary Characteristics. Geological Society, London, Memoirs., 22, 7-20. Talma, A.S., Vogel, J.C. (1993) A Simplified Approach to Calibrating 14C Dates. *Radiocarbon,* 35(2), 317-322. Tan, P. (2006) Introduction to data mining. *In:* Anon. Pearson Education India, 160-170.

Talma, A.S., Vogel, J.C. (1993) A Simplified Approach to Calibrating 14C Dates. *Radiocarbon,* 35(2), 317-322.

Taylor, J., Dowdeswell, J.A. and Kenyon, N.H. (2000) Canyons and late Quaternary sedimentation on the North Norwegian margin. Marine Geology, 166(1-4), pp.1-9.

Tan, P. (2006) Introduction to data mining. *In:* Anon.Pearson Education India, 160-170.

Thorsnes, T., Erikstad, L., Dolan, M.F.J., Bellec, V.K. (2009) Submarine landscapes along the Lofoten-Vesterålen-Senja margin, northern Norway. *Norwegian Journal of Geology/Norsk Geologisk Forening,* 89

Toms, L.T. (2010) *Late Quaternary stratigraphy and sediment distribution on current-swept slopes, west Porcupine Bank, offshore Ireland.* PhD thesis ed. Dublin, Ireland: University College Dublin, UCD.

Toucanne, S., Soulet, G., Freslon, N., Silva Jacinto, R., Dennielou, B., Zaragosi, S., Eynaud, F., Bourillet, J.F., Bayon, G. (2015) Millennial-scale fluctuations of the European Ice Sheet at the end of the last glacial, and their potential impact on global climate. *Quaternary Science Reviews,* 123, 113-133.

Tripsanas, E.K., Piper, D.J.W. (2008) Glaciogenic debris-flow deposits of Orphan Basin, offshore eastern Canada: sedimentological and rheological properties, origin, and relationship to meltwater discharge. *Journal of Sedimentary Research,* 78(11), 724-744.

Unnithan, V., Shannon, P.M., McGrane, K., Readman, P.W., Jacob, A.W.B., Keary, R., Kenyon, N.H. (2001) Slope instability and sediment redistribution in the Rockall Trough: constraints from GLORIA. *The Petroleum Exploration of Ireland's Offshore Basins,* Geological Society of London (Special publication, London, 188), 439-454.

van Aken, H.M. (2000) The hydrography of the mid-latitude northeast Atlantic Ocean: I: The deep water masses. *Deep Sea Research Part I: Oceanographic Research Papers,* 47(5), 757-788.

Waelbroeck, C., Duplessy, J.C., Michel, E., Labeyrie, L., Paillard, D., Duprat, J. (2001) The timing of the last deglaciation in the North Atlantic climate records. *Nature*, 412, 724–727.

Wanamaker Jr, A.D., Butler, P.G., Scourse, J.D., Heinemeier, J., Eiríksson, J., Knudsen, K.L., Richardson, C.A. (2012) Surface changes in the North Atlantic meridional overturning circulation during the last millennium. *Nature Communications,* 3, 899.

Wang, D., Hesse, R. (1996) Continental slope sedimentation adjacent to an ice-margin. II. Glaciomarine depositional facies on Labrador slope and glacial cycles. *Marine Geology,* 135(1), 65-96.

Weaver, P.P.E., Schultheiss, P.J. (1990) Current methods for obtaining, logging and splitting marine sediment cores. *Marine Geophysical Researches,* 12(1-2), 85-100.

Weaver, P.P.E., Wynn, R.B., Kenyon, N.H., Evans, J. (2000) Continental margin sedimentation, with special reference to the north-east Atlantic margin. *Sedimentology,* 47(s1), 239-256.

Wilson, L.J, Austin, W.E.N. (2002) Millennial and sub-millennial-scale variability in the sediment colour from the Barra Fan, NW Scotland: implications for British ice sheet dynamics. *Glacier-Influenced Sedimentation on High-Latitude Continental Margins. Geological Society, London, Special Publication,* 203, 349-365.

Wilson, L.J., Austin, W.E.N., Jansen, E. (2002) The last British Ice Sheet: growth, maximum extent and deglaciation. *Polar Research,* 21(2), 243-250.

Wood, B.L., Williams, D M., Murray, J. (2017) Effects of the Younger Dryas climate event recorded in sediment near the western Irish seaboard. *Geological Journal.*

Wright, W.B. (1914) *The Quaternary ice age.* Macmillan and Company, limited.

Wynn, R.B., Stow, D.A.V. (2002) Classification and characterisation of deep-water sediment waves. *Marine Geology,* 192(1), 7-22. Zhuravleva, A., Bauch, H.A., Van Nieuwenhove,N. (2017) Last Interglacial (MIS5e) hydrographic shifts linked to meltwater discharges from the East Greenland margin. *Quaternary Science Reviews,* 164, 95-109.

Zhuravleva, A., Bauch, H.A., Van Nieuwenhove, N. (2017) Last Interglacial (MIS5e) hydrographic shifts linked to meltwater discharges from the East Greenland margin. *Quaternary Science Reviews,* 164, 95-109.

Appendix 3

Table 20APC foraminiferal counting: Sampling interval and relative abundances are indicated. The matrix is used for cluster analysis. NPS=Neogloboquadrina pachyderma sinistral; NPD= Neogloboquadrina pachyderma dextral.

Sample (cm)	*O. universa*	*G. bulloides*	*G. glutinata*	*G. inflata*	*G. menardii*	*G. quinqueloba*	*G. scitula*	*G. truncatulinoides*	*NPS*	*NPD*
10	1.8	76.9	0.0	4.2	0.0	10.8	1.2	0.0	0.0	5.1
30	0.0	36.4	0.0	12.5	0.0	12.8	0.3	0.0	10.8	27.1
41	0.0	20.2	0.0	1.4	0.0	3.7	0.3	0.0	71.8	2.6
50	0.0	54.4	0.0	5.3	0.0	8.5	2.2	0.0	26.1	3.5
62.5	0.0	13.0	0.0	0.0	0.0	0.3	0.6	0.0	84.9	1.2
80	0.0	25.3	0.0	0.0	0.0	0.3	0.0	0.0	74.4	0.0
90	0.0	22.8	0.0	0.0	0.0	0.0	0.0	0.0	77.2	0.0
100	0.0	7.6	0.0	0.0	0.0	1.8	0.2	0.0	90.3	0.0
110	0.0	12.0	0.0	0.0	0.0	0.0	0.0	0.0	88.0	0.0
120	0.0	23.7	0.0	0.0	0.0	3.3	1.2	0.0	71.8	0.0
129	1.4	45.7	0.0	8.1	0.0	1.2	1.2	0.0	0.0	42.5
140	0.0	44.8	0.0	0.0	0.0	15.1	0.0	0.0	40.1	0.0
150	0.0	19.4	0.0	0.0	0.0	0.0	0.0	0.0	80.6	0.0
170	0.0	7.2	0.0	0.0	0.0	0.0	0.3	0.0	92.5	0.0
180	0.0	3.1	0.0	0.0	0.0	0.3	0.3	0.0	96.3	0.0
190	0.0	37.2	0.0	1.0	0.0	4.4	3.9	0.0	47.5	5.9
200	0.0	55.5	0.0	0.4	0.0	0.0	0.0	0.0	43.9	0.2
210	0.0	19.8	0.0	0.0	0.0	0.0	0.9	0.0	78.8	0.6
220	0.0	53.4	0.0	0.3	0.0	5.9	1.0	0.0	37.0	2.3
239	0.0	57.2	0.0	0.6	0.0	3.1	1.6	0.0	37.4	0.0
250	0.0	55.2	0.0	1.0	0.0	6.3	2.8	0.0	33.4	1.3
280	0.0	82.2	0.0	0.9	0.0	9.6	0.6	0.0	4.4	2.3
290	0.0	24.4	0.0	0.0	0.0	0.6	0.1	0.0	71.9	3.0
300	0.0	4.2	0.0	0.0	0.0	3.3	0.0	0.0	91.5	0.6
310	0.0	38.3	0.0	1.5	0.0	45.6	9.1	0.3	4.1	1.2
320	0.0	38.7	0.0	2.3	0.0	2.1	1.3	0.0	47.2	8.5
330	0.0	34.0	0.0	2.3	0.0	30.3	5.3	0.0	2.9	25.8
340	0.0	50.4	0.0	4.7	0.0	29.9	1.9	0.0	1.4	11.6
350	0.0	54.7	1.1	4.7	0.0	34.9	1.4	0.0	1.4	1.7
360	0.6	35.8	0.0	15.2	0.6	14.7	1.2	2.1	0.0	29.9
370	0.5	48.3	0.0	7.6	0.5	5.7	2.1	1.0	1.2	33.3

Table 20PC foraminiferal counting: Sampling interval and relative abundances are indicated. The matrix is used for cluster analysis. NPS=Neogloboquadrina pachyderma sinistral; NPD= Neogloboquadrina pachyderma dextral.

Sample (cm)	*Globigerina bulloides*	*Globorotalia inflata*	*Globorotalia menardii*	*Globorotalia quinqueloba*	*Globorotalia scitula*	NPS	NPD
1	70.6	5.3	0.2	0.5	0.2	2.4	20.1
20	13.5	0.0	0.0	0.0	0.0	85.2	1.4
40	10.1	0.3	0.0	0.0	0.0	87.8	1.8
60	8.3	0.0	0.0	0.0	0.0	89.6	1.8
80	30.0	0.2	0.0	0.0	1.6	67.0	1.2
100	19.8	0.1	0.0	6.1	0.5	72.0	1.5
120	16.9	0.0	0.0	0.6	0.3	81.7	0.6
140	8.8	0.0	0.0	0.9	0.0	90.0	0.2
160	30.5	0.4	0.0	12.1	3.2	53.2	0.4
180	13.3	0.0	0.0	0.0	0.0	86.7	0.0
200	10.2	0.0	0.0	2.6	0.5	86.6	0.0
220	6.7	0.0	0.0	1.3	0.0	93.3	0.0
240	26.2	0.2	0.0	3.7	1.8	67.7	0.4
260	51.0	2.5	0.0	25.1	9.0	7.2	5.2
280	22.5	0.0	0.0	5.3	0.6	70.2	1.5
300	63.3	1.2	0.0	3.4	1.8	25.5	4.8
320	68.1	0.2	0.0	7.2	4.5	14.7	5.2
340	36.4	0.0	0.0	2.2	0.3	58.1	3.1
360	48.6	0.5	0.0	16.6	3.0	27.2	4.1
380	52.7	3.2	0.2	30.3	1.7	4.5	7.2

Appendix on CD

In the folders (Appendix 1 and Appendix 2) the reader can find photos, x-radiographs, measured physical properties and results of foraminifera and ice rafted debris counting for all the sediment cores analysed within this PhD project.

Appendix 1 includes the data from the JC106 cores used in Chapter 4.

Appendix 2 includes the data from the CE10008 cores used in Chapter 5.

Appendix 1

The 'Appendix 1' folder contains 3 additional folders. These represent the data collected during JC106 Cruise and presented in Chapter 4. The JC106-128PC, JC106-133PC, JC106-134PC folders include the data for each of the piston cores used, respectively. Each individual folder contains: photos and x-rays presented for each section of the core. The folders also include the results of foraminifera and IRD counting and radiocarbon dating laboratory reports, when available. The DBF-Radiocarbon-all-new calibrations file contains all of the radiocarbon calibrated ages as part of the Britice-Chrono consortium.

JC106-128PC

Photos and x-radiographs

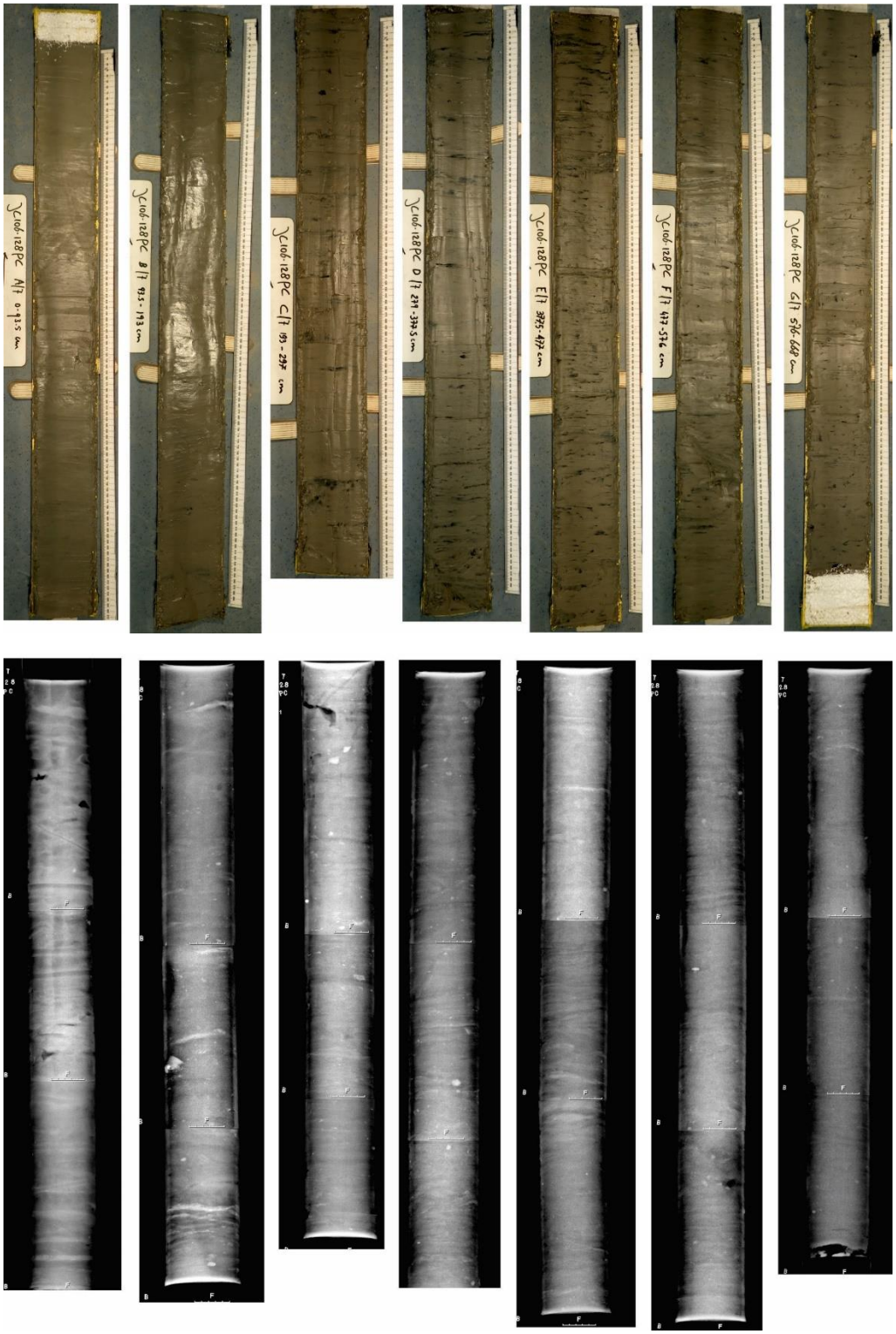

IRD counting

Sample	Weight in container (g)	Container weight (g)	Weight fraction >63 µm (mg):	Weight fraction > 150 µm (mg):	N. split	Weight fraction counted (mg):	IRD grains (counted):	IRD grains in all the fraction > 150 µm:	IRD/mg
20-21	15.2805	11.598	3682.5	1745.4	1	774.3	315	710.0619915	0.192821
39-40	15.0004	11.403	3597.4	1511.8	3	165.2	405	3706.289346	1.030269
64-65	13.5301	11.3375	2192.6	842.3	2	202	412	1717.958416	0.783526
85-86	12.8693	11.4322	1437.1	467.5	2	99.6	442	2074.648594	1.443636
105-106	12.0539	11.3827	671.2	197.6	1	80.6	386	946.3225806	1.409897
125-126	12.0022	11.5188	606.3	106.4	2	27	172	677.8074074	1.117941
145-146	12.3287	11.6363	692.4	262.9	1	112.6	451	1053.000888	1.520799
165-166	11.8885	11.3287	559.8	224.9	1	131.6	523	893.7895137	1.596623
185-186	11.9241	11.438	486.1	235.5	1	120.1	321	629.4379684	1.294873
205-206	12.108	11.3264	781.6	424.1	1	122.4	494	1711.645425	2.189925
225-226	11.934	11.4669	467.1	213.2	0	213.2	461	461	0.986941
245-246	11.829	11.5117	317.3	100.7	0	100.7	327	327	1.03057
265-266	11.8866	11.553	333.6	155.6	0	155.6	360	360	1.079137
295-296	11.7759	11.5012	274.7	106.8	0	106.8	525	525	1.911176
315-316	11.7063	11.4347	271.6	104.3	0	104.3	290	290	1.067747
335-336	12.561	11.4309	1130.1	518.2	2	110.9	299	1397.130748	1.236289
355-356	14.2986	11.6549	2643.7	1112.8	2	214	534	2776.8	1.050346
373-374	12.277	11.3885	888.5	354.4	1	194.9	447	812.8106721	0.914812
395-396	13.1425	11.6606	1481.9	547.6	2	131.8	390	1620.364188	1.093437
415-416	11.9811	11.2378	743.3	320.5	1	152.8	365	765.5922775	1.029991
435-436	13.1648	11.3742	1790.6	558.2	2	146.9	437	1660.540504	0.927365
455-456	11.97	11.3019	668.1	248.8	1	114	437	953.7333333	1.427531
473-474	13.0983	11.4938	1604.5	685.9	2	192.4	731	2605.992204	1.624177
485-486	13.7906	11.6549	2135.7	931.4	3	118.6	437	3431.887015	1.606914
505-506	12.2532	11.4682	785	345.8	1	171.2	373	753.4077103	0.959755
525-526	12.2455	11.2521	993.4	348.8	1	169.5	470	967.1740413	0.9736
545-546	14.8447	11.575	3269.7	998.1	3	164.4	410	2489.178832	0.761287
565-566	12.9761	11.5918	1384.3	387.3	1	167	543	1259.30479	0.909705
585-586	12.5995	11.593	1006.5	416.6	1	186.1	340	761.1176787	0.756202
605-606	12.2249	11.4379	787	290.8	1	118.5	407	998.7814346	1.2691
625-626	12.5504	11.5884	962	429.3	1	178.9	369	885.4762437	0.920453
645-646	12.8631	11.6612	1201.9	576.9	1	289	488	974.1425606	0.810502
663-664	12.1496	11.5359	613.7	241.2	1	101.6	303	719.3267717	1.172115

JC106-133PC

Photos and x-radiographs

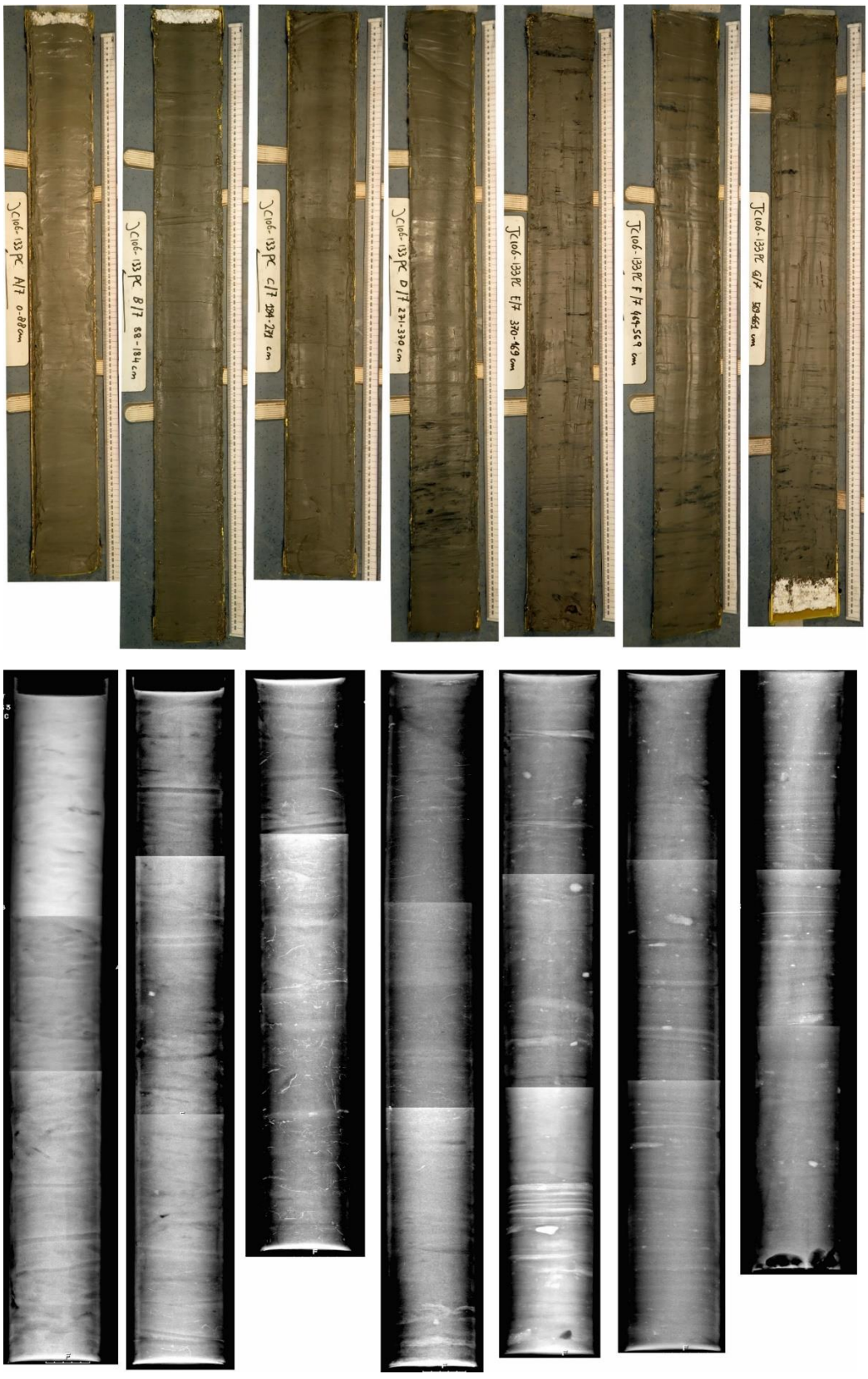

IRD counting

Sample (cm)	Weigth > 63 µm (g):	Weigth fraction > 63 µm (mg):	Weight fraction > 150 µm (mg):	Number split:	Weigth fraction counted (mg):	IRD grains (counted):	IRD grains (in all the fraction >150 µm):	IRD/mg
2_3	0.6837	683.7	302.6	0	302.6	10	10	0.014626298
6_7	1.1052	1105.2	480.7	0	480.7	7	7	0.006333695
20-21	0.6207	620.7	227	0	227	7	7	0.01127759
40-41	0.968	968	391.6	0	391.6	9	9	0.009297521
60-61	0.894	894	291.2	0	291.2	4	4	0.004474273
79-80	1.8163	1816.3	225.9	0	225.9	13	13	0.007157408
99-100	1.5037	1503.7	131.4	0	131.4	22	22	0.014630578
120-121	0.8046	804.6	244	0	244	224	224	0.278399205
140-141	1.0136	1013.6	452.9	2	161.8	406	1136.448702	1.121200377
160-161	1.2545	1254.5	445.8	1	275.4	935	1513.518519	1.206471517
175-176	1.6872	1687.2	621.1	1	348.4	1352	2410.238806	1.428543626
191-192	0.4744	474.4	97	0	97	103	103	0.217116358
215-216	0.4851	485.1	117.7	0	117.7	16	16	0.03298289
235-236	0.2284	228.4	78.4	0	78.4	9	9	0.039404553
255-256	0.2918	291.8	104.6	0	104.6	9	9	0.030843043
275-276	0.1676	167.6	41.5	0	41.5	38	38	0.22673031
295-296	0.1502	150.2	42.4	0	42.4	13	13	0.086551265
315-316	0.1219	121.9	29.9	0	29.9	16	16	0.13125127
335-336	0.3492	349.2	115	0	115	29	29	0.083046964
355-356	0.5322	532.2	326.9	0	326.9	141	141	0.264937993
375-376	0.8686	868.6	295.4	2	68.8	360	1545.697674	1.779527601
395-396	0.658	658	254.1	1	137.3	701	1297.335033	1.971633788
415-416	0.6327	632.7	276.9	1	144.3	667	1279.918919	2.022947556
435-436	0.2791	279.1	101.7	1	63.6	307	490.9103774	1.758904971
453-454	0.3022	302.2	107.6	0	107.6	707	707	2.339510258
475-476	0.4034	403.4	180.6	1	73.5	301	739.6	1.833415964
495-496	0.4883	488.3	174.9	1	85.6	410	837.7219626	1.715588701
515-516	0.3352	335.2	115.8	1	66.1	320	560.6051437	1.672449713
535-536	0.6457	645.7	212.7	1	115.3	555	1023.837814	1.585624616
555-556	0.199	199	74.1	0	74.1	291	291	1.462311558
575-576	0.3642	364.2	125.7	1	62.6	371	744.9632588	2.04547847
585-586	1.1978	1197.8	935	1	115.8	534	4311.658031	3.599647713
594-595	0.3418	341.8	155.5	0	155.5	546	546	1.597425395
615-616	0.2365	236.5	77.2	0	77.2	357	357	1.509513742
635-636	0.5643	564.3	163.5	1	77.6	376	792.2164948	1.403892424
655-656	0.5227	522.7	270.9	0	270.9	611	611	1.168930553

NPS counting

Sample (cm)	N split	Weigth >150μm (g):	Weigth fraction counted (g):	N planktonic in fraction counted:	N NPS	Abundance NPS
2_3	5	0.3026	0.061	1132	0	0
6_7	6	0.4807	0.0599	695	0	0
20-21	5	0.227	0.0534	601	0	0
40-41	6	0.3916	0.0478	410	0	0
60-61	6	0.2912	0.0556	549	0	0
79-80	5	0.2259	0.0545	964	0	0
99-100	5	0.1314	0.0491	497	4	0.804828974
120-121	5	0.244	0.0552	358	16	4.469273743
140-141	4	0.4529	0.0871	333	105	31.53153153
160-161	2	0.4458	0.1763	693	644	92.92929293
175-176	3	0.6211	0.1239	307	261	85.01628664
191-192	3	0.097	0.0688	712	67	9.41011236
215-216	3	0.1177	0.0142	764	13	1.701570681
235-236	3	0.0784	0.01	317	1	0.315457413
255-256	3	0.1046	0.0125	354	2	0.564971751
275-276	1	0.0415	0.0244	1182	53	4.48392555
295-296	2	0.0424	0.0112	410	4	0.975609756
315-316	2	0.0299	0.0086	399	49	12.28070175
335-336	3	0.115	0.0141	333	7	2.102102102
355-356	4	0.3269	0.024	308	12	3.896103896
375-376	1	0.2954	0.1373	532	487	91.54135338
395-396	0	0.2541	0.2541	408	389	95.34313725
415-416	1	0.2769	0.1372	347	331	95.38904899
435-436	0	0.1017	0.1017	375	353	94.13333333
453-454	0	0.1076	0.1076	265	243	91.69811321
475-476	0	0.1806	0.1806	485	446	91.95876289
495-496	0	0.1749	0.1749	513	468	91.22807018
515-516	0	0.1158	0.1158	200	181	90.5
535-536	0	0.2127	0.2127	129	119	92.24806202
555-556	0	0.0741	0.0741	255	235	92.15686275
575-576	0	0.1257	0.1257	300	276	92
585-586	0	0.935	0.935	239	218	91.21338912
594-595	0	0.1555	0.1555	90	80	88.88888889
615-616	0	0.0772	0.0772	332	309	93.07228916
635-636	0	0.1635	0.1635	460	396	86.08695652
655-656	1	0.2709	0.1586	1110	925	83.33333333

CALIBRATION OF RADIOCARBON AGE TO CALENDAR YEARS

(Variables: C13/C12 = -0.1 0/00 : Delta-R = -16 ± 55 : Glob res = -200 to 500 : lab. mult = 1)

Laboratory number	Beta450231 : JC106-133PC
Conventional radiocarbon age	15050 ± 50 BP

f 5066 ± 74 Adjusted for local reservoir correction prior to calibration

Calibrated Result (95% Probability)	Cal BC 16045 to 15720 (Cal BP 17995 to 17670)
Intercept of radiocarbon age with calibration curve	Cal BC 15925 (Cal BP 17875)
Calibrated Result (68% Probability)	Cal BC 15985 to 15835 (Cal BP 17935 to 17785)

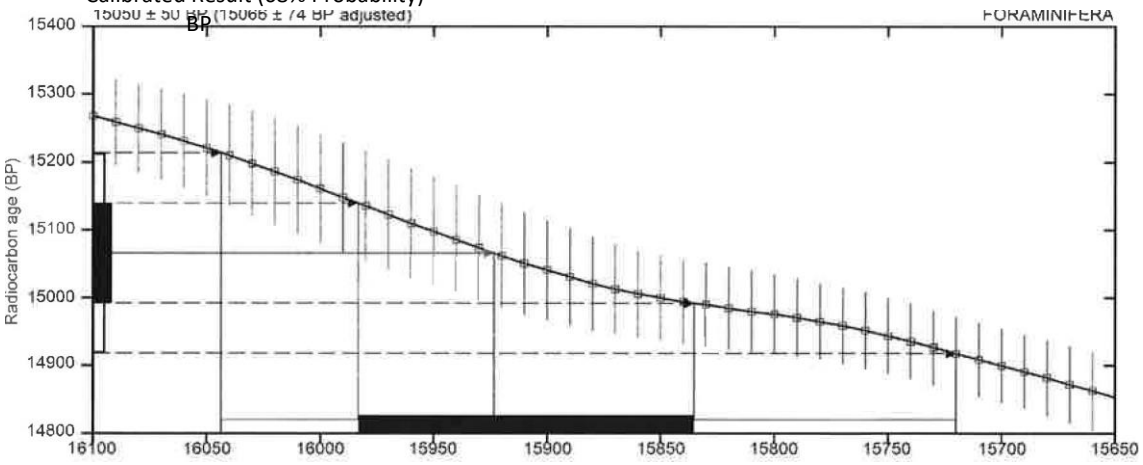

Database used

MARINE13

References

Mathematics used for calibration scenario

A Simplified Approach to Calibrating C14 Dates, Talma, A_ S , Vogel, J 1993, Radiocarbon 35(2):31

References to MARINE13 database

Reimer PO, Bard E, Bayliss A, Beck JW, Blackwell PG, Bronk Ramsey C, Buck CE, Cheng H; Edwards RL, Fnednch M, Grootes PM, Guilderson TP_

Hafiidason H, Hajdas l, Hatté C, Heaton TJ, Hoffmann DC, Hogg AG, Hughen KAT Kaiser KF, Kromer B, Manning SW, Niu M, Reimer RW, Richards DA, Scott EM, Southon JR, Staff RA, Turney CSM, van der Phchtd 2013 JntCa113 and Marine13 radiocarbon age calibration curves 0—50,000 years cal BP Radiocarbon55(4):18

Beta Analytic Radiocarbon Dating Laboratory

4985 S W. 74th Court, Miami. Florida 33155 • Tel: (305)667-5167 • Fax: (305)663-0964 • Email: beta@radiocarbon.com

CALIBRATION OF RADIOCARBON AGE TO CALENDAR YEARS

(Variables: C13/C12 = -0.2 o/oo : Delta-R = -16 ± 55 : Glob res = -200 to 500 : lab. mult = 1)

Laboratory number **Beta-441865 : JC106-133PC-175-176CM**

Conventional radiocarbon age **11200 ± 30 BP**

11216 ± 63 Adjusted for local reservoir correction prior to calibration

Calibrated Result (95% Probability) **Cal BC 10835 to 10665 (Cal BP 12785 to 12615)**

Intercept of radiocarbon age with calibration Cal BC 10740 (Cal BP 12690) curve

Calibrated Result (68% Probability) Cal BC 10780 to 10700 (Cal BP 12730 to 12650)

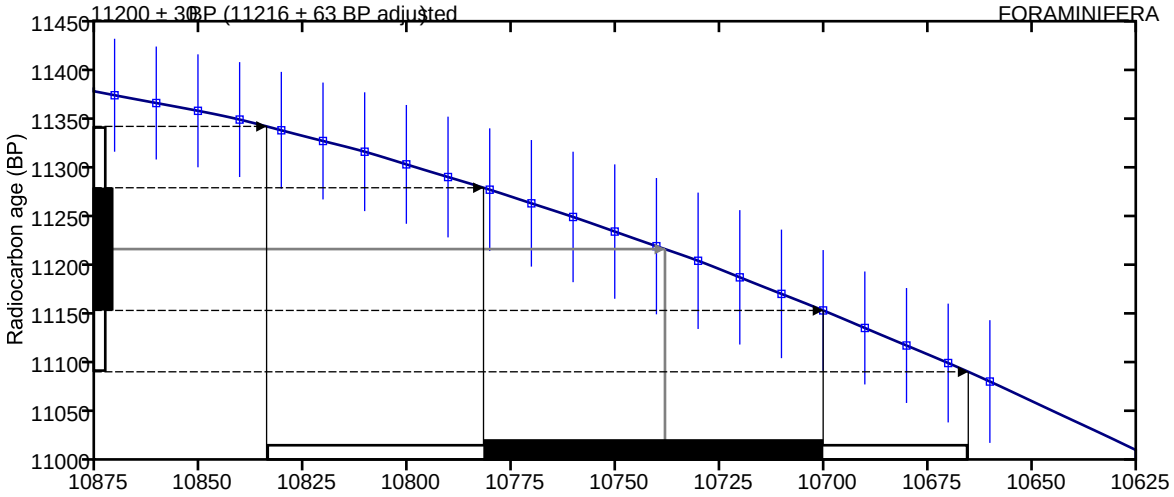

C

al BC **Database used MARINE13**

References

Mathematics used for calibration scenario

A Simplified Approach to Calibrating C14 Dates, Talma, A. S., Vogel, J. C., 1993, Radiocarbon 35(2):317-322

JC106-134PC

Photos and x-radiographs

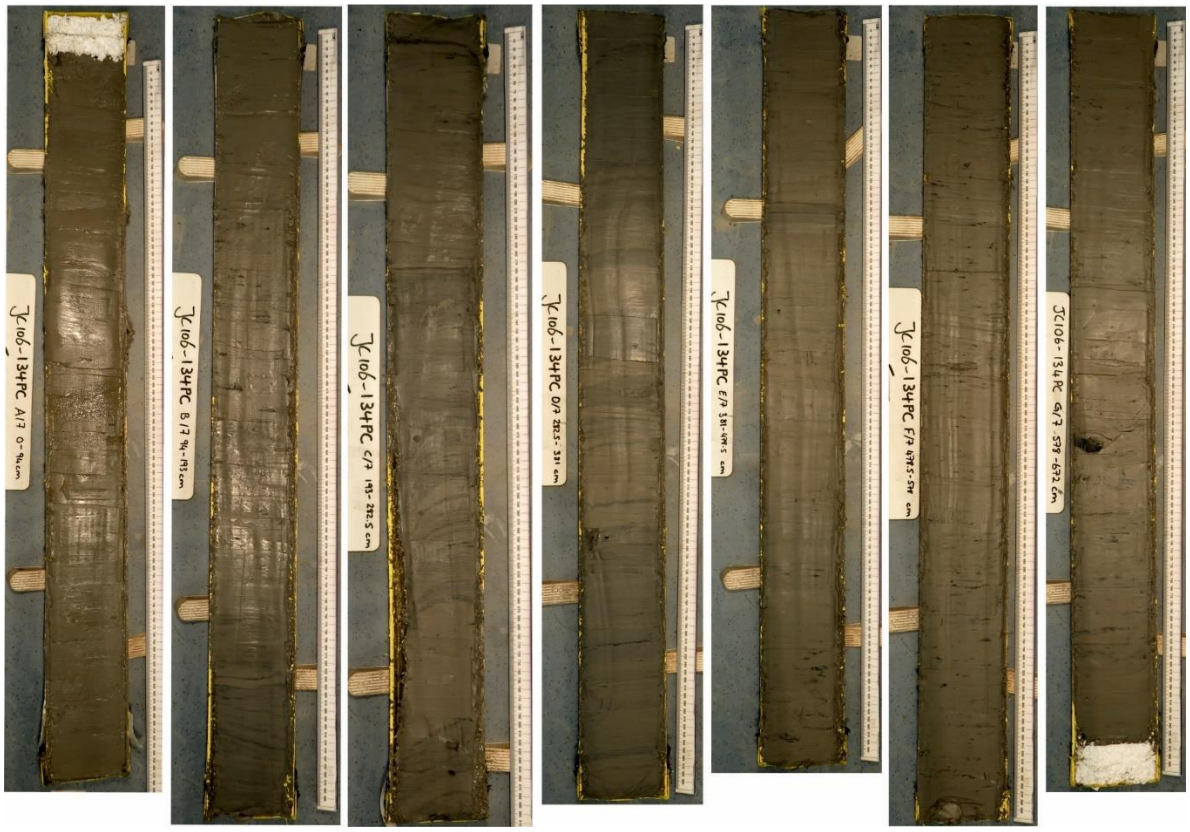

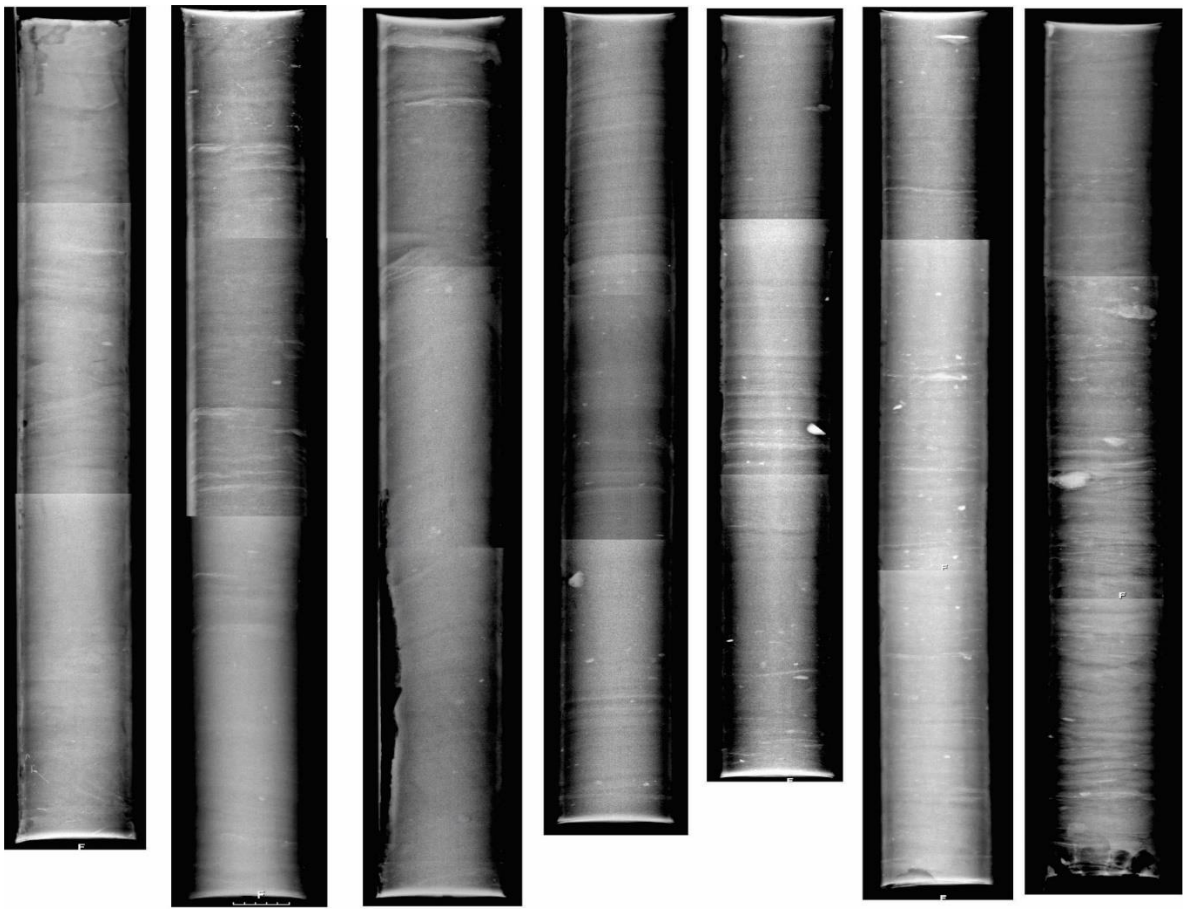

Sample (cm)	Weight in container (g):	Weight > 63 µm (g):	Weight > 63 µm (mg):	Weight fraction > 150 µm (mg):	Number split:	Weight fraction counted (mg):	IRD grains counted:	IRD grains (in all the fraction > 150):	IRD/mg (concentration):
10_11	13.7805	2.048	2048	459.2	2	148	384	1191.437838	0.581756757
30_31	13.966	2.3201	2320.1	577.2	2	147	359	1409.62449	0.607570574
50_51	15.0749	3.5938	3593.8	1290.5	3	150.5	580	4973.355482	1.383870967
60_61#	30.4853	1.4807	1480.7	158.4	1	80.8	444	870.4158416	0.587840779
70_71	12.008	0.5905	590.5	64.7	0	64.7	311	311	0.526672312
80_81	15.0866	0.6146	614.6	83.8	0	83.8	197	197	0.32053368
90_91	11.7715	0.291	291	120.1	0	120.1	11	11	0.037800687
110_111	12.2031	0.3539	353.9	59.3	1	59.3	349	349	0.986154281
130_131	11.9338	0.4757	475.7	87.4	0	87.4	367	367	0.771494639
150_151	12.6993	1.2205	1220.5	161.7	1	93.4	394	682.117773	0.558883878
170_171	12.4598	0.8324	832.4	113.3	1	53.8	308	648.6319703	0.779231103
190_191	12.316	0.6734	673.4	151.4	1	90	559	940.3622222	1.396439296
210_211	12.3083	0.5427	542.7	146.8	0	146.8	392	392	0.722314354
230_231	12.0333	0.6433	643.3	154.2	0	154.2	511	511	0.794341676
250_251	11.8496	0.3823	382.3	102.1	0	102.1	339	339	0.886738164
270_271	11.6647	0.2508	250.8	80.1	0	250.8	609	609	2.428229665
290_291	12.6138	1.0008	1000.8	150.3	0	150.3	880	880	0.879296563
310_311	11.9623	0.2778	277.8	57.3	0	57.3	222	222	0.799136069
330_331	12.1989	0.5468	546.8	192.8	1	60.2	324	1037.66113	1.89769775
350_351#	29.3162	5.9604	5960.4	5377.4	1	57.6	430	40143.78472	6.73508233
370_371	12.0388	0.4518	451.8	122.9	0	122.9	526	526	1.164231961
390_391	11.7939	0.2772	277.2	102.6	1	54.4	242	456.4191176	1.646533613
410_411	11.8338	0.3802	380.2	128.2	0	128.2	423	423	1.11257233
430_431	11.7997	0.2705	270.5	94.8	1	60	352	556.16	2.056044362
450_451	12.0655	0.5166	516.6	88.4	0	88.4	610	610	1.180797522
470_471	12.0718	0.5492	549.2	113.2	0	113.2	526	526	0.957756737
490_491	11.8414	0.2995	299.5	126.5	0	126.5	273	273	0.911519199
510_511	12.0992	0.4584	458.4	250.3	1	130.8	404	773.0978593	1.686513655
530_531	14.4971	0.436	436	243.9	1	115.7	362	750.2817632	1.720829732
550_551	12.0514	0.4451	445.1	228.4	2	49	289	1347.093878	3.026497141
570_571	12.0393	0.4307	430.7	233.7	1	233.7	365	365	0.847457627
590_591	12.1983	0.4497	449.7	254.1	1	109	327	762.3	1.695130087
610_611	11.8302	0.3791	379.1	151.4	1	84.3	390	700.4270463	1.847604976
630_631	11.8939	0.3823	382.3	100.3	1	48.7	314	646.698152	1.691598619
650_651	11.8019	0.234	234	96.8	0	96.8	413	413	1.764957265
669_670	11.7751	0.1596	159.6	57.2	0	57.2	307	307	1.923558897

DBF radiocarbon-all calibrations

Transect	Cruise	Core	Status	Publication Code	DR 0 from	to	Sample Identifier	Latitude N	Longitude	+/- 2σ (cal yrs BP)	Water depth (m)	DR 300 from	to	Location	No sections	Sample depth (cm)	Sample type	Conventional Radiocarbon Age (years BP)	+/- 1σ (radiocarbon yrs BP)	Calibrated Age (cal yrs BP) R = 0 years	+/- 2σ (cal yrs BP)	Calibrated Age (cal yrs BP) R = 300 years	+/- 2σ (cal yrs BP)	Calibrated Age (cal yrs BP) R = 700 years	+/- 2σ (cal yrs BP)
T7	JC106	134PC	Analysed	SUERC-6	T7-134PC-588		56.44471	-9.32123	1036	Malin Sea	7	8-593 (G/	Foraminif	15022	43	17800	169	17443	180	16863	225				
T7	JC106	134PC	Analysed	SUERC-6	T7-134PC-60		56.44471	-9.32123	1036	Malin Sea	7	0-61 (A/7	Foraminif	13174	40	15214	141	14635	359	13955	137				
T7	JC106	128PC	Analysed	SUERC-6	T7-128PC-125		56.17147	-9.61674	1475	Malin Sea		125-128	Neoglobo	13707	41	15995	180	15552	221	14960	231				
T7	JC106	133PC	Analysed	SUERC-6	T7-133PC-375		56.44450	-9.67221	1537	Malin Sea		375-376	Mixed for	15270	43	18070	169	17750	174	17250	194				
T7	JC106	133PC	Analysed	SUERC-6	T7-133PC-433		56.44450	-9.67221	1537	Malin Sea		433-438	Neoglobo	14355	41	16915	220	16457	210	15928	176				

Lab ID	Sample	Conventional Radiocarbon Age (years BP)	+/- 1σ (radiocarbon yrs BP)	DR 0 from	to	Calibrated Age (cal yrs BP) R = 0 years	+/- 2σ (cal yrs BP)	DR 300 from	to	Calibrated Age (cal yrs BP) R = 300 years	+/- 2σ (cal yrs BP)	DR 700 from	to	Calibrated Age (cal yrs BP) R = 700 years	+/- 2σ (cal yrs BP)
Beta-4418	T7-133PC-175-176	11200	30	12781	12597	12689	92	12590	12286	12438	152	11906	11407	11656.5	249.5
Beta-4502	T7-133PC-583-588	15050	50	17998	17652	17825	173	17661	17274	17467.5	193.5	17128	16646	16887	241

Appendix 2

The 'Appendix 2' folder contains 2 additional folders. These represent the data collected during Cruise CE10008 and used in Chapter 5. The 20APC and 20PC folders contain: photos, x-rays and oxygen stable isotopes data, when available.

20PC

Photos and x-radiographs

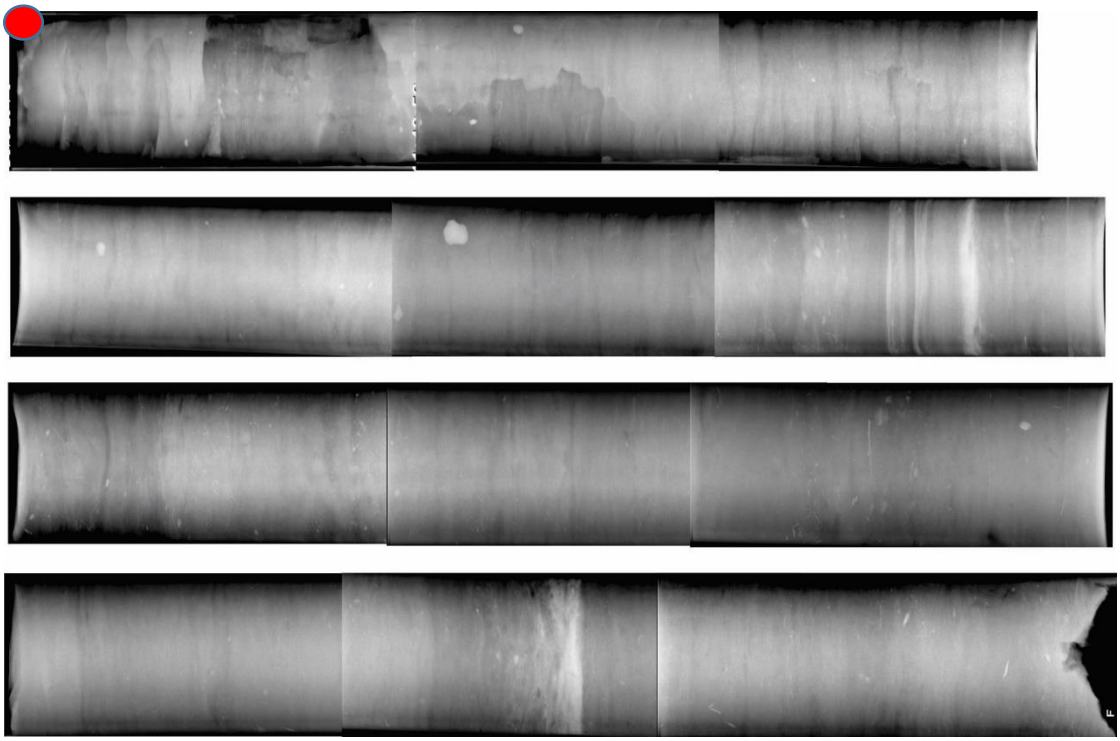

NOTE: The red dot indicates the core top

20APC

Photos and x-radiographs

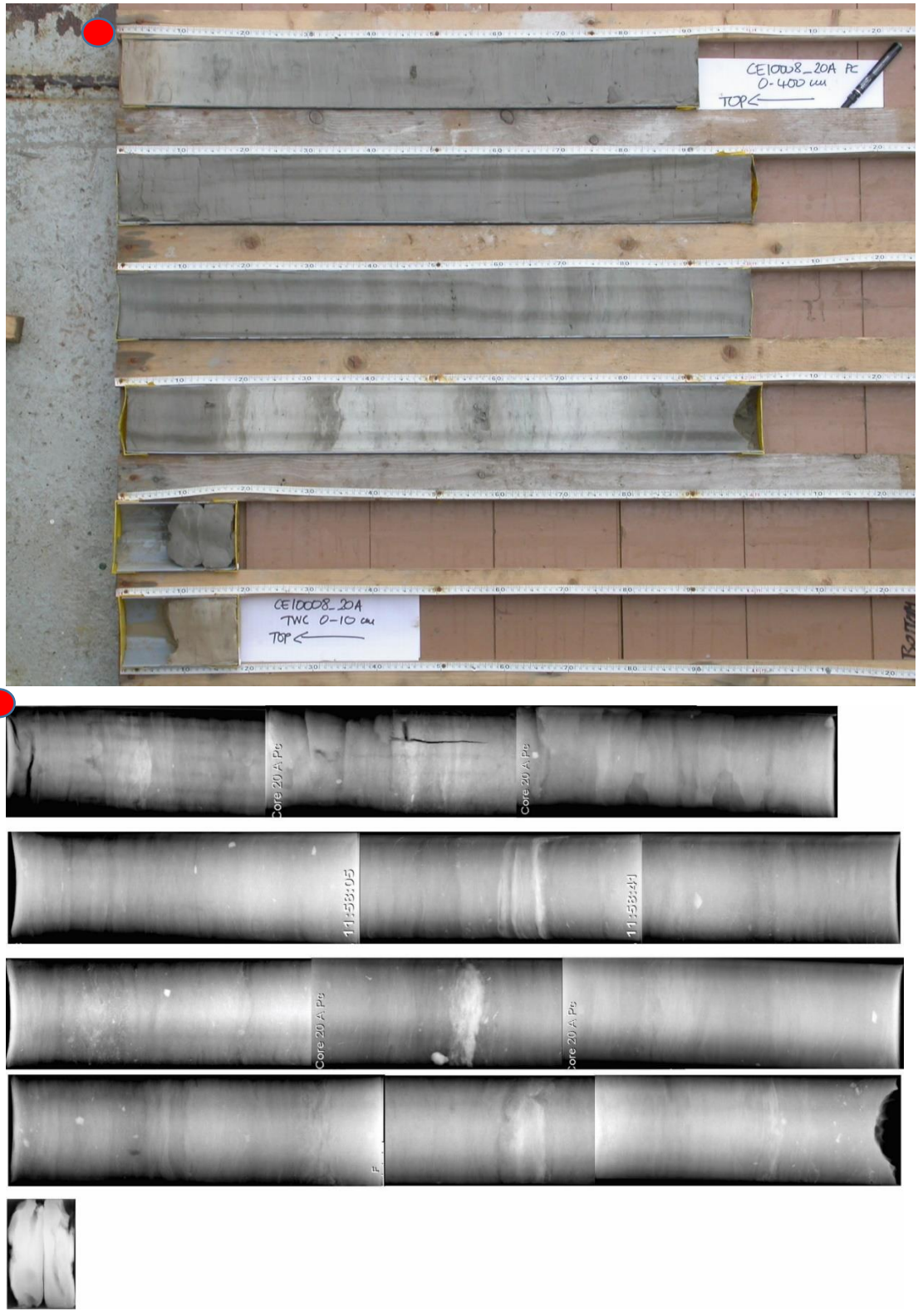

NOTE: The red dot indicates the core top.

20APC stable isotopes data

Sample Code	Sample Weight	Result δ-$^{13}C_{V\text{-}PDB}$ (‰)	Result δ-$^{18}O_{V\text{-}PDB}$ (‰)
3	0.8	-0.05	1.48
5	0.5	-0.03	1.64
8	0.8	-0.24	1.50
8.5	0.6	-0.20	4.73
10	0.7	-0.10	1.36
15	1.1	-0.04	2.02
19	0.7	-0.56	1.99
25	0.5	-0.46	2.67
28	0.7	-0.50	2.67
30	1.3	-0.29	2.77
41	0.8	-0.57	2.67
42	0.8	-1.06	2.54
50	1	-0.55	2.93
53	0.3	-0.04	3.98
58	0.3	0.01	3.78
62.5	0.3	-0.91	4.01
67	0.6	-0.46	4.58
80	0.3	-0.84	3.60
85	0.8	-0.50	4.08
88	0.6	-0.73	4.12
90	0.5	-0.71	4.12
95	0.3	-0.53	4.26
97	0.6	-0.36	4.45
100	0.3	-0.91	3.54
105	0.4	-1.04	3.61
110	0.3	-1.17	3.75
113	0.6	-0.44	4.38
120	0.3	-0.81	4.14
125	0.3	-1.07	3.73
129	0.9	0.04	1.63
134.5	0.7	-0.66	3.44
140	0.9	-0.25	3.66
141	0.9	-0.28	3.21
142	0.7	-0.51	3.14
160	0.3	-1.56	3.47
165	0.2	-1.62	4.62
170	0.3	-1.18	3.90
171	0.6	-0.19	3.05
172	0.4	-0.52	4.12
180	0.3	-0.64	3.18
184	0.8	-0.26	3.12
190	1	-0.38	3.82
195	1	-0.39	2.79
200	0.3	-0.48	3.13
205	0.3	-0.63	3.60
210	0.5	-0.36	3.16
214	1.2	-0.08	2.91
217	0.7	-0.08	3.03
220	1	0.00	2.86
223	0.8	-0.17	3.10
224	1.1	-0.07	2.66
229	0.8	-0.10	3.10
231	0.8	-0.11	2.91
234	0.8	-0.12	3.19
239	1.2	0.21	3.29
244	0.8	-0.44	2.99
250	0.6	-0.40	2.94
254	0.8	-0.17	2.78
256	0.6	-0.23	2.76
260	0.8	-0.29	2.78
263	0.7	-0.40	2.71
267	1.2	-0.12	2.85
271	0.6	0.00	2.70
275	0.7	-0.41	2.90
280	0.9	-0.36	3.23
285	1	-0.62	2.93
286	0.7	-1.00	2.64
288	0.7	-0.90	2.44
290	0.6	-1.14	2.75
296	0.8	-0.40	2.82
300	0.3	-1.31	2.78
305	0.8	-0.22	2.87
310	0.9	0.30	2.93
314	0.7	0.04	2.56
320	0.4	-0.63	2.07
322	0.6	-0.23	2.44
326	0.7	0.04	2.51
330	0.8	-0.37	2.67
336	0.7	-0.34	2.29
340	1.1	-0.38	2.13
345	0.8	-0.51	2.15
350	0.8	-0.09	2.58
355	0.5	-0.63	1.77
358	0.8	-0.24	2.03
360	0.8	-0.09	2.04
365	0.8	-0.37	1.53
370	0.6	-0.72	1.46